Three-Dimensional Model Test Study of the New Breakwaters at Playa Blanca, Lanzarote

Andersen, Thomas Lykke; Garborg, Karsten; Stagsted, Esben Rubech

Publication date:
2012

Document Version
Early version, also known as pre-print

Three-dimensional Model Test Study of the New Breakwaters at Playa Blanca, Lanzarote

October 2012

Thomas Lykke Andersen
Karsten Garborg
Esben Rubeck Stagsted

Client: SENER Ingenería y Sistemas S.A.

DCE Contract Report No. 129

AALBORG UNIVERSITY
Department of Civil Engineering

Hydraulics and Coastal Engineering Laboratory
Department of Civil Engineering
Aalborg University, Denmark

DCE Contract Report No. 129

Three-dimensional Model Test Study of the New Breakwaters at Playa Blanca, Lanzarote

by

Thomas Lykke Andersen
Karsten Garborg
Esben Rubeck Stagsted

October 2012

Scientific Publications at the Department of Civil Engineering

Technical Reports are published for timely dissemination of research results and scientific work carried out at the Department of Civil Engineering (DCE) at Aalborg University. This medium allows publication of more detailed explanations and results than typically allowed in scientific journals.

Technical Memoranda are produced to enable the preliminary dissemination of scientific work by the personnel of the DCE where such release is deemed to be appropriate. Documents of this kind may be incomplete or temporary versions of papers—or part of continuing work. This should be kept in mind when references are given to publications of this kind.

Contract Reports are produced to report scientific work carried out under contract. Publications of this kind contain confidential matter and are reserved for the sponsors and the DCE. Therefore, Contract Reports are generally not available for public circulation.

Lecture Notes contain material produced by the lecturers at the DCE for educational purposes. This may be scientific notes, lecture books, example problems or manuals for laboratory work, or computer programs developed at the DCE.

Theses are monograms or collections of papers published to report the scientific work carried out at the DCE to obtain a degree as either PhD or Doctor of Technology. The thesis is publicly available after the defence of the degree.

Latest News is published to enable rapid communication of information about scientific work carried out at the DCE. This includes the status of research projects, developments in the laboratories, information about collaborative work and recent research results.

Published 2012 by
Aalborg University
Department of Civil Engineering
Sohngaardsholmsvej 57,
DK-9000 Aalborg, Denmark

Printed in Denmark at Aalborg University

DCE Contract Report No. 129

Preface

This report present the results of 3-D physical model tests (length scale 1:42.5) carried out in a wave bassin at Department of Civil Engineering, Aalborg University (AAU) on behalf of SENER Ingenería y Sistemas S.A.

Associate Prof. Thomas Lykke Andersen was in charge of the model tests, assisted by B.Sc. Karsten Garborg and B.Sc. Esben Rubeck Stagsted. Engineer assistant Niels Drustrup and Leif Mortensen assisted in the laboratory with the construction and instrumentation of the model. The model construction, testing and reporting were performed during August and September 2012. The present version of the report is a revised version with corrections to the figures in Appendix A.

For further information please contact Associate Prof. Thomas Lykke Andersen (tla@civil.aau.dk)

Contents

Introduction 1

This report deals with a three-dimensional model study test of the new rubble mound and caisson breakwater at Port of Playa Blanca, Lanzarote. The objective of the work is to verify the structural and hydraulic responses of the new breakwaters for waves approaching from SW and SSW. Focus is on the trunk sections close to the corner connecting the two breakwaters.

The model tests include:

- Tests at increasing wave height for two water levels and two peaks periods.
- Recording of pressures on the base slab and front of the crown wall of the rubble mound breakwater, and on the front of the caisson. The horizontal wave force and tilting moment around the heel are documented for the pressure distribution giving minimum stability against sliding and overturning respectively.
- Measurement of the average overtopping discharge behind the crown wall of the rubble mound and caisson breakwater, where the measurements on the rubble mound includes the spatial distribution of the discharge. Characteristic situations have been video recorded.
- Investigation of toe and berm stability on the caisson and armour on the rubble mound, using photo overlay technique.

3-D model tests of the caisson breakwater in the port were performed for design and overload conditions in scale 1:42.5. Unless otherwise specified, all values given in this report are prototype values assuming Froude scaling. Table 1.1 lists the scales, assuming a factor 1.025 due to salt water in prototype and fresh water in the model.

Parameter	Unit		Scale
Length	[m]		$1 : 42.5$
Volume	[m^3]	$1 : 42.5^3 =$	$1 : 76.8 \cdot 10^3$
Time	[$m^{0.5}$]	$1 : 42.5^{0.5} =$	$1 : 6.52$
Discharge	[$m^3/(s \cdot m)$]	$1 : 42.5^{1.5} =$	$1 : 277$
Velocity	[m/s]	$1 : 42.5^{0.5} =$	$1 : 6.52$
Mass	[kg]	$1 : 42.5^3 \cdot 1.025 =$	$1 : 78.7 \cdot 10^3$
Force	[N]	$1 : 42.5^3 \cdot 1.025 =$	$1 : 78.7 \cdot 10^3$
Force/m	[N/m]	$1 : 42.5^2 \cdot 1.025 =$	$1 : 1.85 \cdot 10^3$
Pressure	[N/m^2]	$1 : 42.5 \cdot 1.025 =$	$1 : 43.6$
Moment	[Nm]	$1 : 42.5^4 \cdot 1.025 =$	$1 : 3.34 \cdot 10^6$

Table 1.1. Scale relations between model and prototype.

Model Set-up and Instrumentation 2

2.1 Model set-up in basin

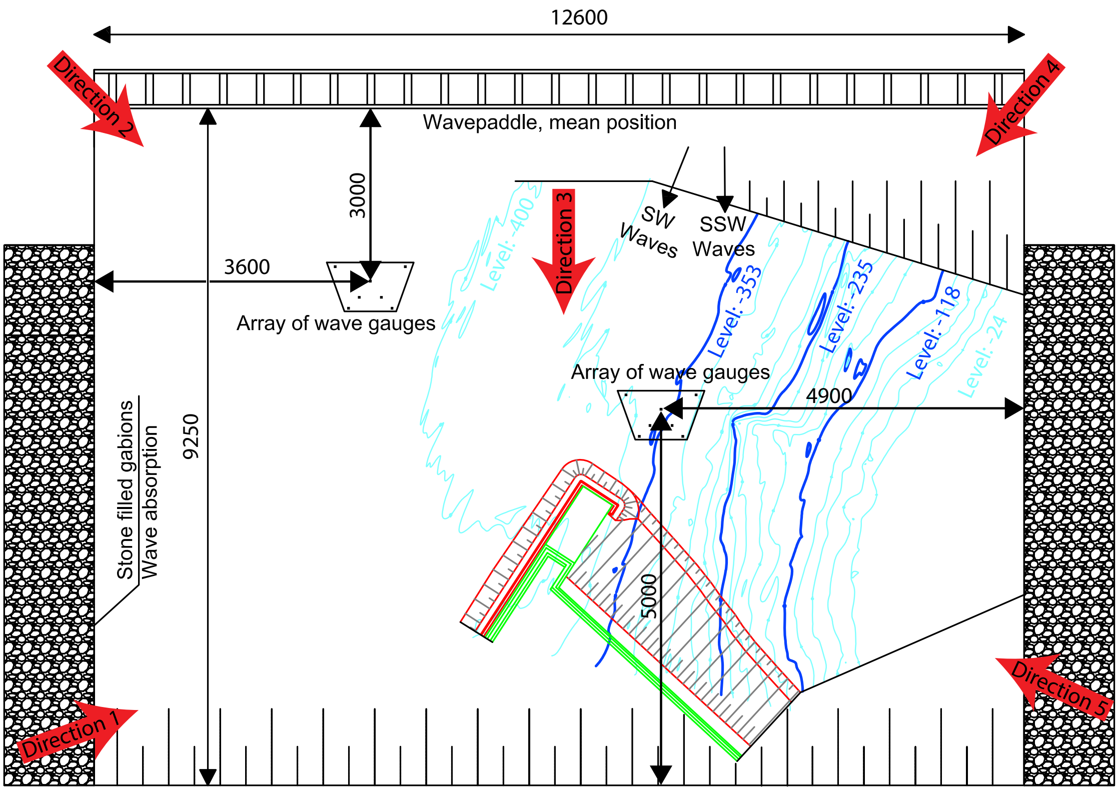

Figure 2.1. Set-up in the basin (model values in millimetres). The red arrows shows the angle of view in Figure 2.3 to 2.7.

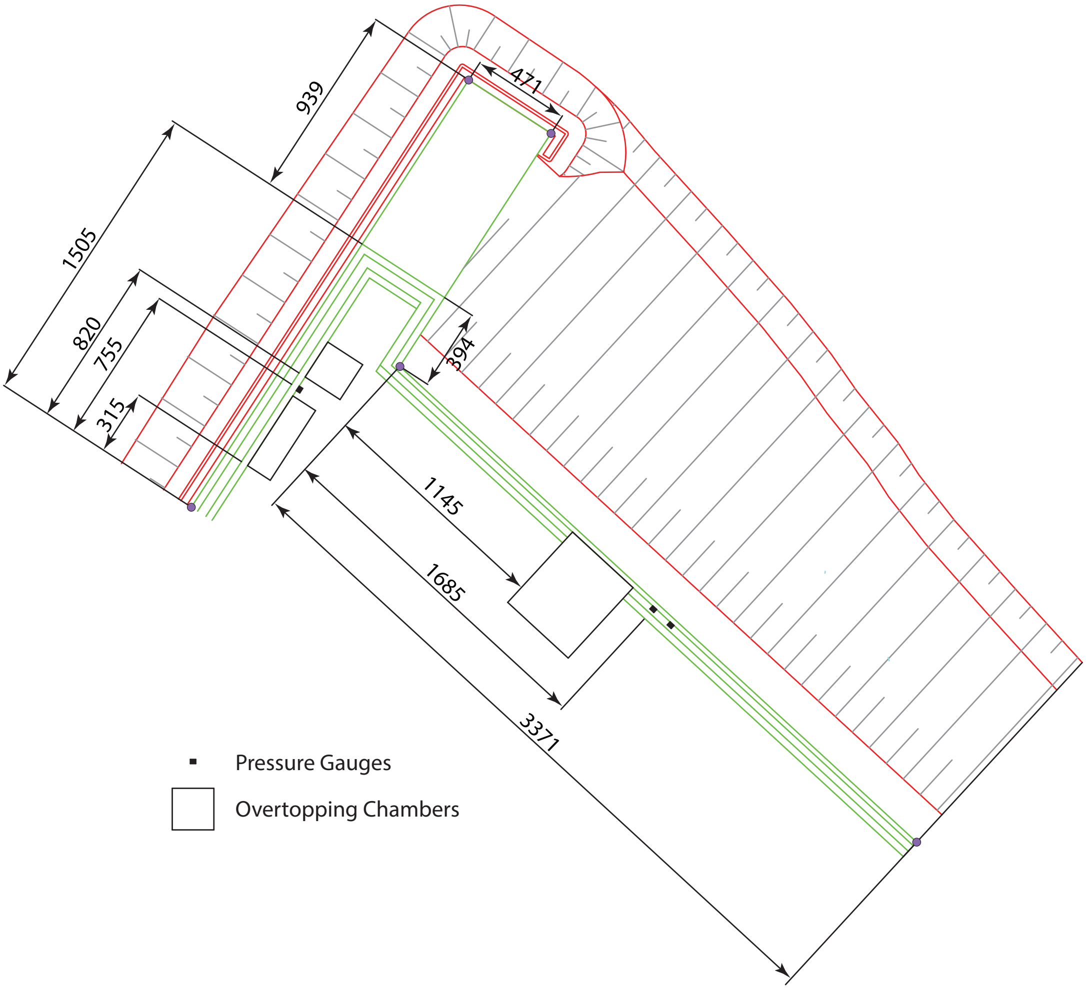

Figure 2.2. Set-up of the instrumentation in the basin (model values in millimetres).

Figure 2.3. Picture taken from direction 1.

Figure 2.4. Picture taken from direction 2.

Figure 2.5. Picture taken from direction 3.

Figure 2.6. Picture taken from direction 4.

Figure 2.7. Picture taken from direction 5.

Figure 2.8. Picture of the model with water and waves.

2.2 Prototype bathymetry and cross-sections

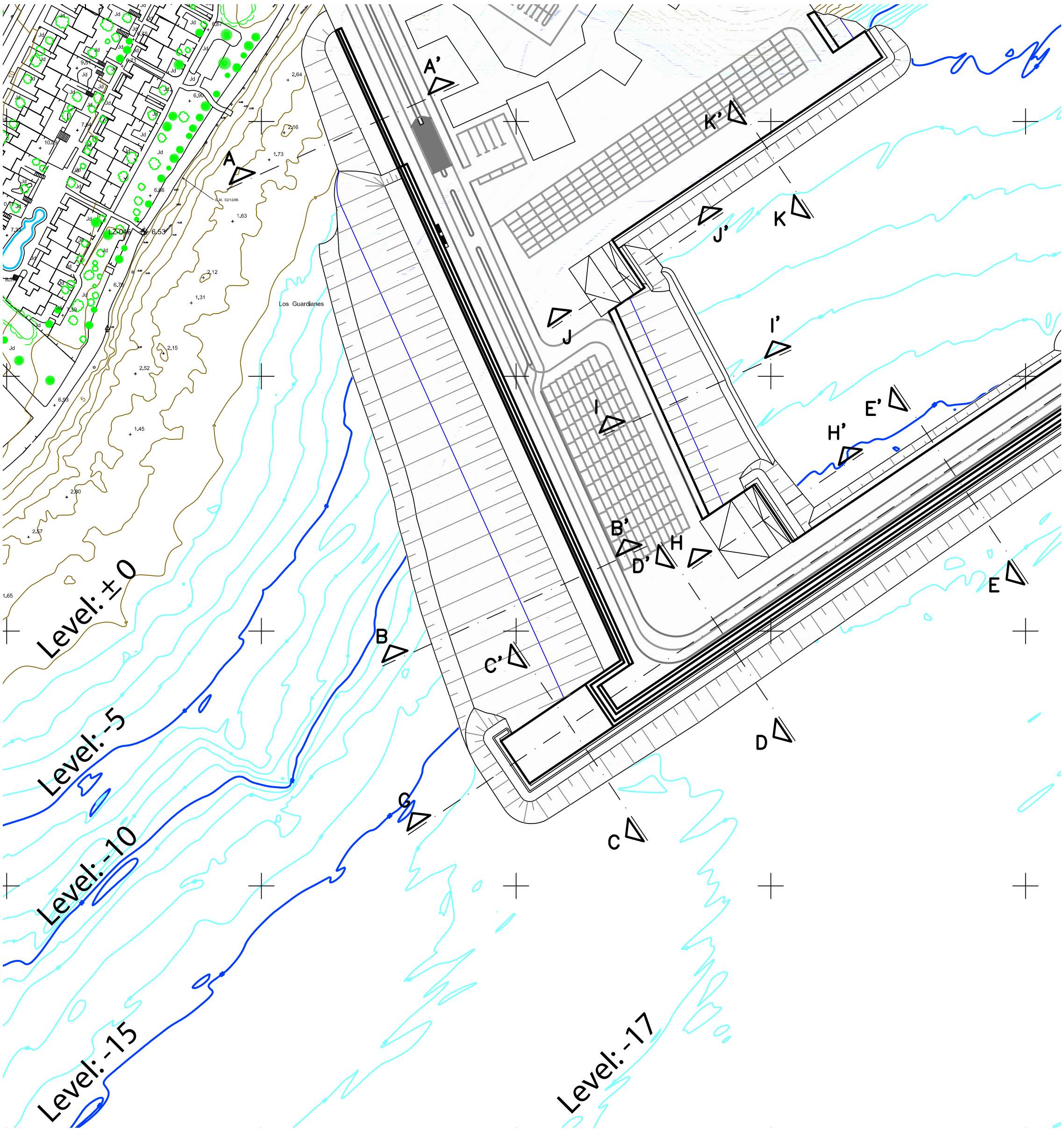

Figure 2.9. Overview of prototype with bathymetry (prototype values in metres).

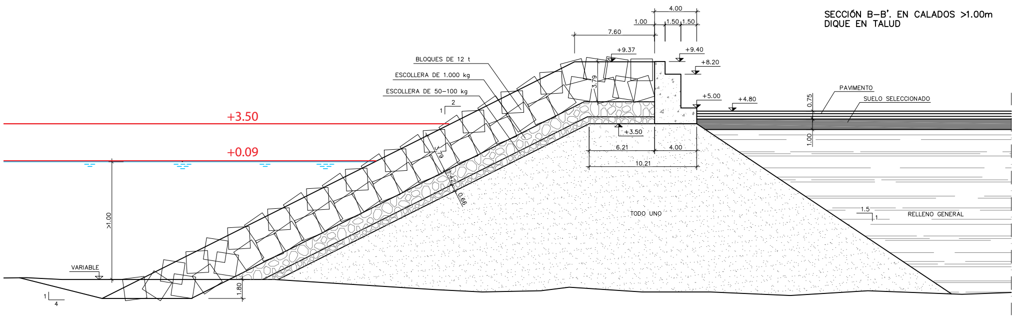

Figure 2.10. Prototype cross-section of cut B-B' (prototype values in metres). Model with impermeable membrane on rear slope.

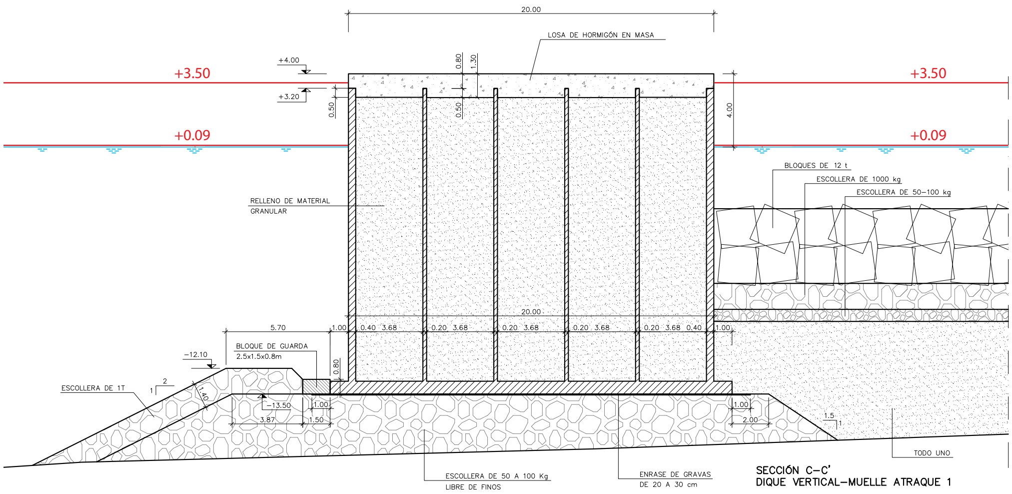

Figure 2.11. Prototype cross-section of cut C-C' (prototype values in metres).

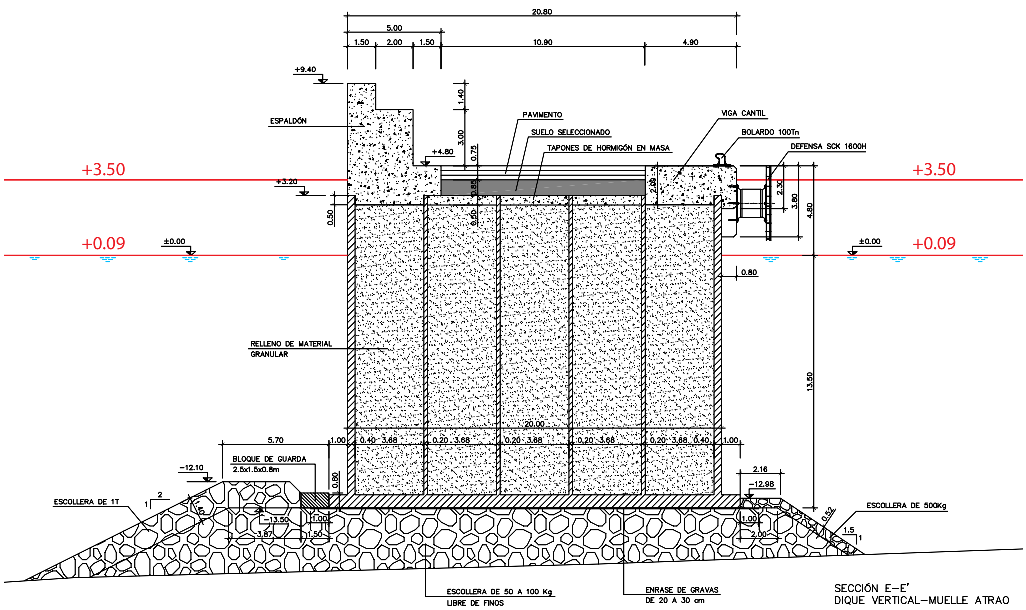

Figure 2.12. Prototype cross-section of cut E-E' (prototype values in metres).

2.3 Materials

The foundation for the caisson breakwater was constructed of two types of rock/gravel and parallelepipeds foot protection blocks. The rubble-mound breakwater was constructed with a core of gravel, a rock armour layer and cubes. The specifications for these materials are given in Table 2.1 and Table 2.2 for rubble mound and caisson foundation. A histogram of the mass of the stones are shown in Figure 2.13.

Placing density of cubes was 0.449 units/m^2.

The nominal diameter was calculated as:

$$D_{n50} = \left(\frac{W_{50}}{\rho_s}\right)^{\frac{1}{3}}$$

D_{n50}	nominal diameter
W_{50}	median weight of the stones
ρ_s	stone density

Type	W_{50} [g]	Size [mm]	Density [t/m^3]	ΔD_{n50} [mm]
Core/filter material	0.30	$D_{n50} = 4.7$	2.87	8.8
Inner armour rock layer	10.4	$D_{n50} = 15.7$	2.71	26.7
Armour cubes, 2 layers	148	40x40x40	2.31	52.6

Table 2.1. Material specifications for rubble mound breakwater (model scale).

Type	W_{50} [g]	Size [mm]	Density [t/m^3]	ΔD_{n50} [mm]
Core/filter material	0.30	$D_{n50} = 4.7$	2.87	8.8
Toe armour rock layer	10.4	$D_{n50} = 15.7$	2.71	26.7
Foot protection blocks	98	59x35x18	2.66	55.5

Table 2.2. Material specifications for caisson breakwater foundation (model scale).

Because of a difference in density for the foot protection blocks at the toe of the caisson (concrete in prototype, $\rho_c = 2.40$ t/m^3, aluminium in model, $\rho_{alu} = 2.66$ t/m^3), the target $\Delta D_{n50} = 48.2$ mm was not achieved and all wave heights relating to stability of protection blocks should be lowered by a factor of $\frac{55.5 \text{ mm}}{48.2 \text{ mm}} = 1.15$. The wave heights that has been corrected with this factor will be denoted H^*_{m0}.

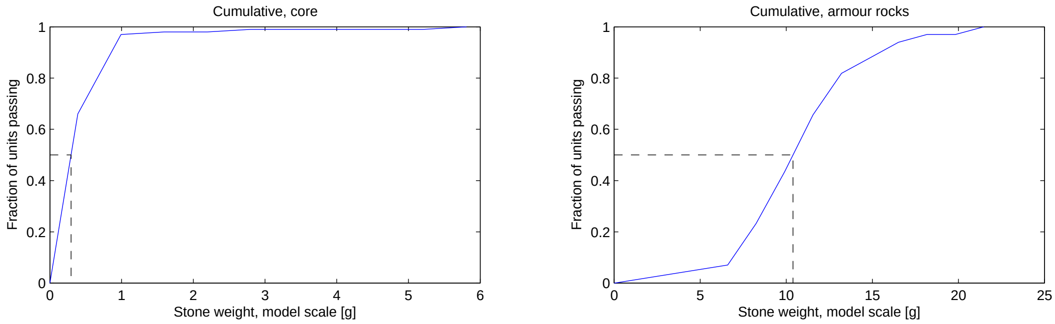

Figure 2.13. Grain curves of materials.

Due to lack of number of cube armour units, the cubes were substituted with parallelepipeds, with the same weight and density, on a stretch of the inner armour layer shown on Figure 2.14. The overtopping discharge and pressure were measured on the part of the rubble mound with the correct cube armour layer.

Figure 2.14. Inner armour layer. Note the cubes were substituted with parallelepipeds armour block in the inner layer on a stretch of the rubble mound.

2.4 Pressure gauges

Druck PMP Unik 5000 pressure gauges were used to measure the wave loads on the crown wall and the caisson breakwater. 10 and 6 pressure gauges were located at the front and bottom of the crown wall on the rubble-mound breakwater and 9 pressure gauges were located at the front face of the caisson breakwater.

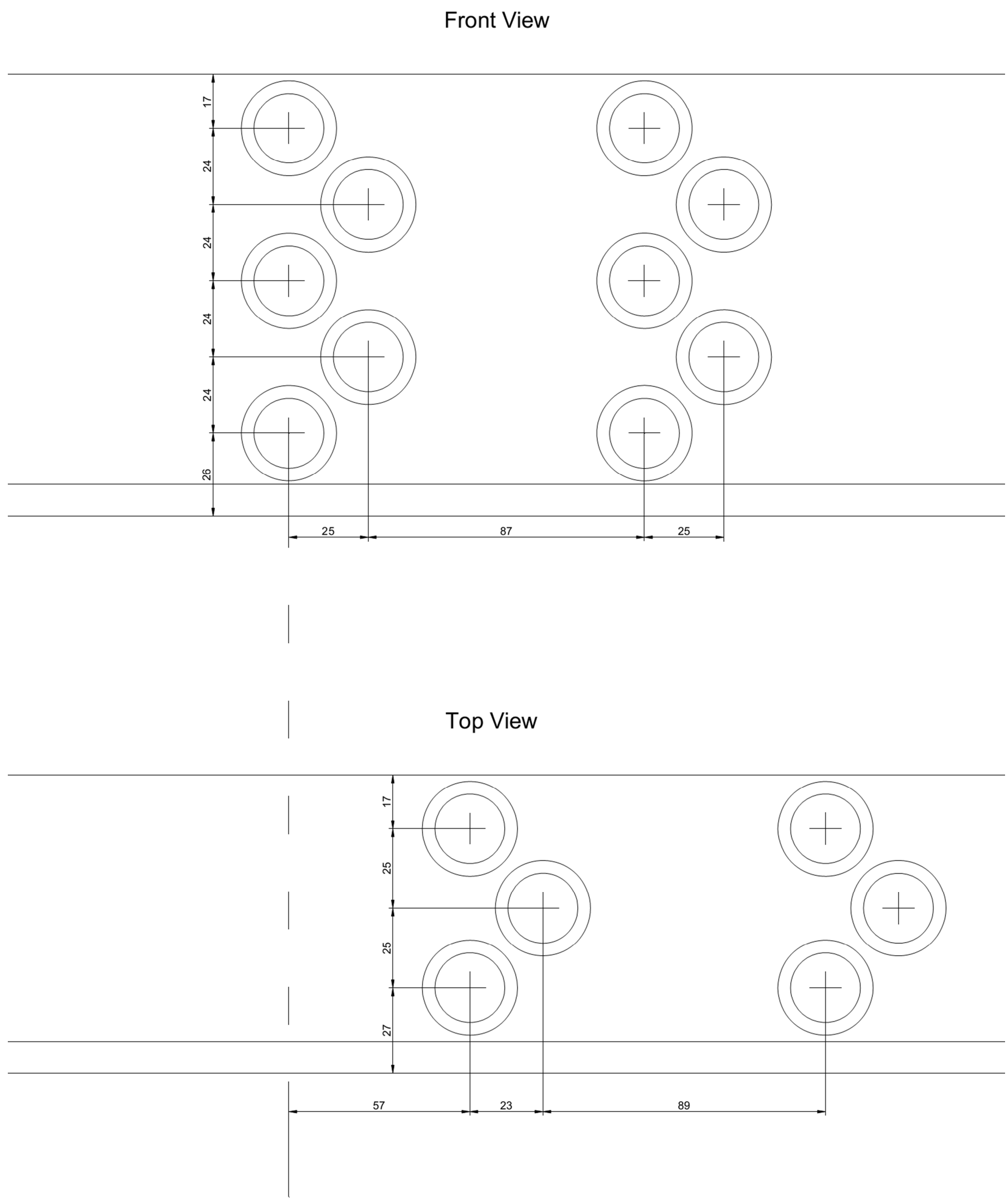

Figure 2.15. Pressure gauge locations at the crown wall on the rubble mound breakwater (annotations in millimetres in model scale).

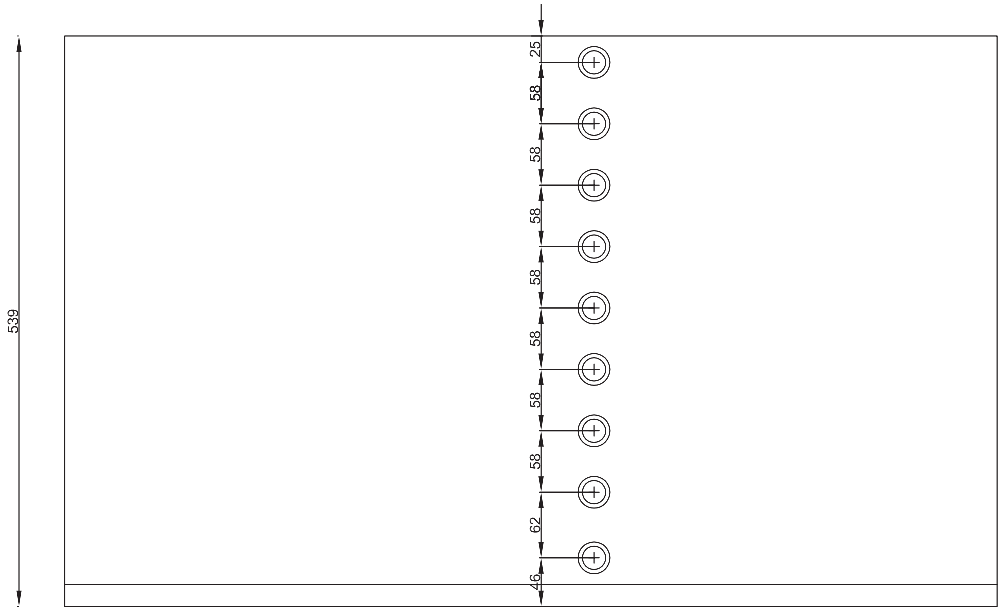

Figure 2.16. Pressure gauge locations on the caisson breakwater (annotations in millimetres in model scale).

Calibration

The pressure gauges were initially verified to be linear. Hereafter the pressure gauges were calibrated after installation with two water depths (in both cases all pressure gauges were fully submerged), as shown on Figure 2.17. The calibration was checked after completion of the test programme. The offset was found by measuring the signal for 20 seconds at the beginning of each test, before inducing waves, thereby excluding hydrostatic pressure from the measurements.

Figure 2.17. Calibration of pressure gauges at different water depths.

2.5 Wave gauges

Two wave gauge arrays, consisting of five and seven wave gauges, were located in the basin, as shown on Figure 2.18. The five gauge array was used to identify the wave height of the generated waves (H_{m0}^{Gen}), and the seven gauge array was placed in front of the breakwater to identify the waves besides the model and on horizontal bed, and thereby the influence of shoaling and refraction due to the bathymetry in front of the rubble mound(H_{m0}^{Break}).

Figure 2.18. The wave gauge arrays as positioned in the basin.

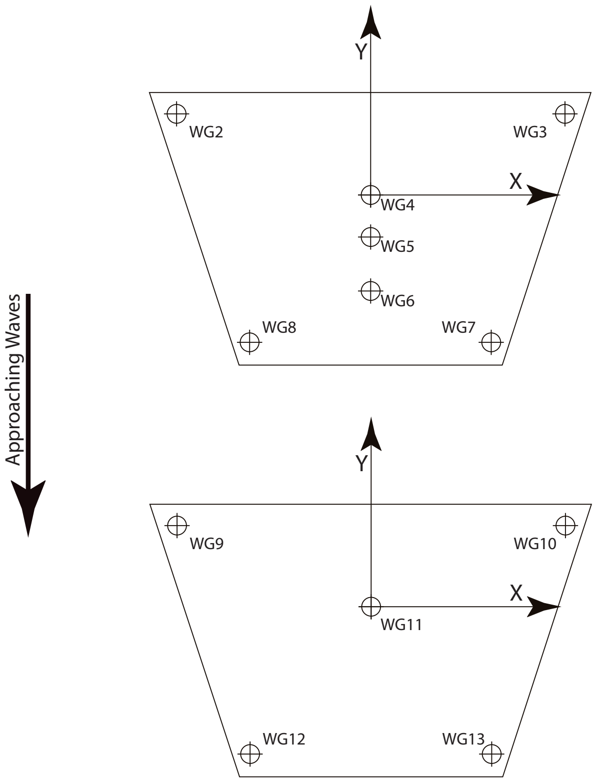

	X	Y
WG2	- 47.5 cm	15.9 cm
WG3	47.5 cm	15.9 cm
WG4	0.0 cm	0.0 cm
WG5	0.0 cm	- 13.0 cm
WG6	0.0 cm	- 33.0 cm
WG7	29.5 cm	-40.4 cm
WG8	- 29.5 cm	-40.4 cm

	X	Y
WG9	- 47.5 cm	15.9 cm
WG10	47.5 cm	15.9 cm
WG11	0.0 cm	0.0 cm
WG12	- 29.5 cm	-40.4 cm
WG13	29.5 cm	-40.4 cm

Figure 2.19. Wave gauge positions in the array (model scale).

2.6 Overtopping chambers

Figure 2.20 and 2.21 shows the overtopping chambers installed on the rubble-mound and the caisson.

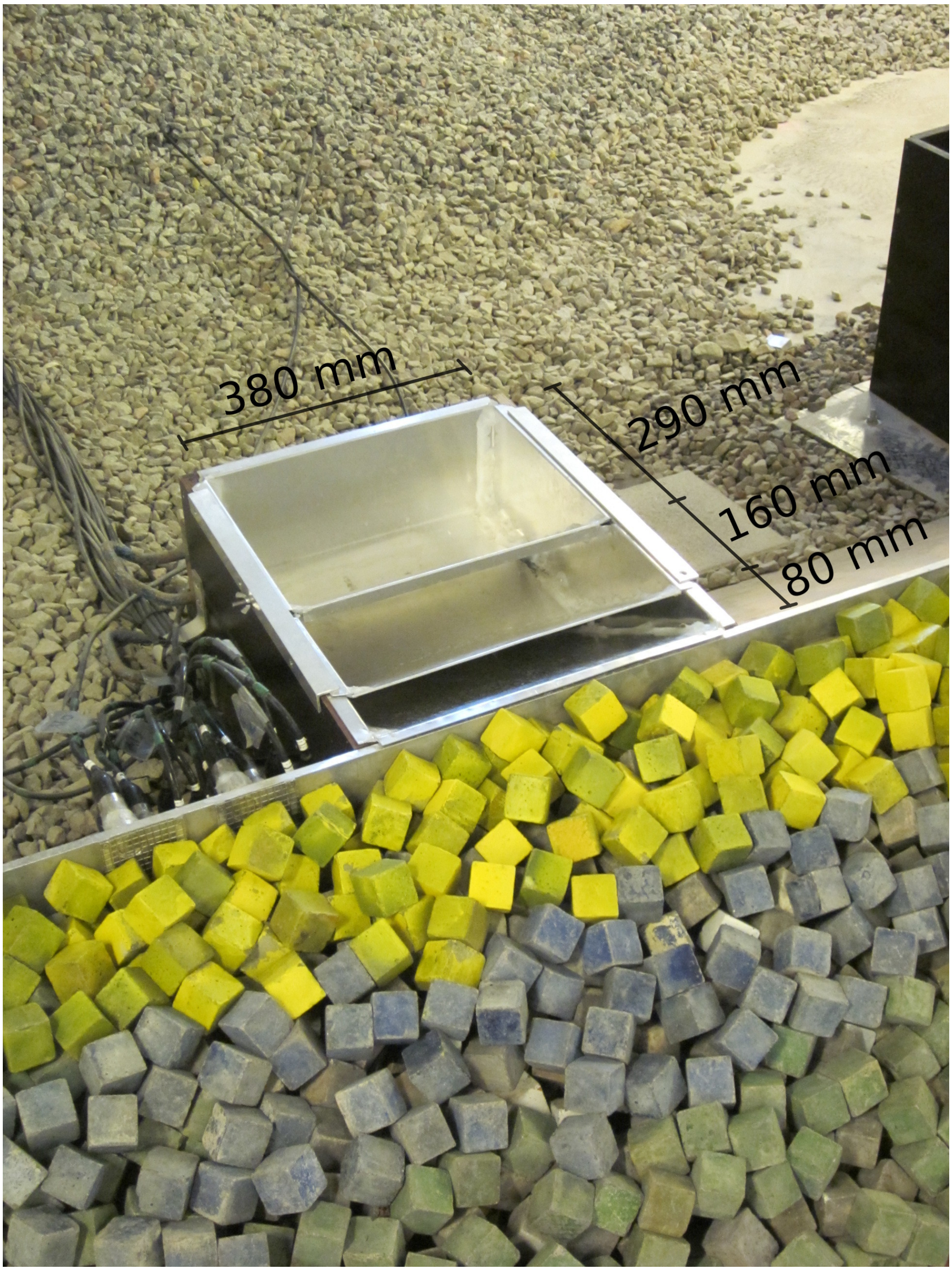

Figure 2.20. Overtopping chambers for rubble-mound. Annotations are in model scale.

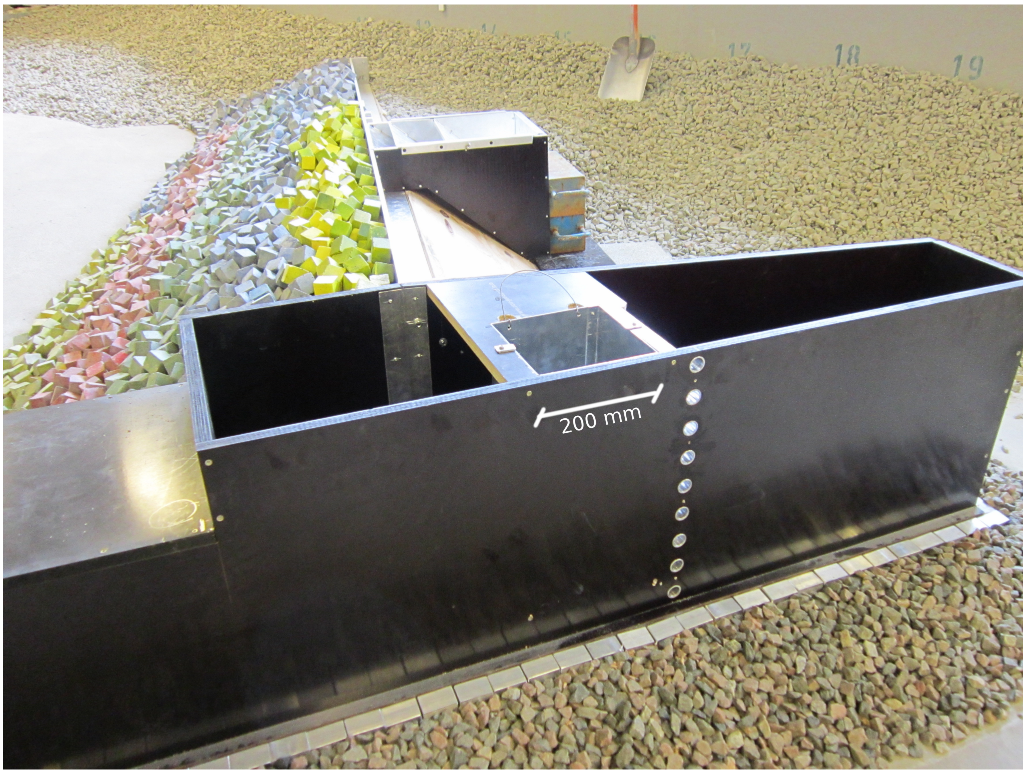

Figure 2.21. Overtopping chamber for caisson. Annotations are in model scale.

2.7 Stability

Stability of the rock and cube armour layers on the rubble-mound breakwater and the toe protection of the caisson breakwater were detected by visual observations, using photos taken before and after each test. For each test photos were taken from specific locations of interest.

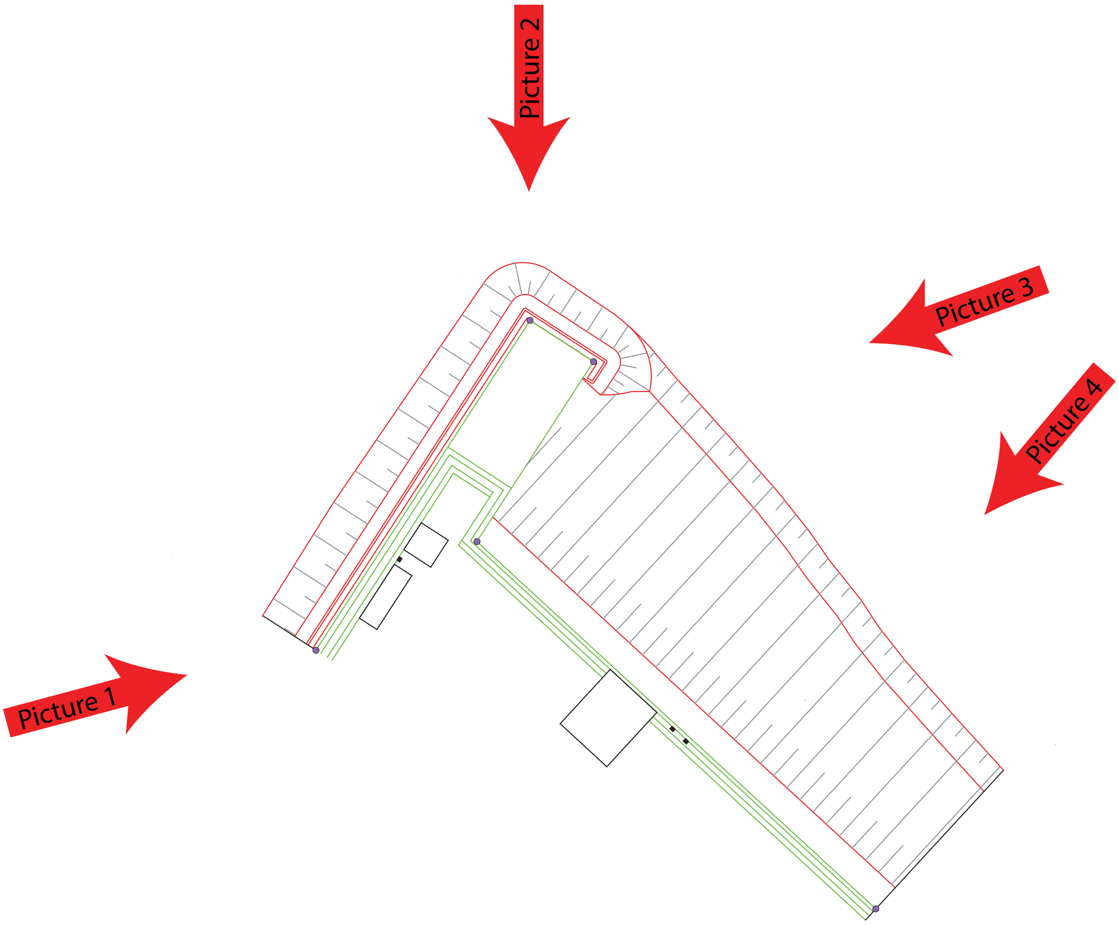

Figure 2.22. Set-up of the rubble mound and caisson breakwater, with indications of where the stability picture are taken from.

Wave Generation and Analysis 3

3.1 Sea States

Low and high water conditions were tested corresponding to +0.09 and +3.50 respectively.

Peak wave periods of 8 s and 16 s were used. The wave height were increased stepwise, with the following significant wave heights as target: 2.0 m, 2.5 m, 3.0 m, 3.5 m, 4.0 m and 4.5 m. A significant wave height of 3.7 m was estimated by SENER to have a return period of 500 years.

A JONSWAP spectrum with peak enhancement parameter $\gamma = 3.3$ were used.

A directional spreading of $s = 10$ (corresponding to a standard deviation of 25°) was used.

3.2 Wave Generation

3-D irregular waves were generated by the AWASYS system with the Filtered White Noise generation method. Because of a high amount of passive absorption in the basin, active absorption of the reflected waves were not used.

3.3 Wave Analysis

The data acquisition was done using a NI USB-6225 acquisition box and the WaveLab software package. The Wavelab software package was also used to analyse the measured surface elevations, splitting incident and reflected spectra on the basis of the BDM method (Hashimoto et al. 1987).

In a few tests wave gauge 8 and 9 were not working (mainly tests with 8 s waves) and were in these cases left out of the wave analysis.

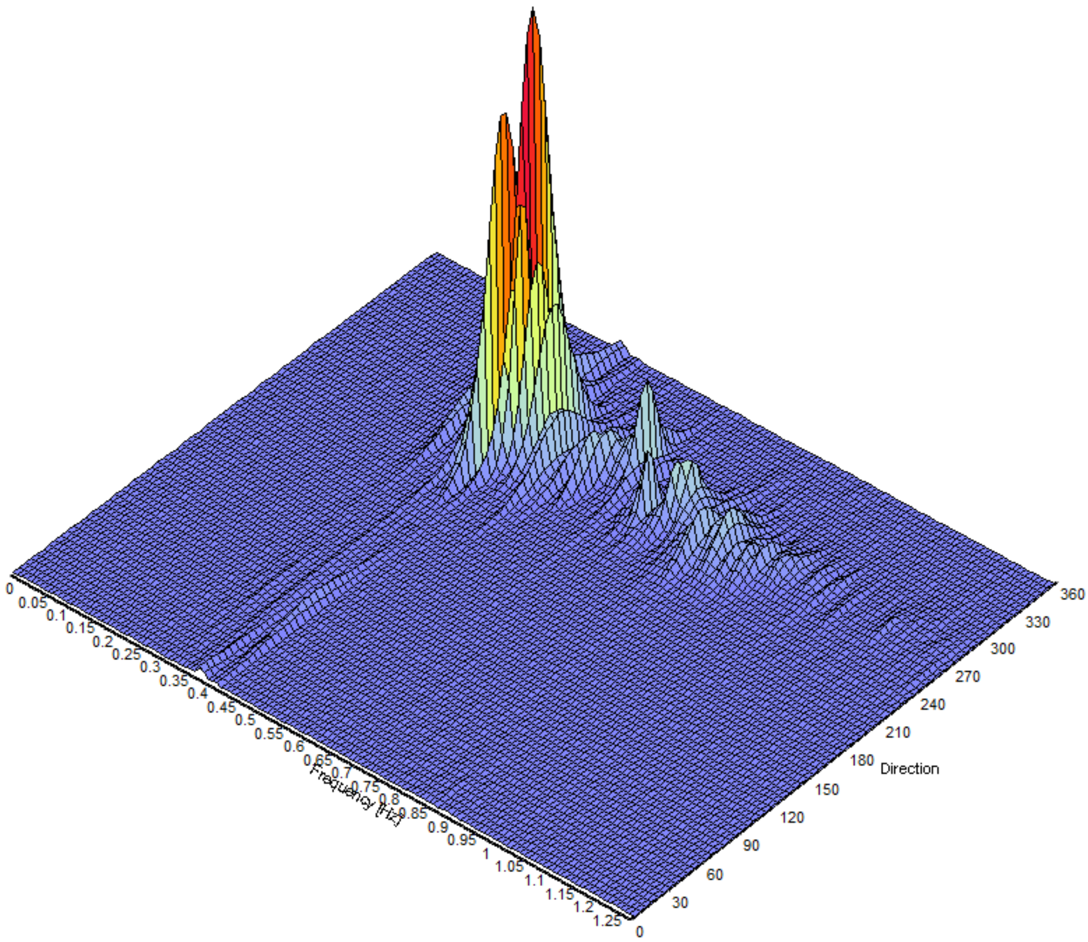

Figure 3.1. 3D variance spectrum of measured waves.

Analysis Method for Wave Induced Loads on Crown Wall and Caisson 4

Wave forces are calculated by numerical pressure integration.

Impact loads were not expected because $H_s/h_s < 0.35$ for the caisson and for the crown wall the entire height is protected by cubes. A sample frequency of 500 Hz (model scale) was used with a moving average of 5 samples to smoothen the signal.

Figure 4.1 and 4.2 shows the location of pressure gauges used for the wave force integration for the crown wall and the caisson breakwater. The numerical integration procedure is explained in the following.

4.1 Crown wall loads

On the crown wall two rows of pressure cells are available and the average of the two are used to calculate the overall forces.

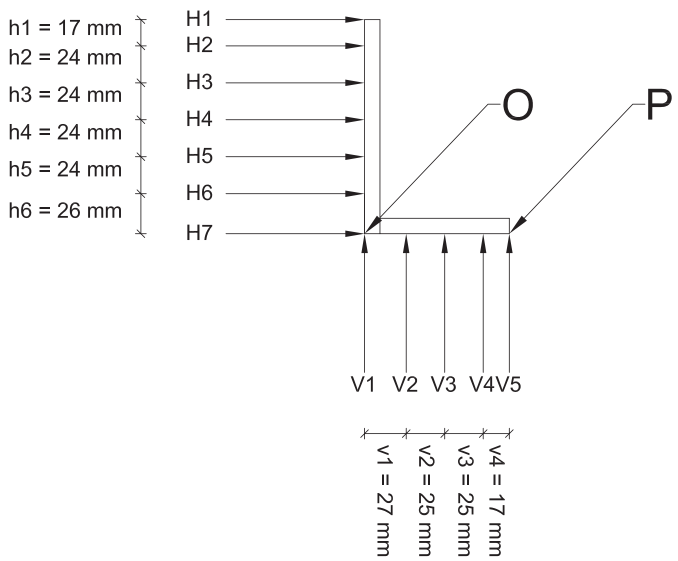

Figure 4.1. Location of pressure gauges on crown wall (model scale).

Assumptions regarding crown wall loads:

The horizontal pressure was assumed uniform from gauge H_2 and to the top of the model (H_1). The pressure at the front foot corner of the model (H_7, V_1), was found by linear extrapolation of H_5 and H_6. The pressure was assumed to be equal around the corner.

$$\begin{aligned} H_1 &= H_2 \\ V_1 = H_7 &= H_6 - \frac{H_5 - H_6}{h_5}\ h_6 \end{aligned}$$

Pressure at the heal (V_5) is found by linear extrapolation of V_3 and V_4.

$$V_5 = V_4 - \frac{V_3 - V_4}{v_4}\ v_5$$

4.1.1 Horizontal wave induced force and related moment

Contribution to F_H from pressure on h_n:

$$\begin{aligned} \Delta F_{H,hn} &= \tfrac{1}{2} h_n \left(H_n + H_{n+1}\right) \\ \Delta M_{F_{H,hn}} &= \tfrac{1}{2} h_n \left[\left(\sum_{i=n+1}^{6} h_i \right) \left(H_n + H_{n+1}\right) + h_n \left(\tfrac{2}{3} H_n + \tfrac{1}{3} H_{n+1}\right) \right] \\ F_{H,} &= \sum_{n=1}^{6} \Delta F_{H,hn} \\ M^P_{F_H} &= \sum_{n=1}^{6} \Delta M_{F_{H,hn}} \end{aligned}$$

4.1.2 Vertical wave induced force and related moment

$$F_V = \sum_{n=1}^{4} \tfrac{1}{2} v_n \left(V_n + V_{n+1}\right)$$
$$M_{F_V}^{O} = \sum_{n=1}^{4} \left(\tfrac{1}{2} v_n \left[\left(\sum_{i=1}^{n} v_i \right) \cdot \left(V_n + V_{n+1}\right) + v_n \left(\tfrac{1}{3} V_n + \tfrac{2}{3} V_{n+1} \right) \right] \right)$$

Moment around the rear corner of the base plate:

$$M_{F_V}^{P} = \left(\left(\sum_{i=1}^{4} v_i \right) - \frac{M_{F_V}^{O}}{F_V} \right) F_V$$

4.2 Caisson loads

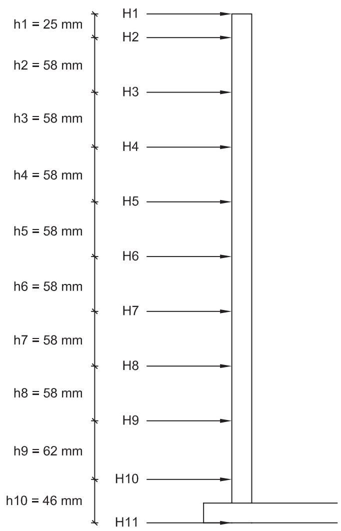

Figure 4.2. Location of pressure gauges on caisson (model scale).

Assumptions regarding caisson loads:

The horizontal pressure was assumed uniform from gauge H_2 and to the top of the model (H_1). The pressure at the front foot corner of the model (H_{11}), was found by linear extrapolation of H_9 and H_{10}. The pressure was assumed to be equal around the toe of the caisson, and the toe is therefore neglected.

$$H_1 = H_2$$
$$H_{11} = H_{10} - \frac{H_9 - H_{10}}{h_9} \; h_{10}$$

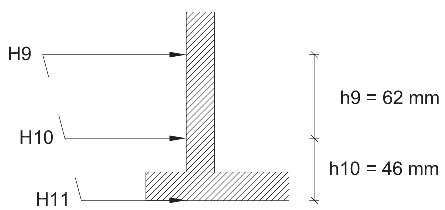

The uplift force is estimated by assuming a triangular distribution of the pressure underneath the caisson. The pressure V_1 is assumed equal to H_{11} and the pressure at the heel of the caisson is assumed to be zero.

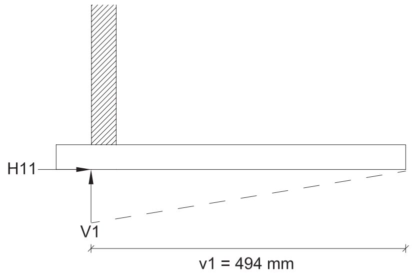

$$V_1 = H_{11}$$

4.2.1 Horizontal wave induced force and related moment

Contribution to F_H from pressure on h_n:

$$\Delta F_{H,hn} = \tfrac{1}{2} h_n \left(H_n + H_{n+1} \right)$$

$$\Delta M_{F_{H,hn}} = \tfrac{1}{2} h_n \left[\left(\sum_{i=n+1}^{10} h_i \right) \left(H_n + H_{n+1} \right) + h_n \left(\tfrac{2}{3} H_n + \tfrac{1}{3} H_{n+1} \right) \right]$$

$$F_{H,} = \sum_{n=1}^{11} \Delta F_{H,hn}$$

$$M^P_{F_H} = \sum_{n=1}^{11} \Delta M_{F_{H,hn}}$$

4.2.2 Vertical wave induced force and related moment

$$F_V = \tfrac{1}{2} V_1 \ v_1$$

$$M^P_{F_V} = \tfrac{1}{3} V_1 \ v_1^2$$

Test Programme 5

The test programme is shown in Table 5.1. The number of waves in each test was at least 1,500.

Test no. 2.2.6 was re-done for 2 hours (≈ 2.930 waves) to see the prolonged effect on armour stability. In the following the 2 hour-test is denoted (2.2.6).

	Prototype data				Model data			
Test no.	SWL [m]	T_p [s]	H_{m0}^{Gen} [m]	H_{m0}^{Break} [m]	SWL [m]	T_p [s]	H_{m0}^{Gen} [m]	H_{m0}^{Break} [m]
1.1.1	0.09	8	2.21	2.42	0.002	1.23	0.052	0.057
1.1.2	0.09	8	2.72	2.66	0.002	1.23	0.064	0.063
1.1.3	0.09	8	3.03	3.11	0.002	1.23	0.071	0.073
1.1.4	0.09	8	3.57	3.90	0.002	1.23	0.084	0.092
1.1.5	0.09	8	3.74	3.87	0.002	1.23	0.088	0.091
1.1.6	0.09	8	4.06	4.27	0.002	1.23	0.096	0.100
1.1.7	0.09	8	4.52	4.63	0.002	1.23	0.106	0.109
1.1.8	0.09	8	4.68	4.66	0.002	1.23	0.110	0.110
1.2.1	0.09	16	2.22	2.18	0.002	2.45	0.052	0.051
1.2.2	0.09	16	2.51	2.68	0.002	2.45	0.059	0.063
1.2.3	0.09	16	2.70	2.97	0.002	2.45	0.063	0.070
1.2.4	0.09	16	3.35	3.17	0.002	2.45	0.079	0.075
1.2.5	0.09	16	3.66	3.90	0.002	2.45	0.086	0.092
1.2.6	0.09	16	4.19	4.41	0.002	2.45	0.099	0.104
1.2.7	0.09	16	4.28	4.64	0.002	2.45	0.101	0.109
2.1.1	3.50	8	2.70	2.52	0.082	1.23	0.063	0.059
2.1.2	3.50	8	3.14	3.12	0.082	1.23	0.074	0.074
2.1.3	3.50	8	3.31	3.13	0.082	1.23	0.078	0.074
2.1.4	3.50	8	3.92	3.83	0.082	1.23	0.092	0.090
2.1.5	3.50	8	4.15	4.11	0.082	1.23	0.098	0.097
2.1.6	3.50	8	4.74	4.47	0.082	1.23	0.112	0.105
2.1.7	3.50	8	4.87	5.05	0.082	1.23	0.115	0.119
2.2.1	3.50	16	2.50	2.63	0.082	2.45	0.059	0.062
2.2.2	3.50	16	3.04	3.04	0.082	2.45	0.072	0.072
2.2.3	3.50	16	3.66	3.68	0.082	2.45	0.086	0.087
2.2.4	3.50	16	3.77	3.79	0.082	2.45	0.089	0.089
2.2.5	3.50	16	4.36	3.98	0.082	2.45	0.103	0.094
2.2.6	3.50	16	4.84	4.72	0.082	2.45	0.114	0.111
(2.2.6)	3.50	16	4.70	4.77	0.082	2.45	0.111	0.112

Table 5.1. Conditions used in each test as measured by the two arrays using BDM method. H_{m0} is the incident spectral wave height.

Caisson Stability Results 6

The results of the wave induced forces and caisson displacement are given in Table 6.1. The safety factor SF$_{slide}$ was calculated using a friction factor of $\mu = 0.6$.

Even for the overload conditions, high safety factors was observed for the very oblique SSW waves. It should though be taken into account that the uplift is not measured and is based on a triangular distribution. The tests though indicate that head-on waves (SE) results in loads that are slightly larger than the ones obtained for SSW waves (see Lykke Andersen et al. [2012]).

Stability of the caissons at the heads has not been investigated and these might have lower safety factors than for the trunk section.

Test no.	SWL [m]	T_p [s]	H_{m0}^{Gen} [m]	min g [kN/m]	$F_{H,max}$ [kN/m]	$F_{V,max}$ [kN/m]	M_{max}^{P} [kNm/m]	SF_{slide} [-]	SF_{tilt} [-]
1.1.1	0.09	8	2.21	2453	416	220	6799	6.89	8.10
1.1.2	0.09	8	2.72	2349	507	271	8119	5.64	6.78
1.1.3	0.09	8	3.03	2299	536	277	8723	5.29	6.31
1.1.4	0.09	8	3.57	2097	723	307	11737	3.91	4.69
1.1.5	0.09	8	3.74	2124	688	331	11150	4.13	4.94
1.1.6	0.09	8	4.06	2050	750	347	12073	3.74	4.56
1.1.7	0.09	8	4.52	1874	911	370	14870	3.06	3.70
1.1.8	0.09	8	4.68	1872	901	399	14617	3.08	3.77
1.2.1	0.09	16	2.22	2236	558	353	9555	5.01	5.76
1.2.2	0.09	16	2.51	2078	694	422	11605	4.01	4.74
1.2.3	0.09	16	2.70	2067	670	442	11766	4.09	4.68
1.2.4	0.09	16	3.35	1709	976	539	16613	2.76	3.31
1.2.5	0.09	16	3.66	1520	1132	592	19389	2.35	2.84
1.2.6	0.09	16	4.19	1319	1286	665	22010	2.03	2.50
1.2.7	0.09	16	4.28	1128	1440	840	24730	1.78	2.23
2.1.1	3.50	8	2.70	1874	529	343	9782	4.92	4.80
2.1.2	3.50	8	3.14	1908	516	342	9396	5.23	4.99
2.1.3	3.50	8	3.31	1811	604	335	10644	4.09	4.41
2.1.4	3.50	8	3.92	1675	711	402	12820	3.61	3.66
2.1.5	3.50	8	4.15	1744	676	342	11467	3.62	4.09
2.1.6	3.50	8	4.74	1496	832	438	14908	2.80	3.15
2.1.7	3.50	8	4.87	1510	863	429	15502	2.76	3.03
2.2.1	3.50	16	2.50	1586	738	397	13040	3.15	3.60
2.2.2	3.50	16	3.04	1417	892	434	15342	2.60	3.06
2.2.3	3.50	16	3.66	1077	1160	538	20257	1.93	2.32
2.2.4	3.50	16	3.77	1332	952	468	16574	2.40	2.83
2.2.5	3.50	16	4.36	969	1237	587	21708	1.78	2.16
2.2.6	3.50	16	4.84	818	1380	611	24028	1.60	1.95
(2.2.6)	3.50	16	4.70	882	1322	602	23057	1.67	2.04

Table 6.1. Extreme forces and moments calculated from the pressure readings along with safety factors against sliding and overturning.

Crownwall Stability Results 7

The results of the wave induced forces and crownwall displacement are given in Table 7.1. The safety factor SF$_{slide}$ was calculated using a friction factor of $\mu = 0.6$.

Passive and active soil pressures from the armour in front and pavement behind the crown wall has not been included in the load calculation and in the safety factors.

Test no.	SWL [m]	T_p [s]	H_{m0}^{Break} [m]	Prototype data min g [kN/m]	$F_{H,max}$ [kN/m]	$F_{V,max}$ [kN/m]	M_{max}^P [kNm/m]	SF_{slide} [-]	SF_{tilt} [-]
1.1.1	0.09	8	2.42	224	4	3	16	65.24	46.75
1.1.2	0.09	8	2.66	224	4	3	16	65.98	47.53
1.1.3	0.09	8	3.11	224	3	4	17	65.94	44.90
1.1.4	0.09	8	3.90	224	4	3	16	69.54	47.53
1.1.5	0.09	8	3.87	224	4	3	17	74.78	44.37
1.1.6	0.09	8	4.27	224	4	4	16	67.49	47.19
1.1.7	0.09	8	4.63	224	4	3	16	76.35	49.04
1.1.8	0.09	8	4.66	224	4	4	16	66.65	46.89
1.2.1	0.09	16	2.18	223	4	3	18	52.30	41.85
1.2.2	0.09	16	2.68	223	4	3	20	53.53	38.59
1.2.3	0.09	16	2.97	224	4	3	16	79.97	46.32
1.2.4	0.09	16	3.17	224	4	4	16	72.14	47.28
1.2.5	0.09	16	3.90	224	4	4	17	69.01	44.13
1.2.6	0.09	16	4.41	224	4	4	22	65.05	35.32
1.2.7	0.09	16	4.64	214	10	9	35	23.13	21.59
2.1.1	3.50	8	2.52	210	12	22	46	26.03	16.75
2.1.2	3.50	8	3.12	206	14	24	51	17.72	15.06
2.1.3	3.50	8	3.13	206	13	28	52	25.36	14.66
2.1.4	3.50	8	3.83	206	13	32	53	18.68	14.41
2.1.5	3.50	8	4.11	209	11	30	53	25.57	14.40
2.1.6	3.50	8	4.47	202	15	38	76	15.46	10.05
2.1.7	3.50	8	5.05	200	15	43	86	64.07	8.90
2.2.1	3.50	16	2.63	202	6	37	75	32.97	10.10
2.2.2	3.50	16	3.04	186	14	48	110	14.14	6.95
2.2.3	3.50	16	3.68	162	28	68	163	6.91	4.67
2.2.4	3.50	16	3.79	161	28	70	164	6.77	4.64
2.2.5	3.50	16	3.98	131	47	89	243	3.78	3.14
2.2.6	3.50	16	4.72	-21	169	137	674	0.88	1.13
(2.2.6)	3.50	16	4.77	25	127	136	528	1.20	1.44

Table 7.1. Extreme forces and moments calculated from the pressure readings along with safety factors against sliding and overturning (note soil pressures not included).

Armour Layer and Toe Stability Results 8

8.1 Cube armour layer

Photos of the armour layer taken before and after each test, are shown in appendix B.

Cube armour unit displacements are given in Table 8.1 and cumulative damage is plotted in Figure 8.2. The rubble-mound was divided into three sections, as shown on Figure 8.1. The sections were divided this way because some movement was observed due to turbulence behind the corner of the caisson (section 1) and because a increase in wave energy was also observed along the rubble-mound from section 2 towards section 3, thereby expecting more damage to the armour layer in section 3 than section 2. Section 1, 2 and 3 contains 160, 1600 and 1050 units respectively.

In all sections the cumulative damage has not resulted in visible filter layer.

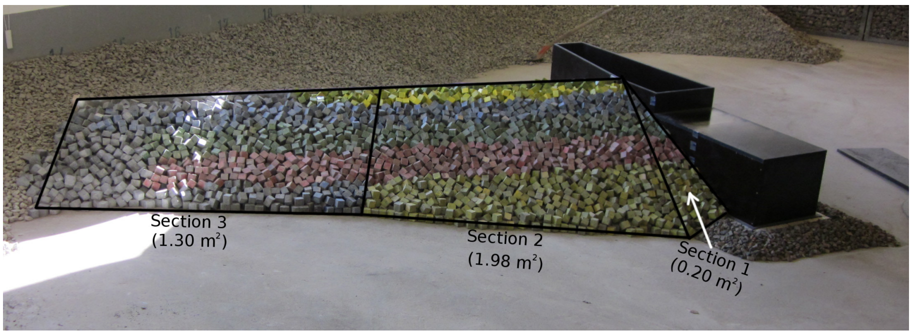

Figure 8.1. Sections used for rubble-mound armour cube stability.

Test no.	SWL	T_p	H_{m0}^{Gen*}	H_{m0}^{Break*}	Displaced units Section 1	Displaced units Section 2	Displaced units Section 3	Cumulative damage Section 1	Cumulative damage Section 2	Cumulative damage Section 3
1.1.1	0.09	8	1.92	2.10	0	0	0	0 (0.00%)	0 (0.00%)	0 (0.00%)
1.1.2	0.09	8	2.37	2.31	0	0	0	0 (0.00%)	0 (0.00%)	0 (0.00%)
1.1.3	0.09	8	2.63	2.70	0	2	2	0 (0.00%)	2 (0.12%)	2 (0.19%)
1.1.4	0.09	8	3.10	3.39	0	0	0	0 (0.00%)	2 (0.12%)	2 (0.19%)
1.1.5	0.09	8	3.25	3.37	0	0	0	0 (0.00%)	2 (0.12%)	2 (0.19%)
1.1.6	0.09	8	3.53	3.71	0	0	4	0 (0.00%)	2 (0.12%)	6 (0.57%)
1.1.7	0.09	8	3.93	4.03	0	0	1	0 (0.00%)	2 (0.12%)	7 (0.67%)
1.1.8	0.09	8	4.07	4.05	1	1	1	1 (0.63%)	3 (0.19%)	8 (0.76%)
1.2.1	0.09	16	1.93	1.90	0	0	2	0 (0.00%)	0 (0.00%)	2 (0.19%)
1.2.2	0.09	16	2.18	2.33	0	0	2	0 (0.00%)	0 (0.00%)	4 (0.38%)
1.2.3	0.09	16	2.35	2.58	1	0	3	1 (0.63%)	0 (0.00%)	7 (0.67%)
1.2.4	0.09	16	2.91	2.76	0	1	0	1 (0.63%)	1 (0.06%)	7 (0.67%)
1.2.5	0.09	16	3.18	3.39	0	0	0	1 (0.63%)	1 (0.06%)	7 (0.67%)
1.2.6	0.09	16	3.64	3.83	3	1	4	4 (2.53%)	2 (0.12%)	11 (1.05%)
1.2.7	0.09	16	3.72	4.03	5	8	3	9 (5.68%)	10 (0.62%)	14 (1.33%)
2.1.1	3.5	8	2.35	2.19	0	0	0	0 (0.00%)	0 (0.00%)	0 (0.00%)
2.1.2	3.5	8	2.73	2.71	0	0	0	0 (0.00%)	0 (0.00%)	0 (0.00%)
2.1.3	3.5	8	2.88	2.72	0	0	0	0 (0.00%)	0 (0.00%)	0 (0.00%)
2.1.4	3.5	8	3.41	3.33	0	0	0	0 (0.00%)	0 (0.00%)	0 (0.00%)
2.1.5	3.5	8	3.61	3.57	0	0	0	0 (0.00%)	0 (0.00%)	0 (0.00%)
2.1.6	3.5	8	4.12	3.89	0	0	0	0 (0.00%)	0 (0.00%)	0 (0.00%)
2.1.7	3.5	8	4.23	4.39	0	1	3	0 (0.00%)	1 (0.06%)	3 (0.29%)
2.2.1	3.5	16	2.17	2.29	0	0	0	0 (0.00%)	0 (0.00%)	0 (0.00%)
2.2.2	3.5	16	2.64	2.64	0	0	0	0 (0.00%)	0 (0.00%)	0 (0.00%)
2.2.3	3.5	16	3.18	3.20	0	0	0	0 (0.00%)	0 (0.00%)	0 (0.00%)
2.2.4	3.5	16	3.28	3.30	0	0	0	0 (0.00%)	0 (0.00%)	0 (0.00%)
2.2.5	3.5	16	3.79	3.46	1	0	1	1 (0.63%)	0 (0.00%)	1 (0.1%)
2.2.6	3.5	16	4.21	4.10	0	2	3	1 (0.63%)	2 (0.12%)	4 (0.38%)
(2.2.6)	3.5	16	4.09	4.15	1	0	4	2 (6.95%)	2 (0.12%)	8 (4.19%)

Table 8.1. Number of displaced units in each test and cumulative damage of cube armour layer (given in percentage of total number of cubes in section).

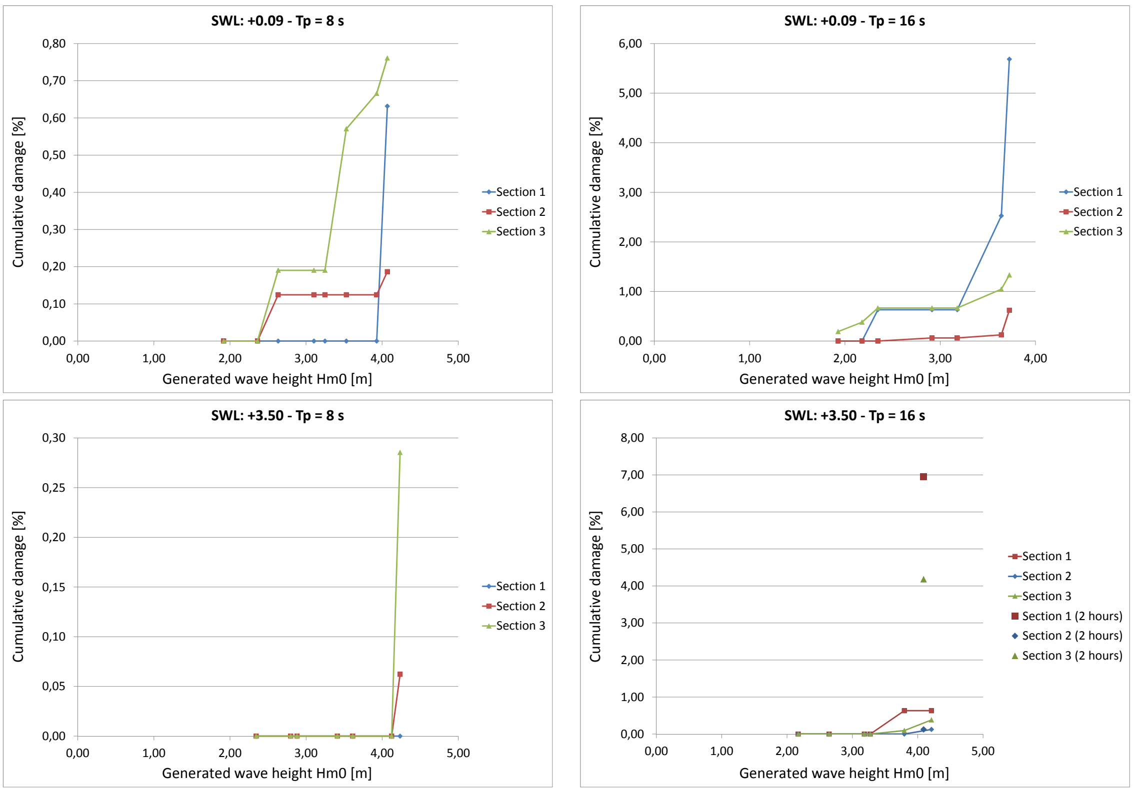

Figure 8.2. Cumulative damage of cube armour layer.

8.2 Caisson toe

Movement of foot protection blocks was observed near front corner of caisson at a wave height of $H_{m0}^{Break*} = 2.33$ m, with SWL +0.09 and $T_p = 16$ s. See Figure 8.3 for example (note $H_{m0}^{Break*} = 4.03$ m).

Filter material was exposed beneath the blocks, but no further exposure of the filter material was observed.

Similar movement for caisson foundation at the head compared to the front corner, see Figure 8.4, with a wave height of $H_{m0}^{Break*} = 3.83$ m, SWL +0.09 and $T_p = 16$ s. Significant movement of foot protection blocks at $H_{m0}^{Break*} = 4.03$ m.

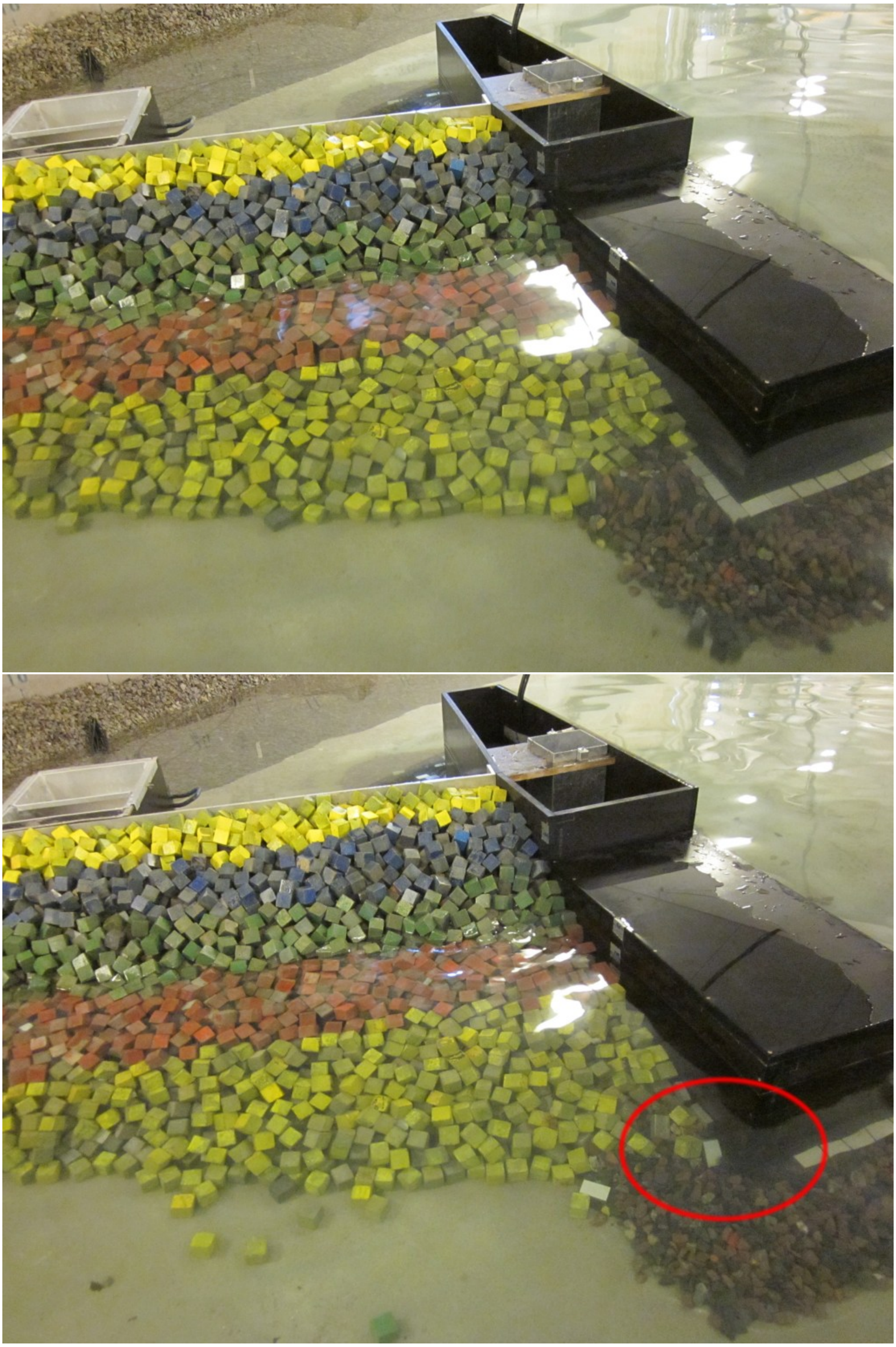

Figure 8.3. Front corner, before and after test no. 1.2.7 - SWL: +0.09, T_p: 16 s, $H_{m0}^{Break} = 4.64$ m, $H_{m0}^{Break*} = 4.03$ m

Figure 8.4. Caisson head, before and after test no. 1.2.7 - SWL: +0.09, T_p: 16 s, H_{m0}^{Break} = 4.64 m, H_{m0}^{Break*} = 4.03 m

Overtopping Results 9

The measured overtopping discharges are given in Table 9.1. For test no. 2.2.1 and down, a second overtopping chamber was added to the caisson (chamber 2). This was done because run-up on the caisson from the oblique waves were observed, thereby producing more overtopping further along the caisson. This is verified by the average discharges being slightly larger for almost all tests.

For some tests the second overtopping chamber were filled (test no. 2.1.6, 2.1.7, 2.2.6 and (2.2.6)), which means that the measured overtopping might be larger. For some tests, the overtopping chamber 2 was filled over a short amount of time.

					Rubble-mound				Caisson	
						Distribution in % of q_{avg} behind front			Chamber 1	Chamber 2
Test no.	SWL [m]	T_p [s]	H_{m0}^{Gen} [m]	H_{m0}^{Break} [m]	q_{avg} [l/s m]	0-3.4m [%]	3.4-10.2m [%]	10.2-22.5m [%]	$q_{avg,1}$ [l/s m]	$q_{avg,2}$ [l/s m]
1.1.1	0.09	8	2.21	2.42	0.00	0	0	0	0.00	-
1.1.2	0.09	8	2.72	2.66	0.00	0	0	0	0.00	-
1.1.3	0.09	8	3.03	3.11	0.00	0	0	0	0.00	-
1.1.4	0.09	8	3.57	3.90	0.00	0	0	0	0.00	-
1.1.5	0.09	8	3.74	3.87	0.00	0	0	0	0.02	-
1.1.6	0.09	8	4.06	4.27	0.00	0	0	0	0.03	-
1.1.7	0.09	8	4.52	4.63	0.00	0	0	0	0.04	-
1.1.8	0.09	8	4.68	4.66	0.00	0	0	0	0.02	-
1.2.1	0.09	16	2.22	2.18	0.00	0	0	0	0.00	-
1.2.2	0.09	16	2.51	2.68	0.00	0	0	0	0.00	-
1.2.3	0.09	16	2.70	2.97	0.00	0	0	0	0.00	-
1.2.4	0.09	16	3.35	3.17	0.00	0	0	0	0.00	-
1.2.5	0.09	16	3.66	3.90	0.00	0	0	0	0.00	-
1.2.6	0.09	16	4.19	4.41	0.00	0	0	0	0.02	-
1.2.7	0.09	16	4.28	4.64	0.00	26	74	0	0.18	-
2.1.1	3.50	8	2.70	2.52	0.01	0	0	0	0.00	0.00
2.1.2	3.50	8	3.14	3.12	0.00	0	0	0	0.00	0.00
2.1.3	3.50	8	3.31	3.13	0.00	0	0	0	0.01	0.05
2.1.4	3.50	8	3.92	3.83	0.00	0	0	0	0.32	1.22
2.1.5	3.50	8	4.15	4.11	0.00	0	0	0	0.50	0.27
2.1.6	3.50	8	4.74	4.47	0.00	0	100	0	2.24	>2.95
2.1.7	3.50	8	4.87	5.05	0.02	83	17	0	3.35	>2.95
2.2.1	3.50	16	2.50	2.63	0.00	0	0	0	0.00	0.00
2.2.2	3.50	16	3.04	3.04	0.00	0	0	0	0.00	0.00
2.2.3	3.50	16	3.66	3.68	0.00	0	0	0	0.21	0.31
2.2.4	3.50	16	3.77	3.79	0.00	0	0	0	0.00	0.01
2.2.5	3.50	16	4.36	3.98	0.01	73	25	2	0.40	0.88
2.2.6	3.50	16	4.84	4.72	0.21	93	7	1	1.21	>2.61
(2.2.6)	3.50	16	4.70	4.77	0.02	74	23	3	1.31	>2.61

Table 9.1. Measured overtopping at the rubble mound and at the caisson.

The measured average discharges are in Figure 9.1 to 9.7 compared with estimates from

CLASH Neural Network.

Comparison with Neural Network for the caisson

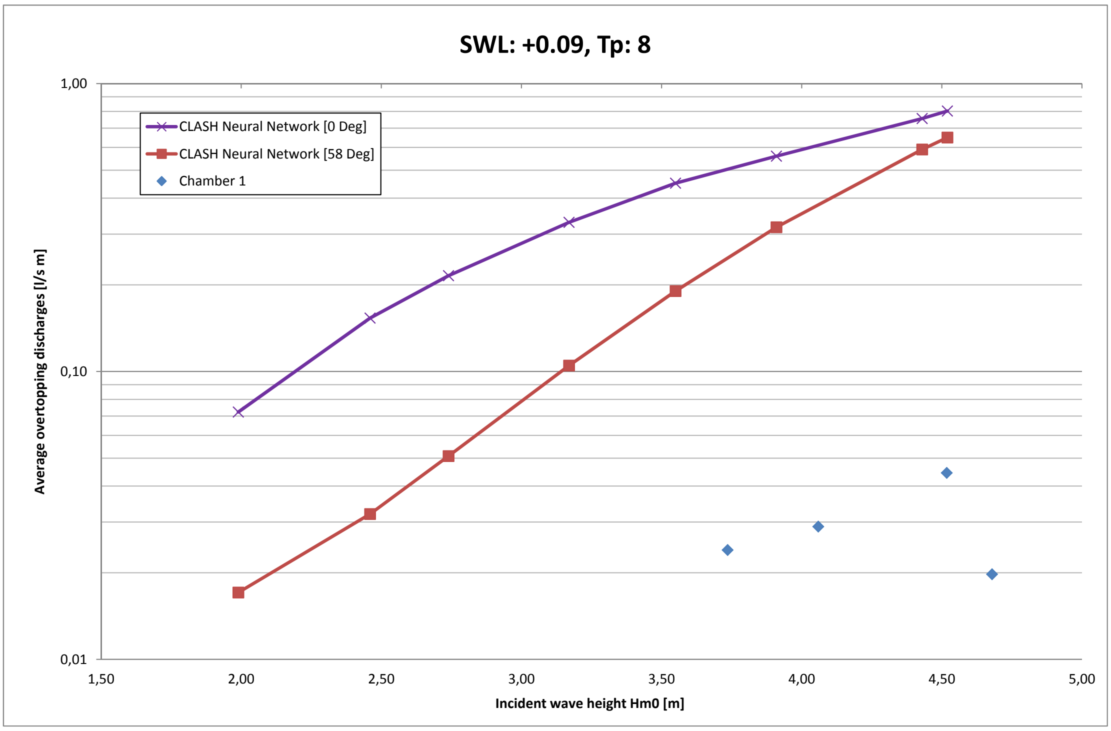

Figure 9.1. Average measured overtopping discharge for the caisson, and estimates from CLASH Neural Network.

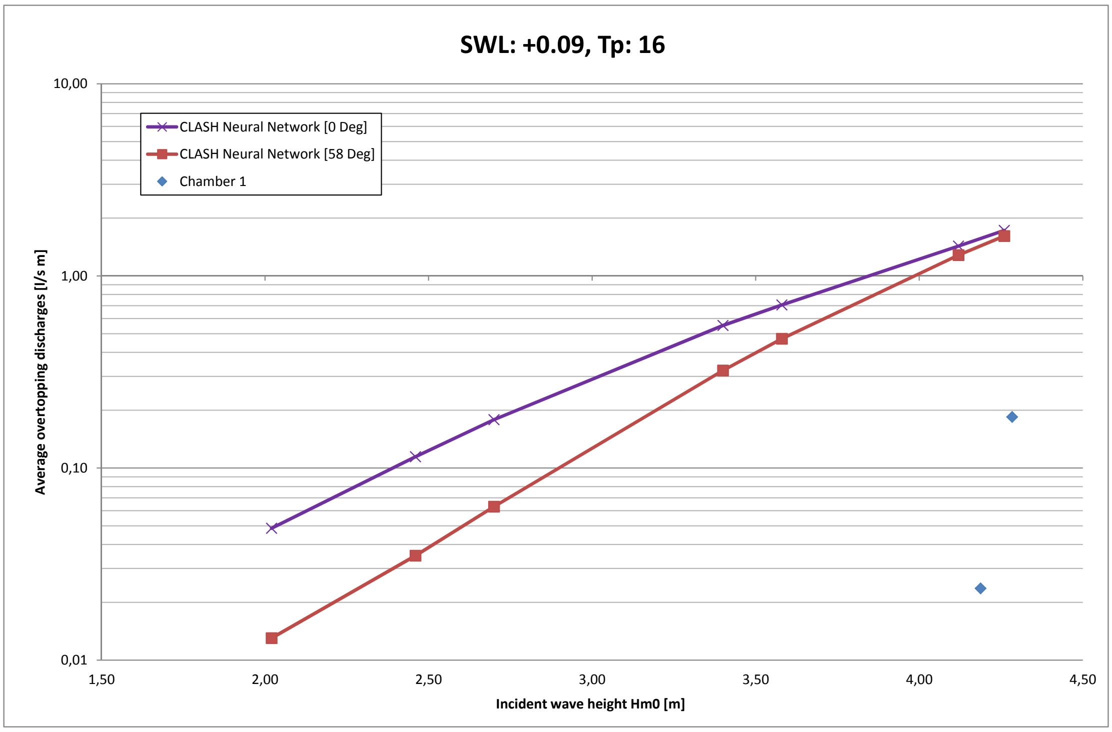

Figure 9.2. Average measured overtopping discharge for the caisson, and estimates from CLASH Neural Network.

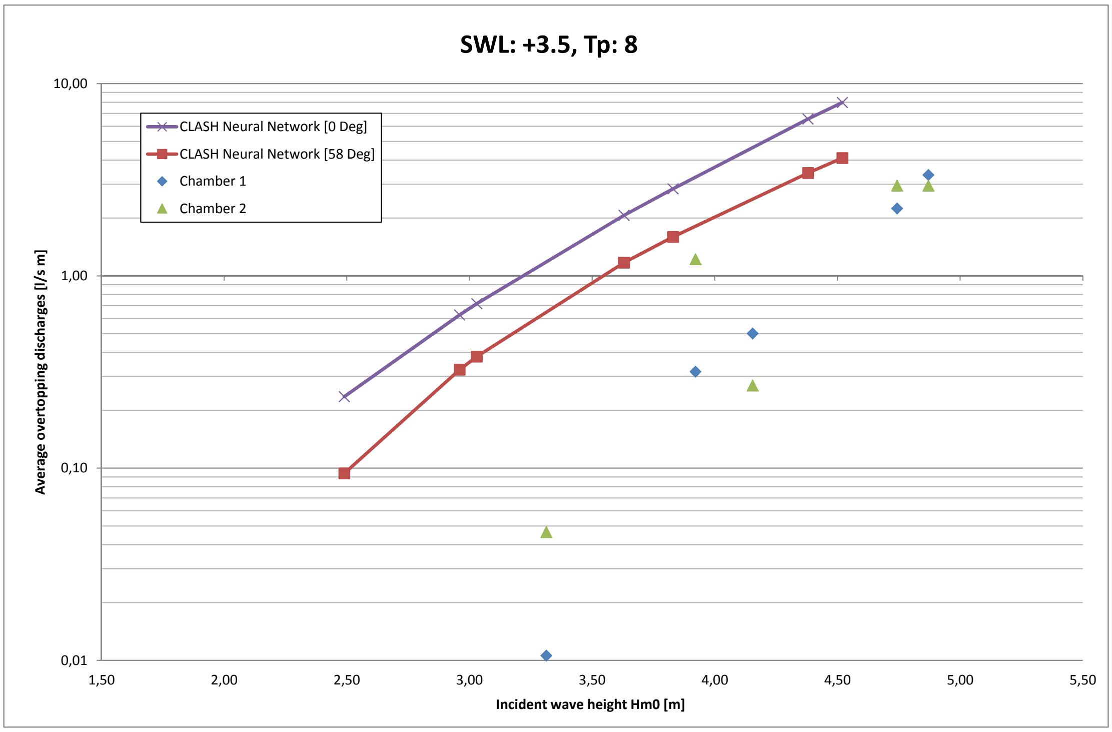

Figure 9.3. Average measured overtopping discharge for the caisson, and estimates from CLASH Neural Network.

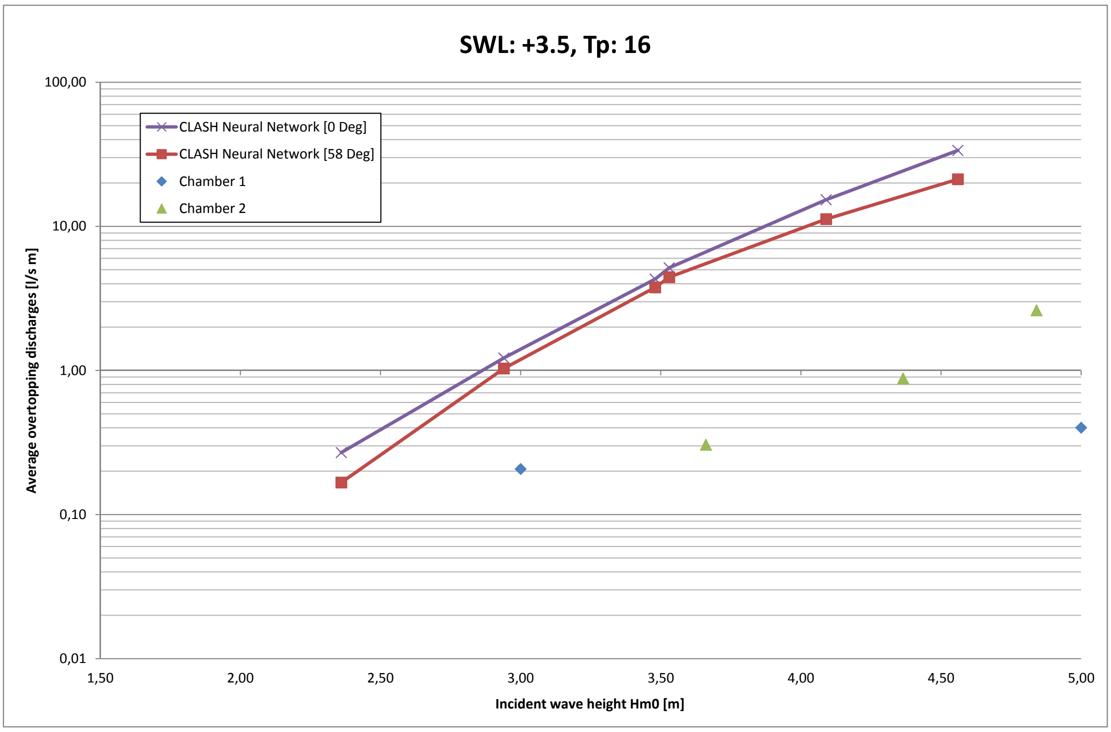

Figure 9.4. Average measured overtopping discharge for the caisson, and estimates from CLASH Neural Network.

Comparrison with Neural Network for the crownwall

Tests with SWL at +0.09 m and waves with a period of 8 seconds did not experience overtopping, and CLASH Neural Network did not estimate any overtopping.

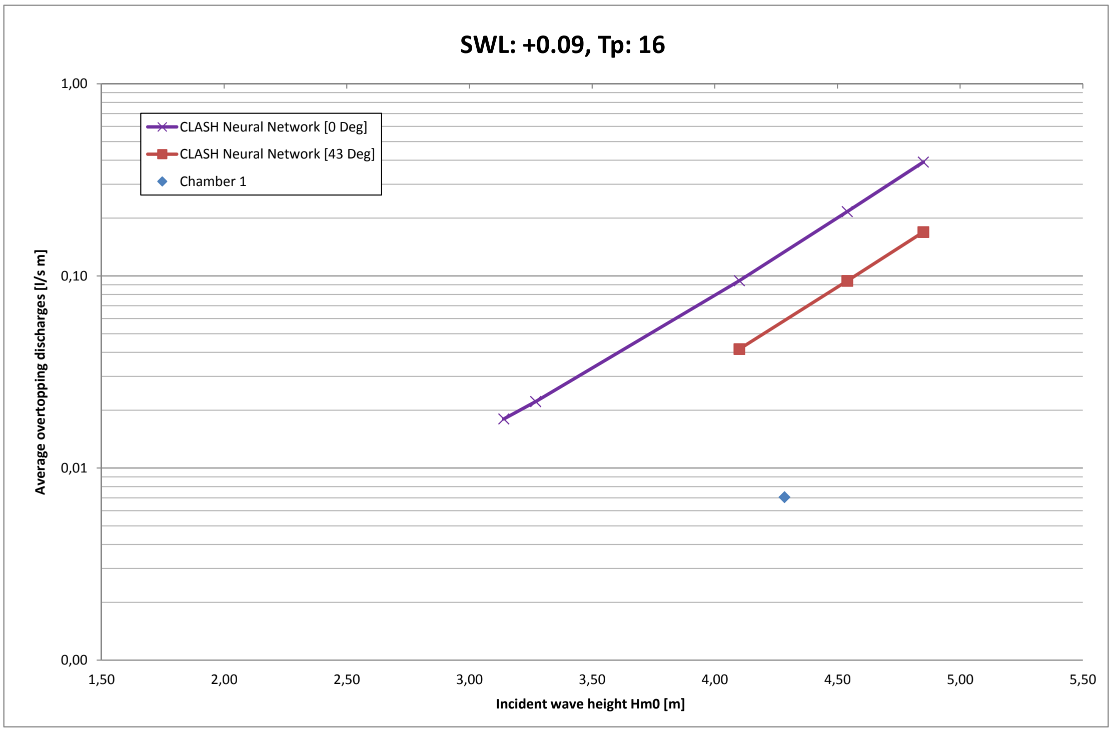

Figure 9.5. Average measured overtopping discharge on the rubble mound, and estimates from CLASH Neural Network.

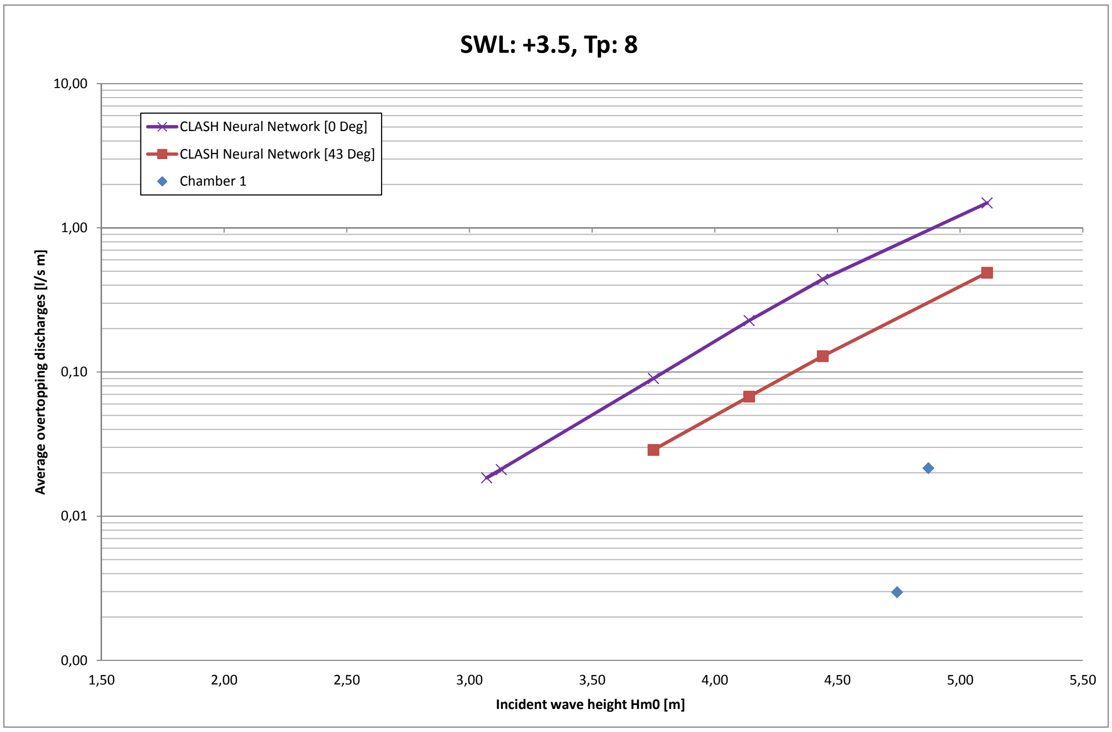

Figure 9.6. Average measured overtopping discharge on the rubble mound, and estimates from CLASH Neural Network.

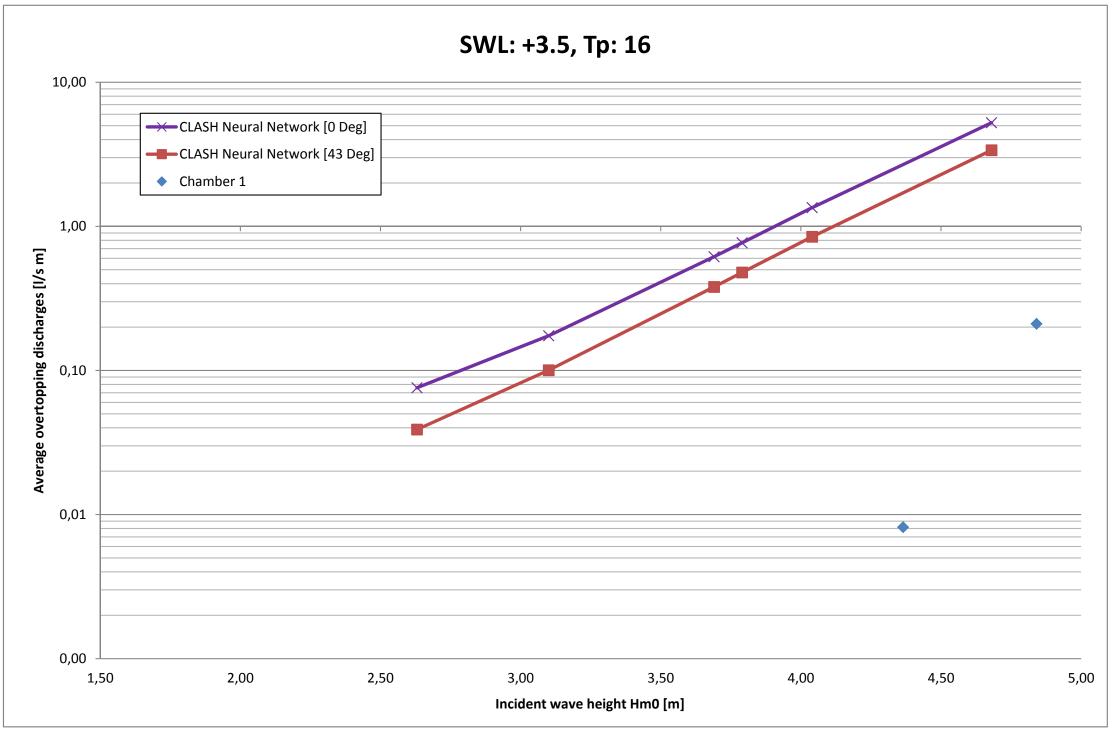

Figure 9.7. Average measured overtopping discharge on the rubble mound, and estimates from CLASH Neural Network.

Conclusions 10

10.1 Stability of armour material

The foundation at the front corner of the caisson turning towards the rubble mound breakwater seems to be unstable for the tests run with a wave period of 16 s period at low water level, as the foot protection block were unstable at $H_{m0}^{Gen*} = 2.18$ m. Regarding the rest of the armour material, the displacements were insignificant for wave heights below $H_{m0}^{Gen*} = 3.73$ m.

10.2 Overtopping discharge

The measured overtopping rates at the rubble mound are very small and significantly smaller than for the caisson. No overtopping occurred for wave heights $H_{m0}^{Gen} \leq 3.74$ m for low water level and $H_{m0}^{Gen} \leq 3.14$ m for high water level. The highest average overtopping discharge measured were $q_{avg} = 3.35$ l/s m for test no. 2.1.7 (SWL: +3.50, $T_p = 8$ s, $H_{m0}^{Gen} = 4.87$ m).

10.3 Stability of caisson and crown wall

Regarding the pressure readings, the caisson and crown wall is stable in the tested conditions, except for test no. 2.2.6 (SWL: +3.50, $T_p = 16$ s, $H_{m0}^{Break} = 4.72$ m), which showed expected sliding of the crown wall. It should be noted that the same test running for 2 hours, test no. (2.2.6), showed no sliding instabilities. In these analyses the soil pressured (active and passive) have been neglected which might change the stability conclusion for the crown wall.

Bibliography

Hashimoto, 1987. *Noriaki Hashimoto*, 1987. Analysis of the directional wave spectrum from field data. Advances in Coastal and Ocean Engineering.

Lykke Andersen, Stagsted, and Garborg, 2012. *Thomas Lykke Andersen, Esben Rubeck Stagsted, and Karsten Garborg*, 2012. Two-dimensional Model Test Study of the New Caisson Breakwater at Playa Blanca, Lanzarote. Aalborg University, DCE Contract Report no. 127.

Characteristic Pressure Readings A

In the following pages, certain characteristic pressure readings are shown. The pressure distribution at the maximum horizontal force, maximum uplift force, maximum overturning moment and minimum value of sliding failure function. Furthermore the maximum reading in each pressure gauge is shown.

A.1 Caisson loads

Test no. 1.1.1, SWL: +0.09, T_p: 8 s, $H_{m0}^{Gen} = 2.21$ m

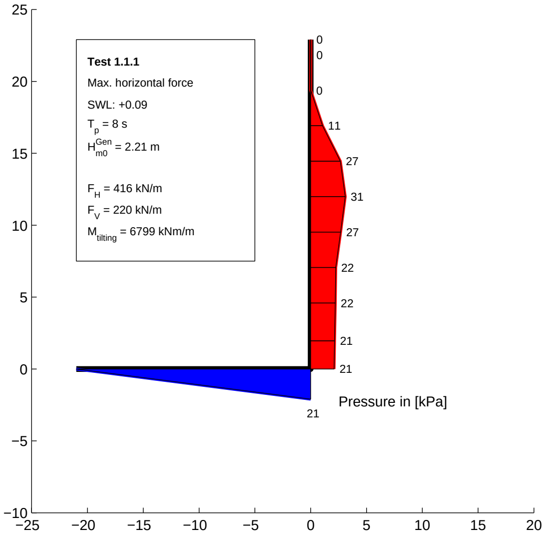

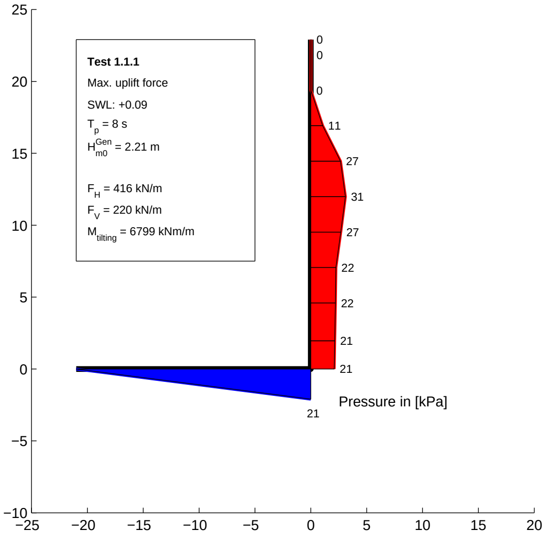

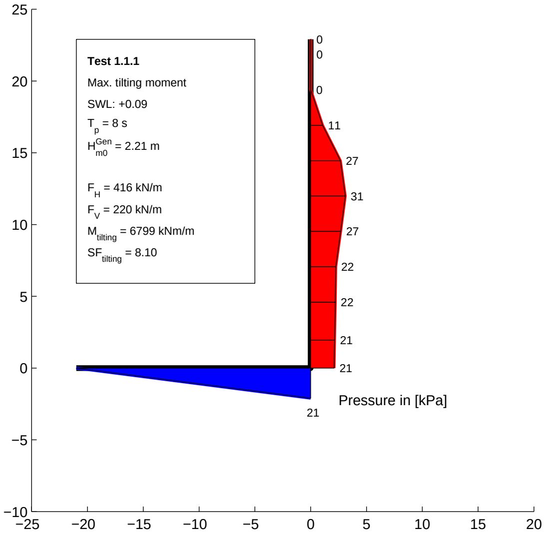

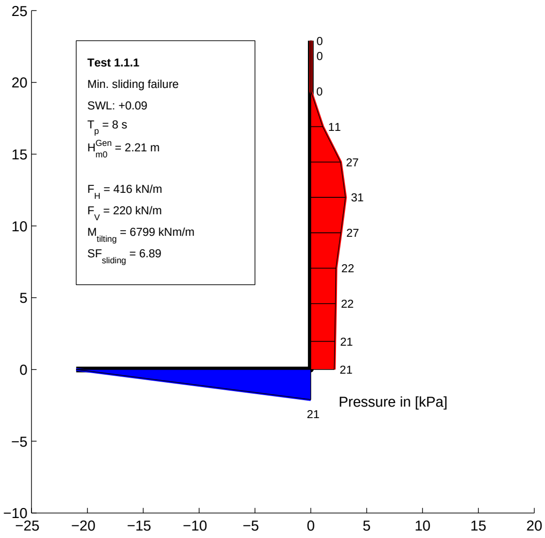

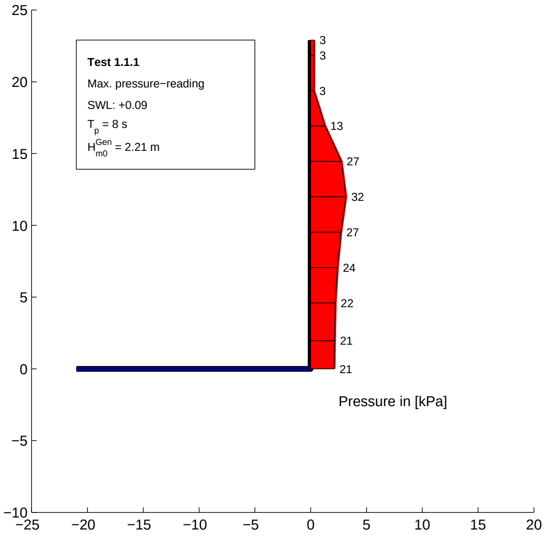

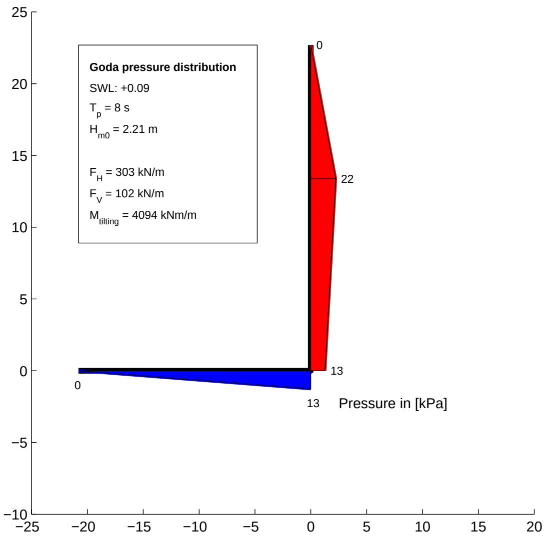

Test no. 1.1.2, SWL: +0.09, T_p: 8 s, $H_{m0}^{Gen} = 2.72$ m

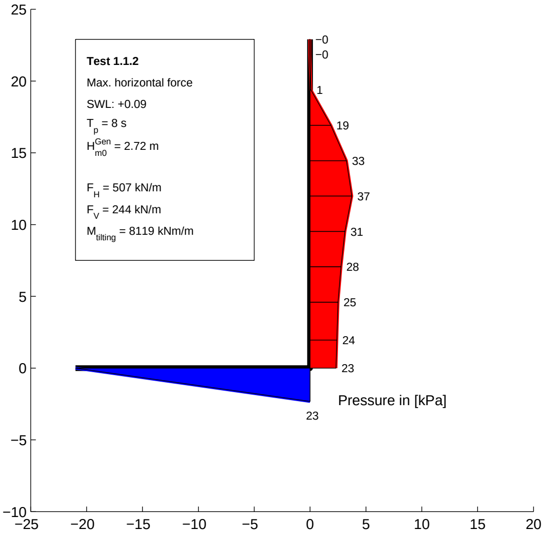

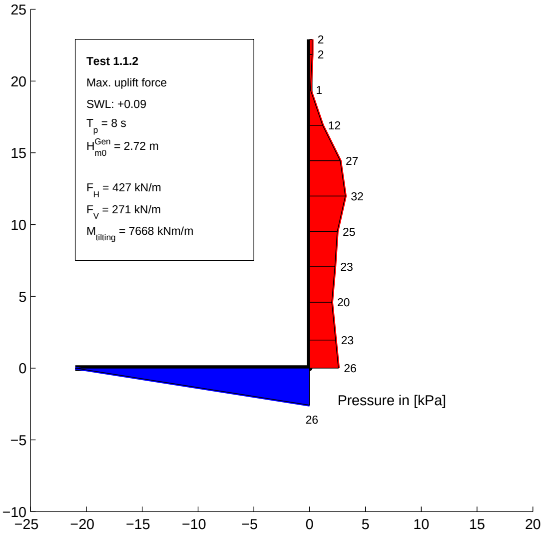

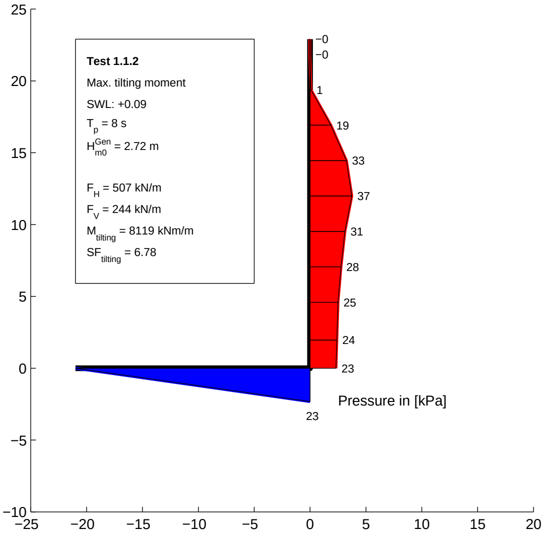

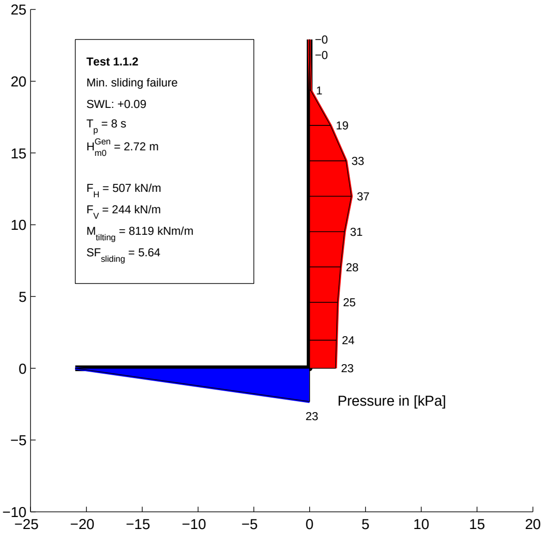

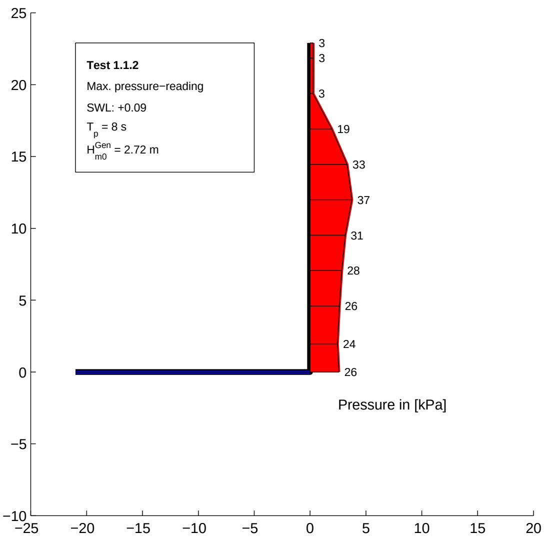

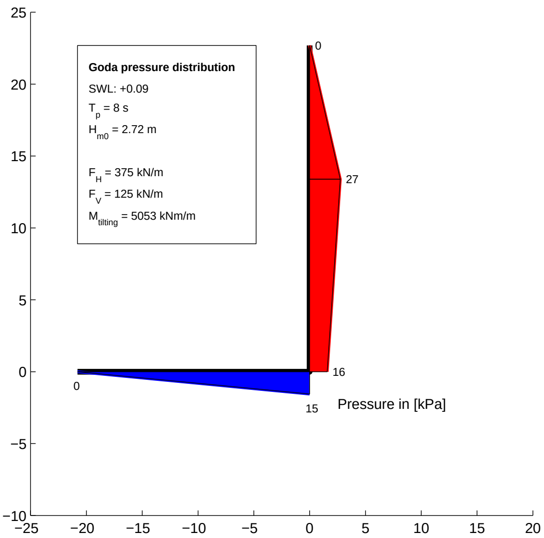

Test no. 1.1.3, SWL: +0.09, T_p: 8 s, $H_{m0}^{Gen} = 3.03$ m

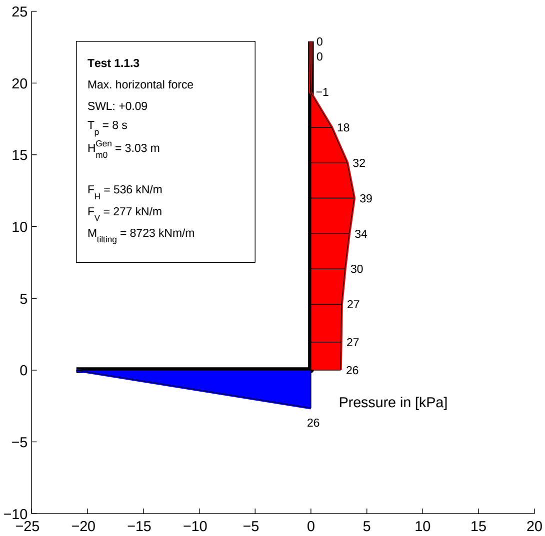

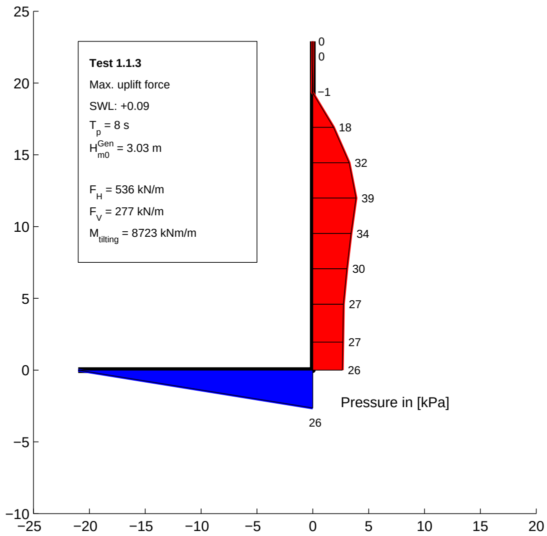

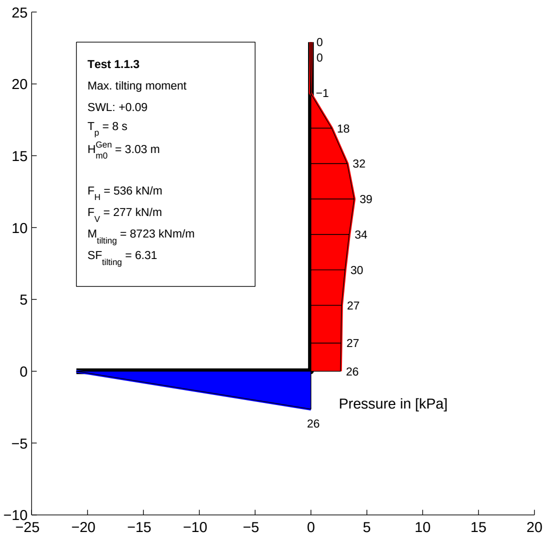

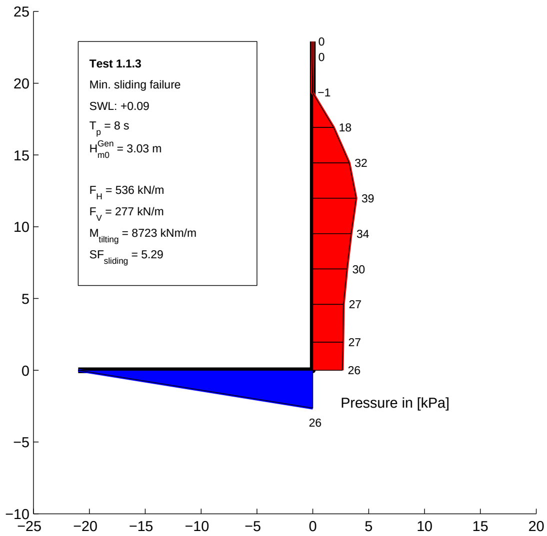

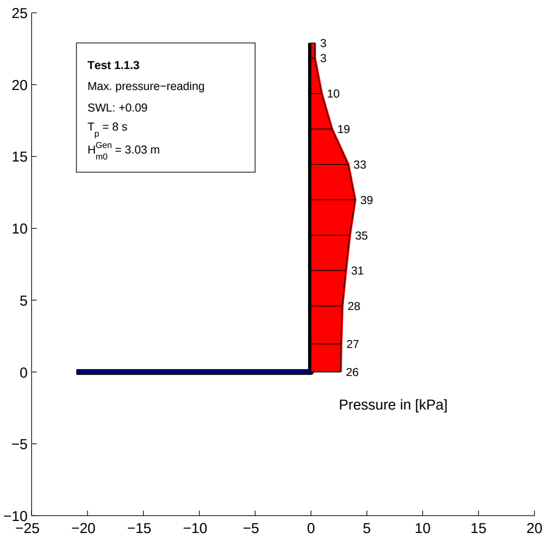

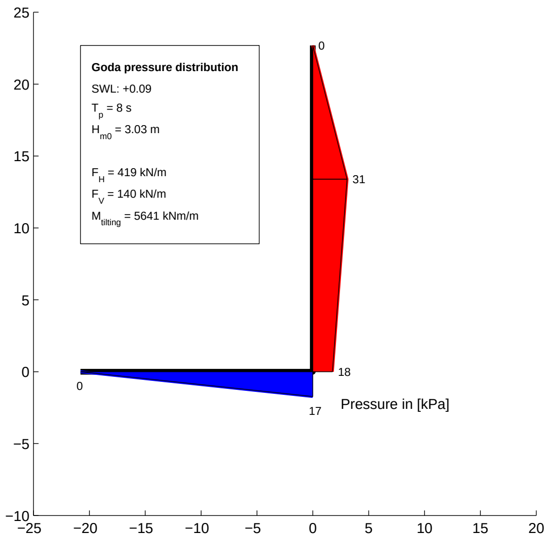

Test no. 1.1.4, SWL: +0.09, T_p: 8 s, $H_{m0}^{Gen} = 3.57$ m

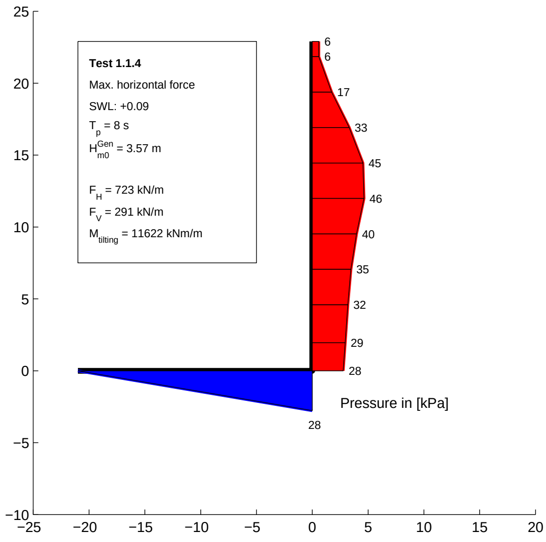

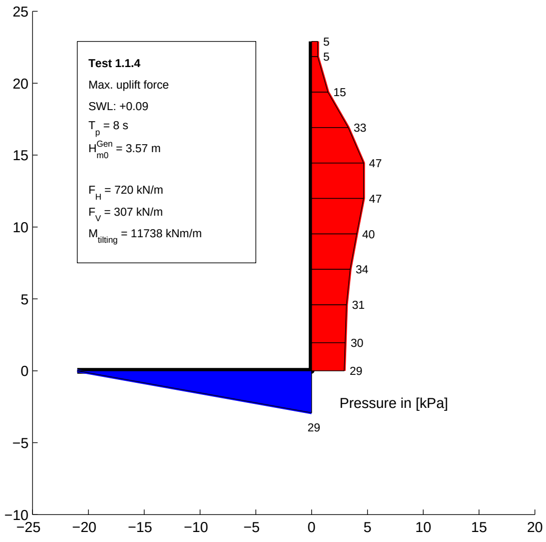

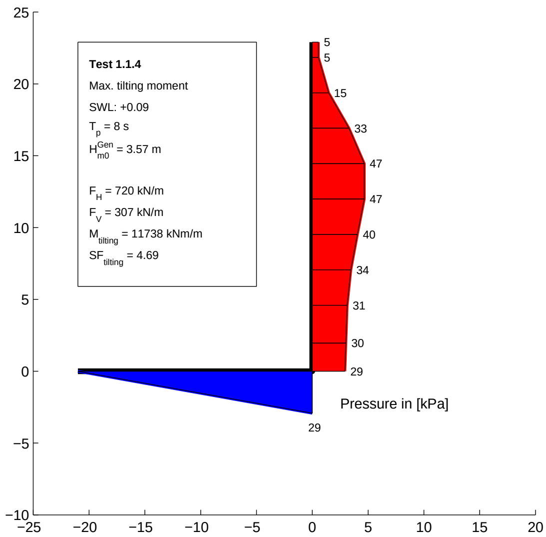

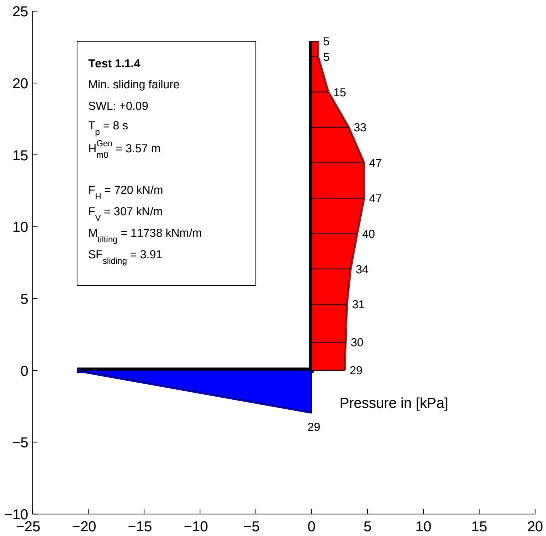

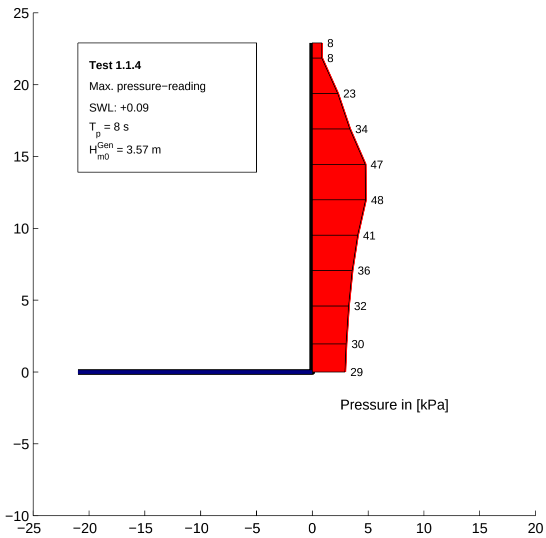

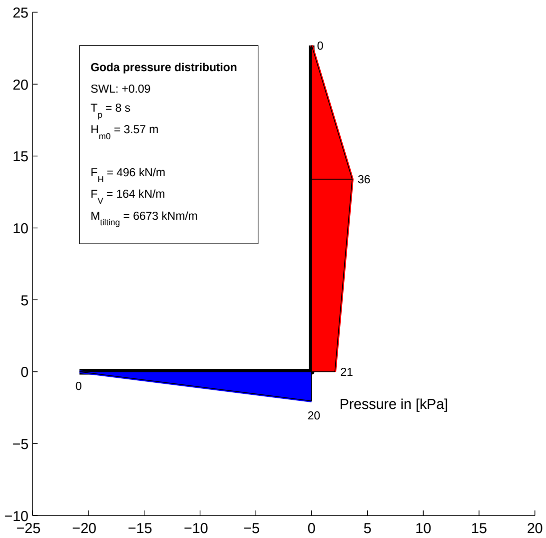

Test no. 1.1.5, SWL: +0.09, T_p: 8 s, $H_{m0}^{Gen} = 3.74$ m

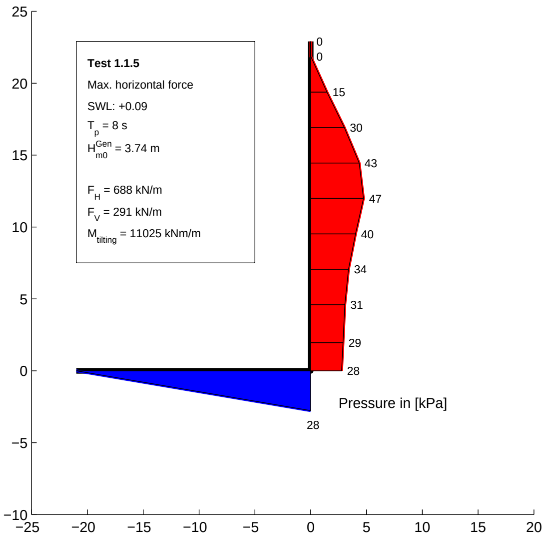

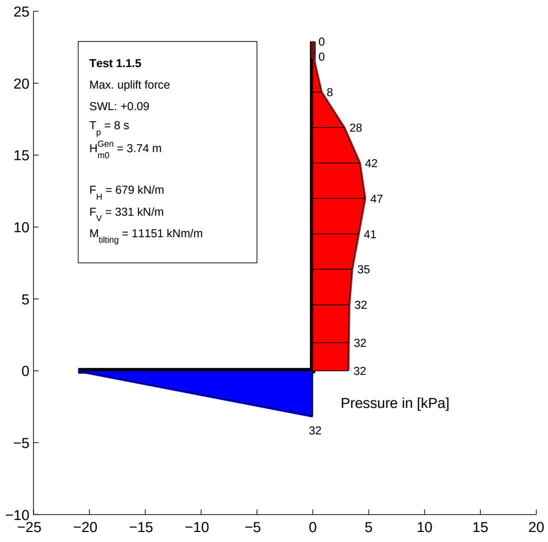

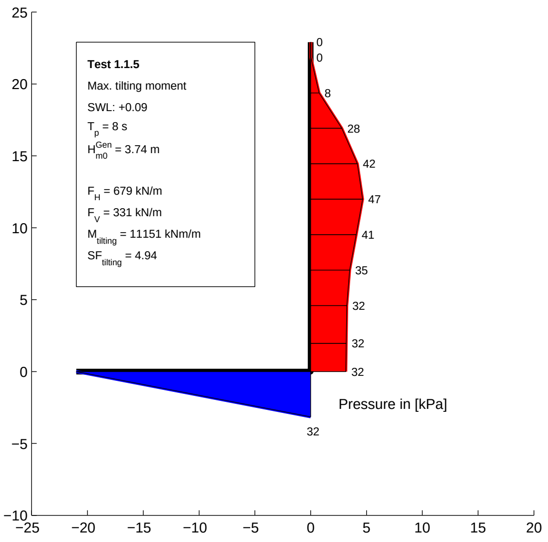

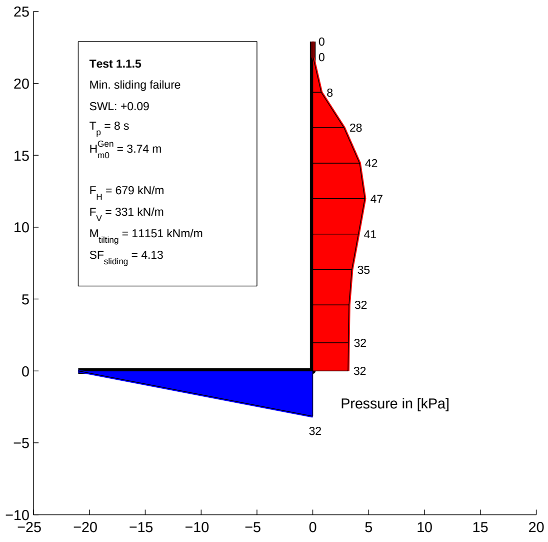

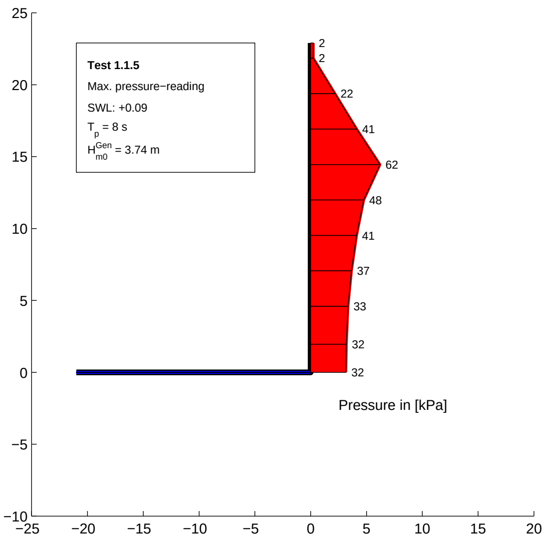

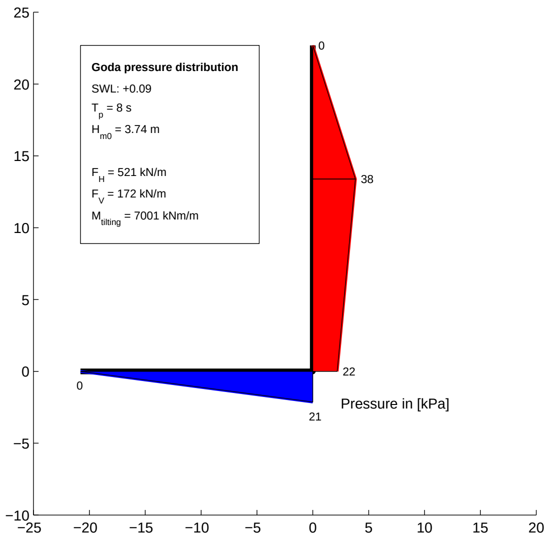

Test no. 1.1.6, SWL: +0.09, T_p: 8 s, $H_{m0}^{Gen} = 4.06$ m

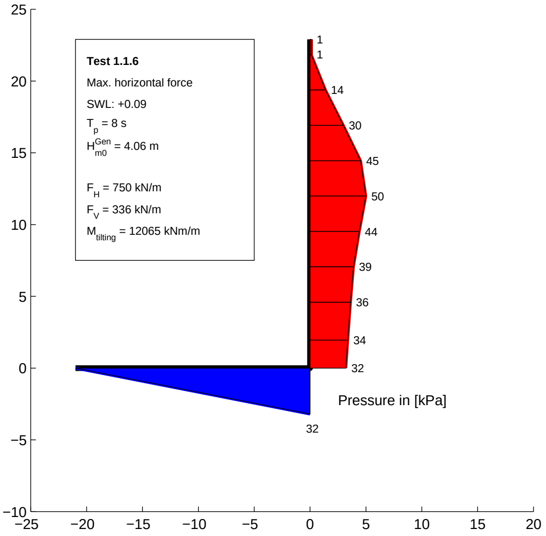

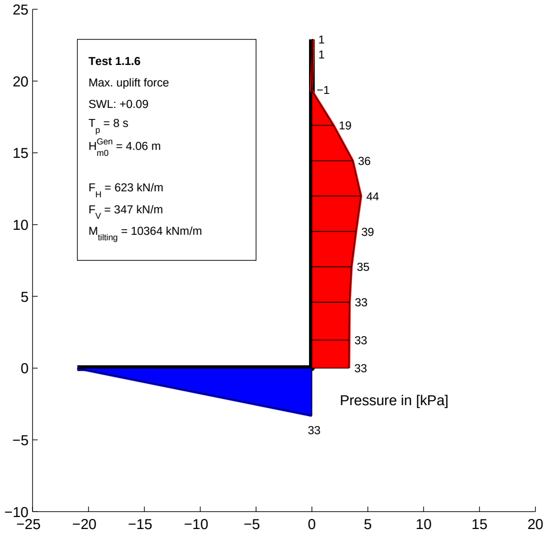

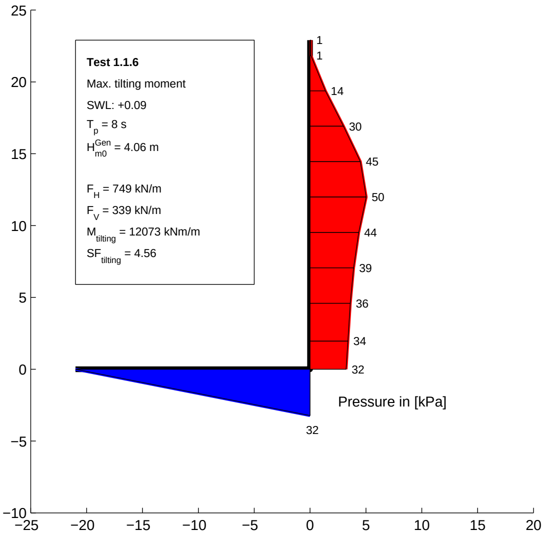

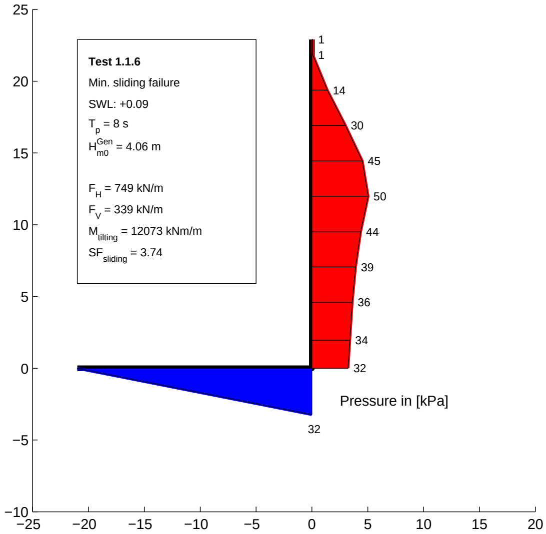

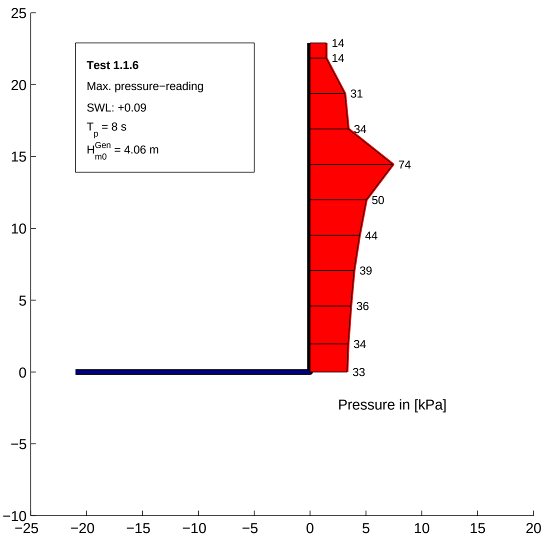

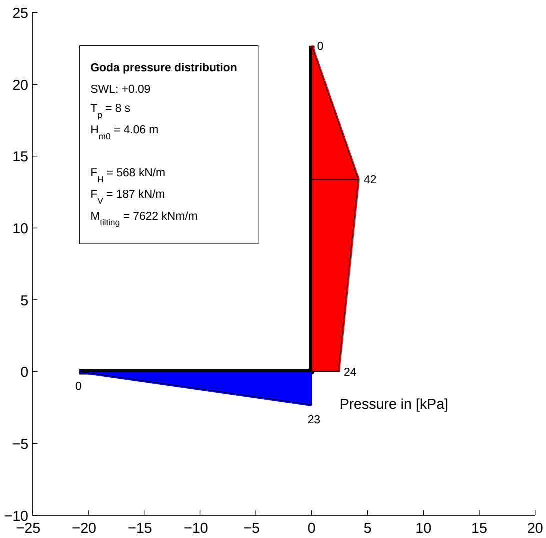

Test no. 1.1.7, SWL: +0.09, T_p: 8 s, $H_{m0}^{Gen} = 4.52$ m

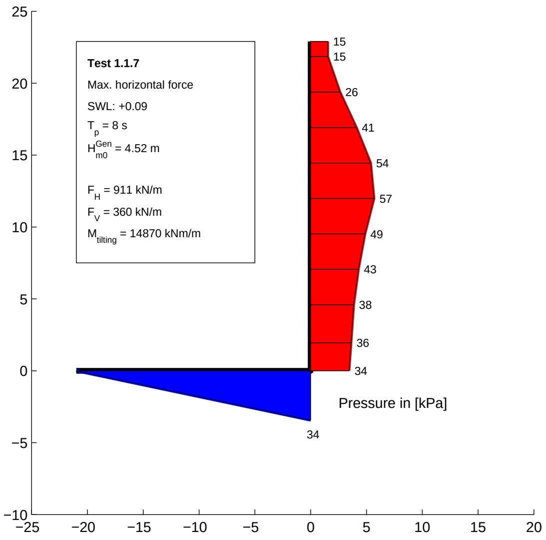

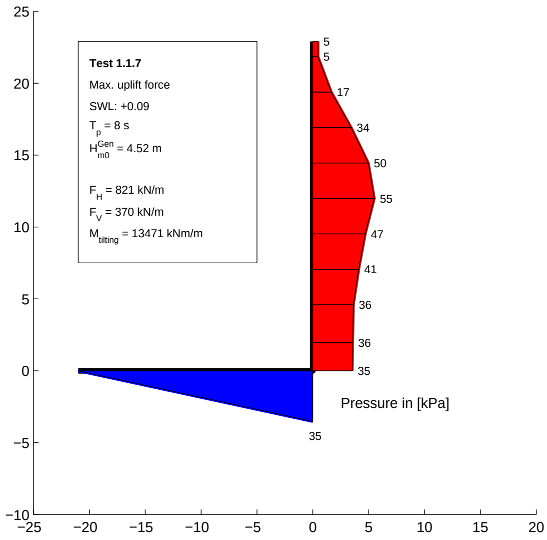

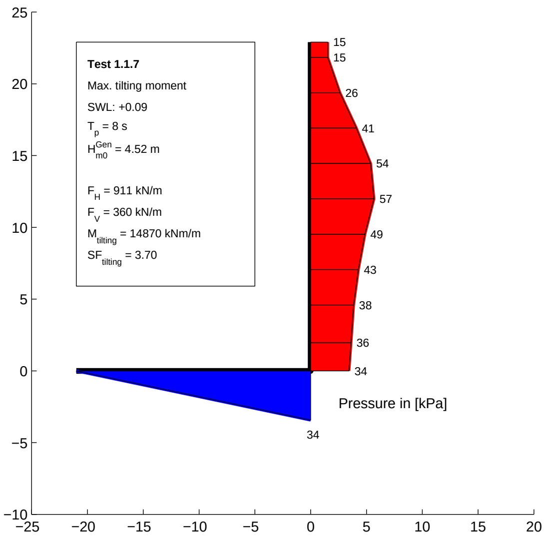

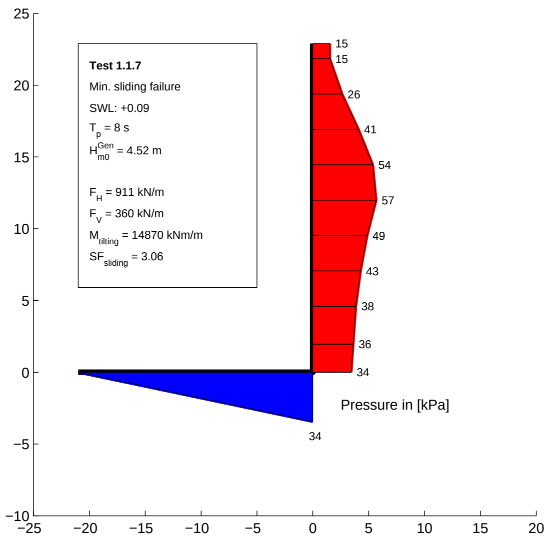

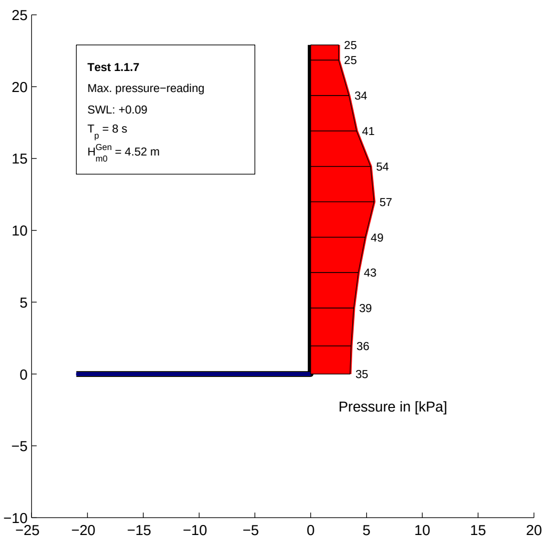

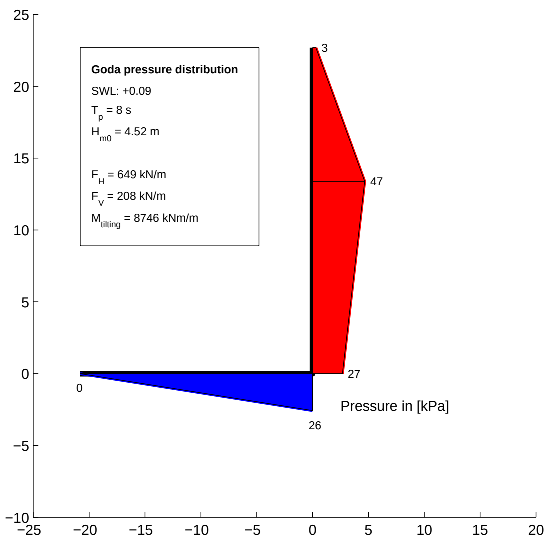

Test no. 1.1.8, SWL: +0.09, T_p: 8 s, $H_{m0}^{Gen} = 4.68$ m

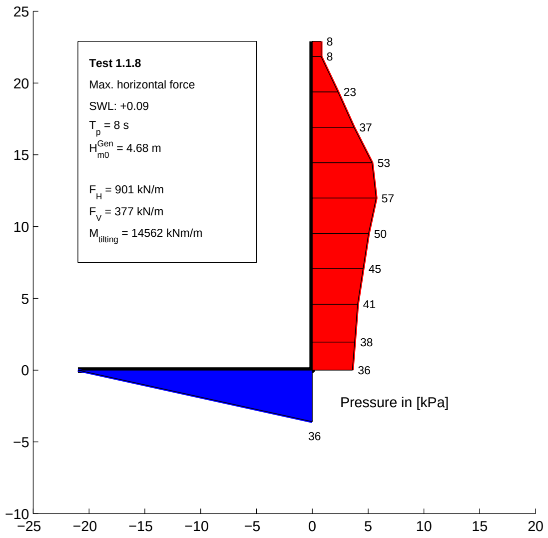

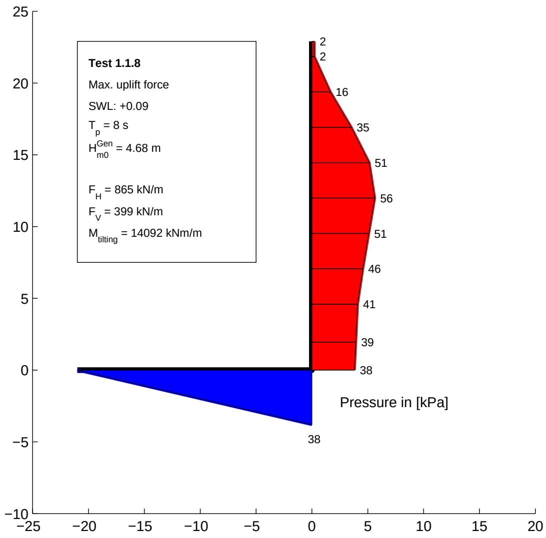

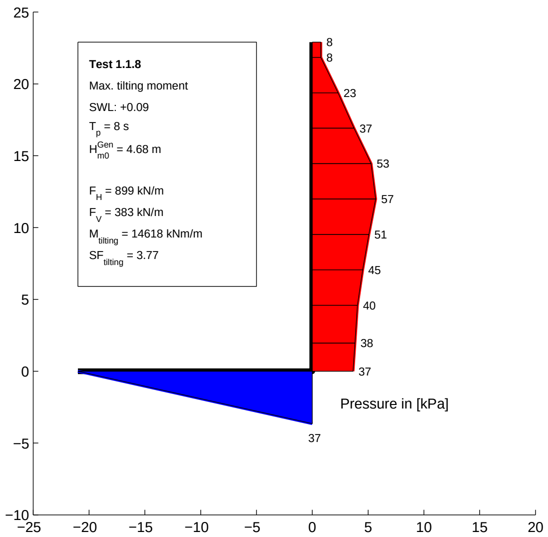

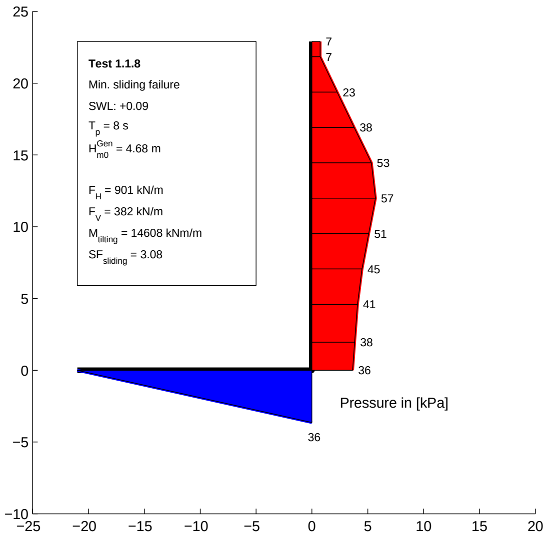

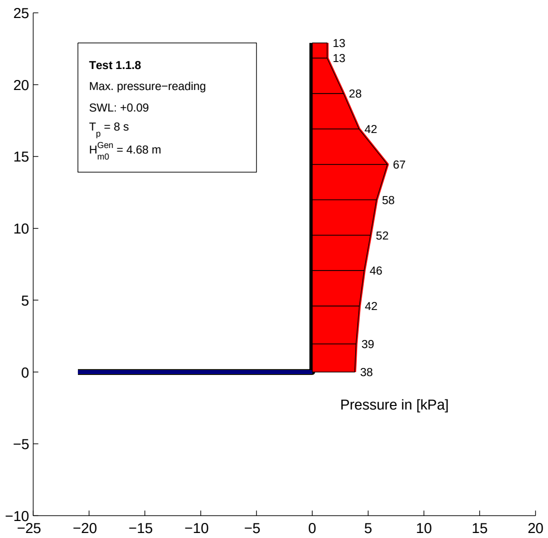

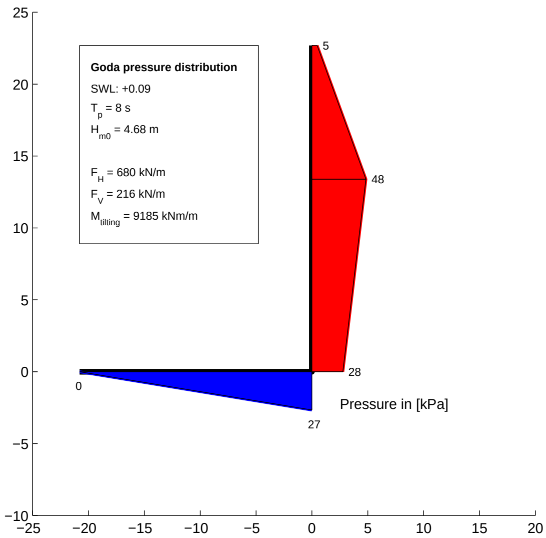

Test no. 1.2.1, SWL: +0.09, T_p: 16 s, $H_{m0}^{Gen} = 2.22$ m

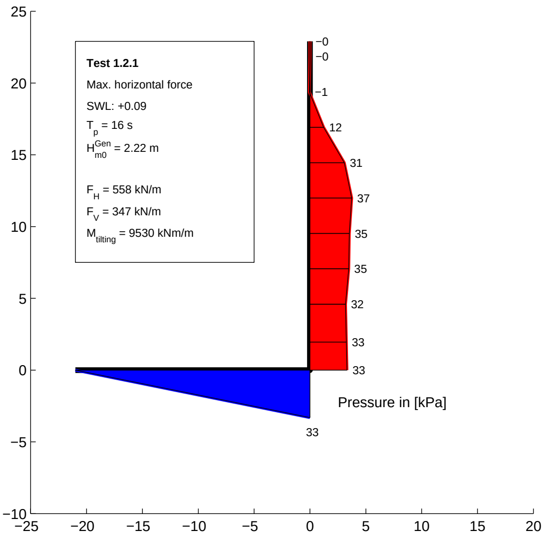

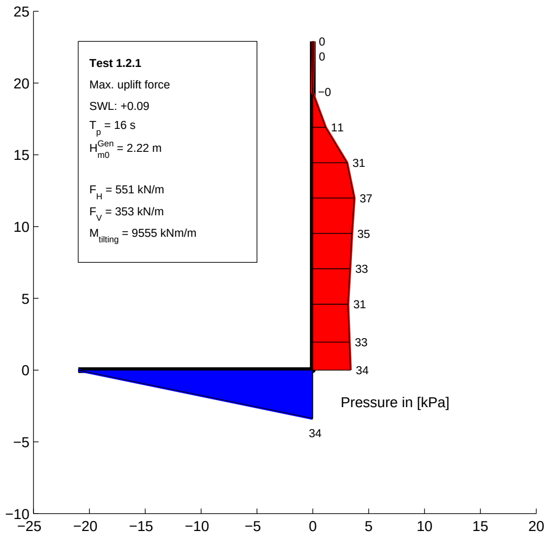

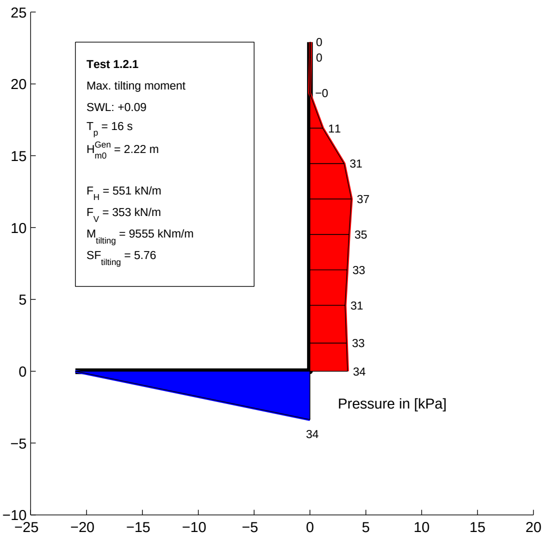

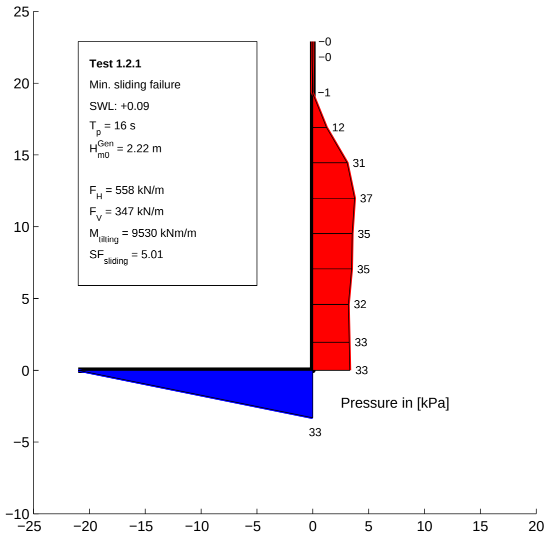

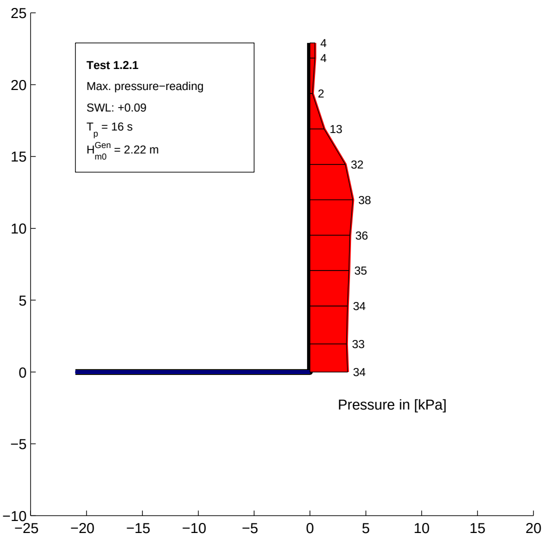

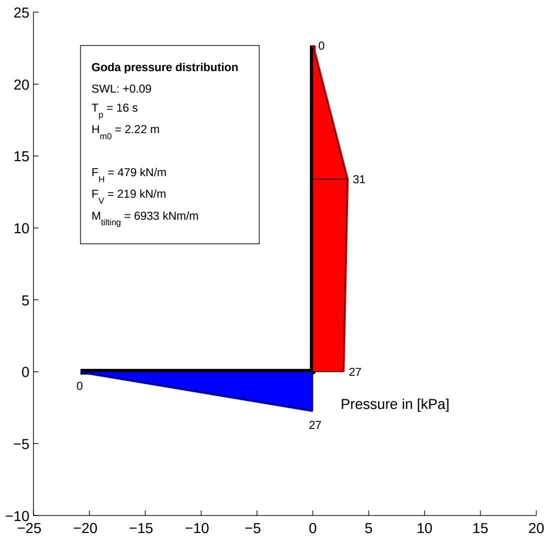

Test no. 1.2.2, SWL: +0.09, T_p: 16 s, $H_{m0}^{Gen} = 2.51$ m

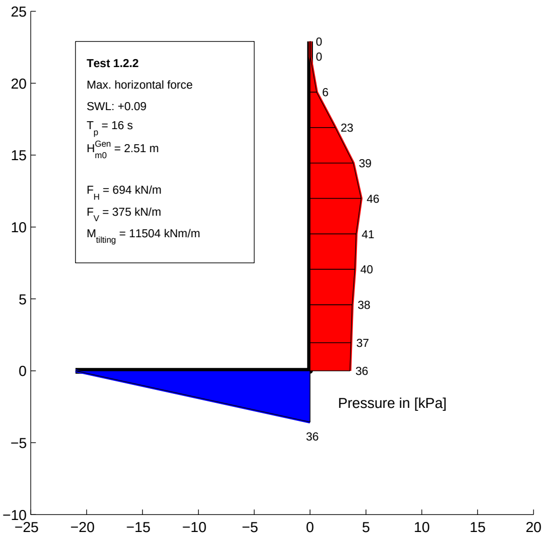

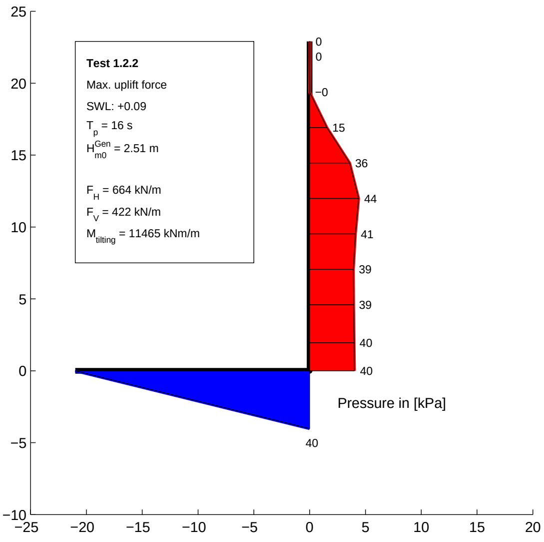

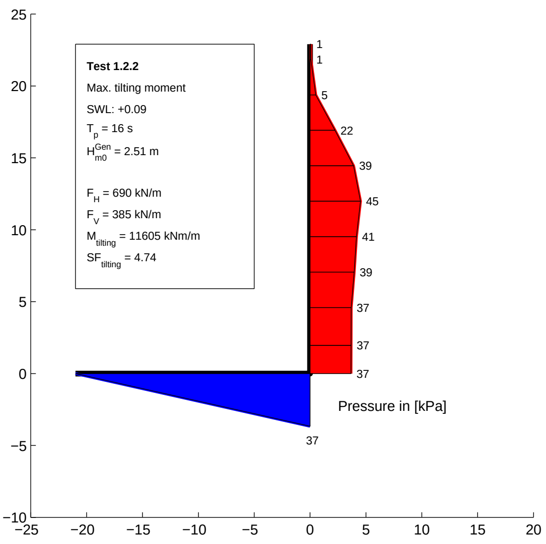

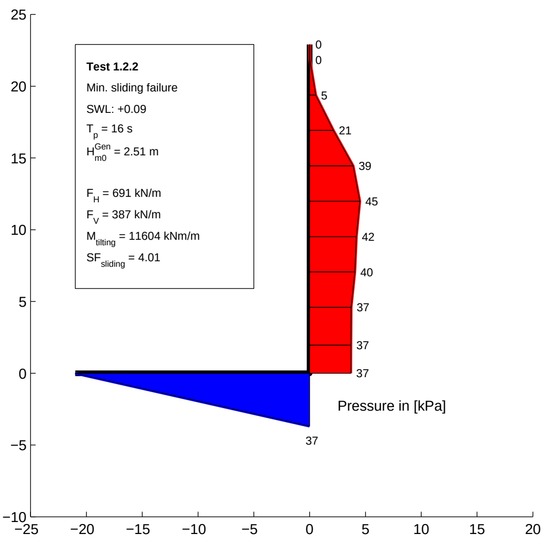

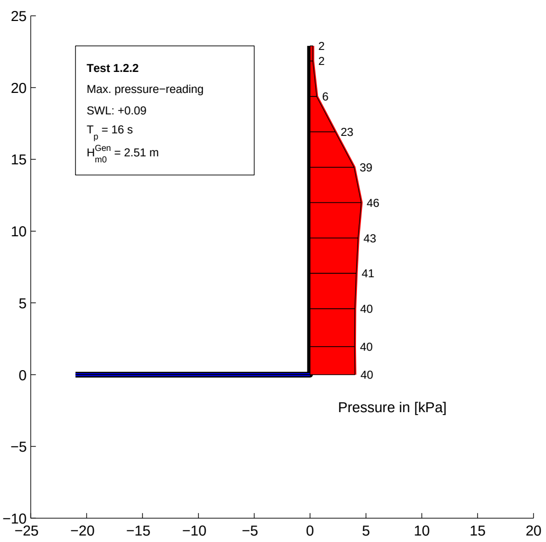

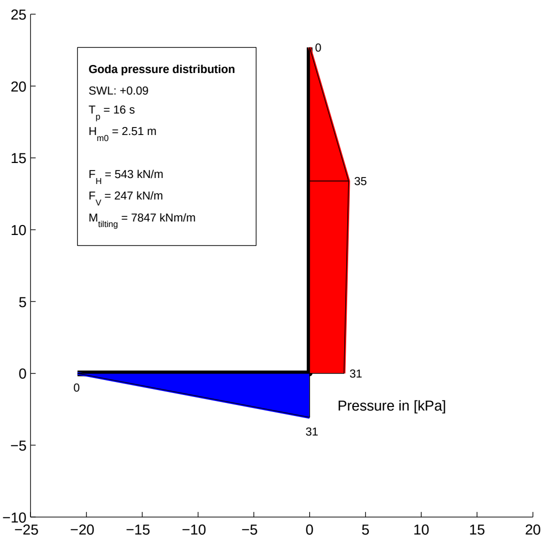

Test no. 1.2.3, SWL: +0.09, T_p: 16 s, $H_{m0}^{Gen} = 2.70$ m

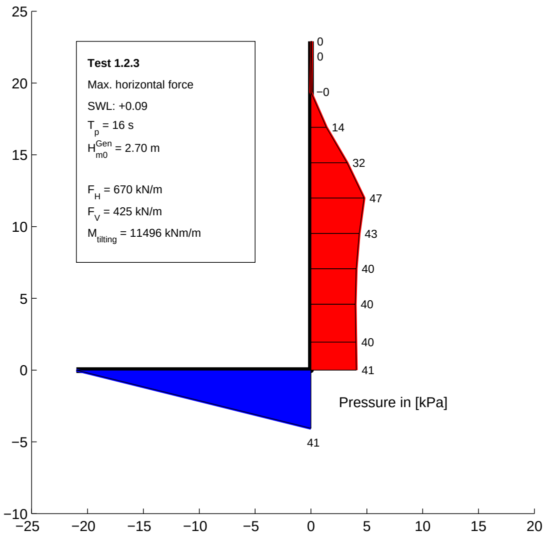

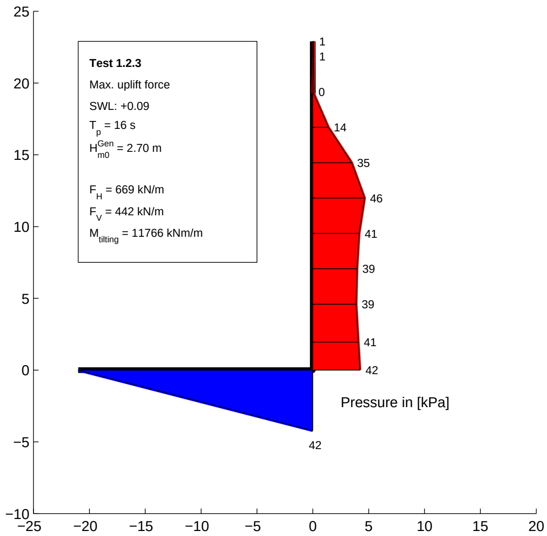

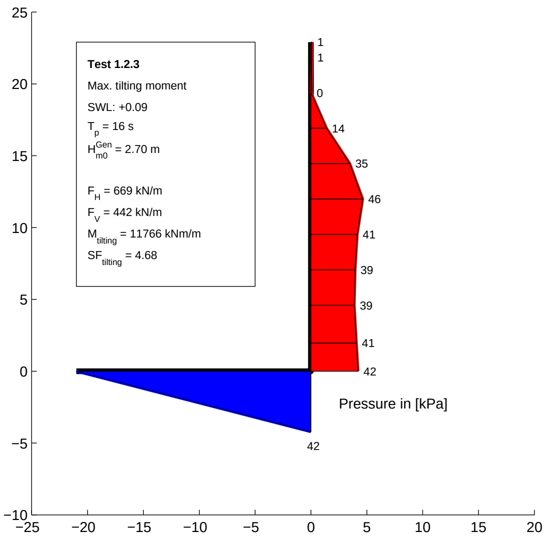

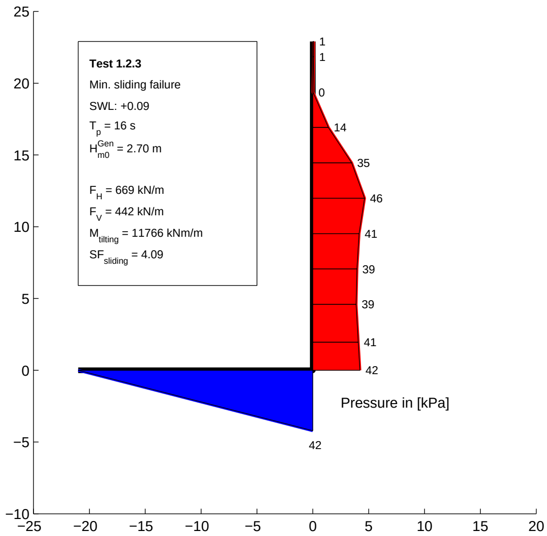

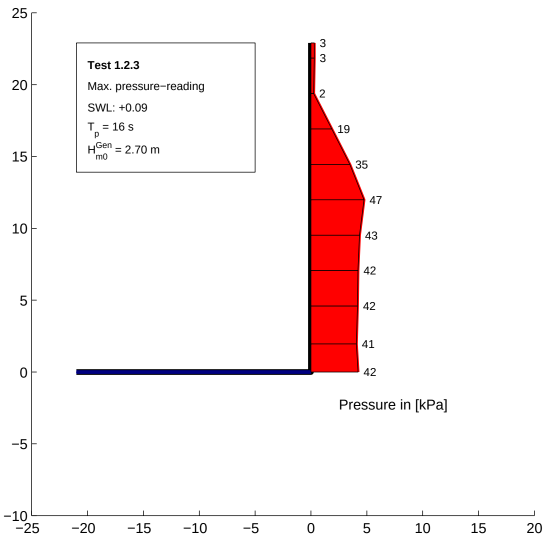

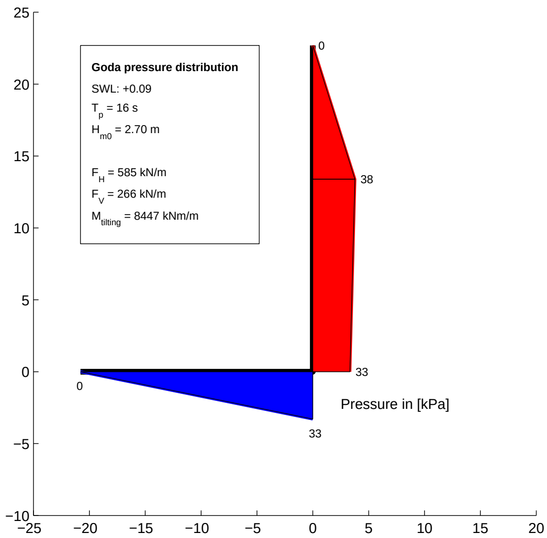

Test no. 1.2.4, SWL: +0.09, T_p: 16 s, $H_{m0}^{Gen} = 3.35$ m

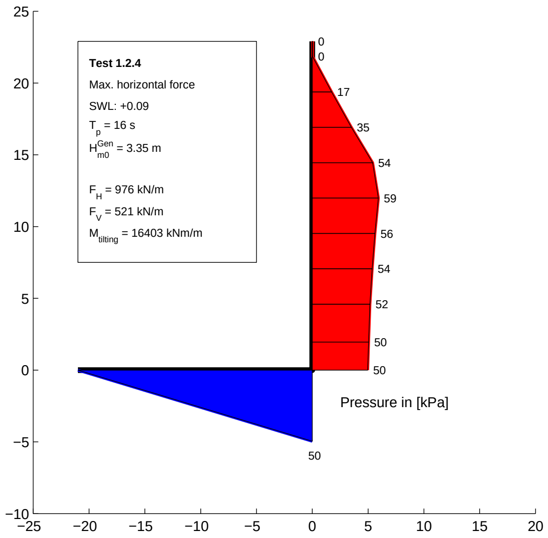

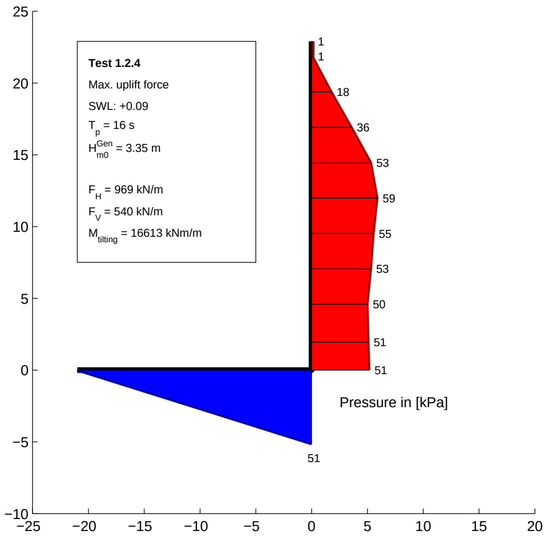

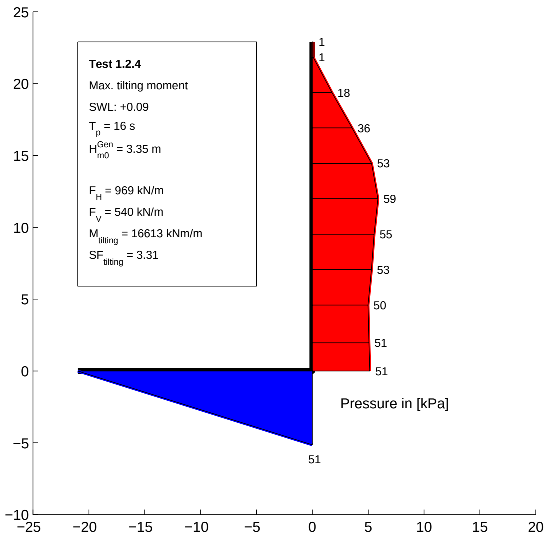

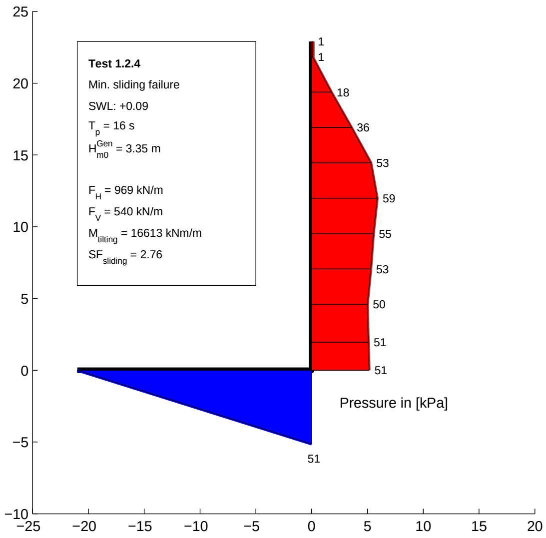

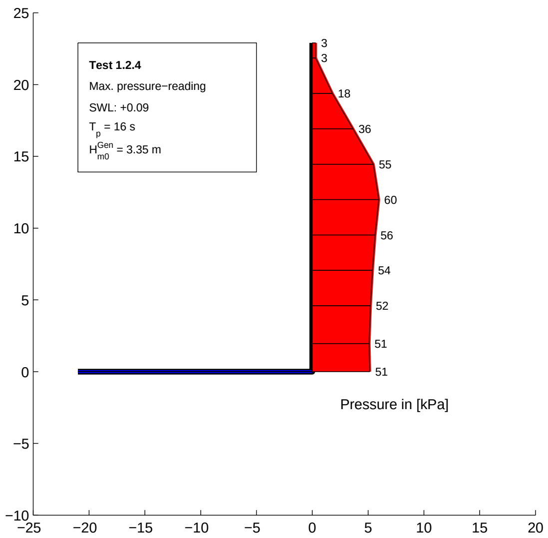

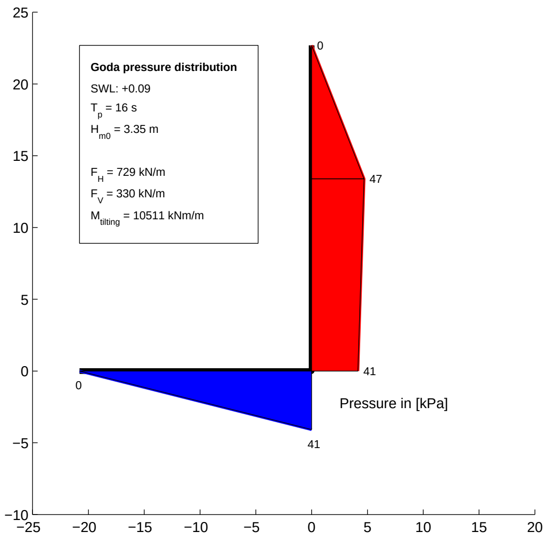

Test no. 1.2.5, SWL: +0.09, T_p: 16 s, $H_{m0}^{Gen} = 3.66$ m

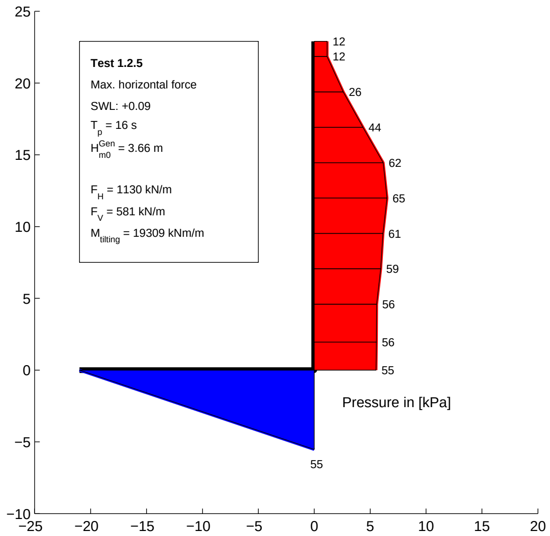

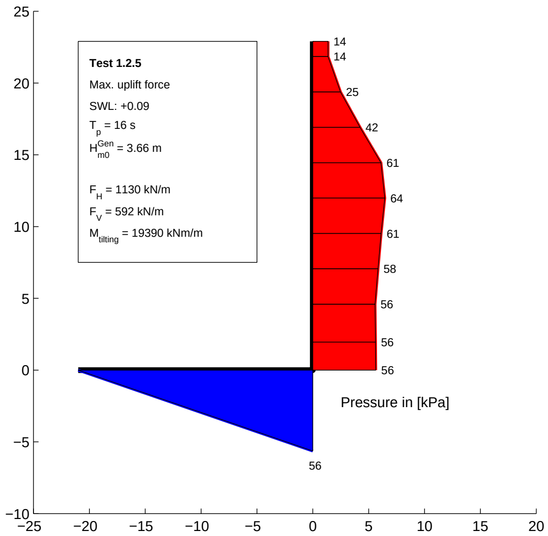

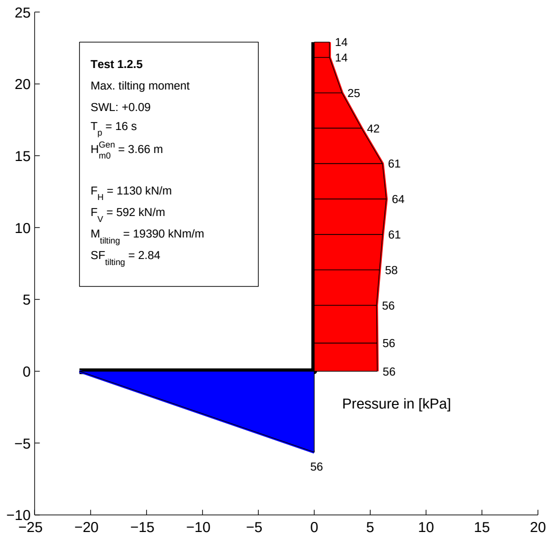

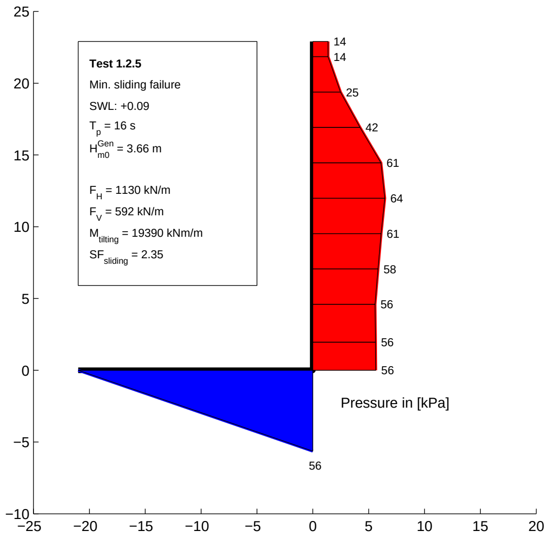

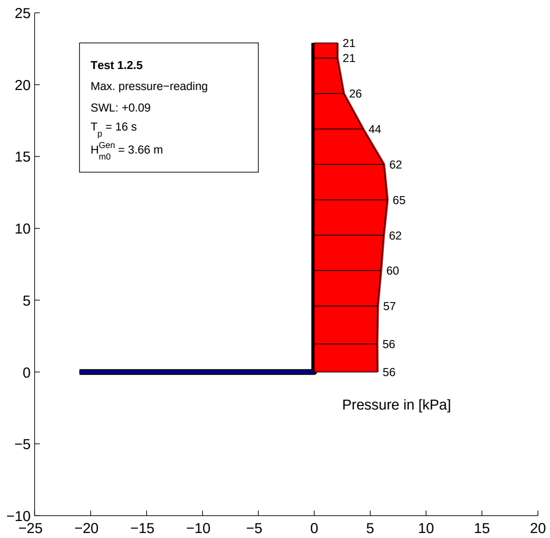

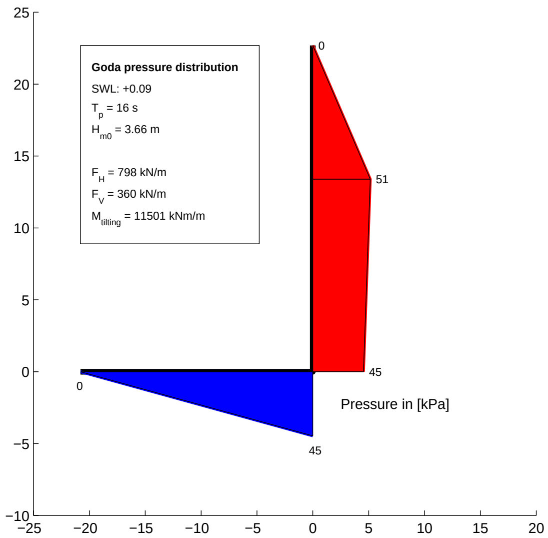

Test no. 1.2.6, SWL: +0.09, T_p: 16 s, $H_{m0}^{Gen} = 4.19$ m

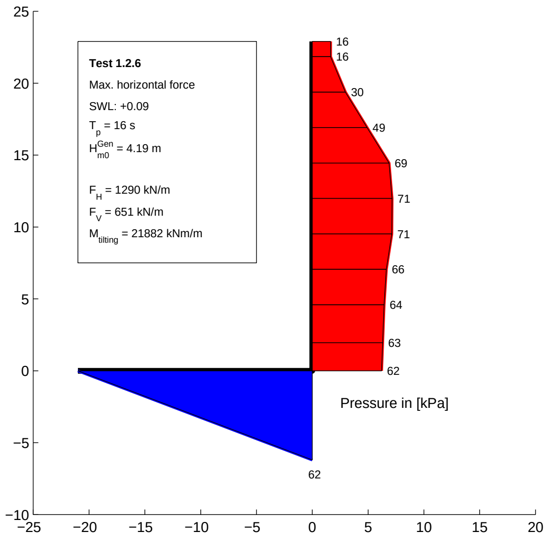

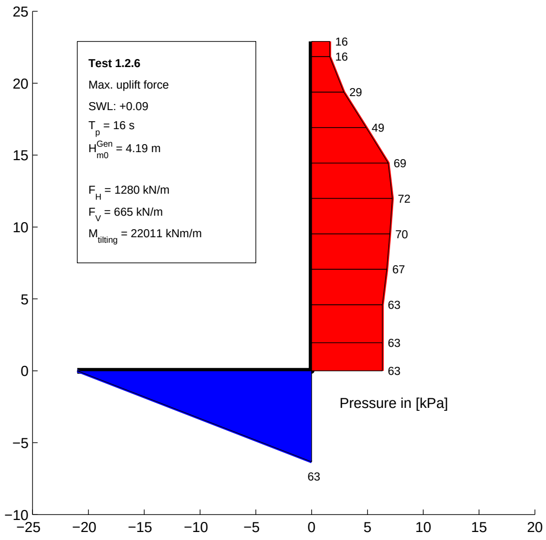

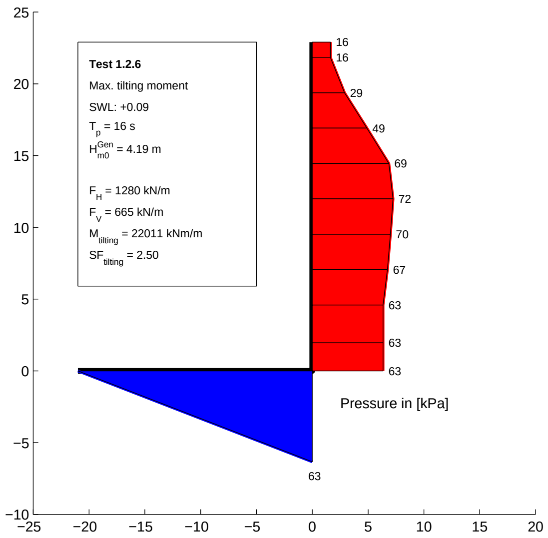

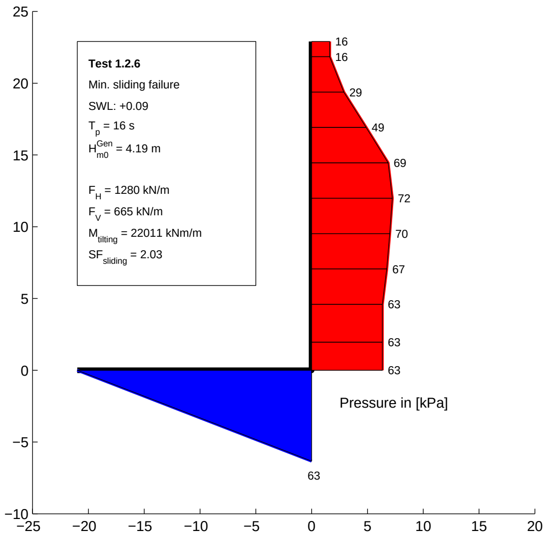

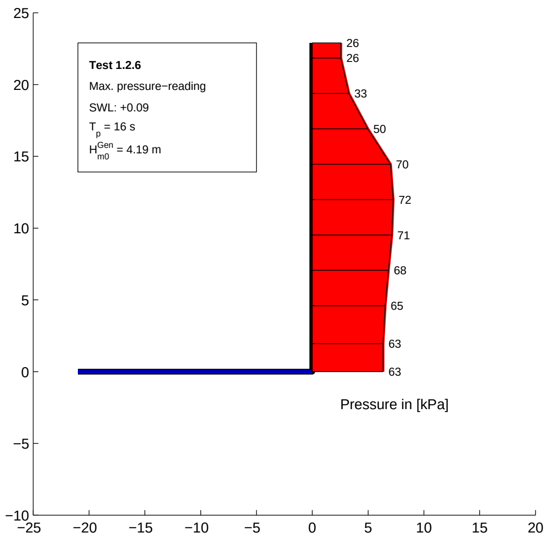

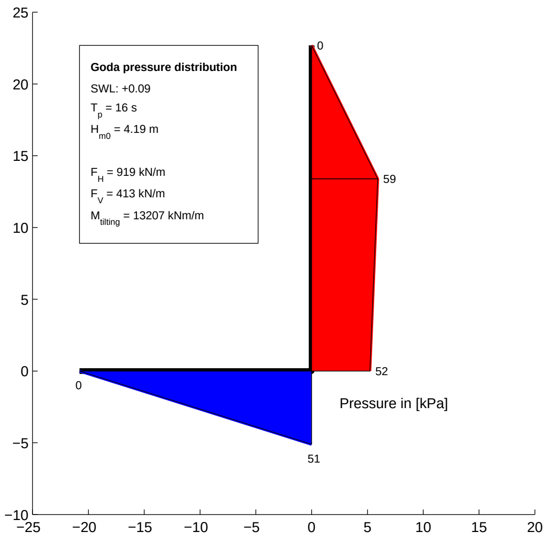

Test no. 1.2.7, SWL: +0.09, T_p: 16 s, $H_{m0}^{Gen} = 4.28$ m

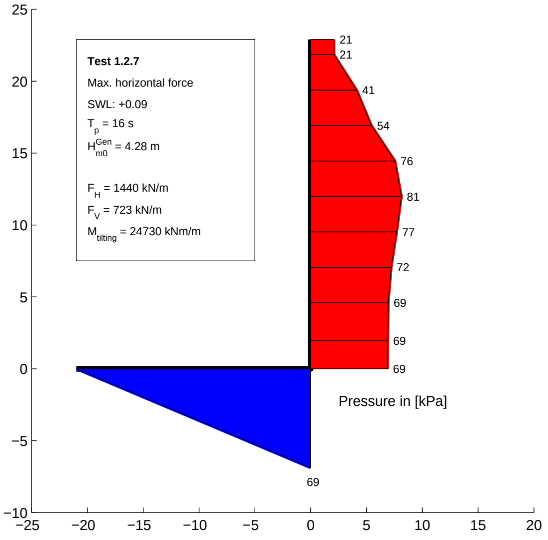

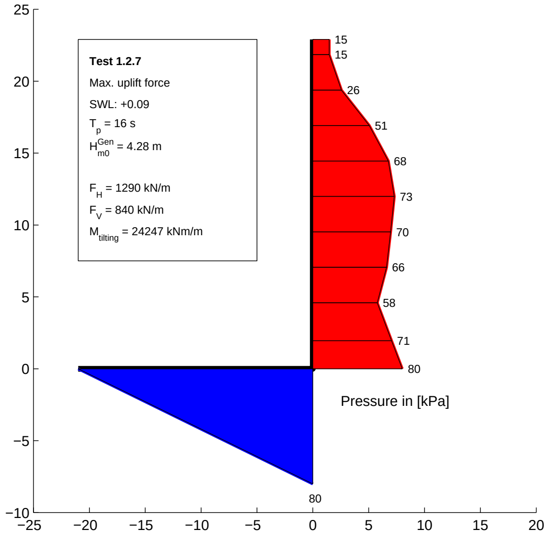

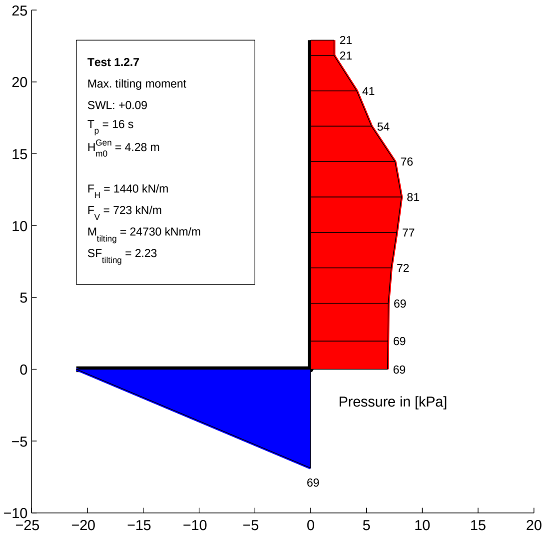

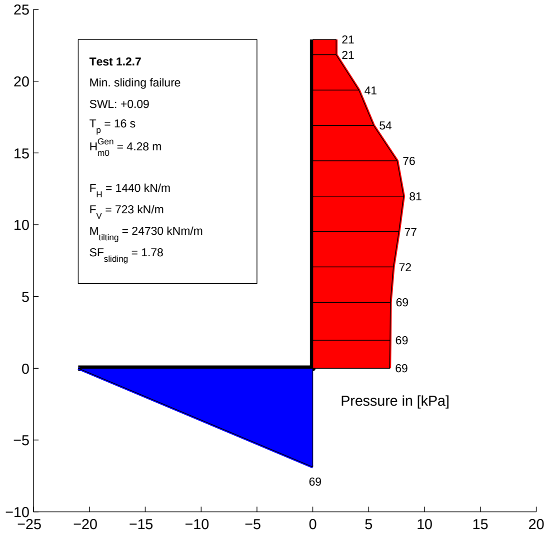

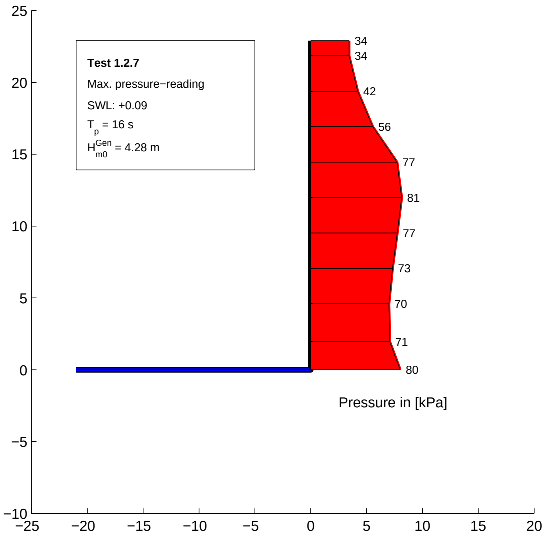

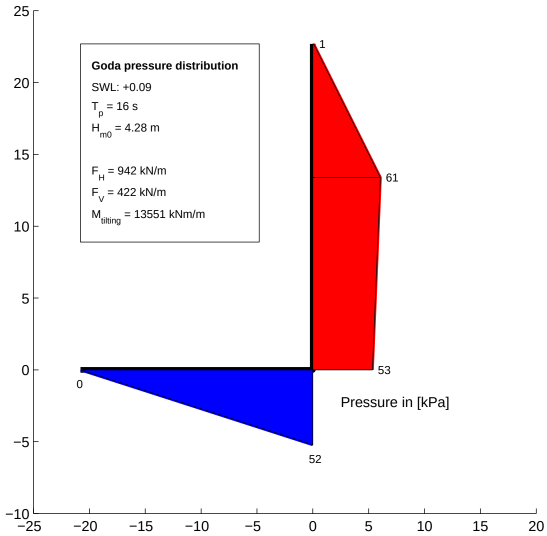

Test no. 2.1.1, SWL: +3.50, T_p: 8 s, $H_{m0}^{Gen} = 2.70$ m

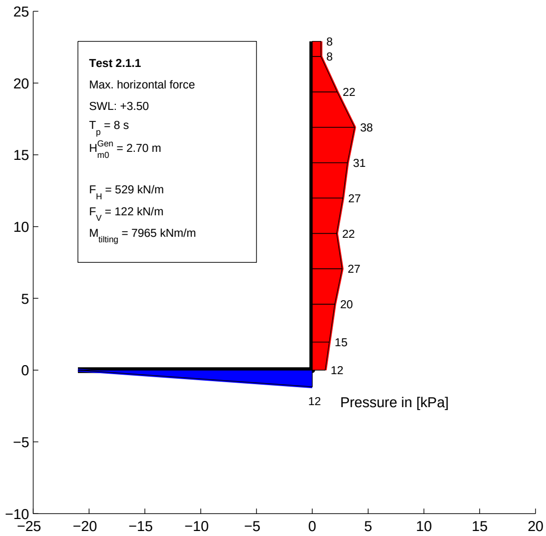

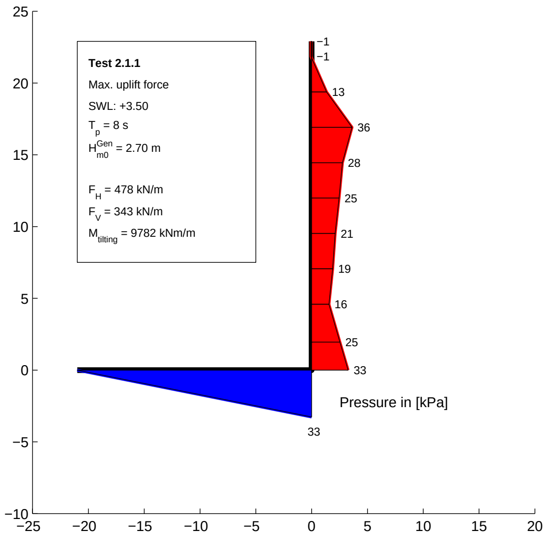

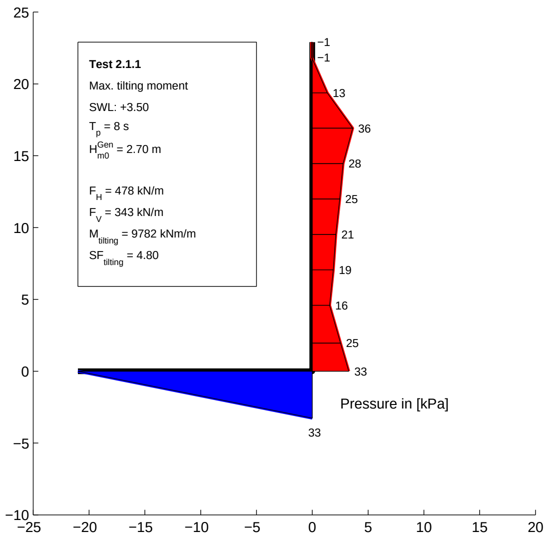

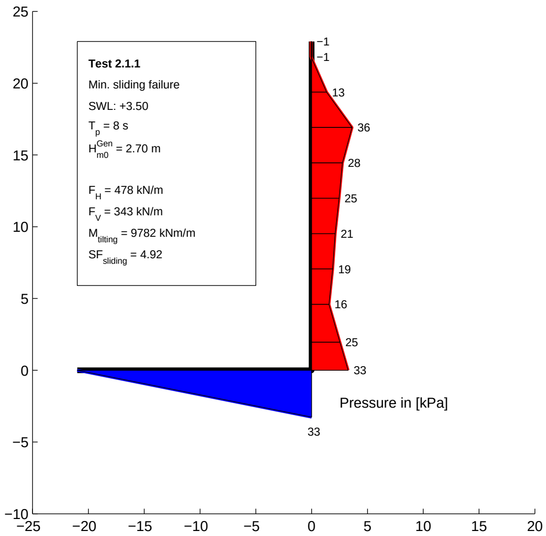

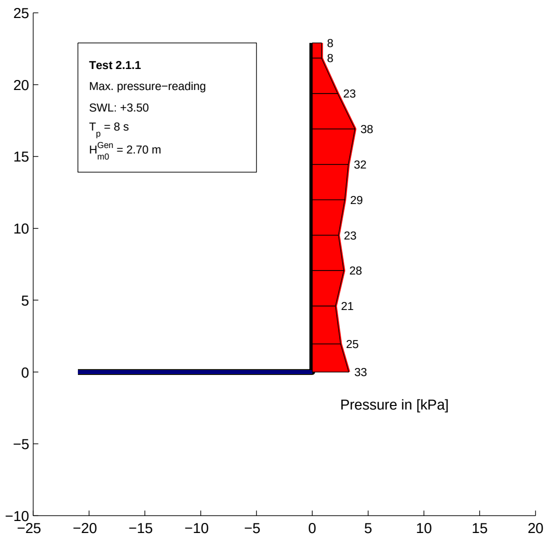

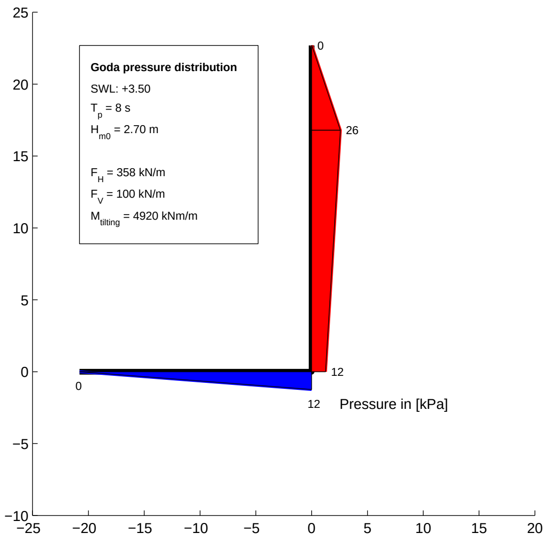

Test no. 2.1.2, SWL: +3.50, T_p: 8 s, $H_{m0}^{Gen} = 3.14$ m

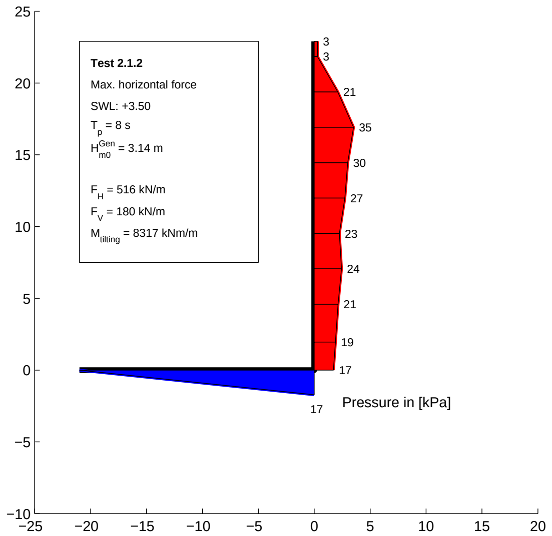

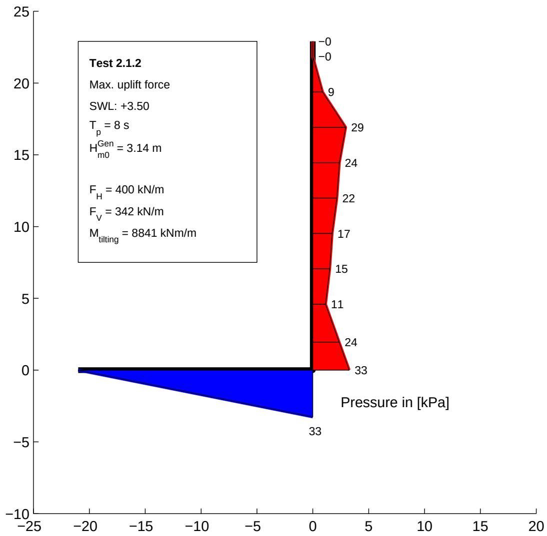

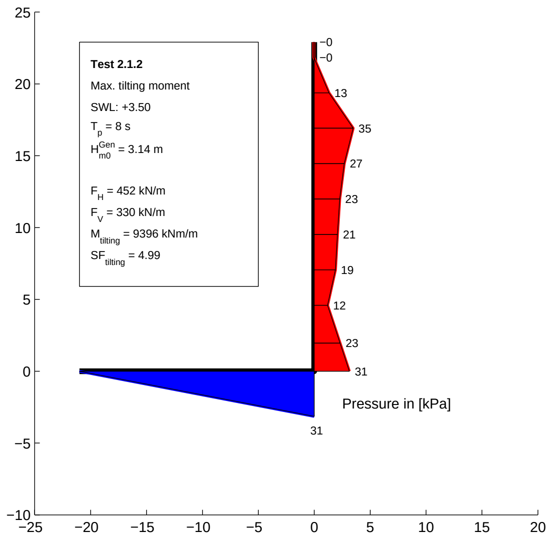

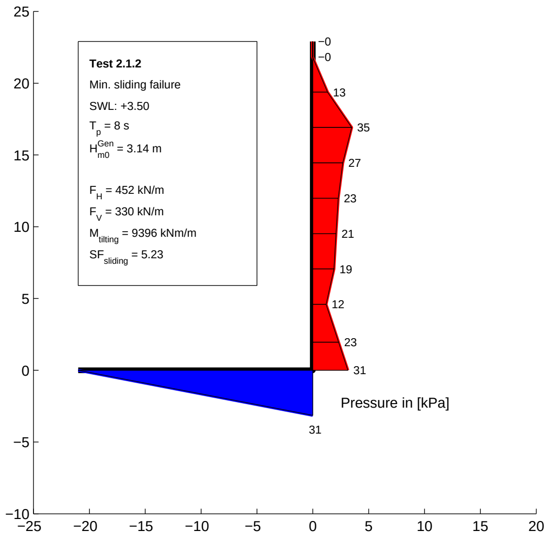

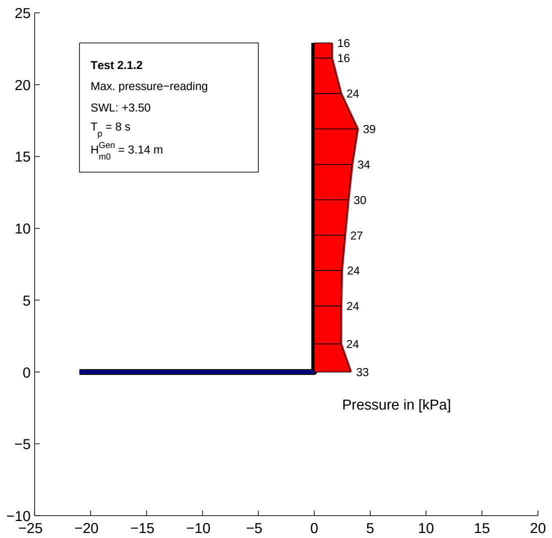

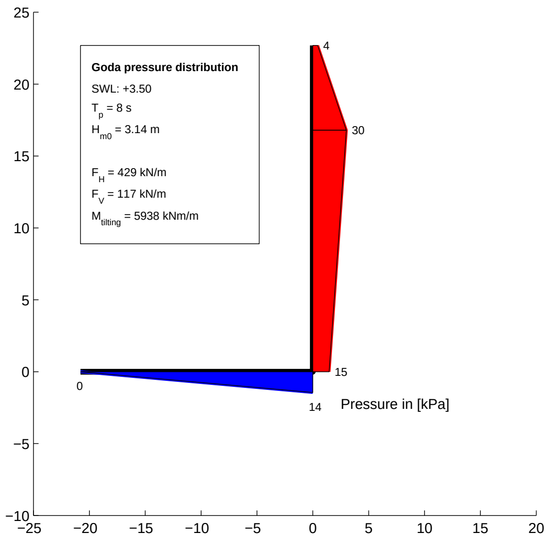

Test no. 2.1.3, SWL: +3.50, T_p: 8 s, $H_{m0}^{Gen} = 3.31$ m

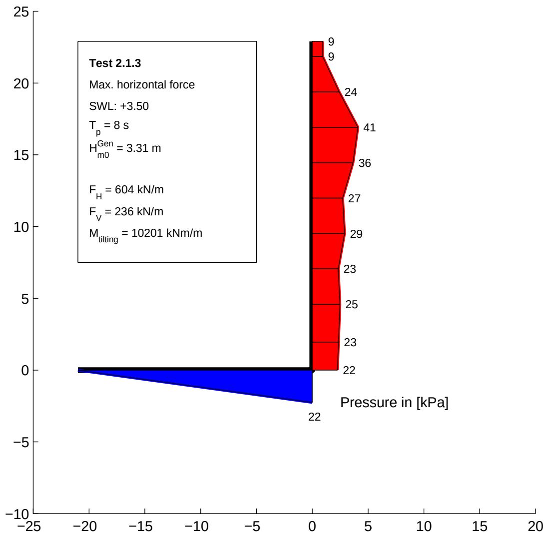

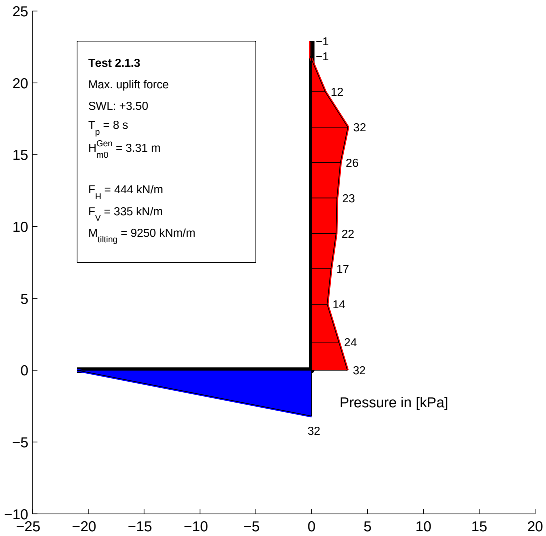

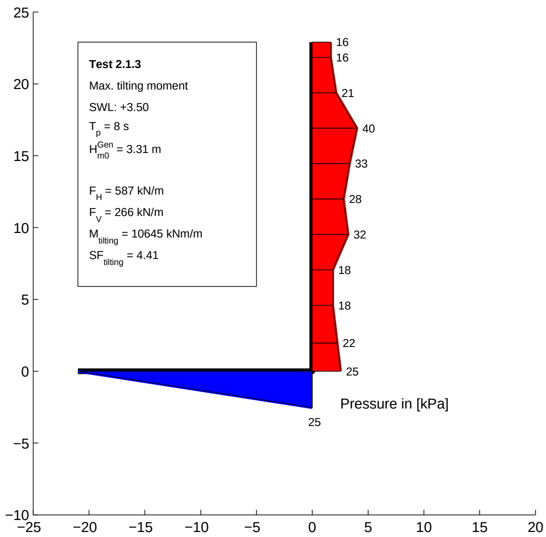

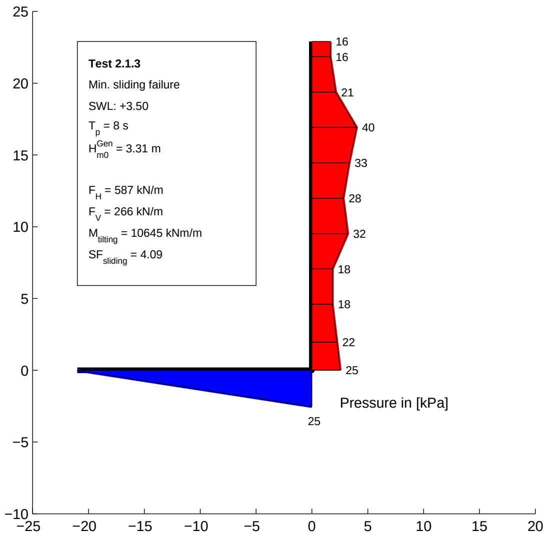

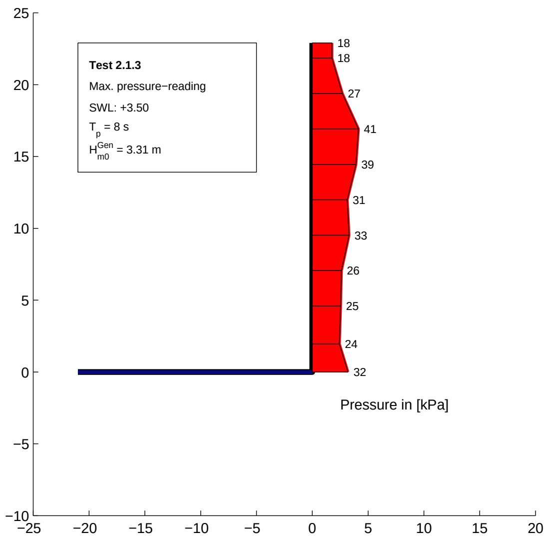

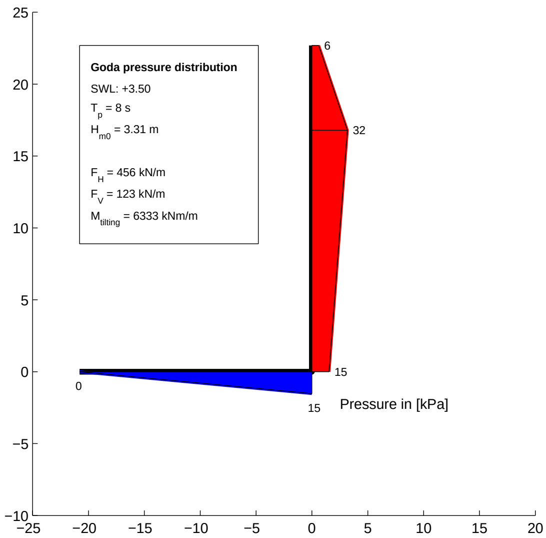

Test no. 2.1.4, SWL: +3.50, T_p: 8 s, $H_{m0}^{Gen} = 3.92$ m

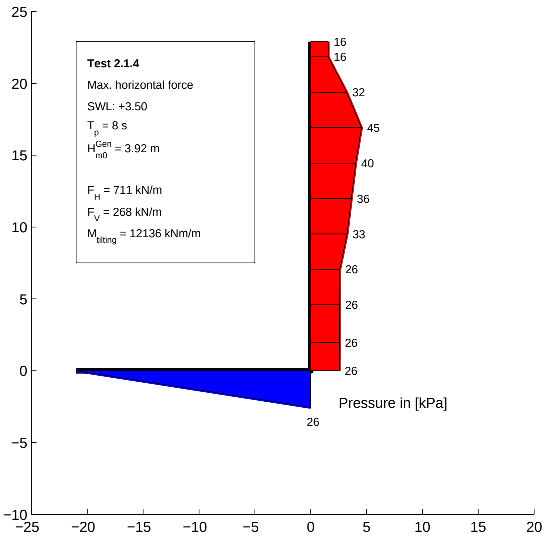

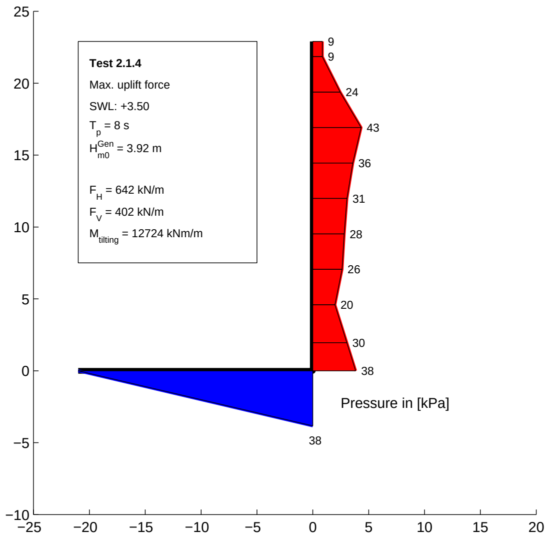

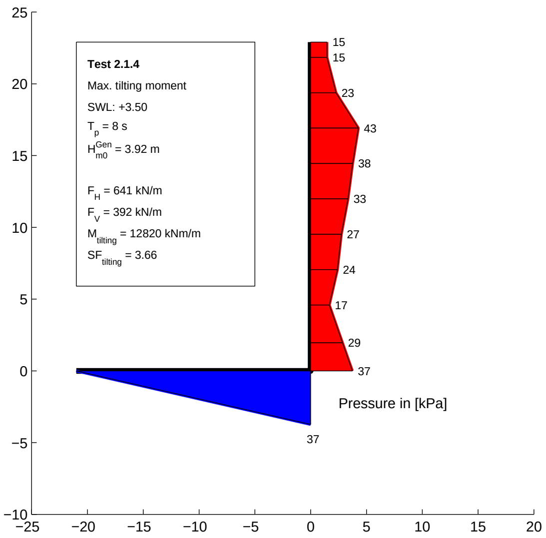

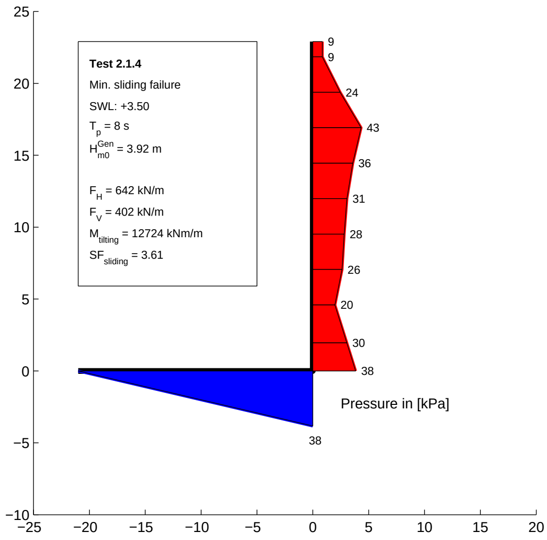

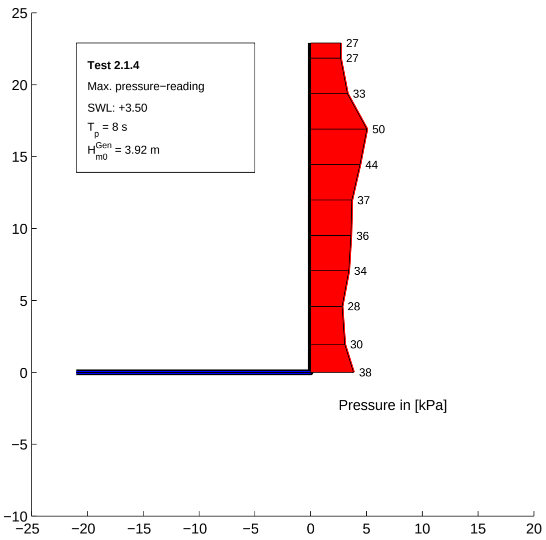

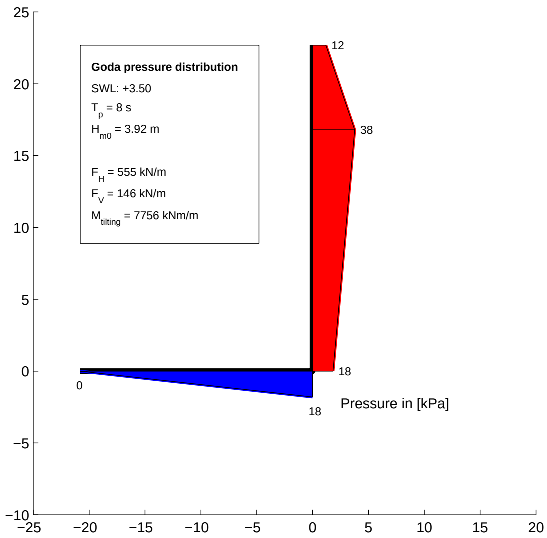

Test no. 2.1.5, SWL: +3.50, T_p: 8 s, $H_{m0}^{Gen} = 4.15$ m

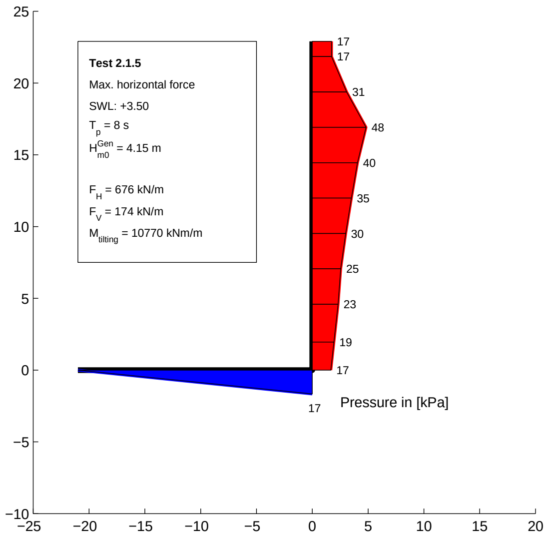

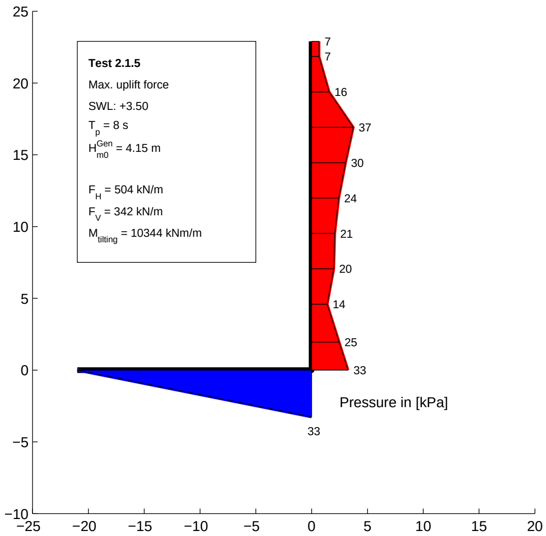

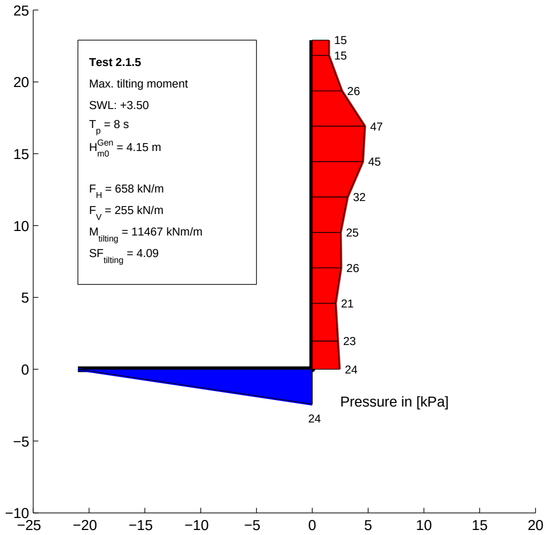

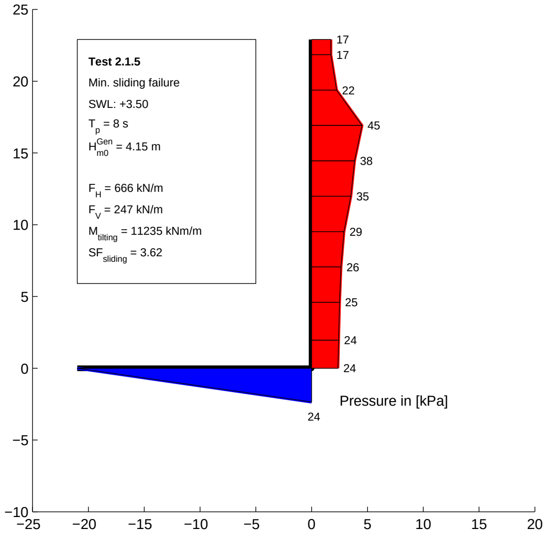

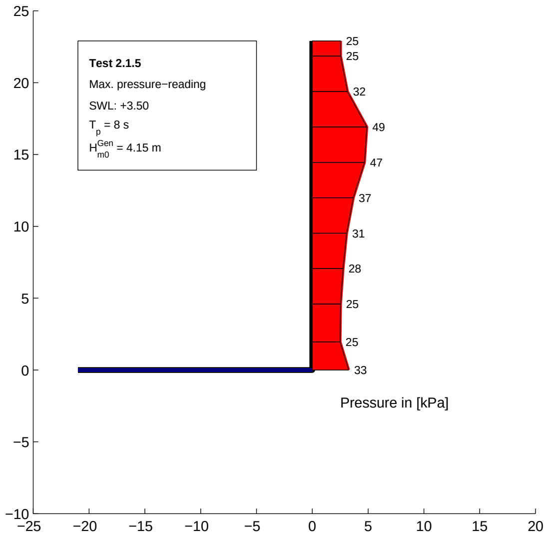

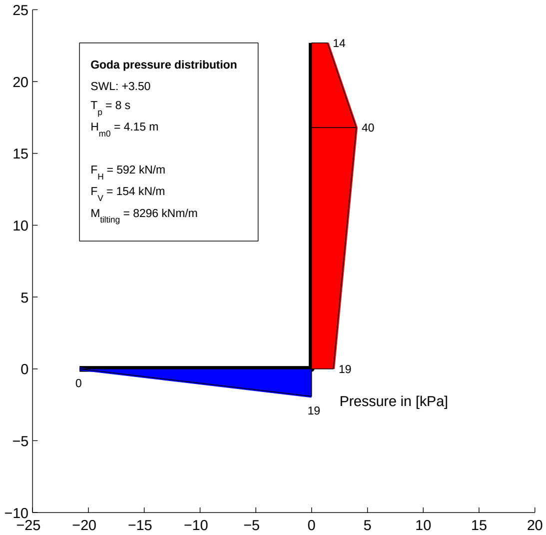

Test no. 2.1.6, SWL: +3.50, T_p: 8 s, $H_{m0}^{Gen} = 4.74$ m

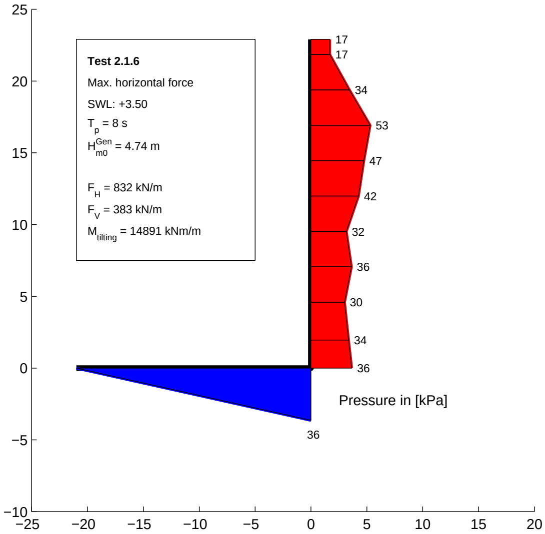

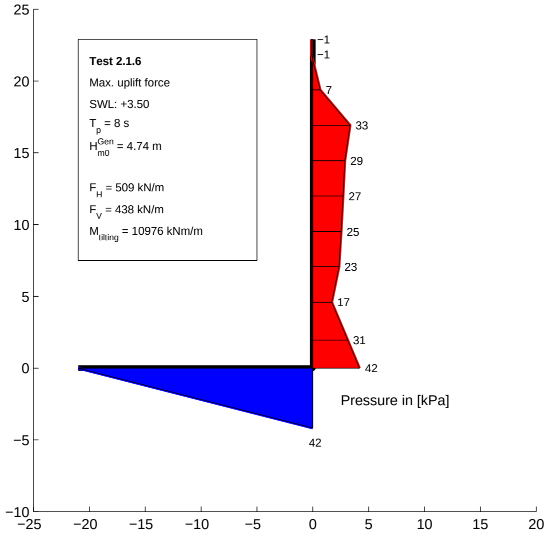

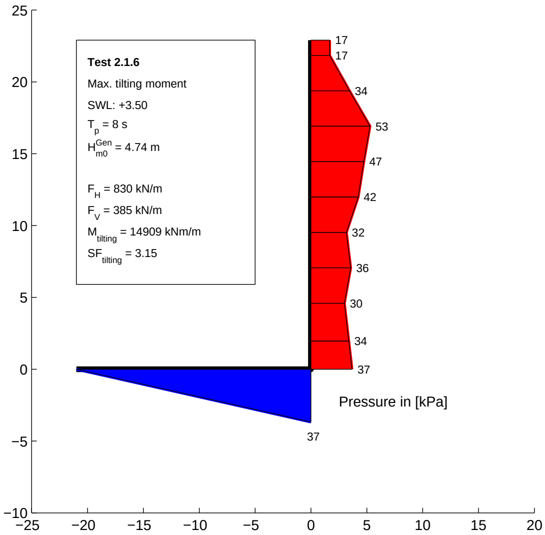

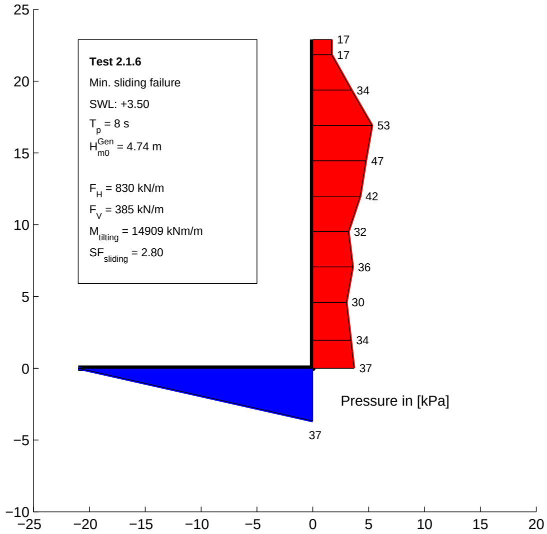

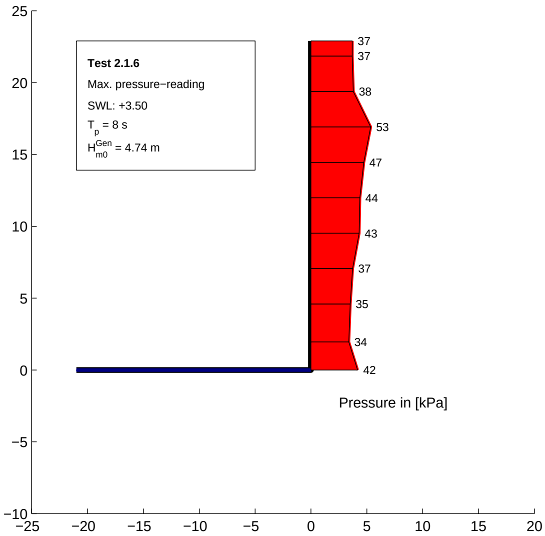

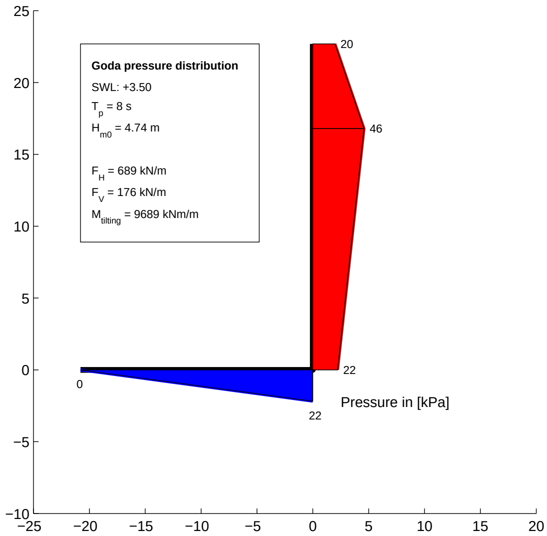

Test no. 2.1.7, SWL: +3.50, T_p: 8 s, $H_{m0}^{Gen} = 4.87$ m

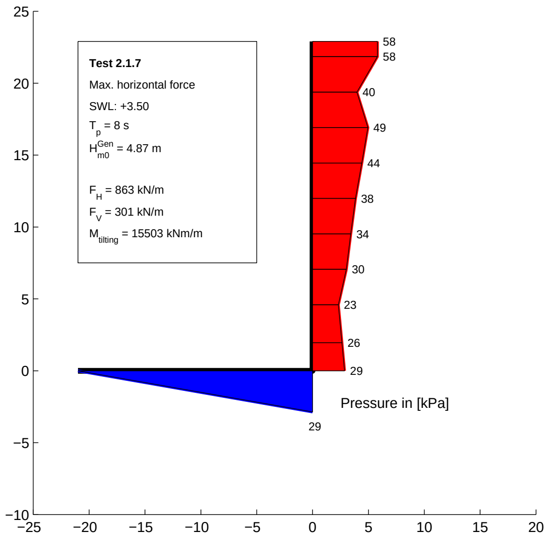

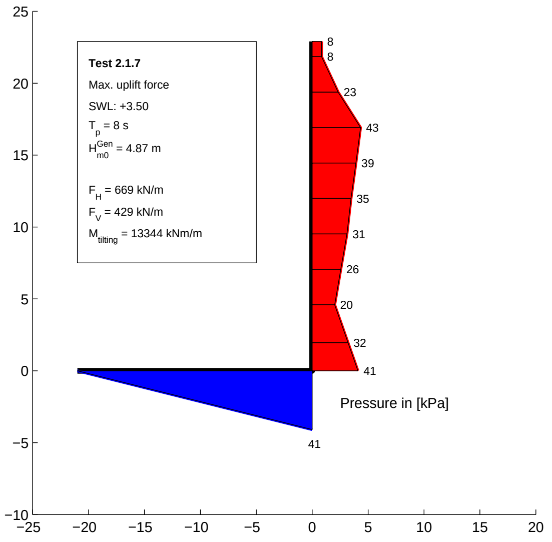

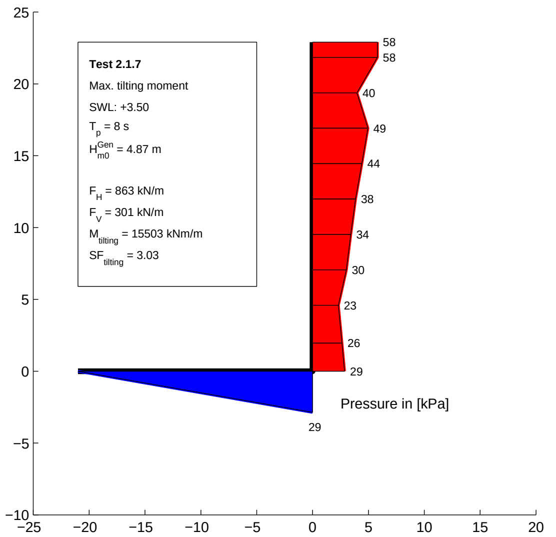

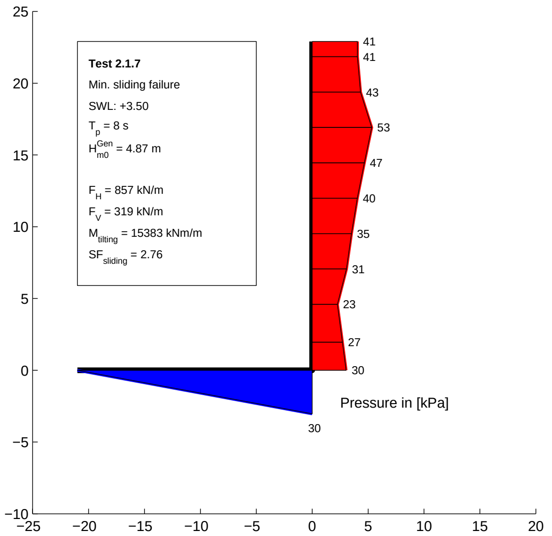

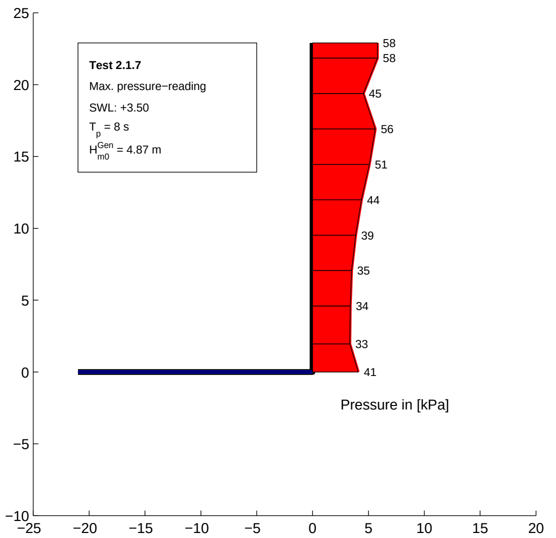

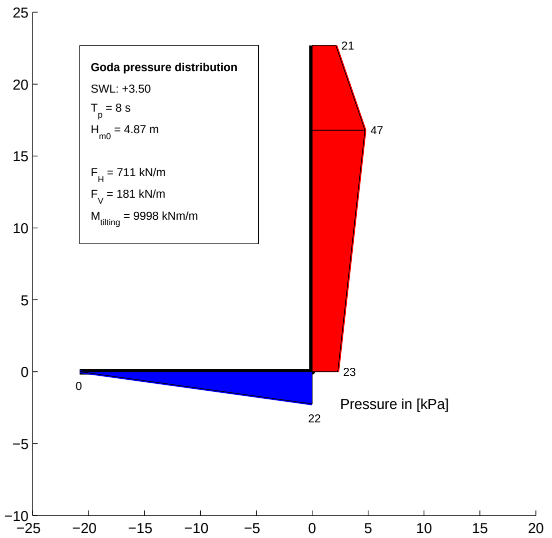

Test no. 2.2.1, SWL: +3.50, T_p: 16 s, $H_{m0}^{Gen} = 2.50$ m

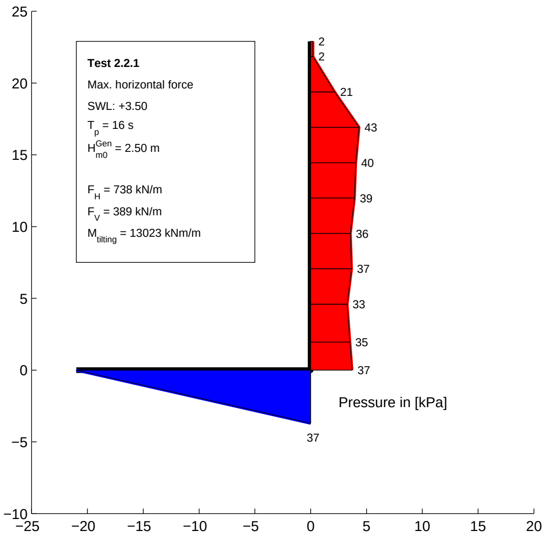

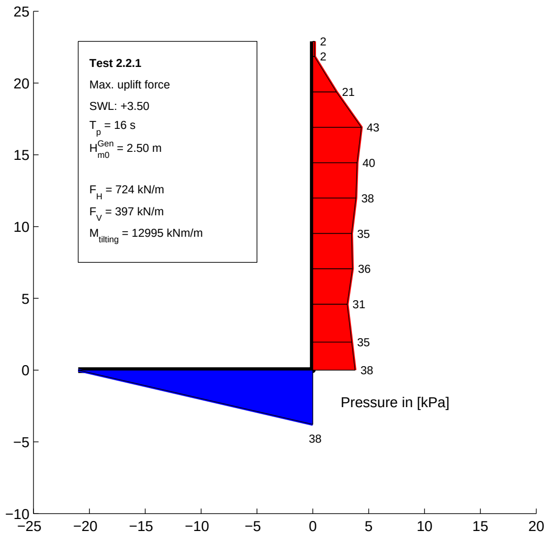

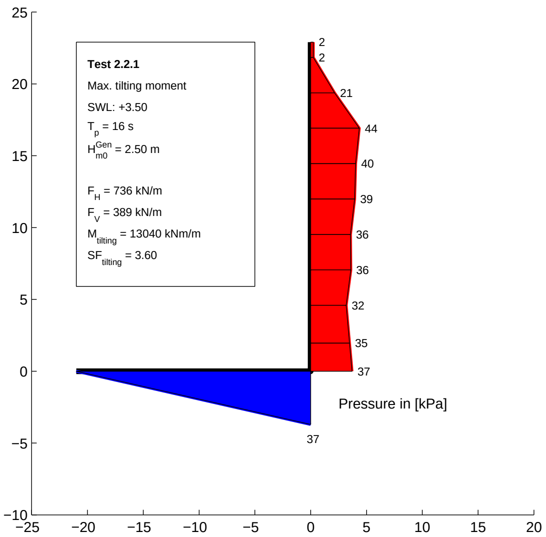

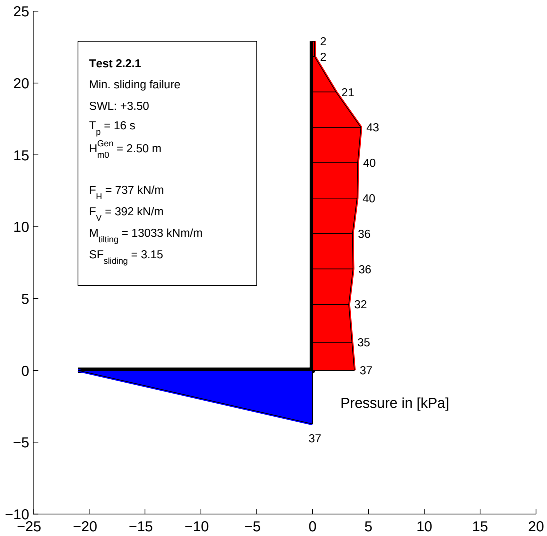

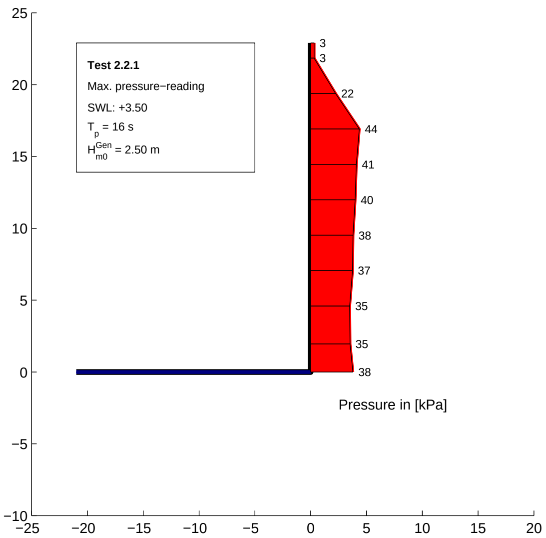

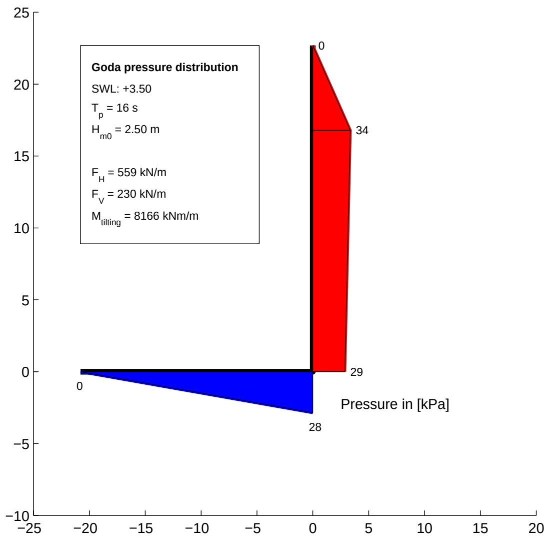

Test no. 2.2.2, SWL: +3.50, $T_\mathbf{p}$: 16 s, $H_{m0}^{Gen} = 3.04$ m

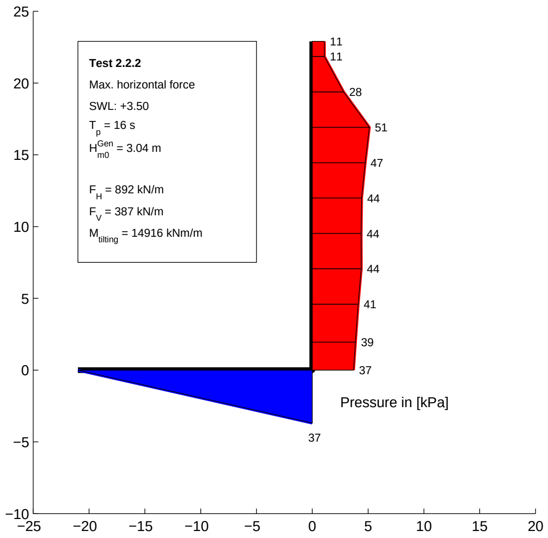

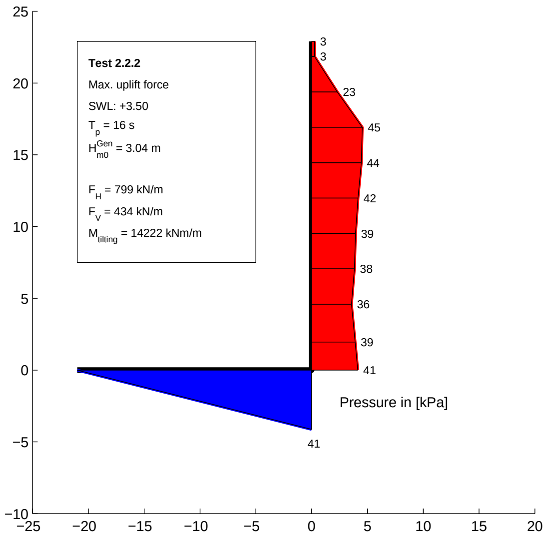

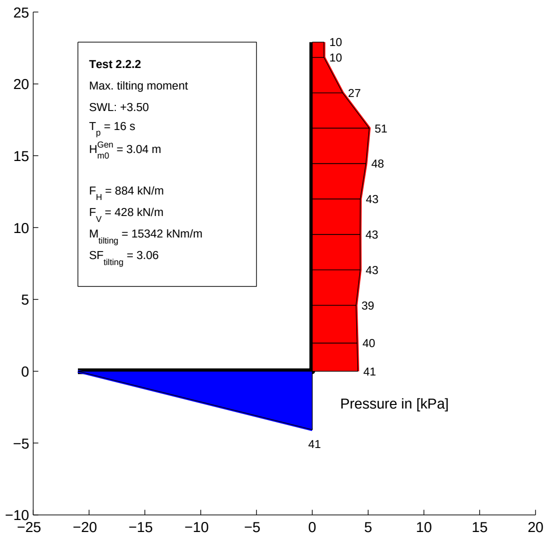

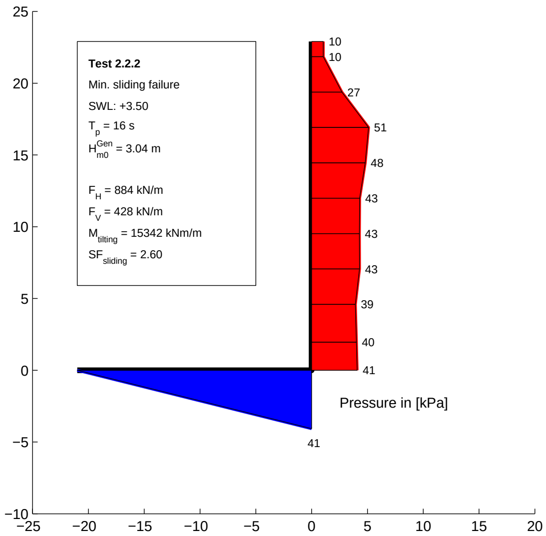

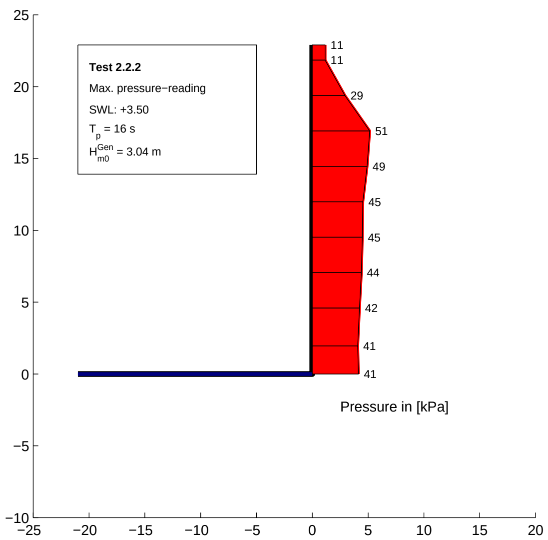

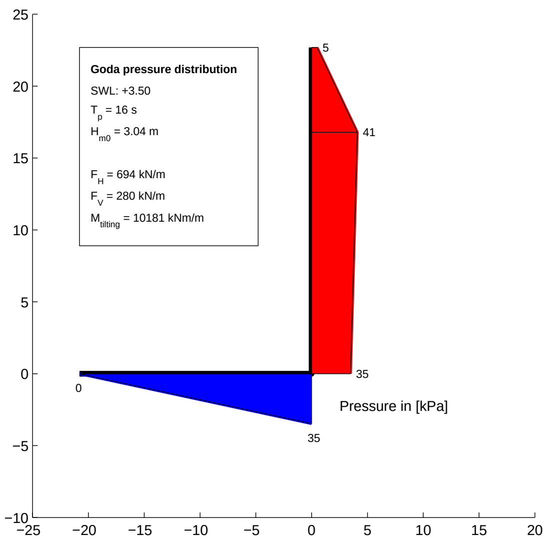

Test no. 2.2.3, SWL: +3.50, T_p: 16 s, $H_{m0}^{Gen} = 3.66$ m

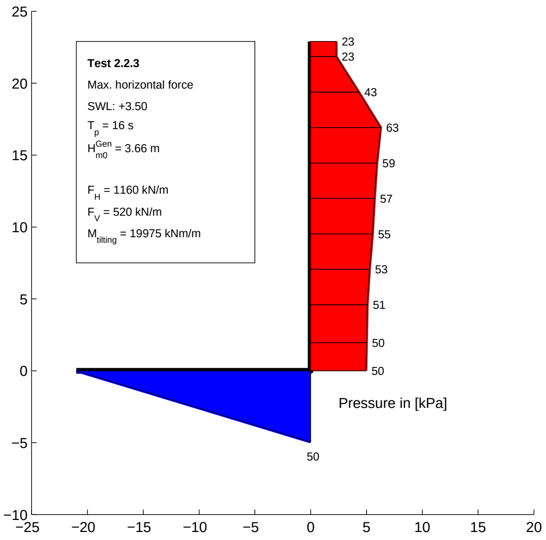

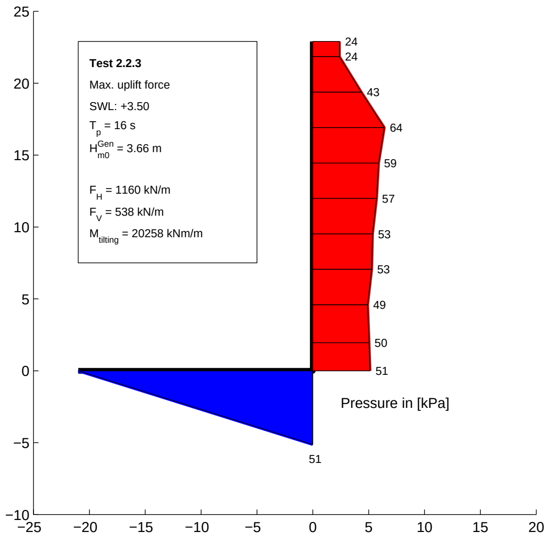

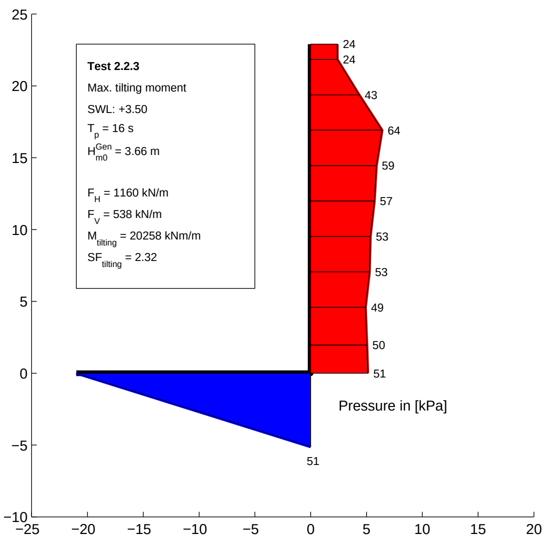

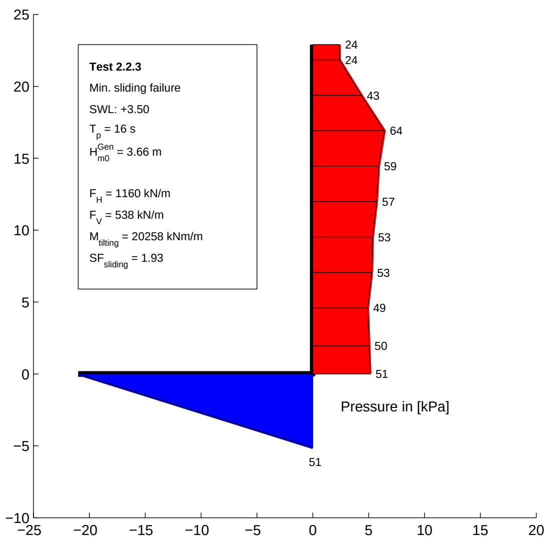

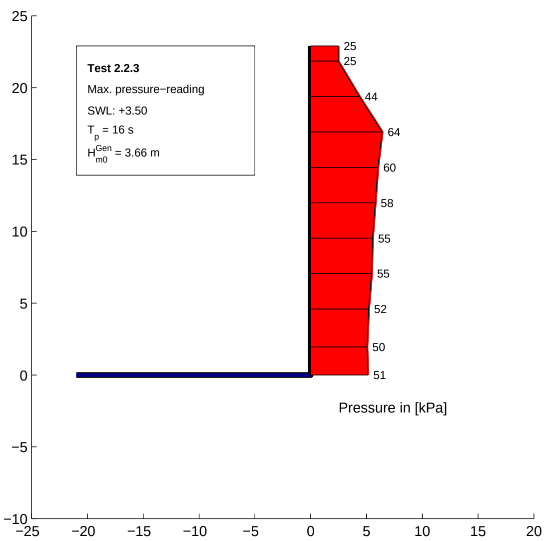

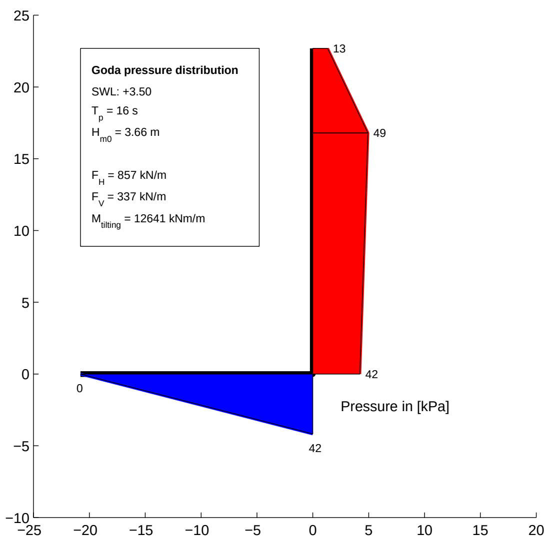

Test no. 2.2.4, SWL: +3.50, T_p: 16 s, $H_{m0}^{Gen} = 3.77$ m

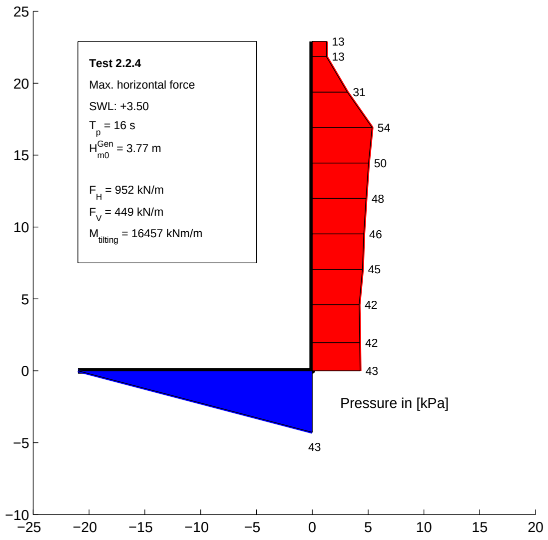

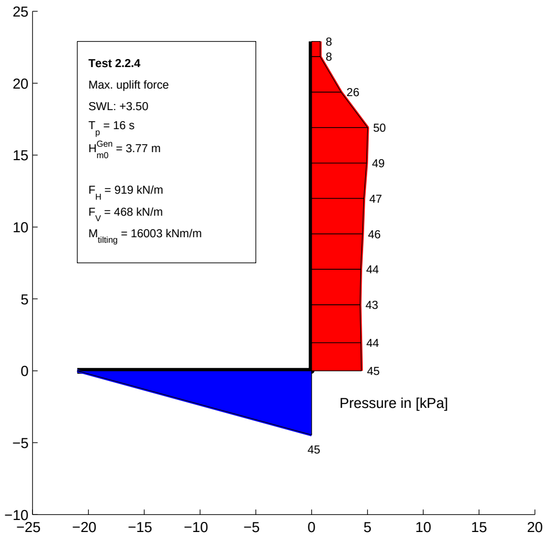

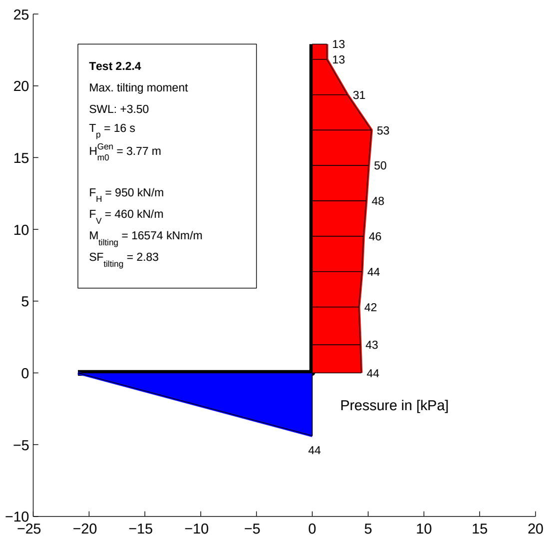

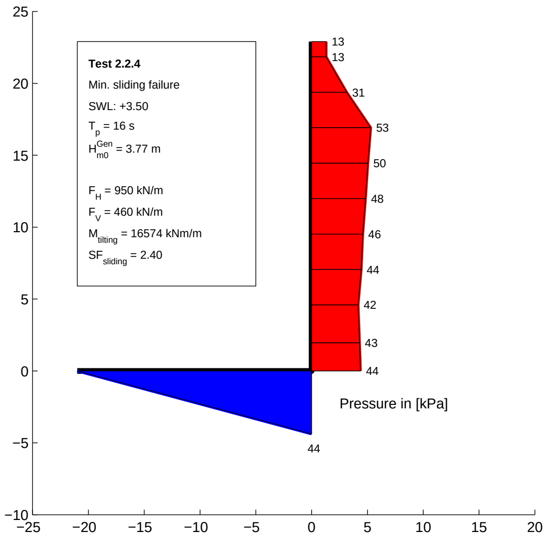

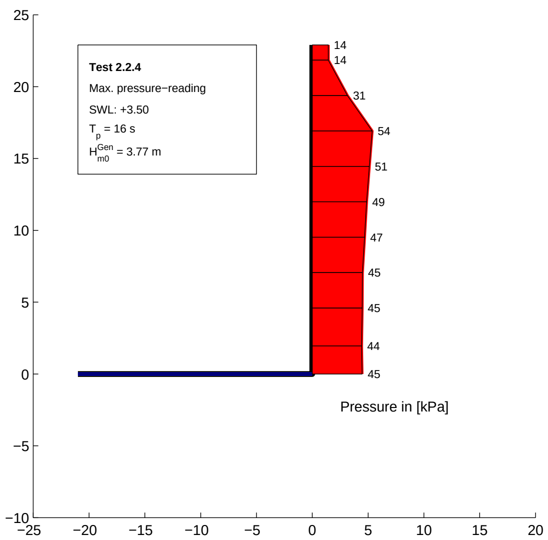

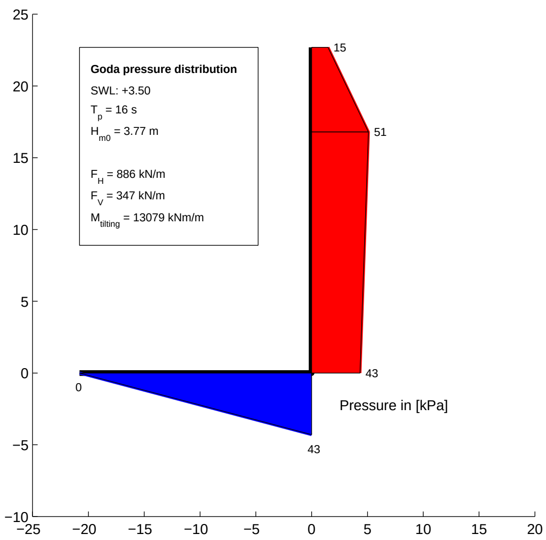

Test no. 2.2.5, SWL: +3.50, T_p: 16 s, $H_{m0}^{Gen} = 4.36$ m

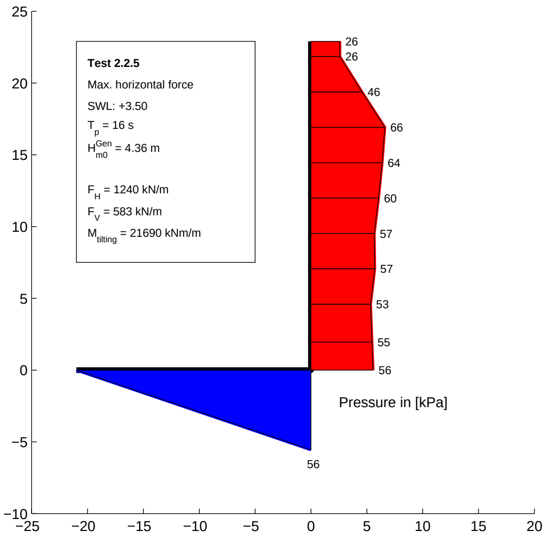

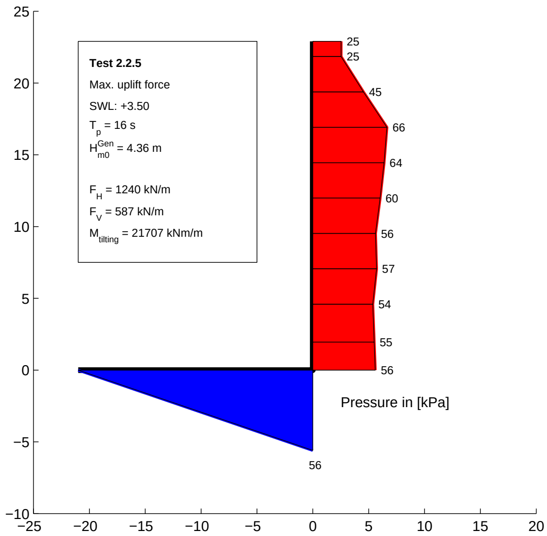

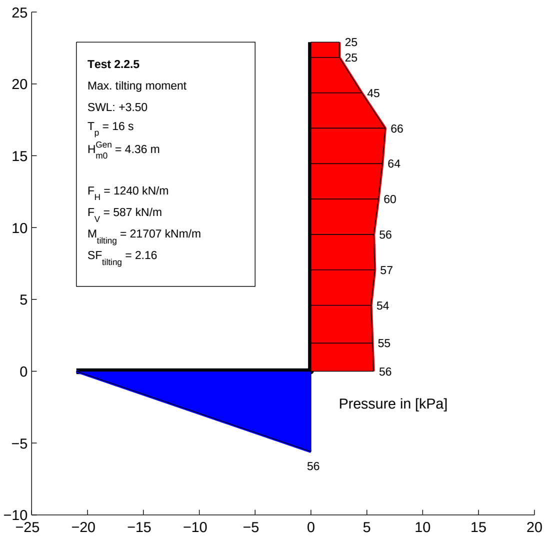

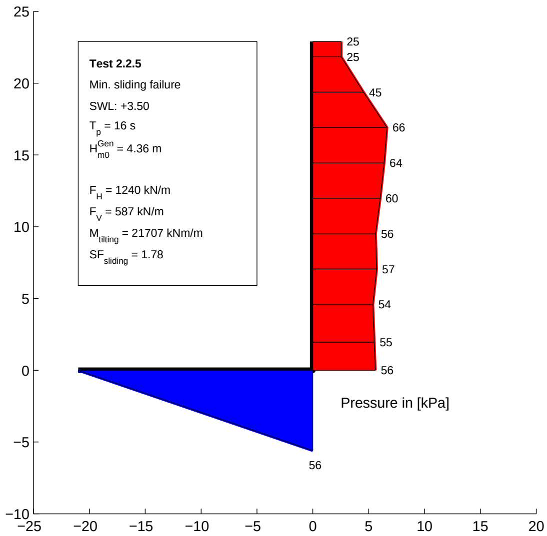

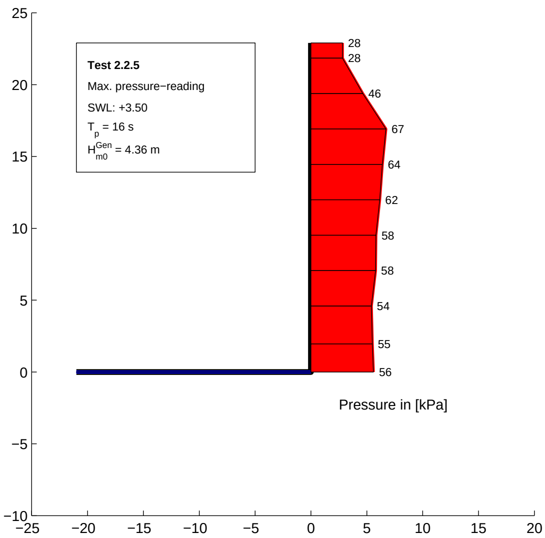

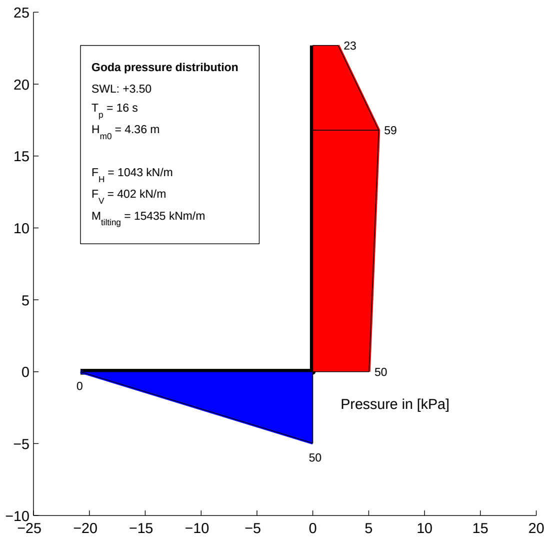

Test no. 2.2.6, SWL: +3.50, T_p: 16 s, $H_{m0}^{Gen} = 4.84$ m

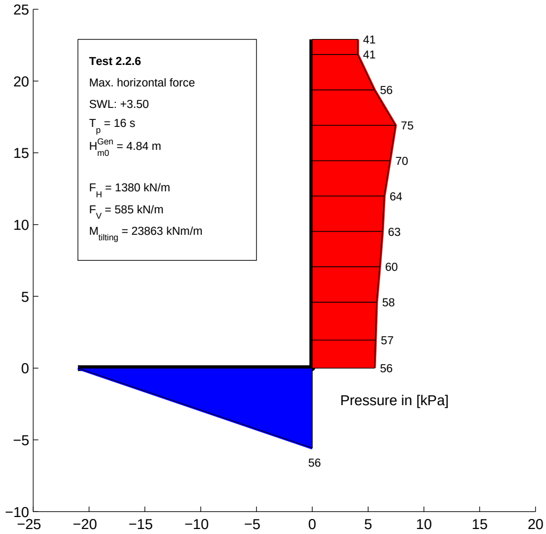

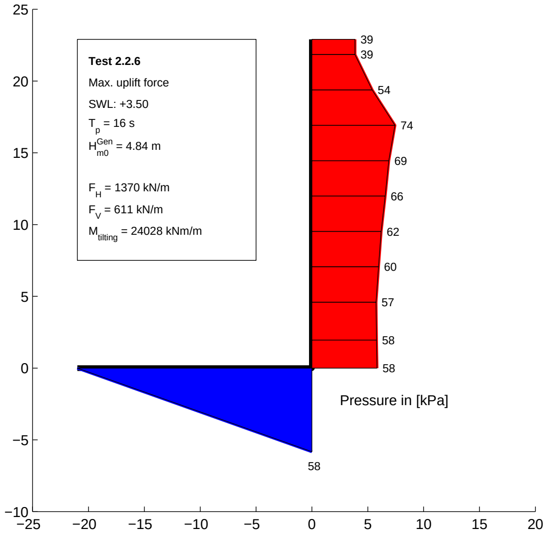

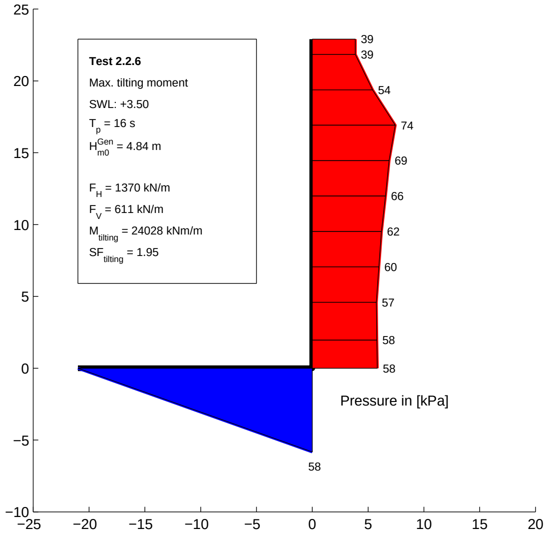

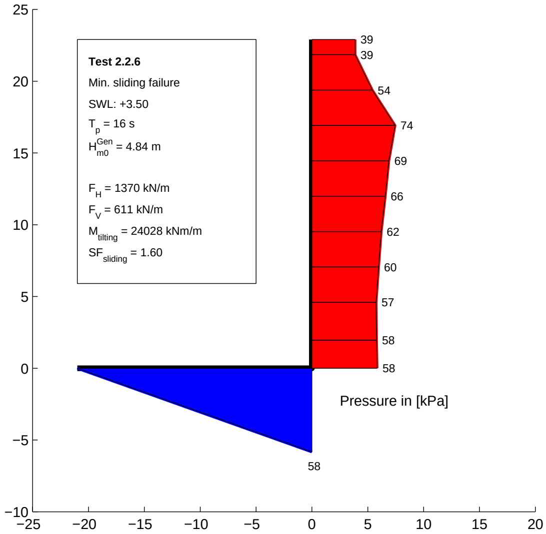

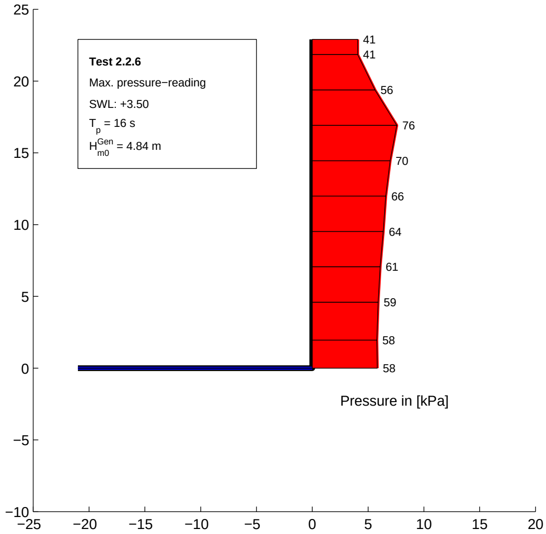

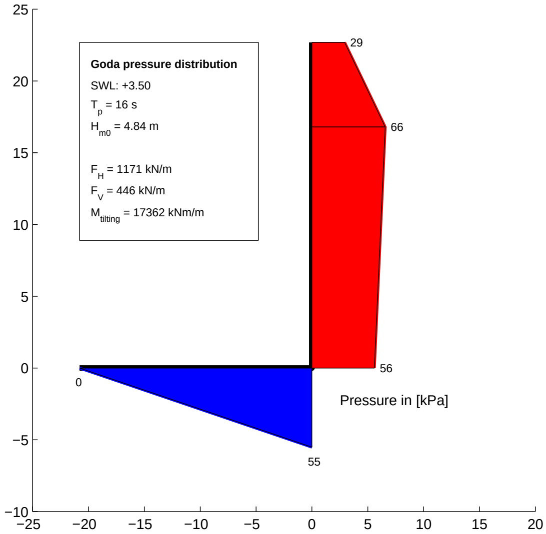

A.2 Crown wall loads

Test no. 1.1.1, SWL: +0.09, T_p: 8 s, $H_{m0}^{Gen} = 2.21$ m

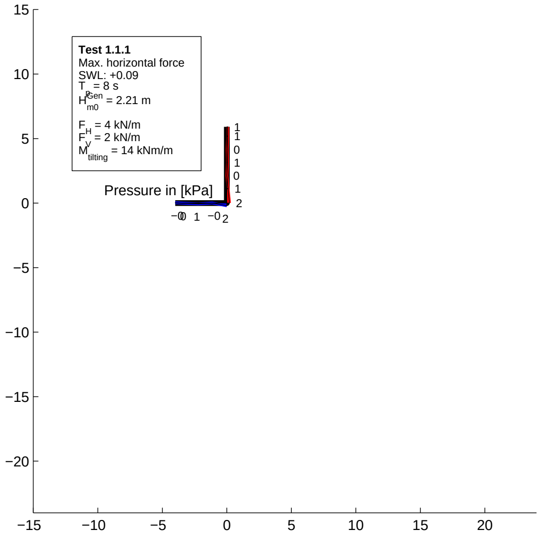

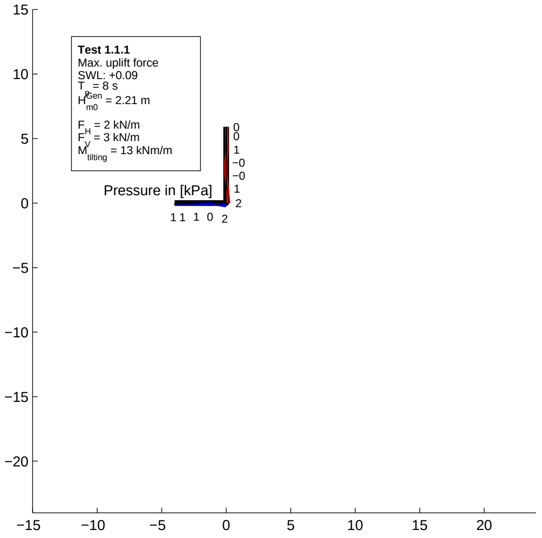

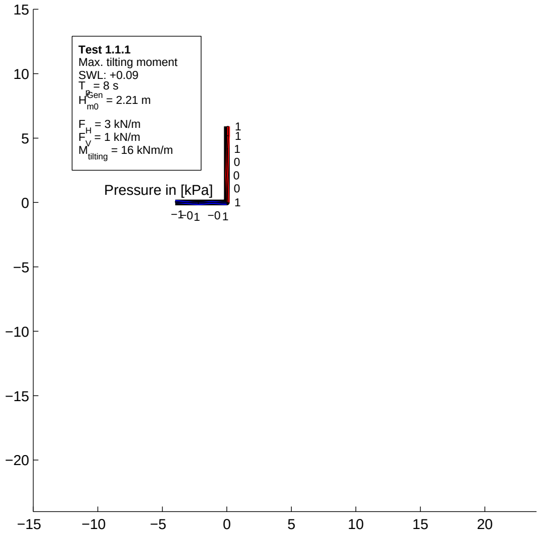

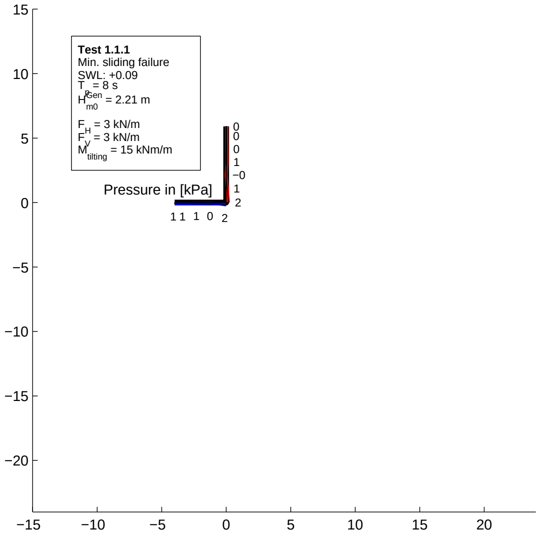

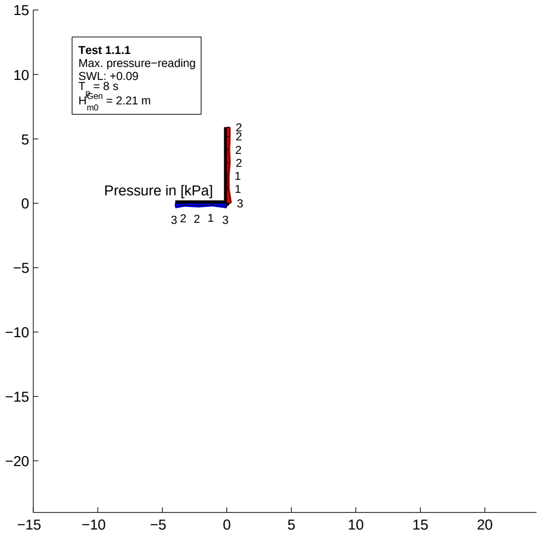

Test no. 1.1.2, SWL: +0.09, $T_\mathbf{p}$: 8 s, $H_{m0}^{Gen} = 2.72$ m

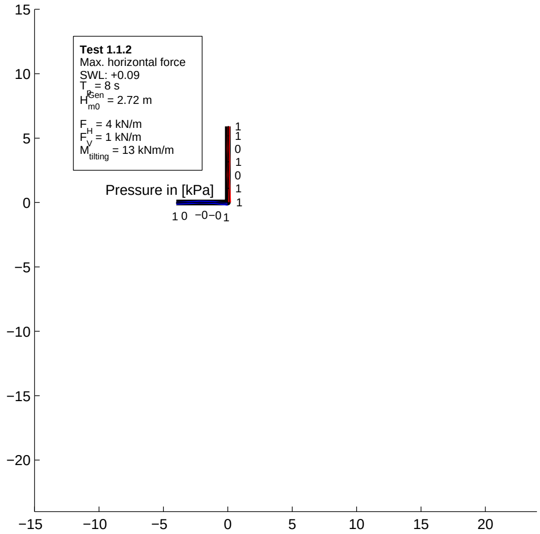

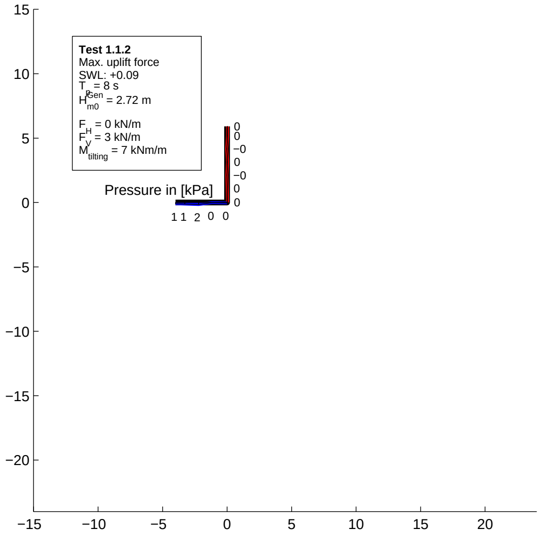

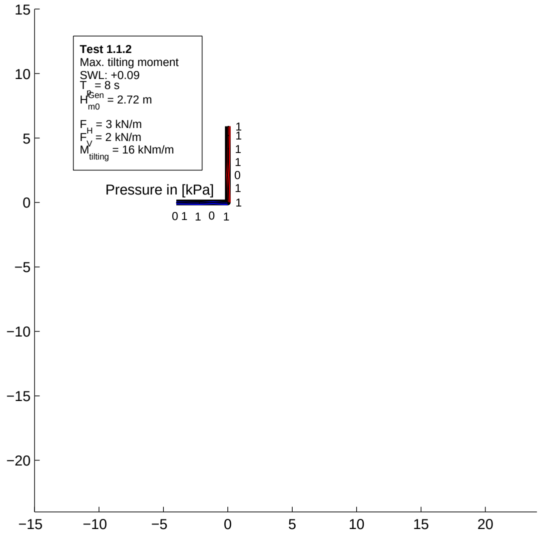

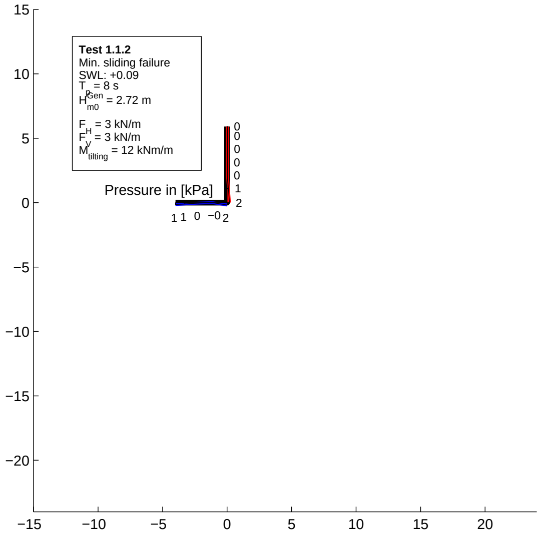

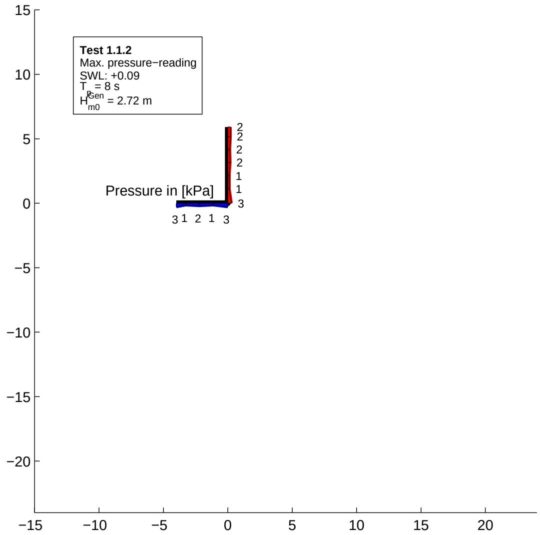

Test no. 1.1.3, SWL: +0.09, T_p: 8 s, $H_{m0}^{Gen} = 3.03$ m

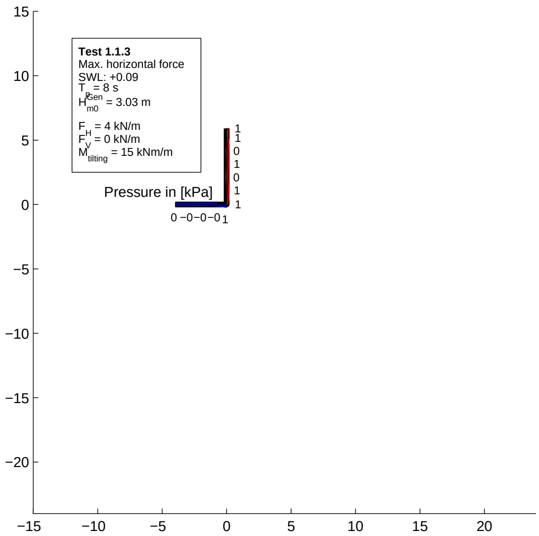

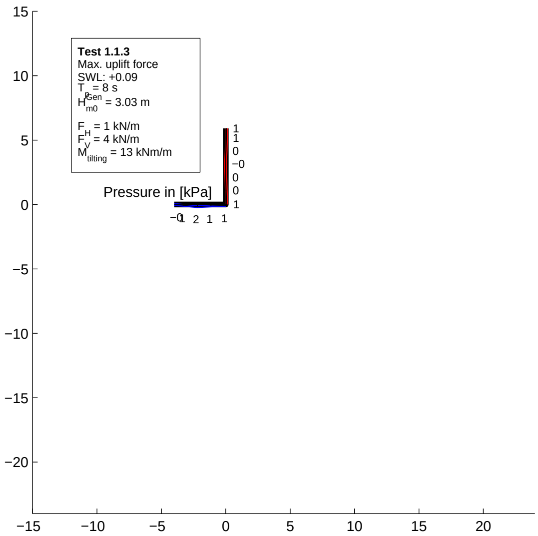

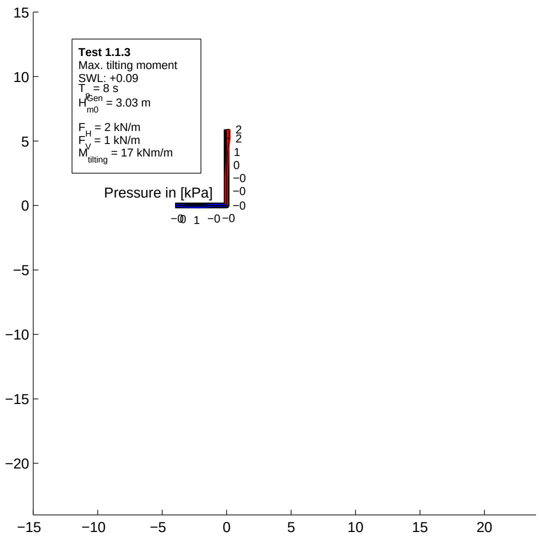

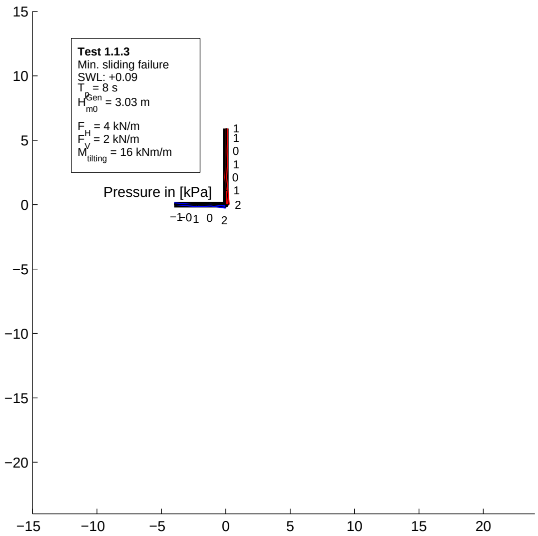

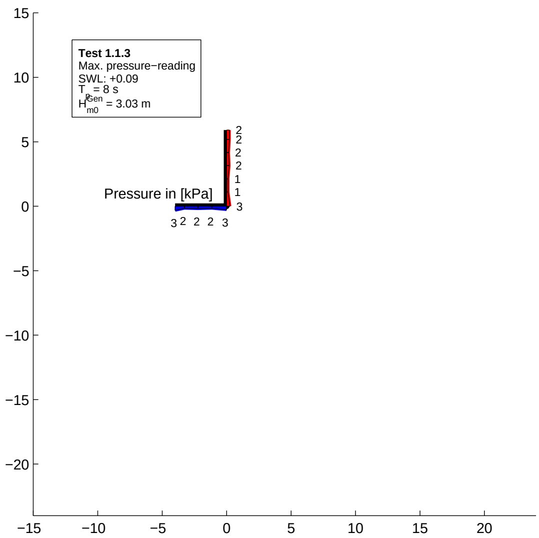

Test no. 1.1.4, SWL: +0.09, $T_{\mathbf{p}}$: 8 s, $H_{m0}^{Gen} = 3.57$ m

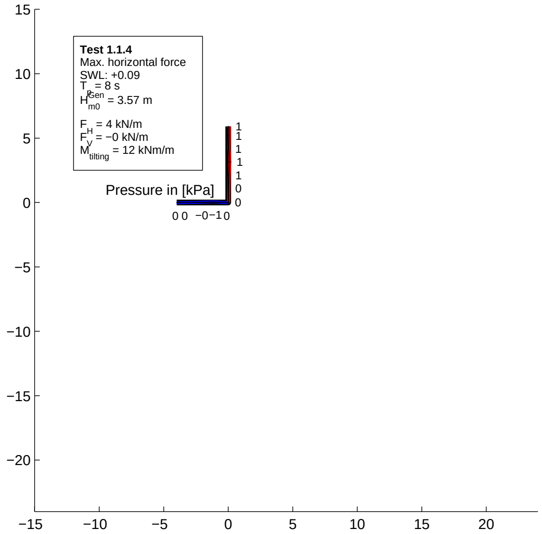

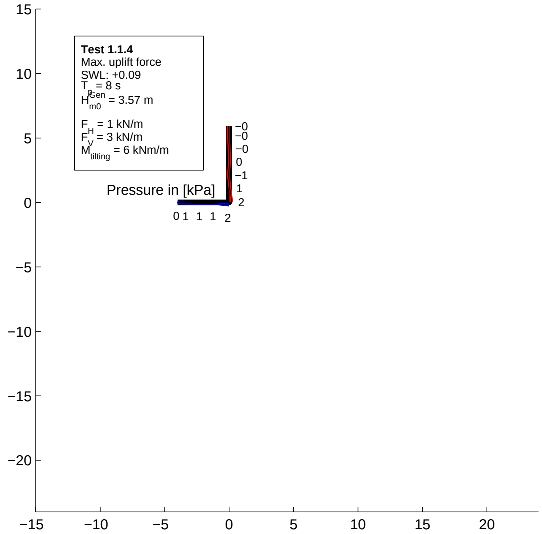

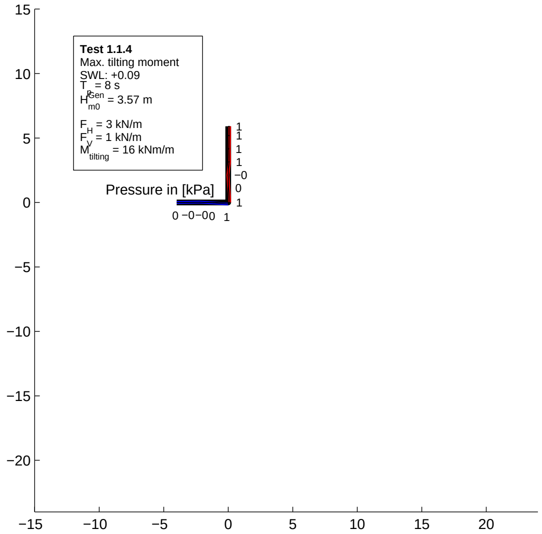

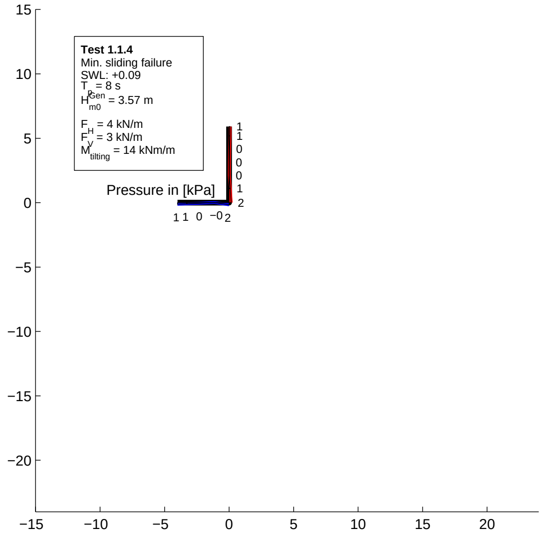

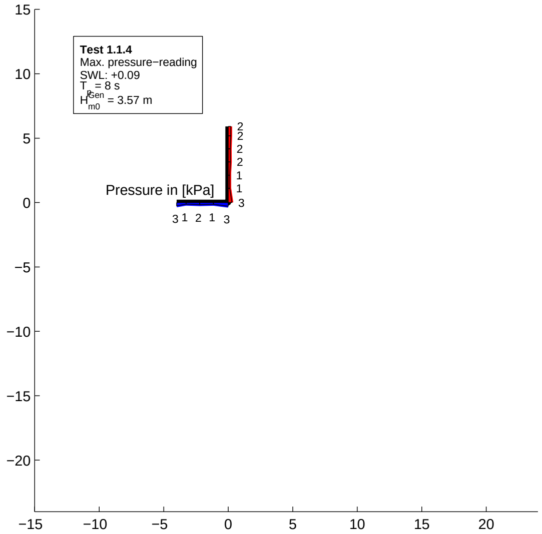

Test no. 1.1.5, SWL: +0.09, T_p: 8 s, $H_{m0}^{Gen} = 3.74$ m

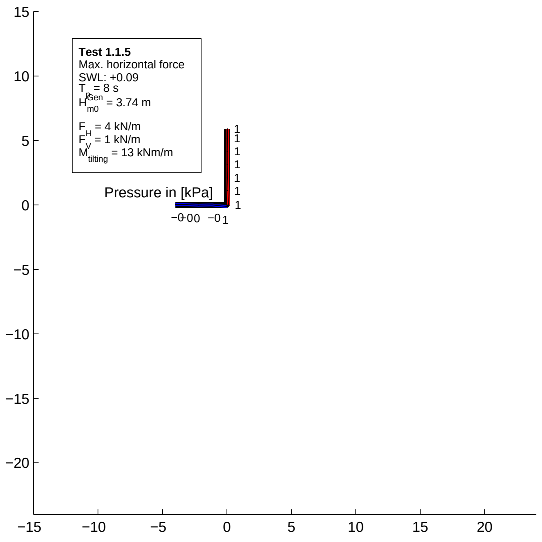

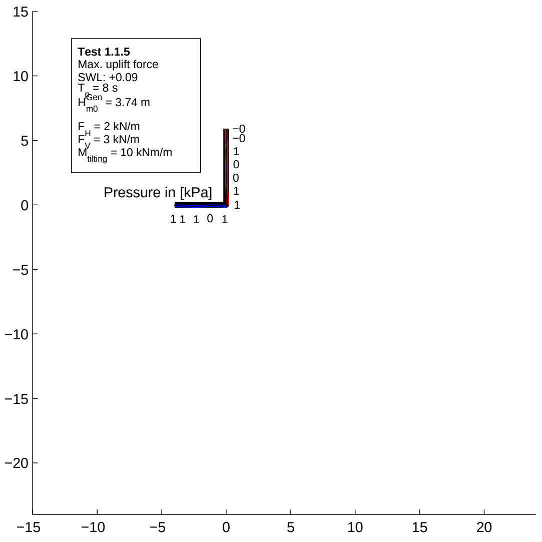

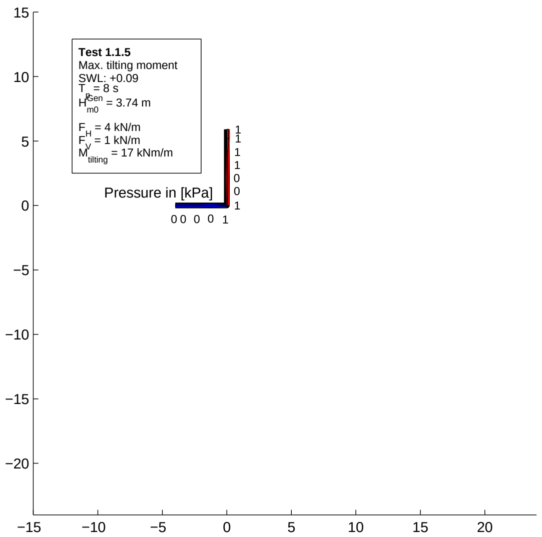

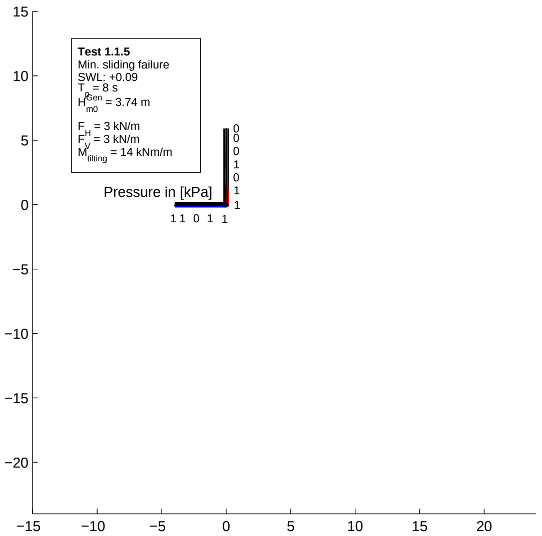

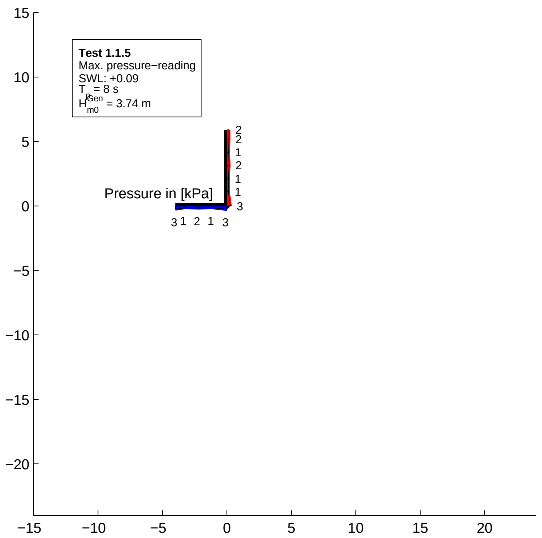

Test no. 1.1.6, SWL: +0.09, T_p: 8 s, $H_{m0}^{Gen} = 4.06$ m

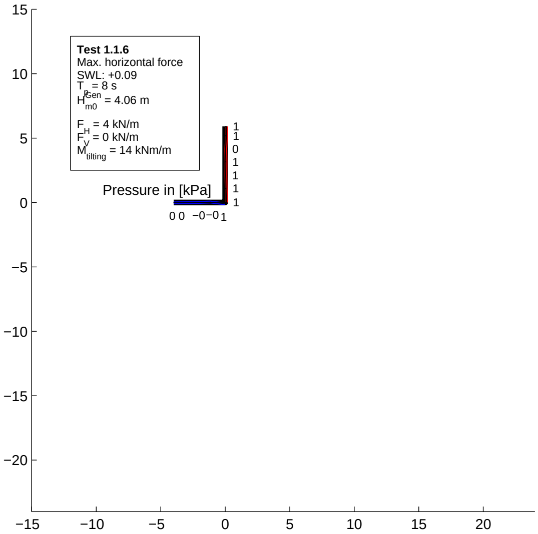

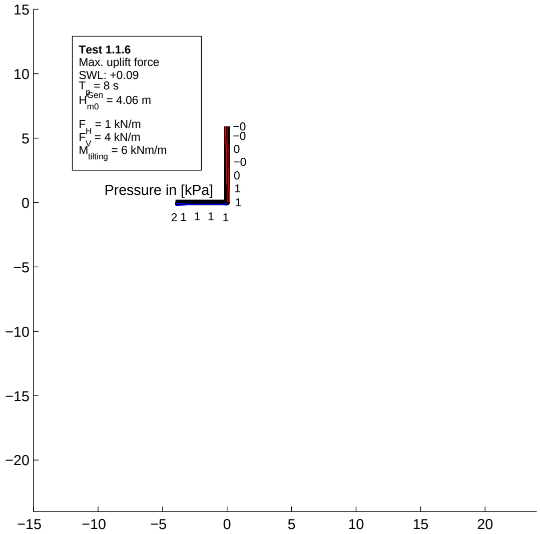

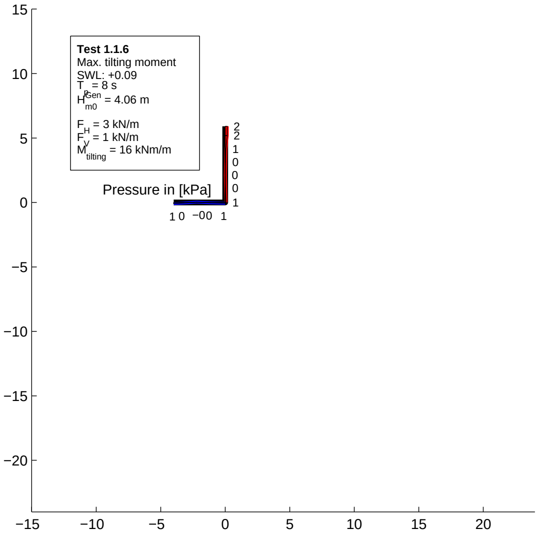

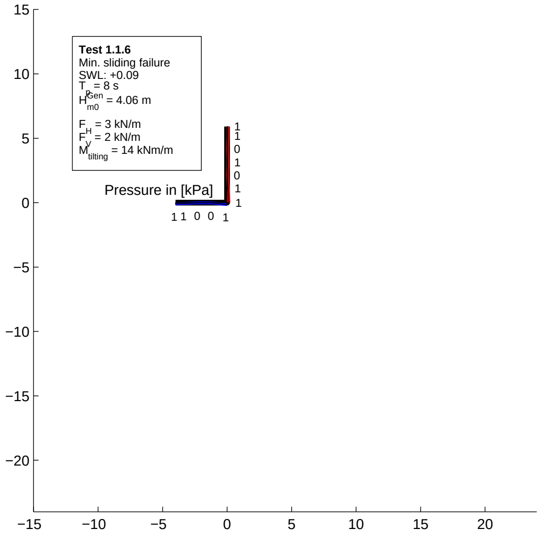

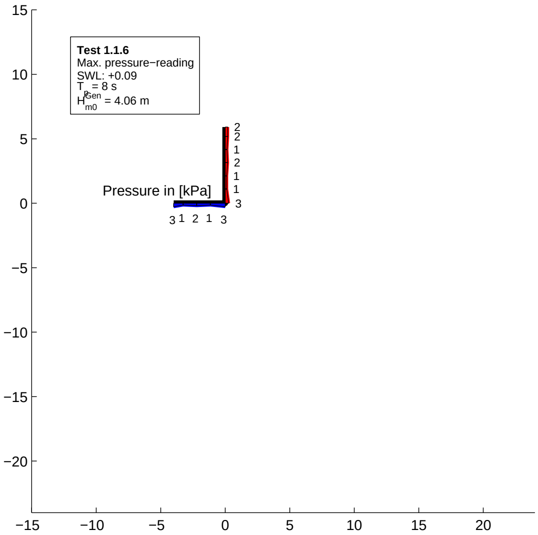

Test no. 1.1.7, SWL: +0.09, T_p: 8 s, $H_{m0}^{Gen} = 4.52$ m

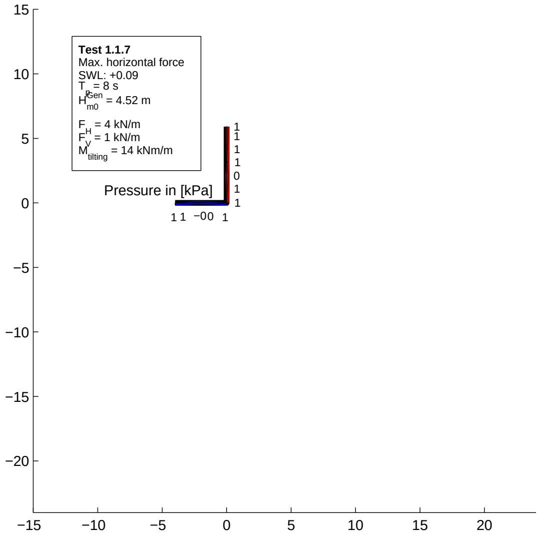

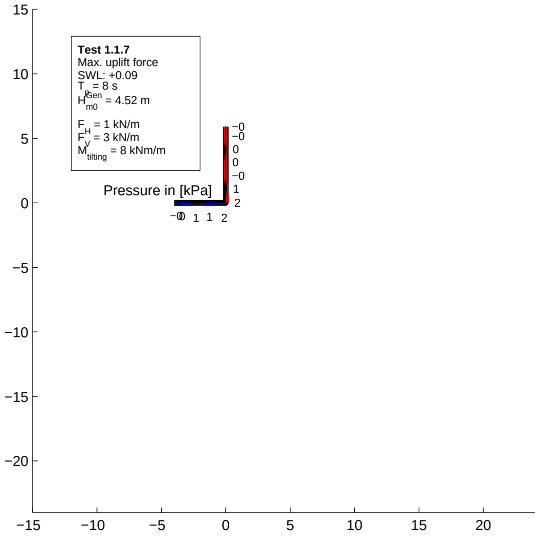

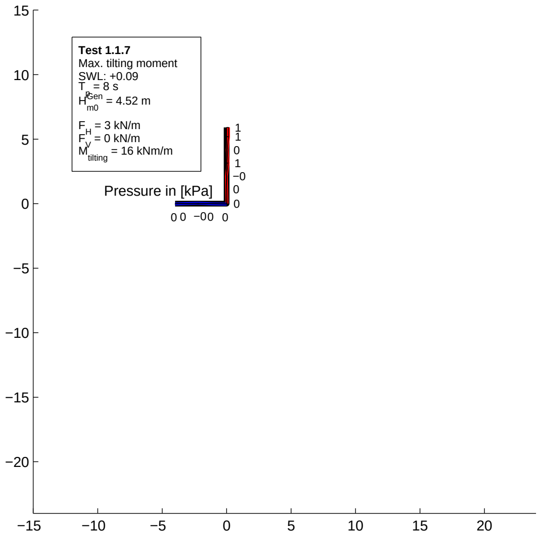

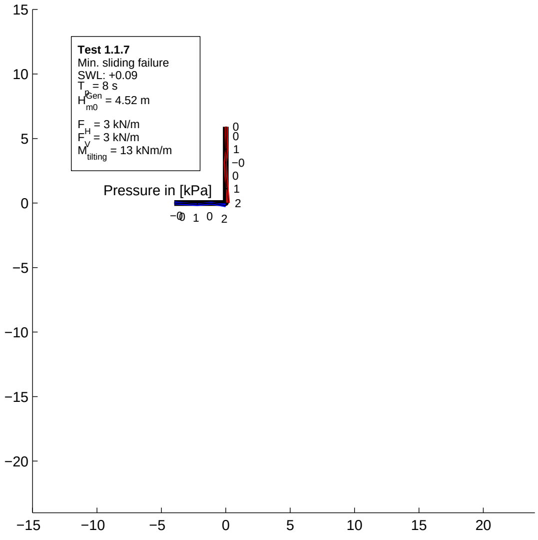

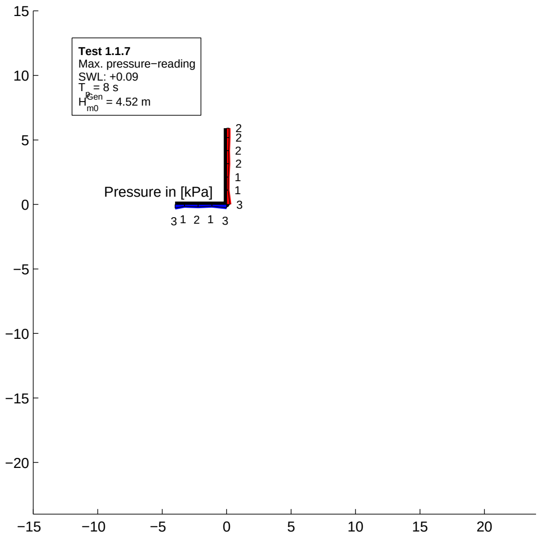

Test no. 1.1.8, SWL: +0.09, T_p: 8 s, $H_{m0}^{Gen} = 4.68$ m

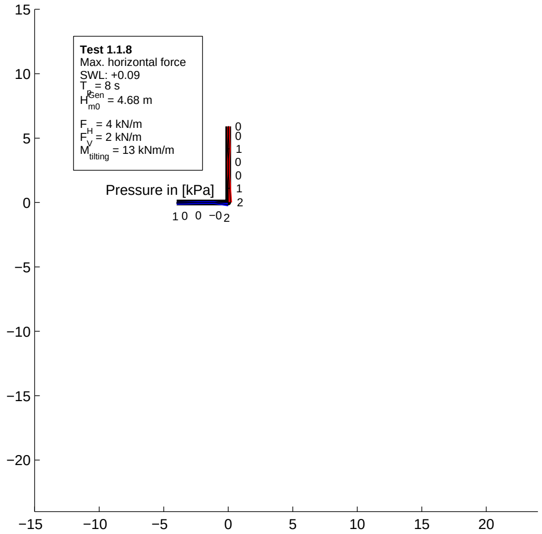

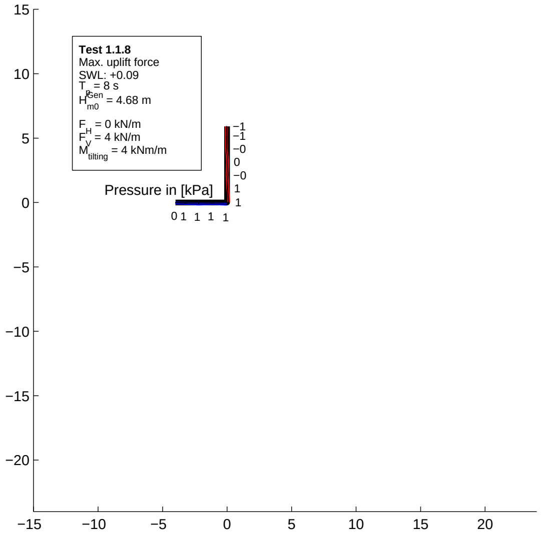

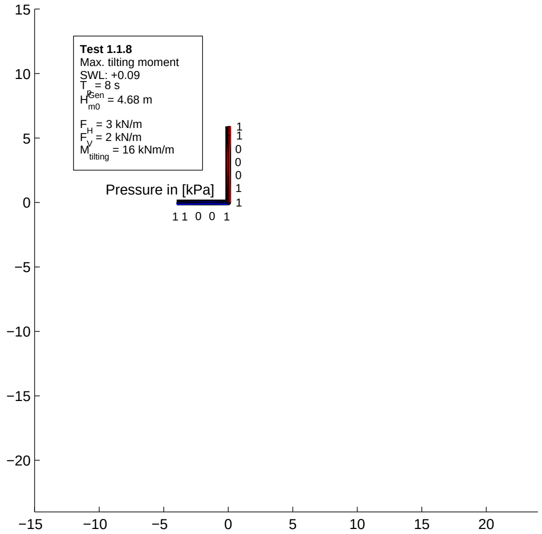

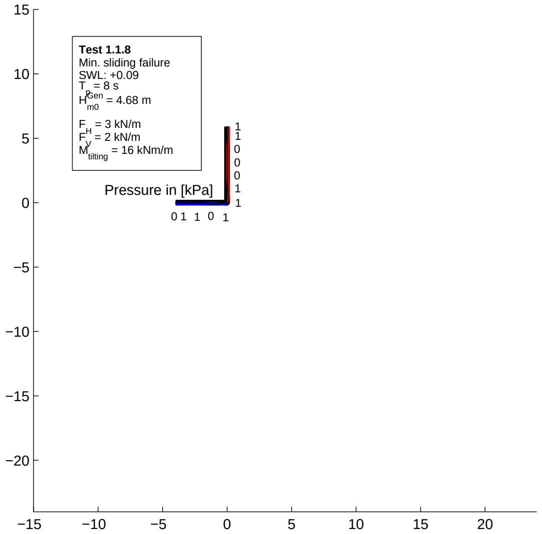

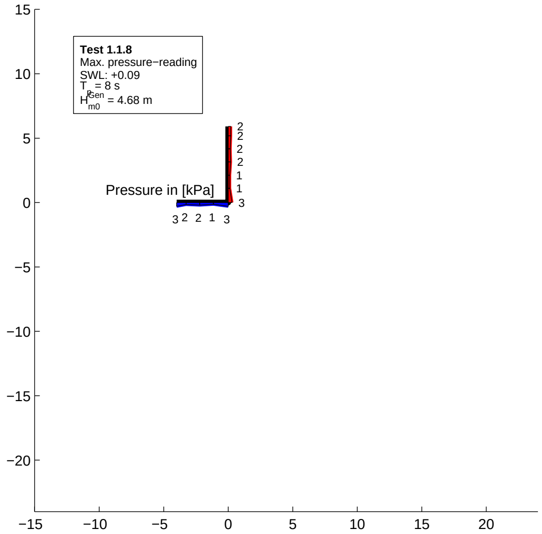

Test no. 1.2.1, SWL: +0.09, T_p: 16 s, $H_{m0}^{Gen} = 2.22$ m

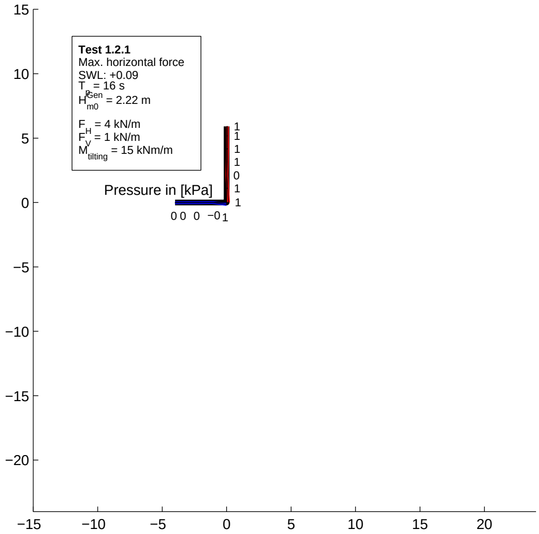

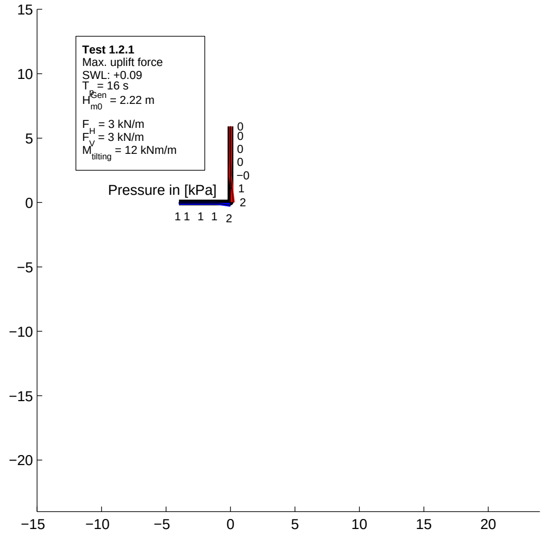

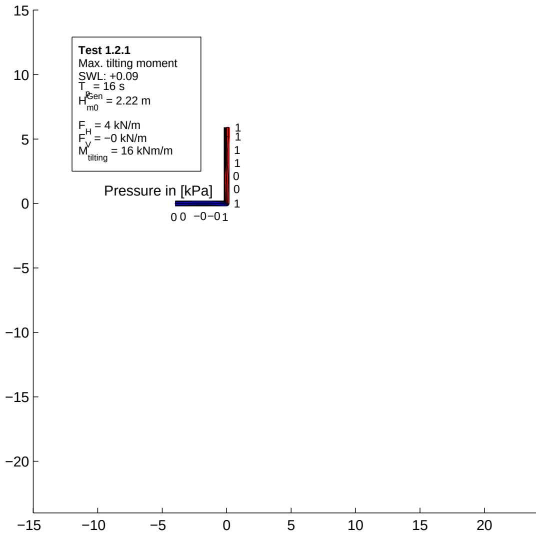

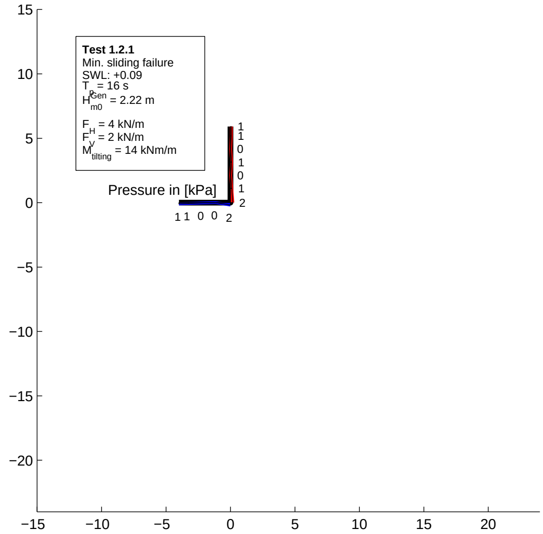

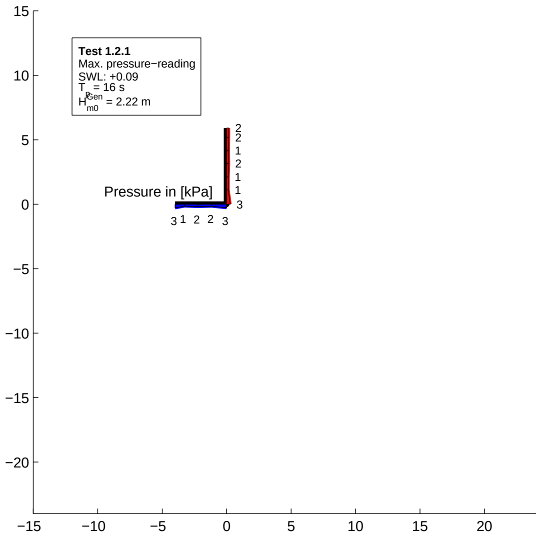

Test no. 1.2.2, SWL: +0.09, $T_{\mathbf{p}}$: 16 s, $H_{m0}^{Gen} = 2.51$ m

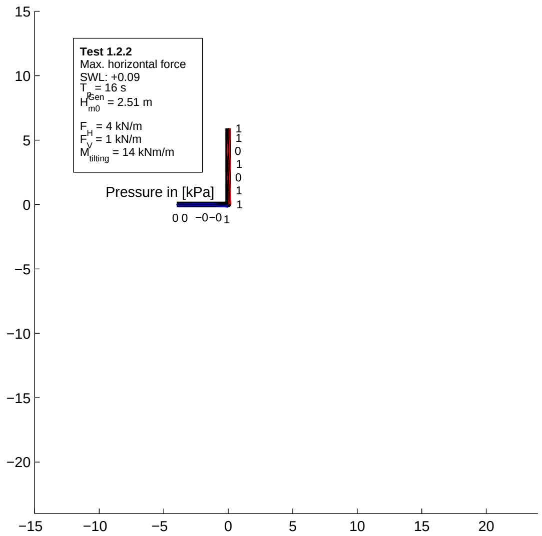

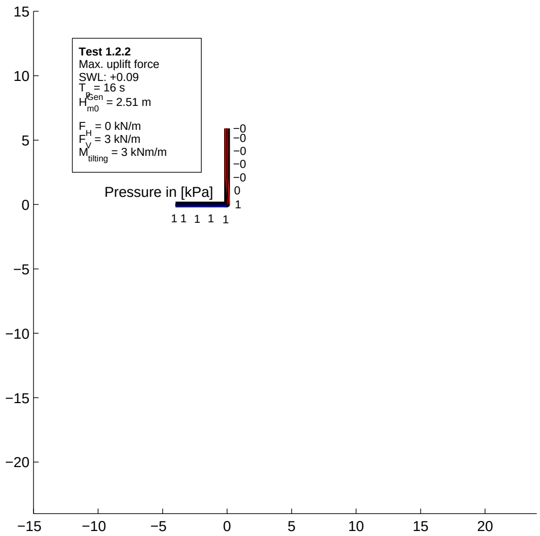

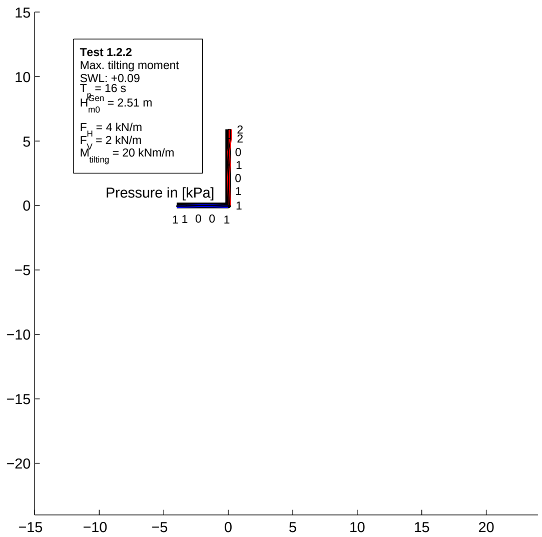

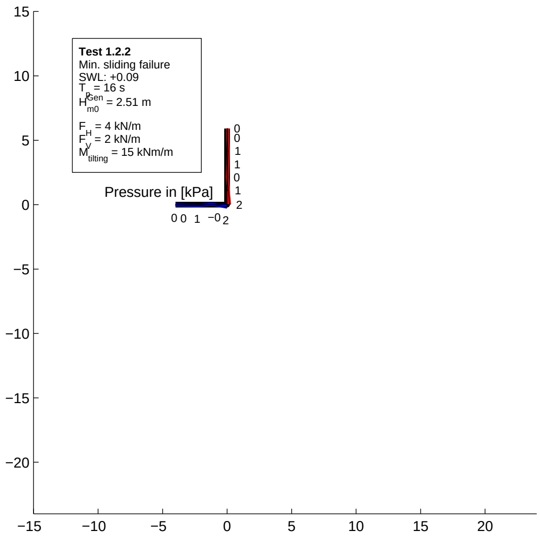

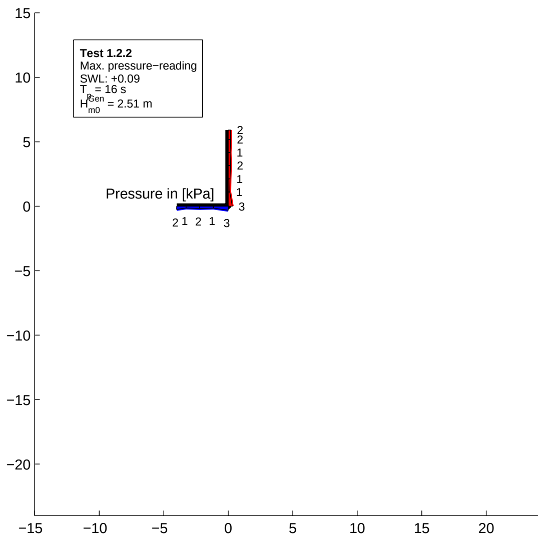

Test no. 1.2.3, SWL: +0.09, $T_\mathbf{p}$: 16 s, $H_{m0}^{Gen} = 2.70$ m

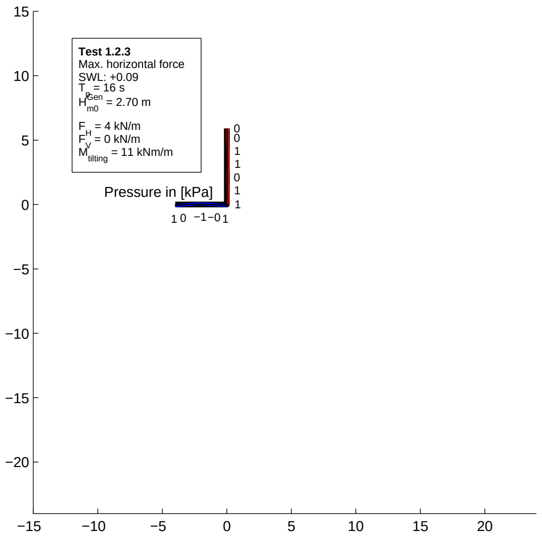

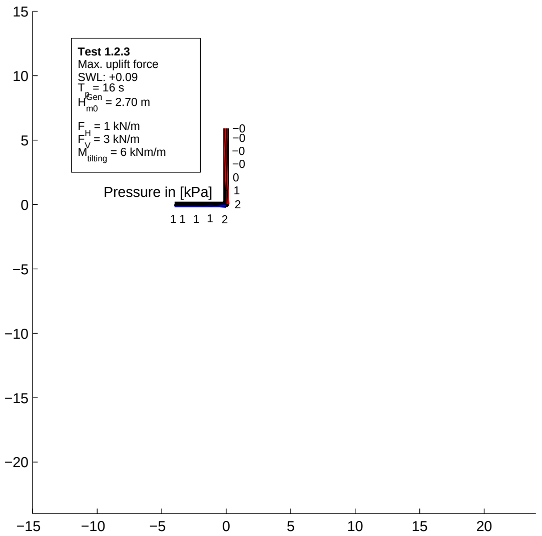

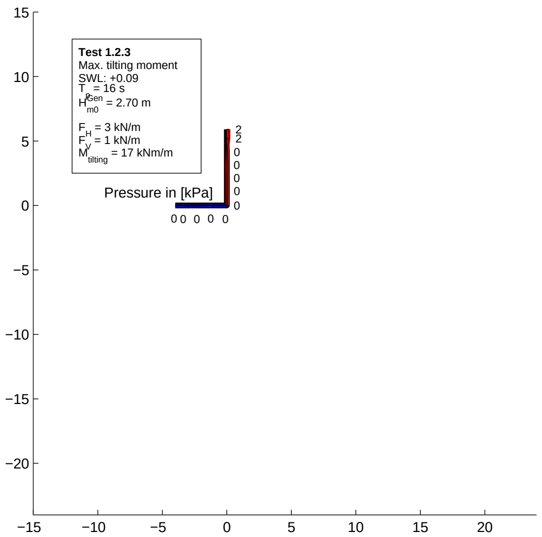

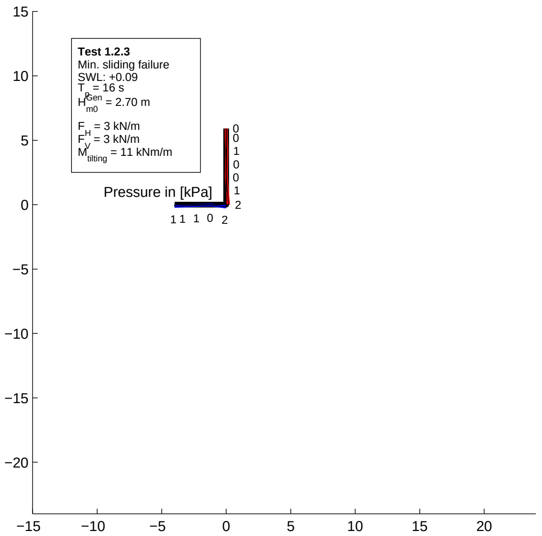

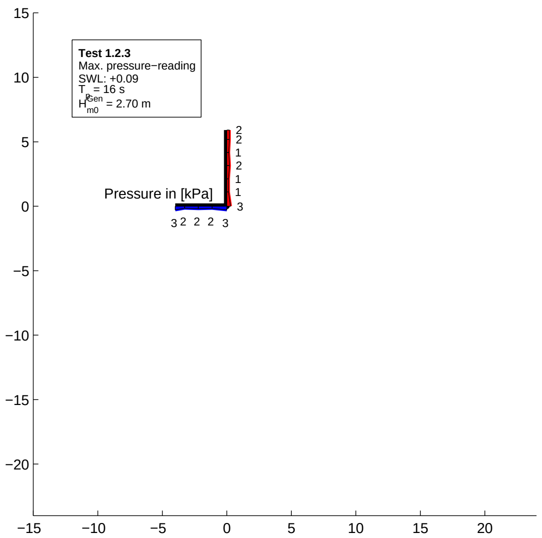

Test no. 1.2.4, SWL: +0.09, $T_\mathbf{p}$: 16 s, $H_{m0}^{Gen} = 3.35$ m

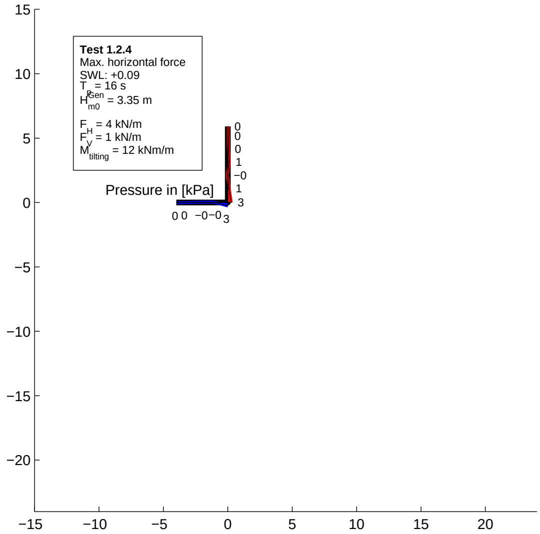

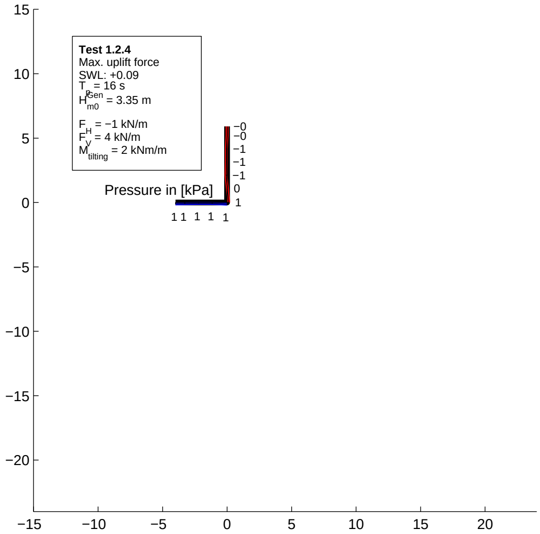

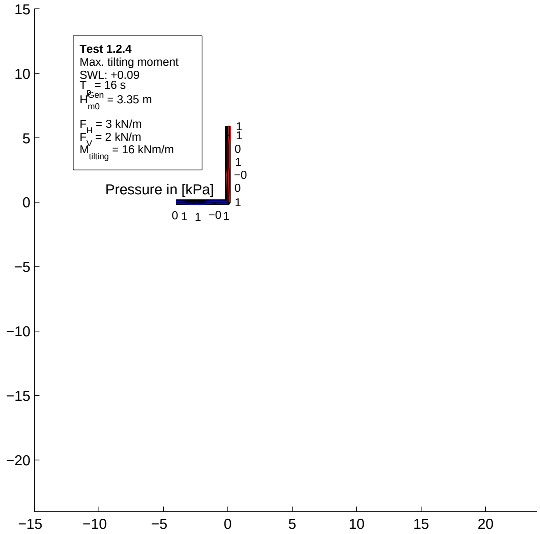

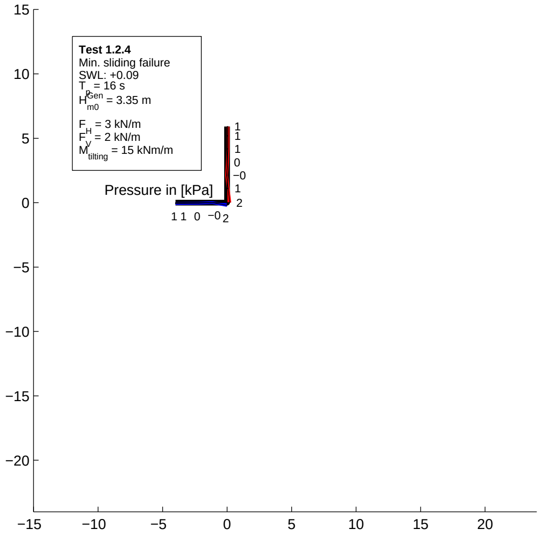

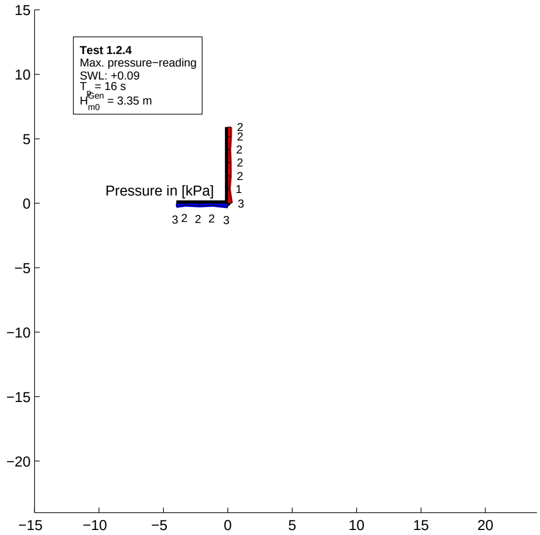

Test no. 1.2.5, SWL: +0.09, T_p: 16 s, $H_{m0}^{Gen} = 3.66$ m

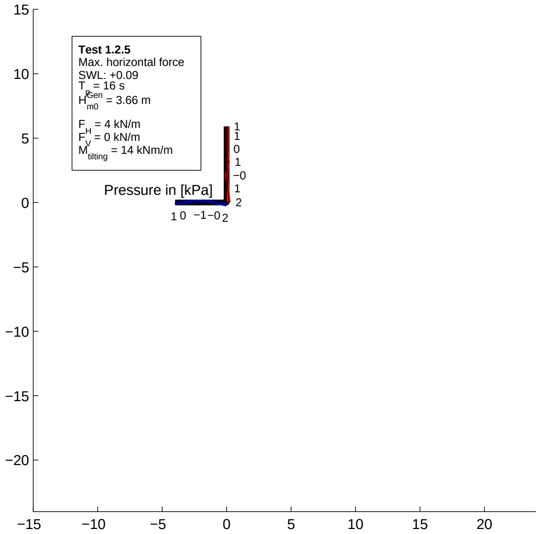

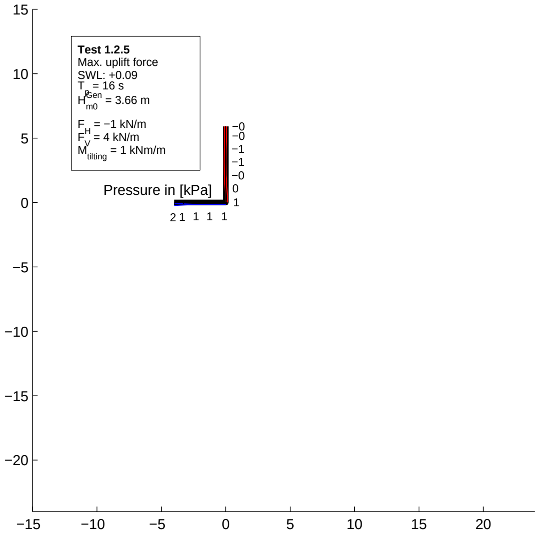

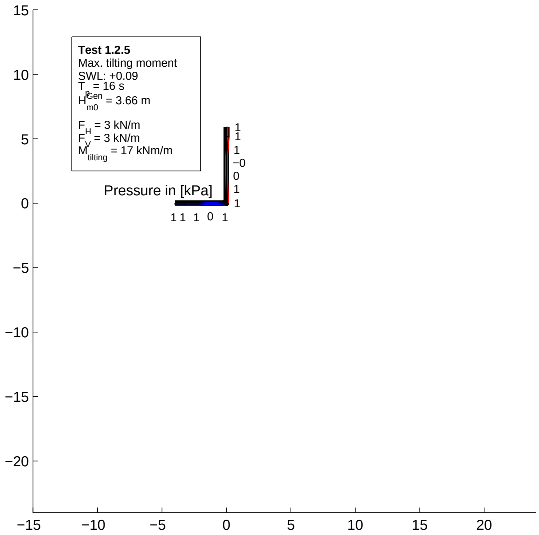

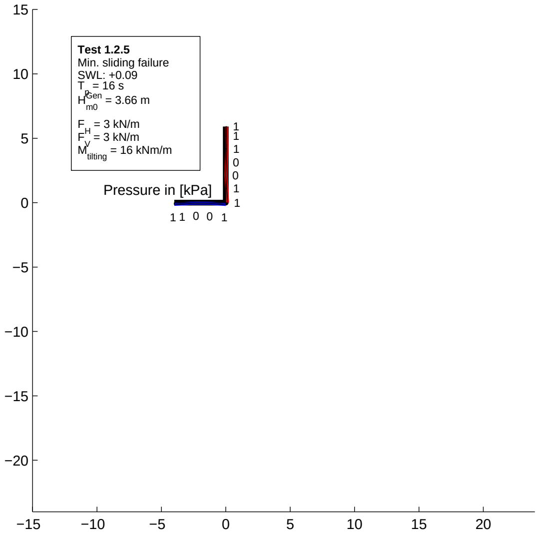

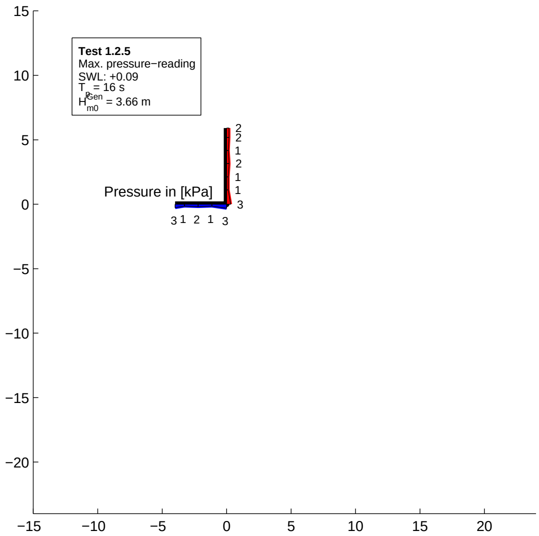

Test no. 1.2.6, SWL: +0.09, $T_\mathbf{p}$: 16 s, $H_{m0}^{Gen} = 4.19$ m

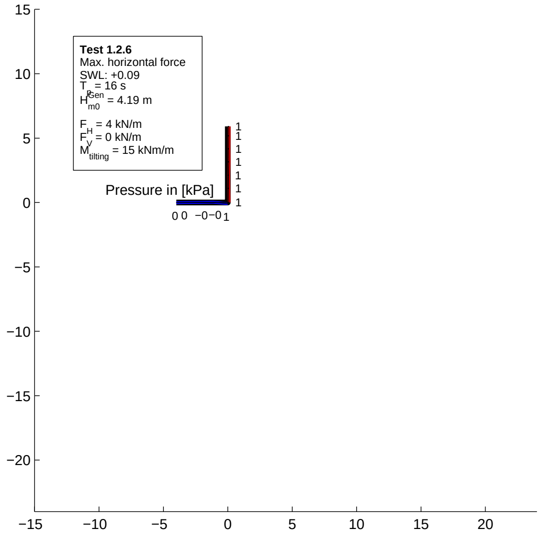

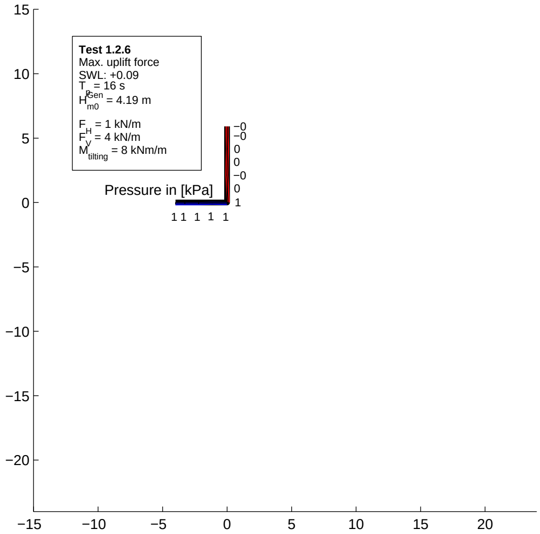

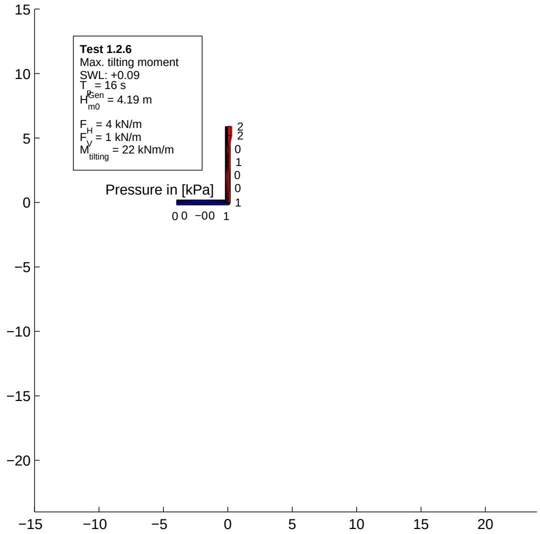

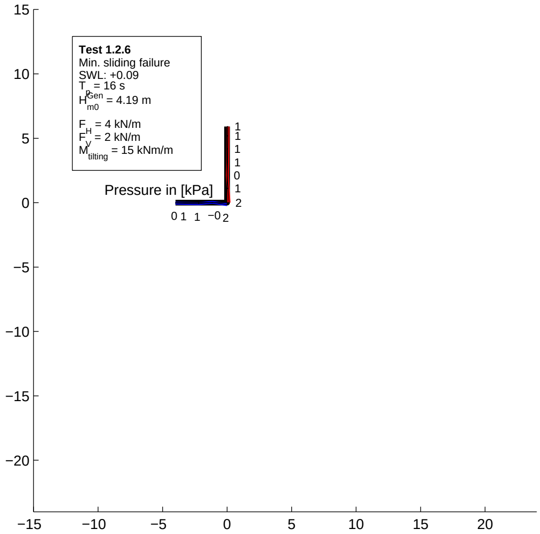

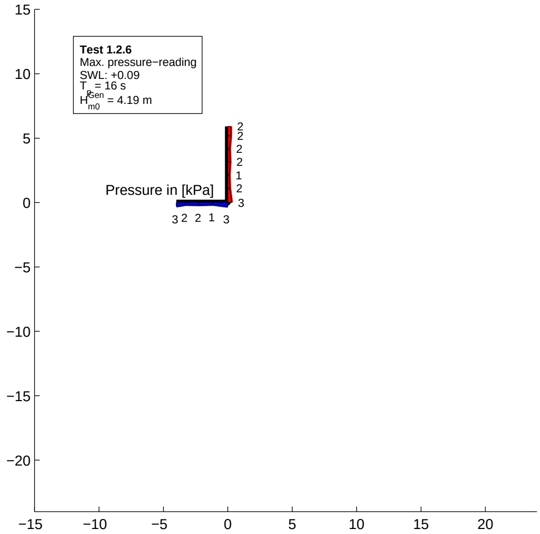

Test no. 1.2.7, SWL: +0.09, $T_\mathbf{p}$: 16 s, $H_{m0}^{Gen} = 4.28$ m

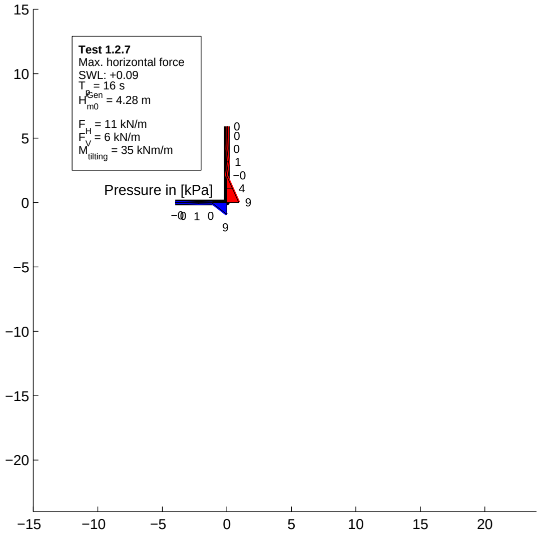

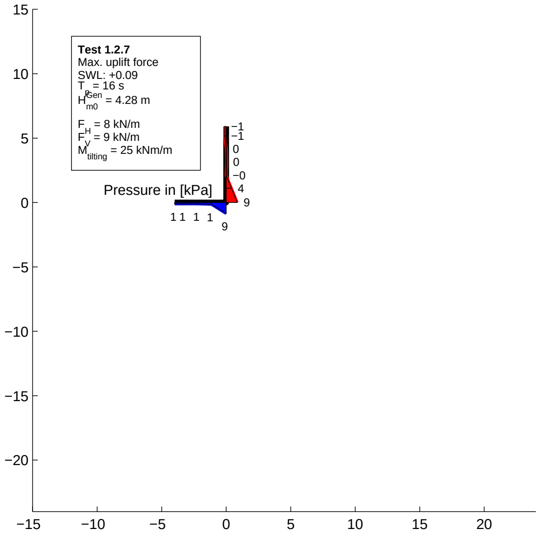

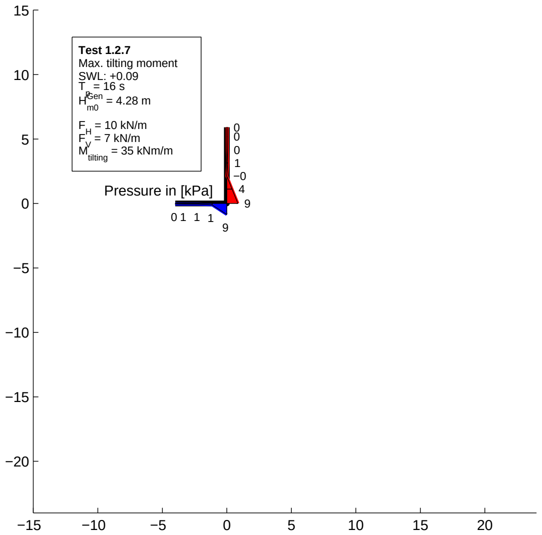

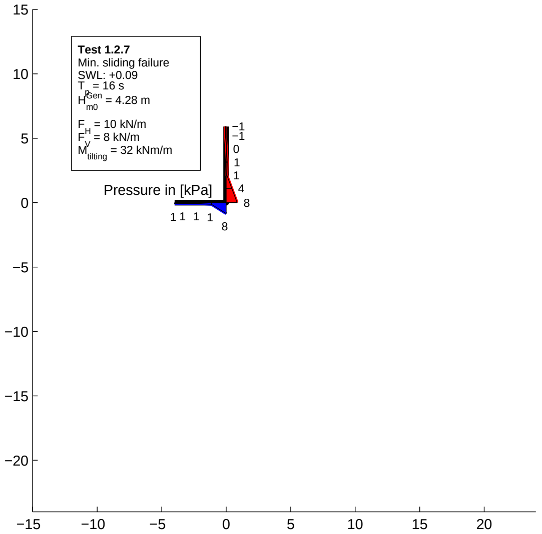

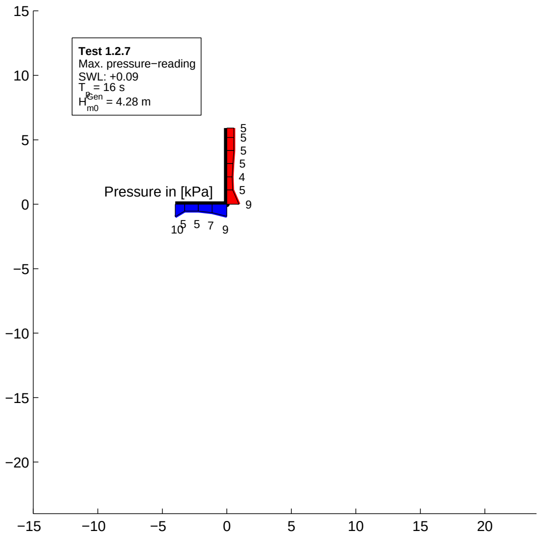

Test no. 2.1.1, SWL: +3.50, T_p: 8 s, $H_{m0}^{Gen} = 2.70$ m

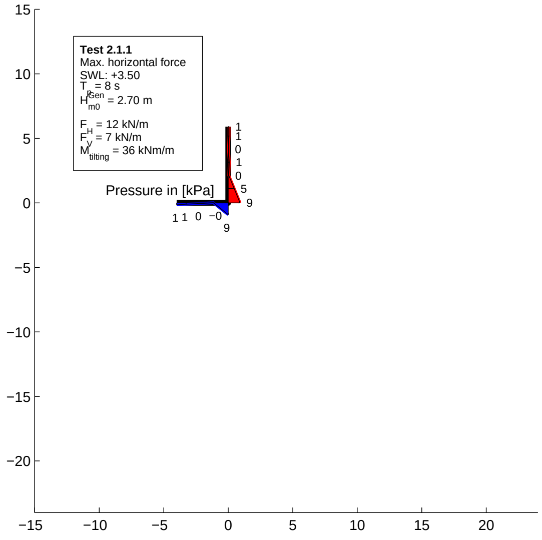

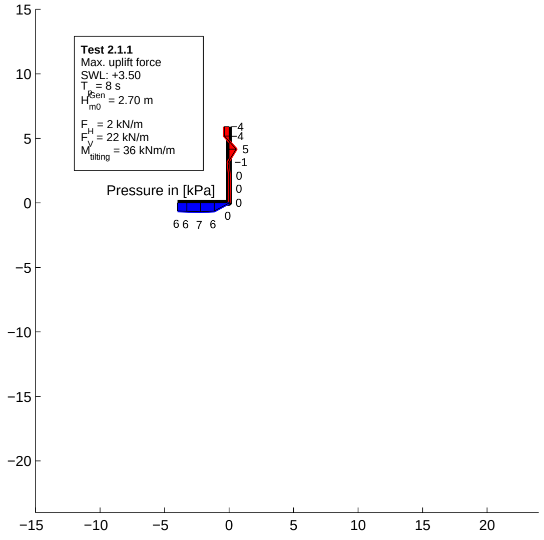

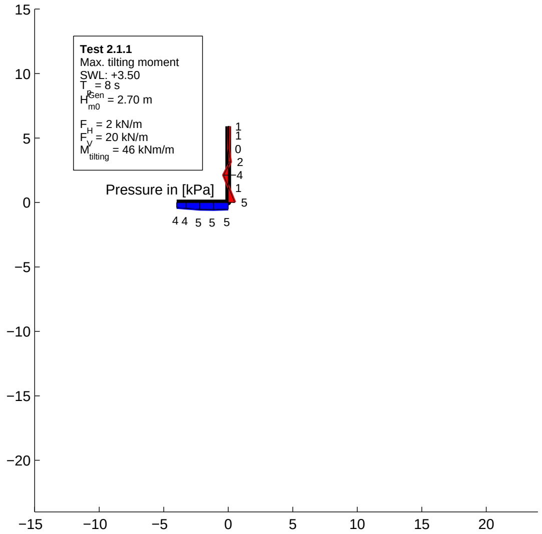

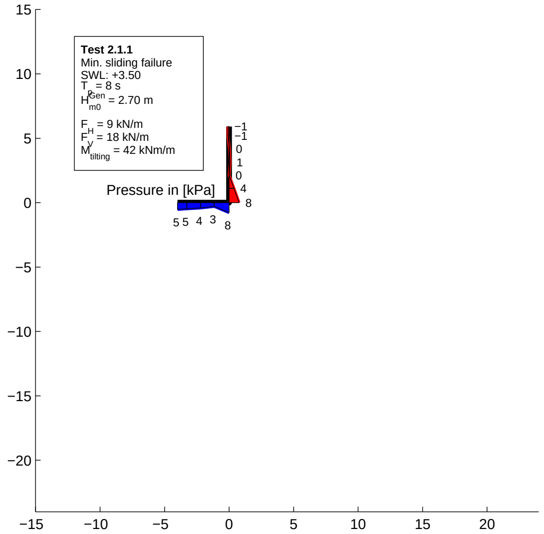

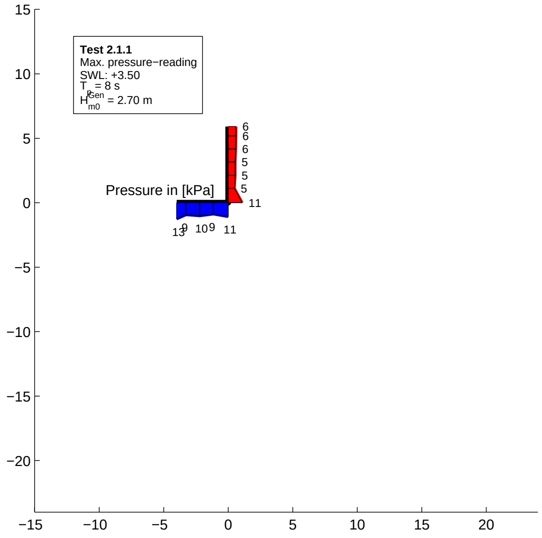

Test no. 2.1.2, SWL: +3.50, T_p: 8 s, $H_{m0}^{Gen} = 3.14$ m

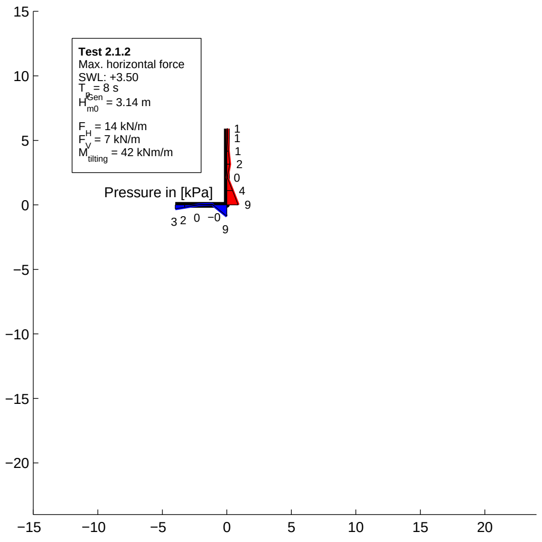

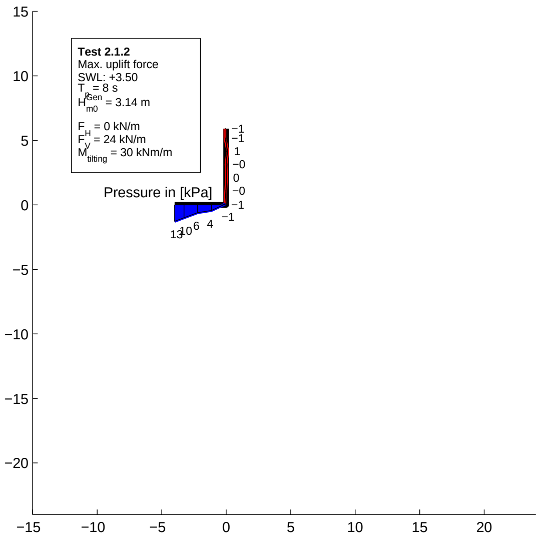

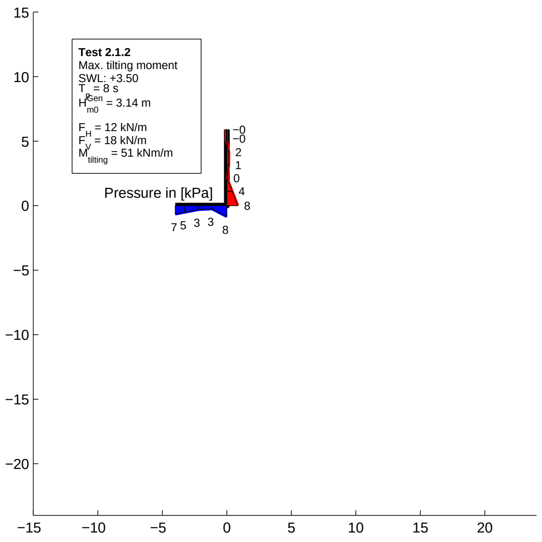

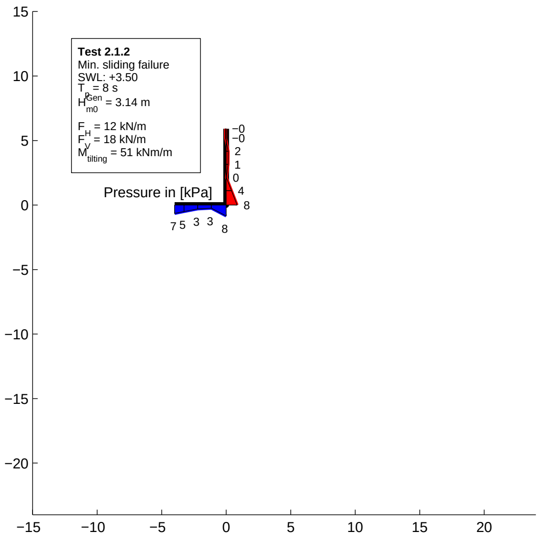

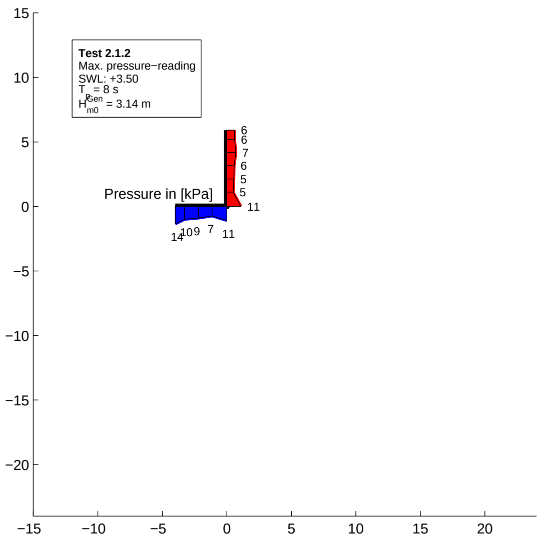

Test no. 2.1.3, SWL: +3.50, T_p: 8 s, $H_{m0}^{Gen} = 3.31$ m

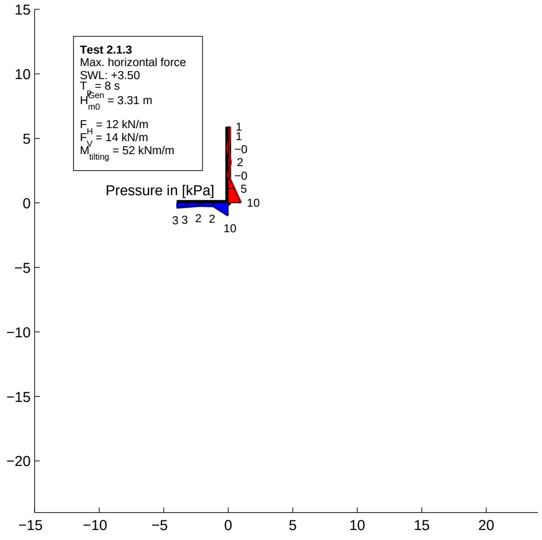

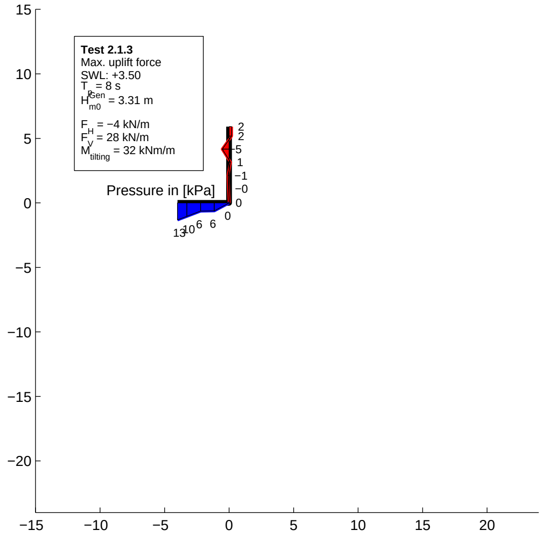

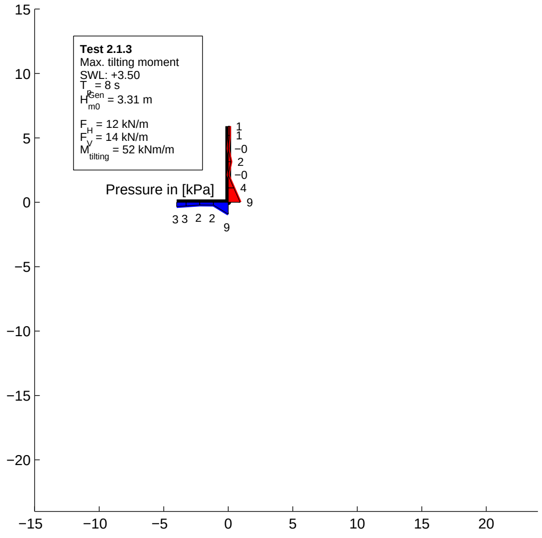

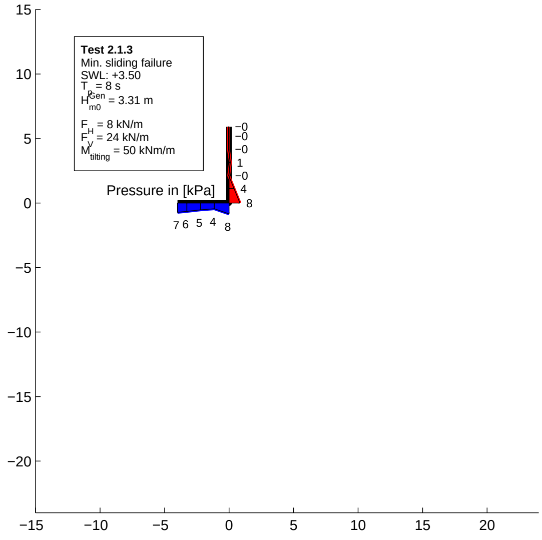

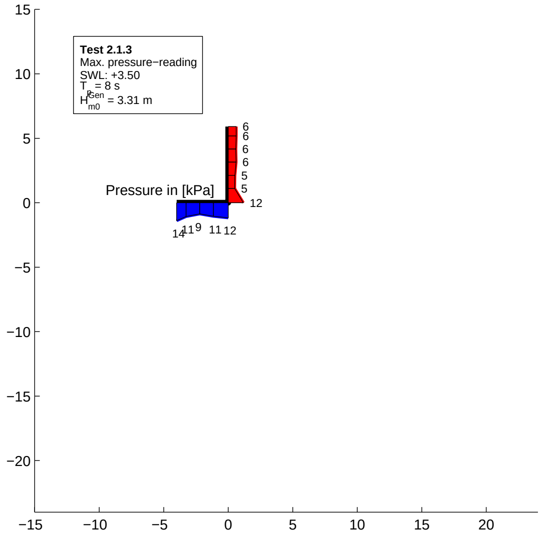

Test no. 2.1.4, SWL: +3.50, T_p: 8 s, $H_{m0}^{Gen} = 3.92$ m

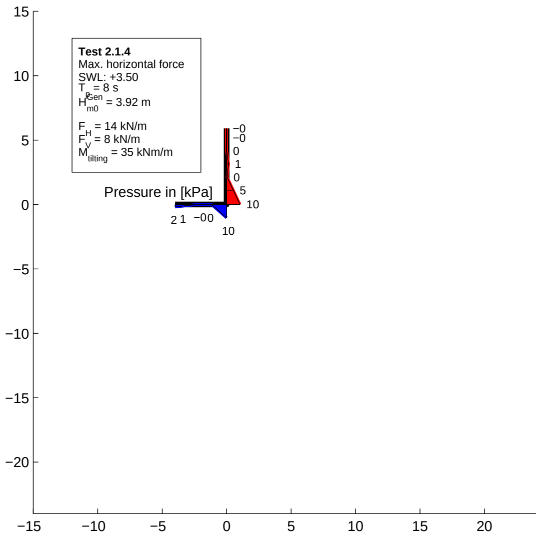

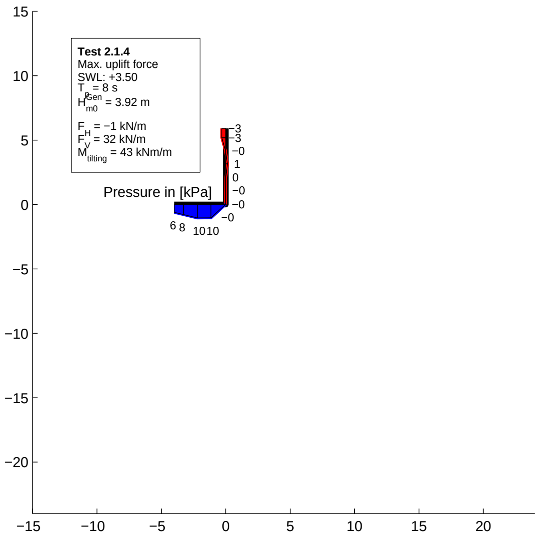

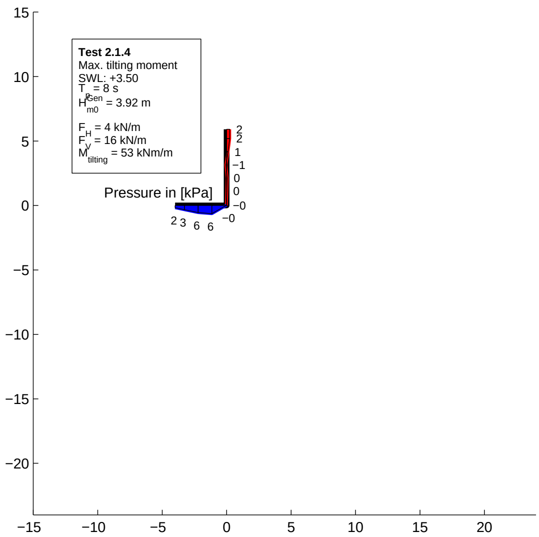

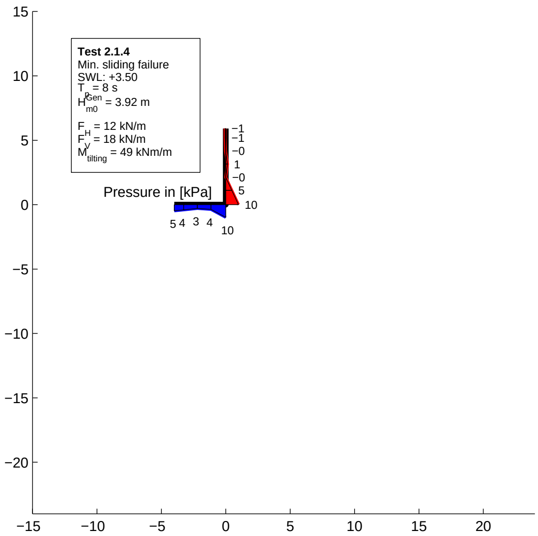

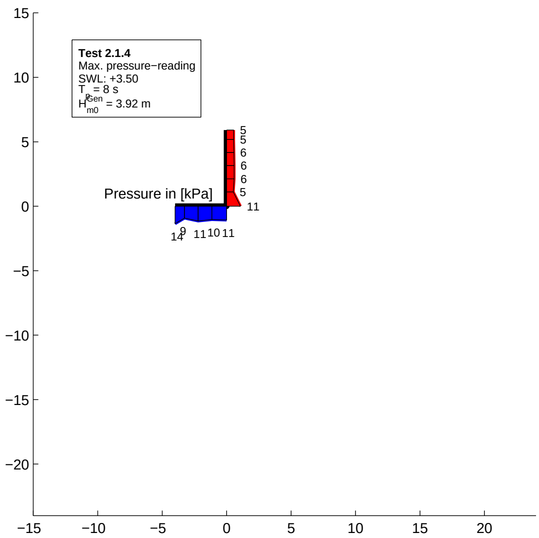

Test no. 2.1.5, SWL: +3.50, T_p: 8 s, $H_{m0}^{Gen} = 4.15$ m

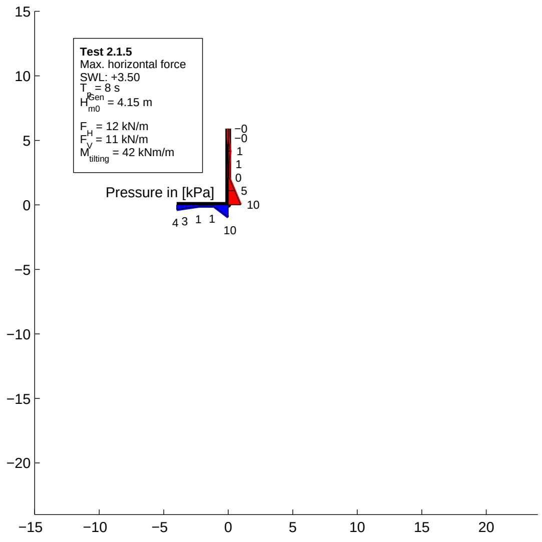

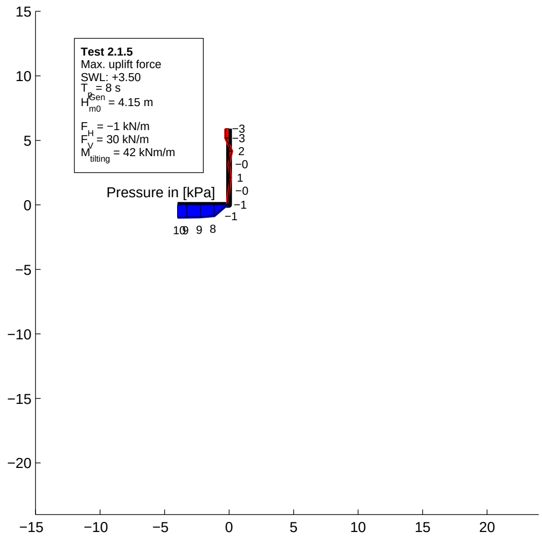

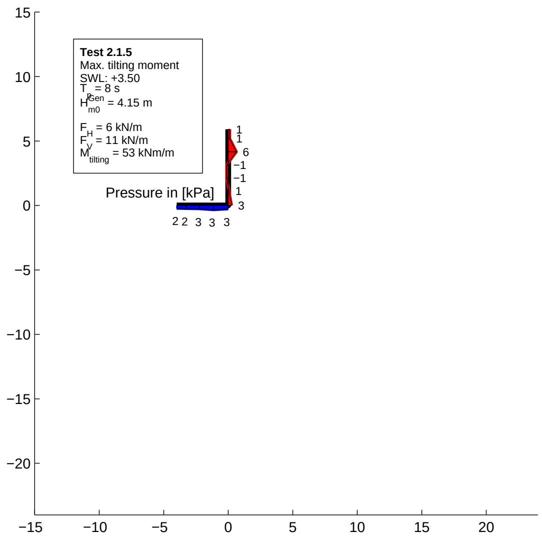

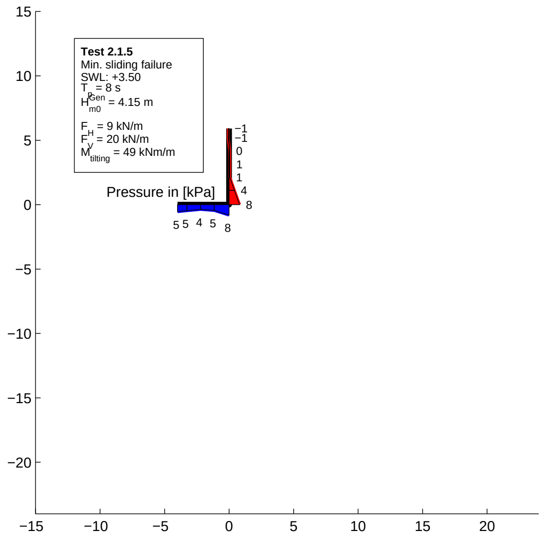

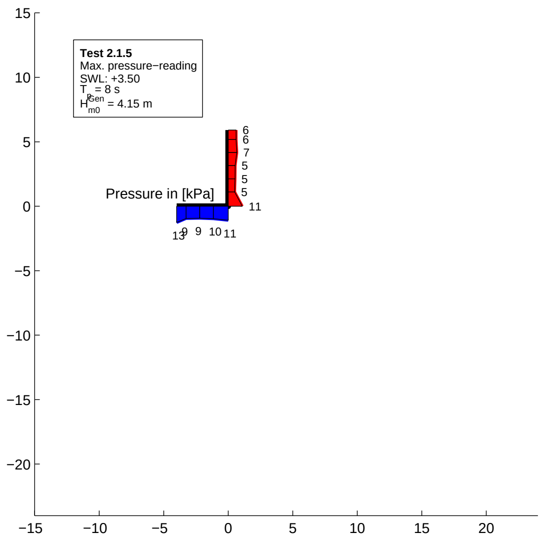

Test no. 2.1.6, SWL: +3.50, T_p: 8 s, $H_{m0}^{Gen} = 4.74$ m

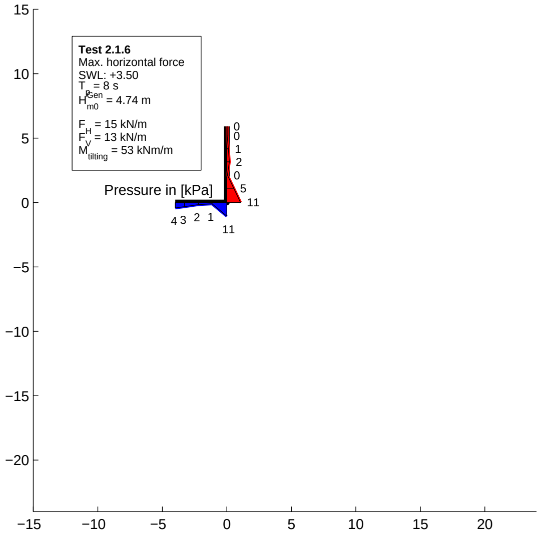

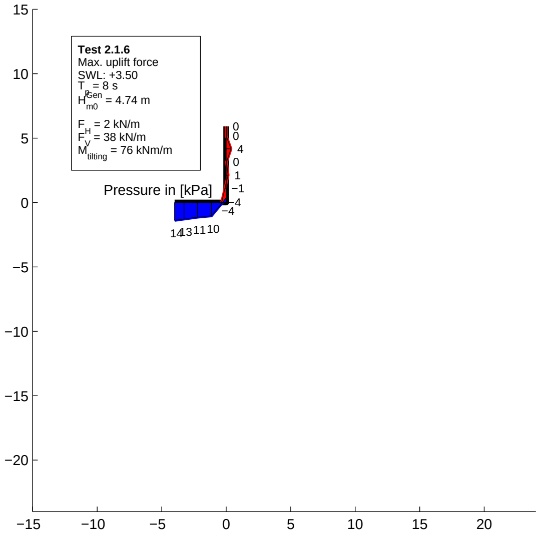

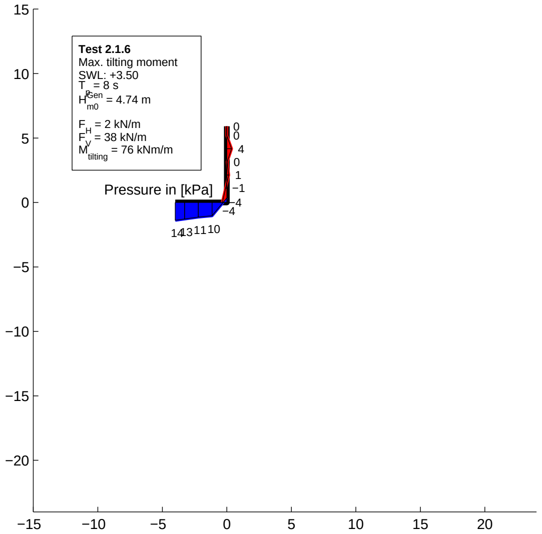

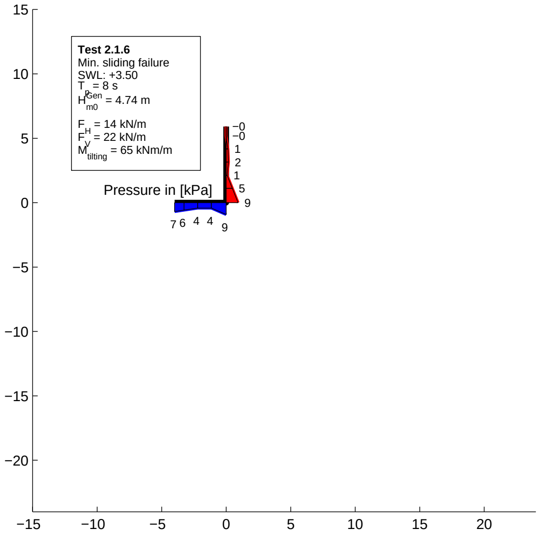

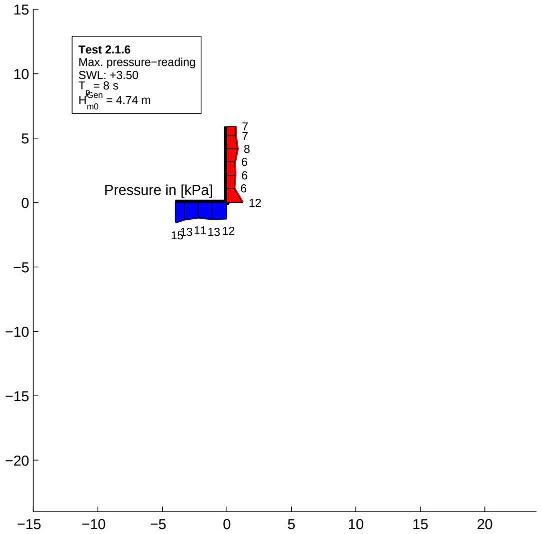

Test no. 2.1.7, SWL: +3.50, T_p: 8 s, $H_{m0}^{Gen} = 4.87$ m

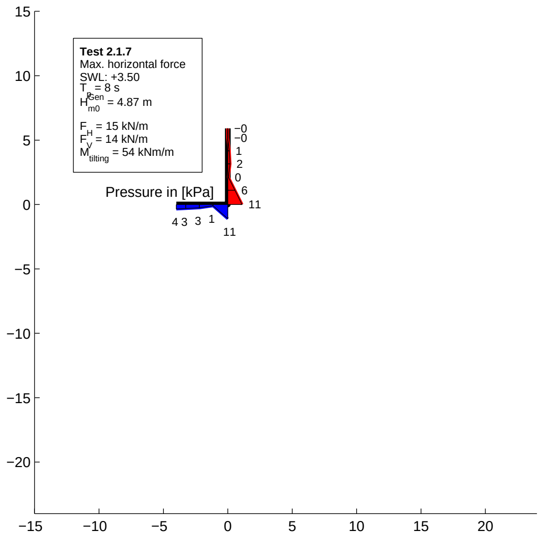

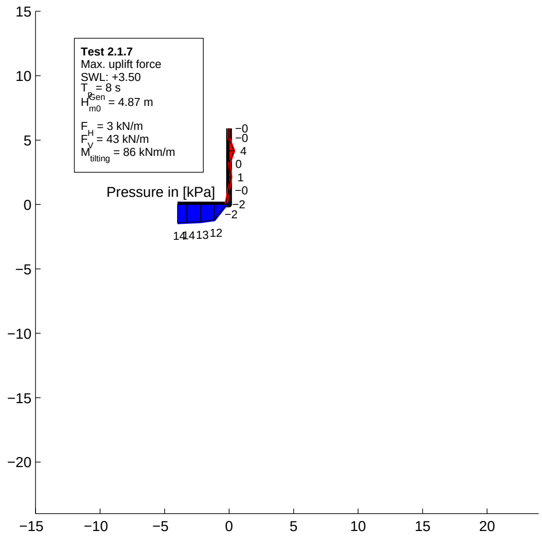

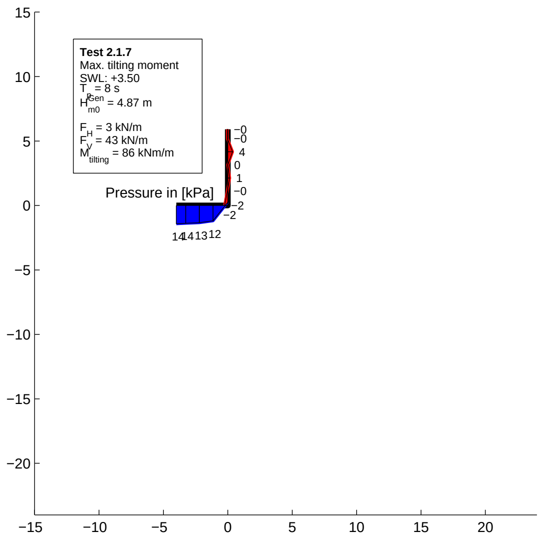

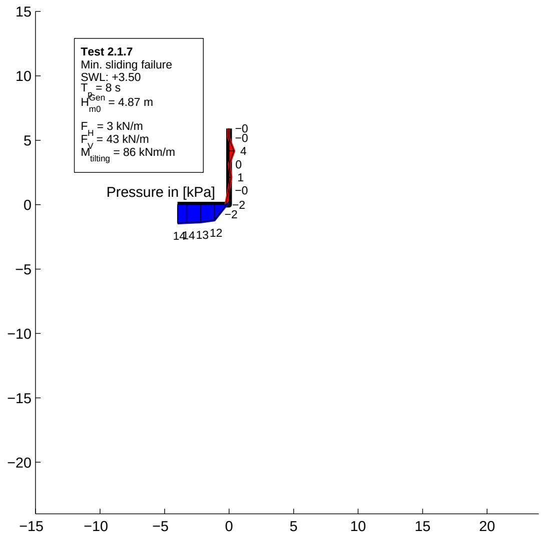

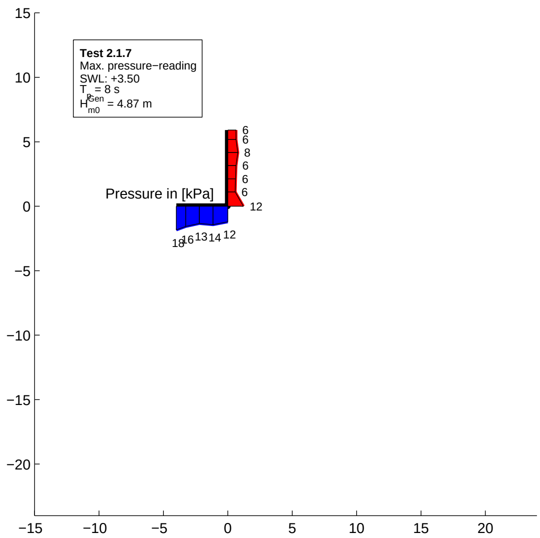

Test no. 2.2.1, SWL: +3.50, T_p: 16 s, $H_{m0}^{Gen} = 2.50$ m

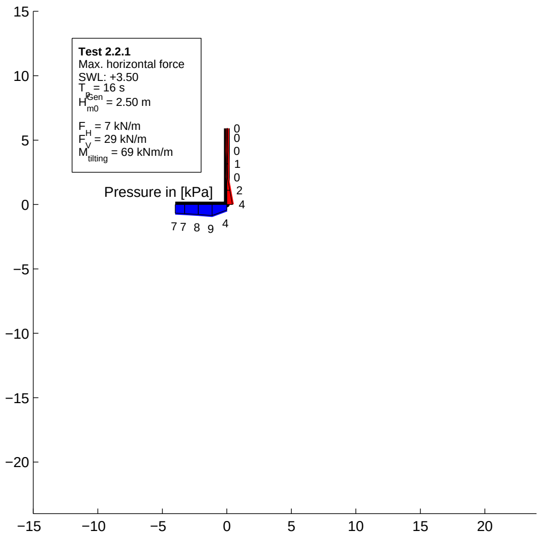

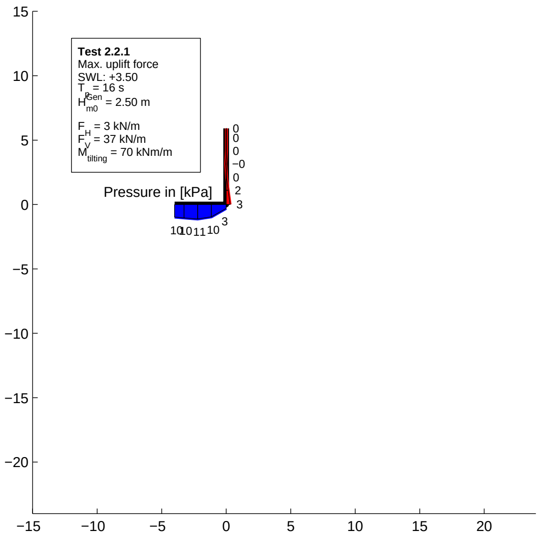

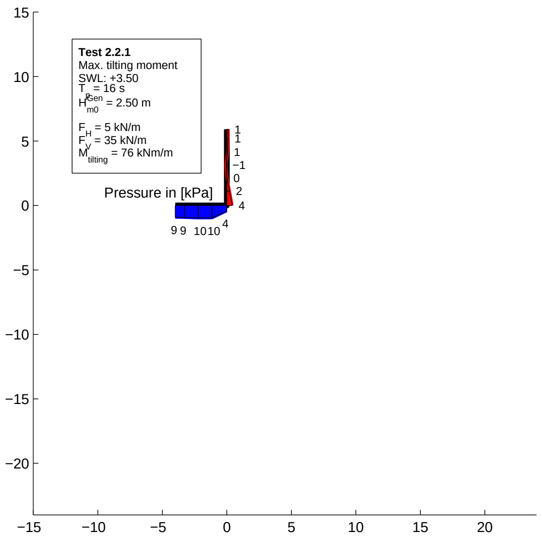

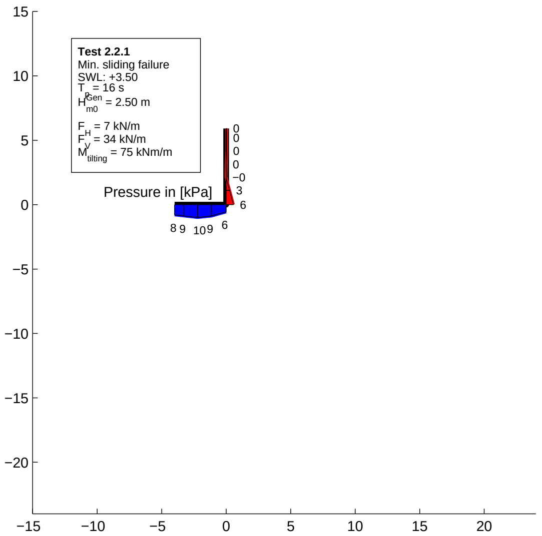

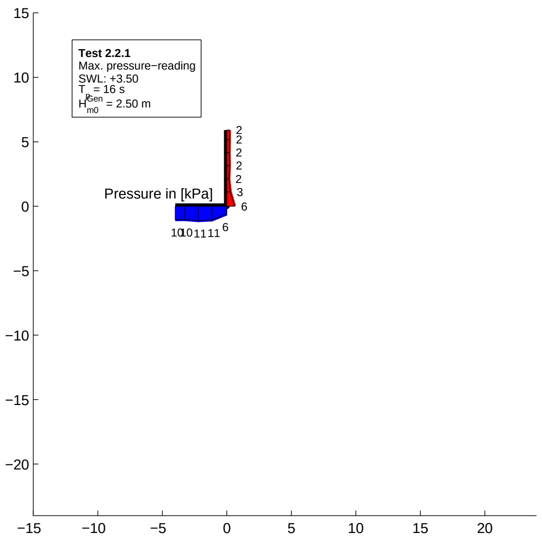

Test no. 2.2.2, SWL: +3.50, T_{p}: 16 s, $H_{m0}^{Gen} = 3.04$ m

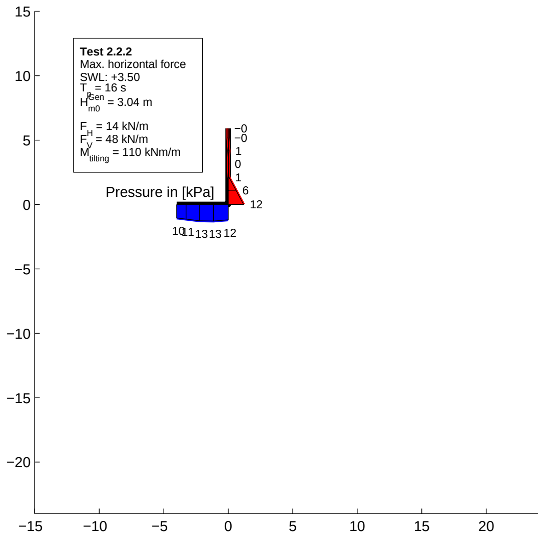

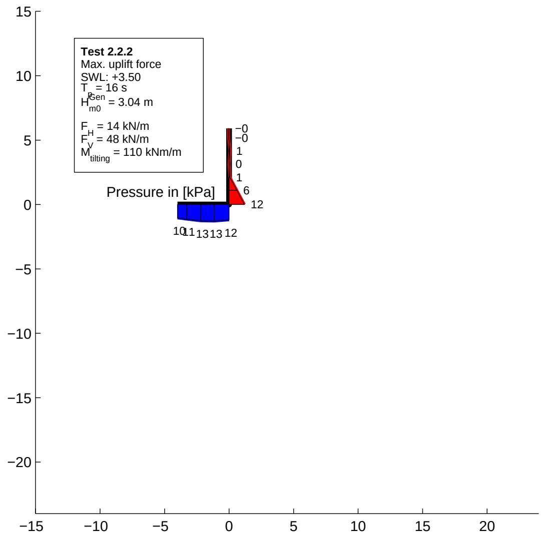

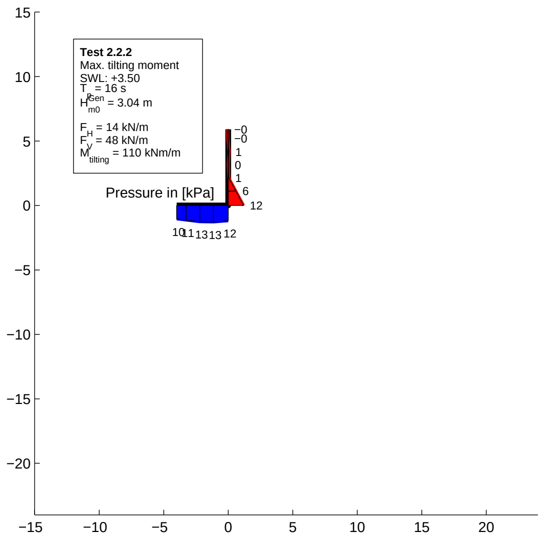

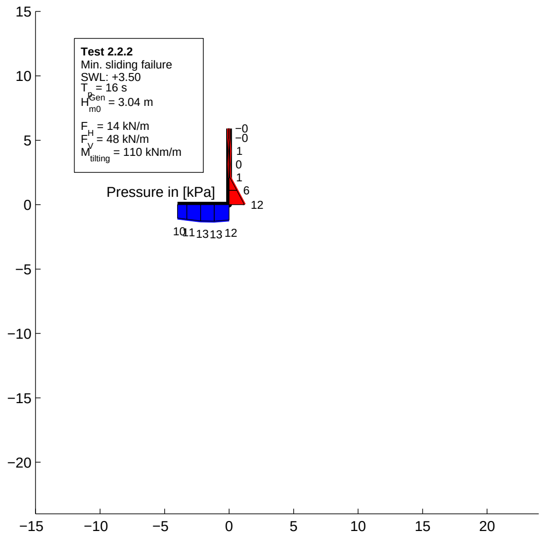

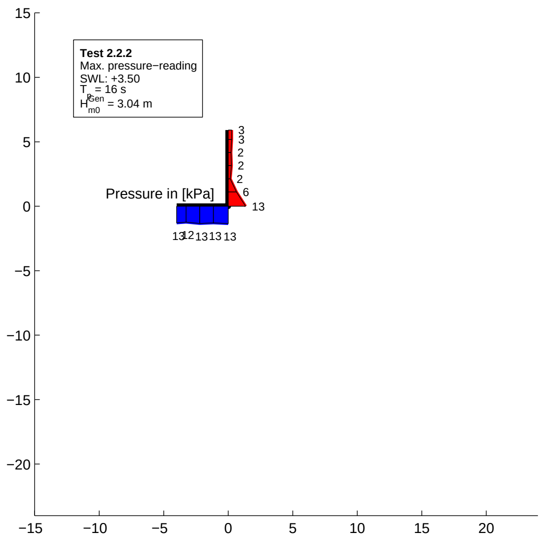

Test no. 2.2.3, SWL: +3.50, $T_\mathbf{p}$: 16 s, $H_{m0}^{Gen} = 3.66$ m

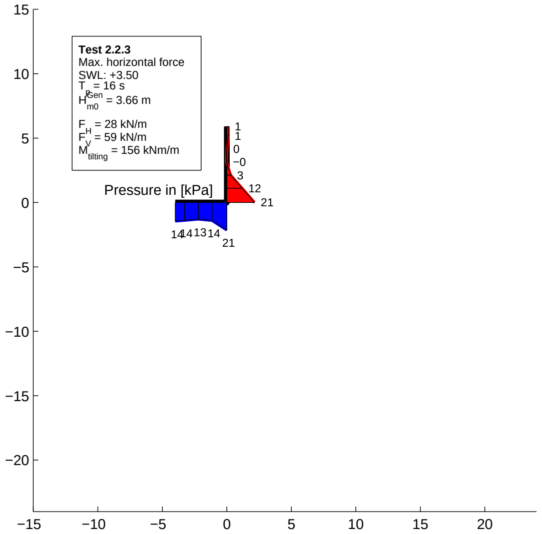

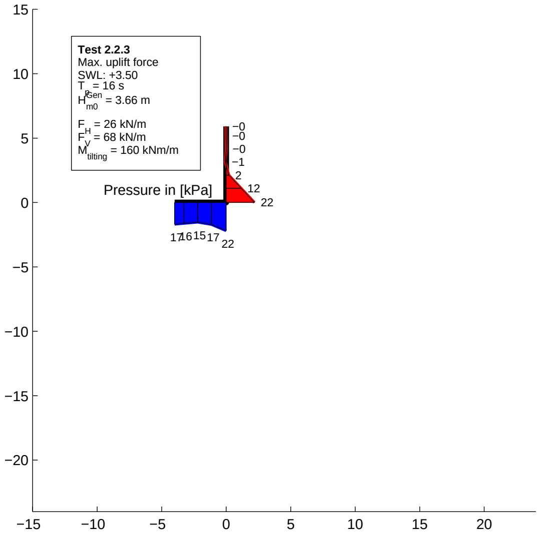

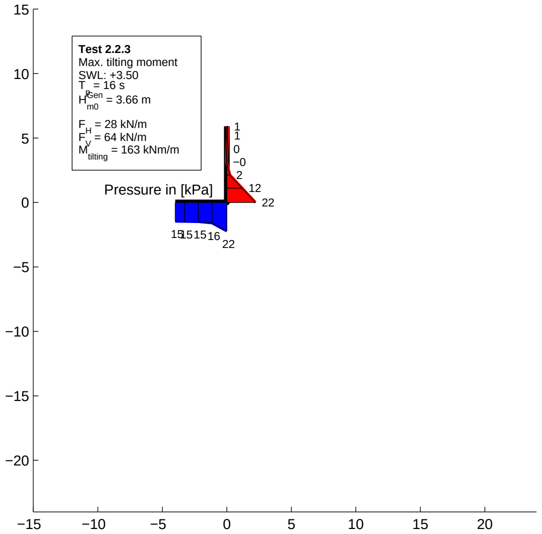

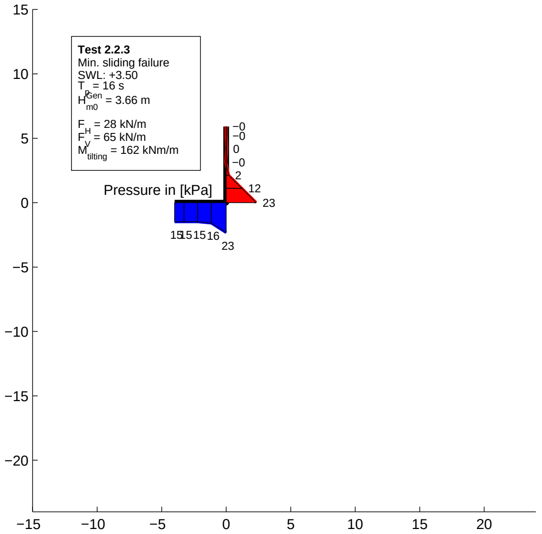

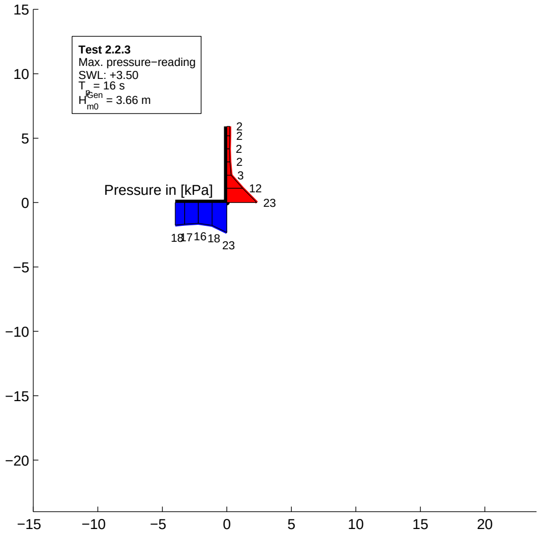

Test no. 2.2.4, SWL: +3.50, T_{p}: 16 s, $H_{m0}^{Gen} = 3.77$ m

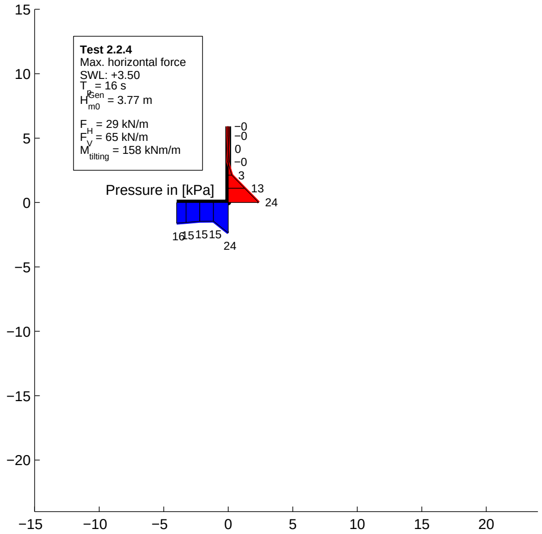

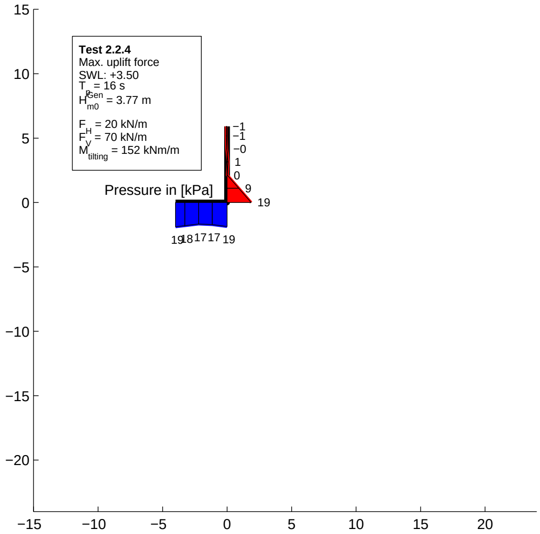

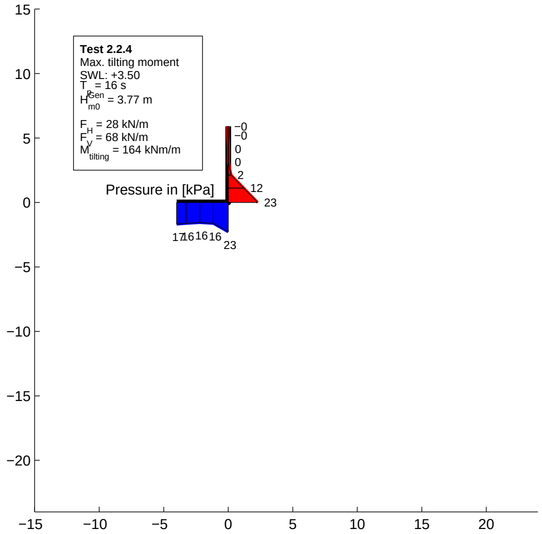

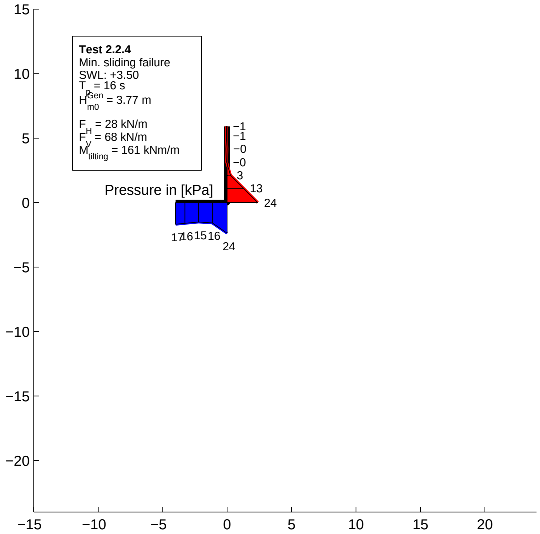

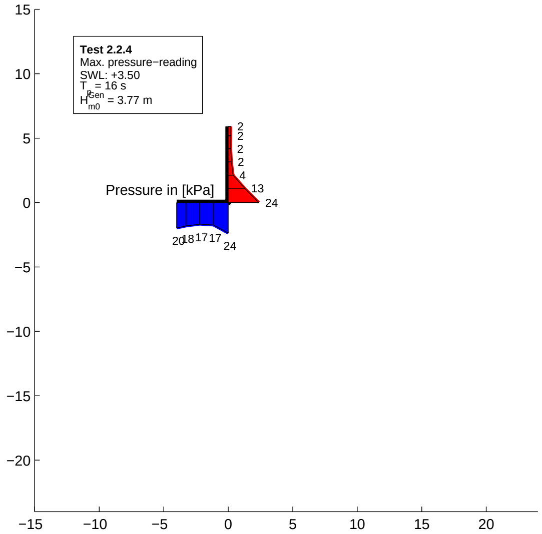

Test no. 2.2.5, SWL: +3.50, T_p: 16 s, $H_{m0}^{Gen} = 4.36$ m

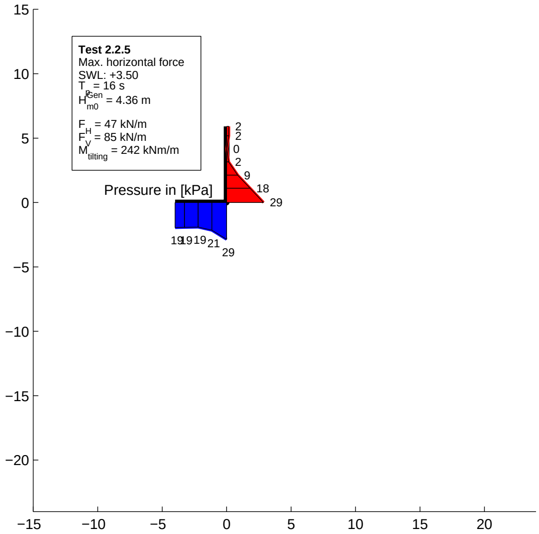

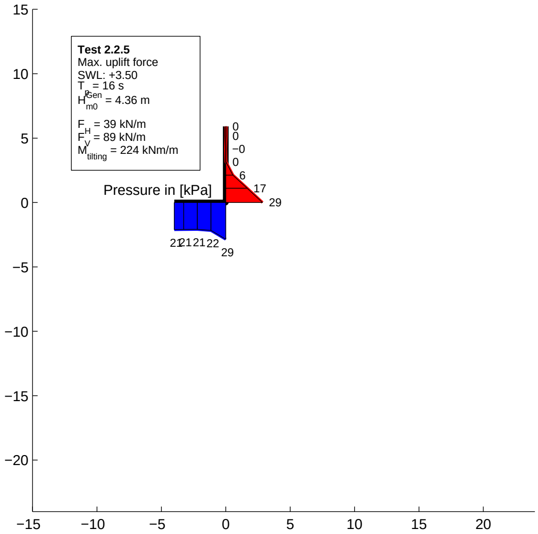

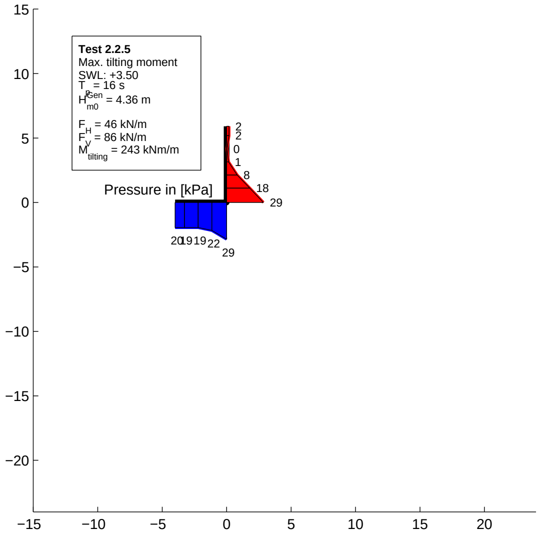

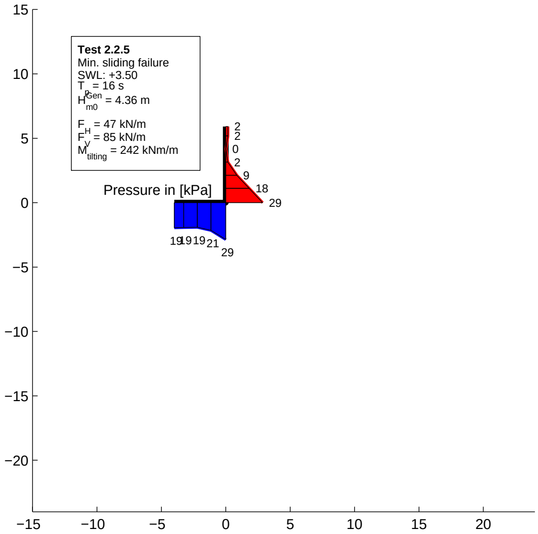

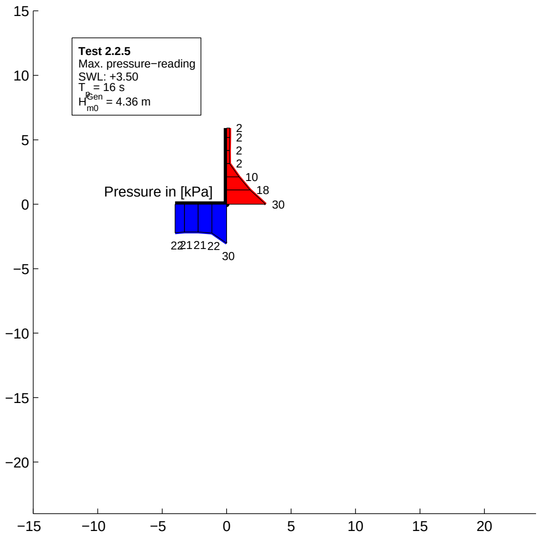

Test no. 2.2.6, SWL: +3.50, T_{p}: 16 s, $H_{m0}^{Gen} = 4.84$ m

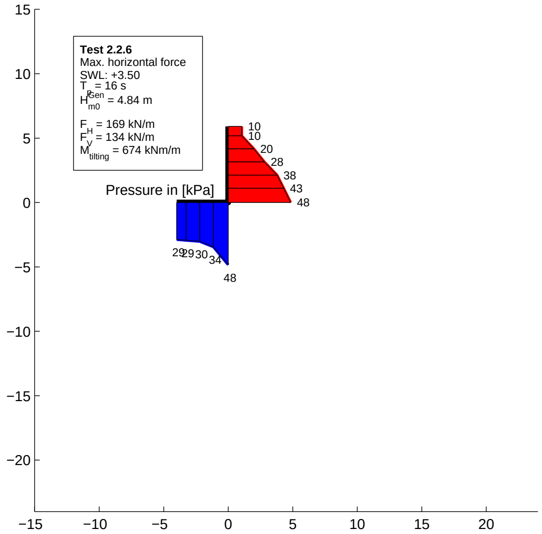

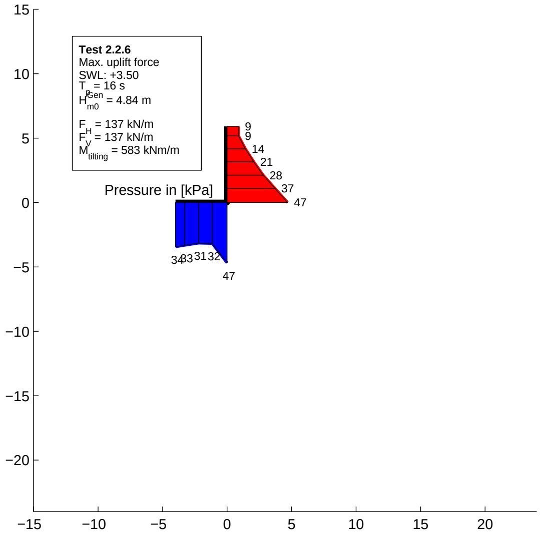

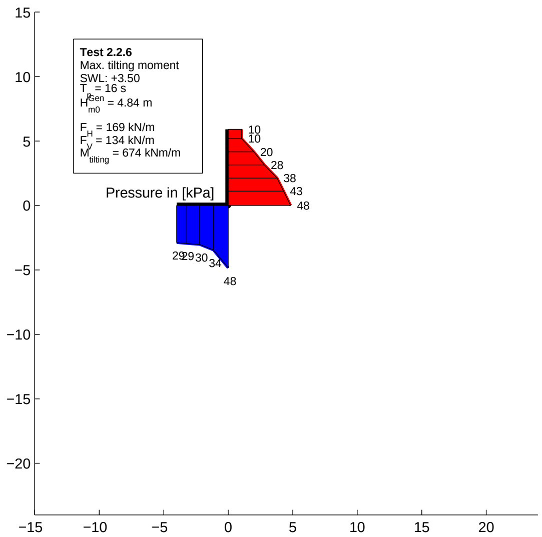

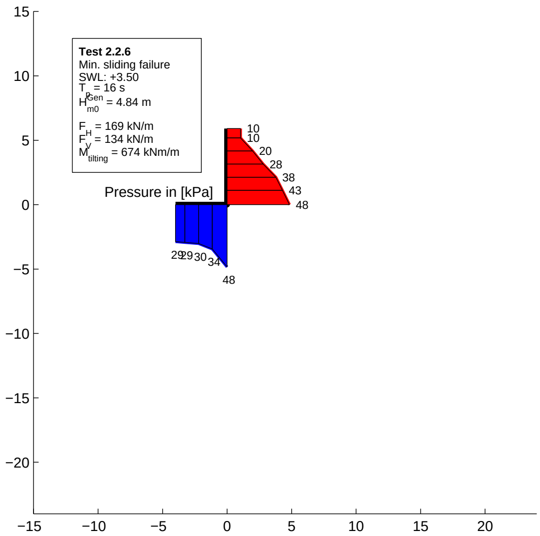

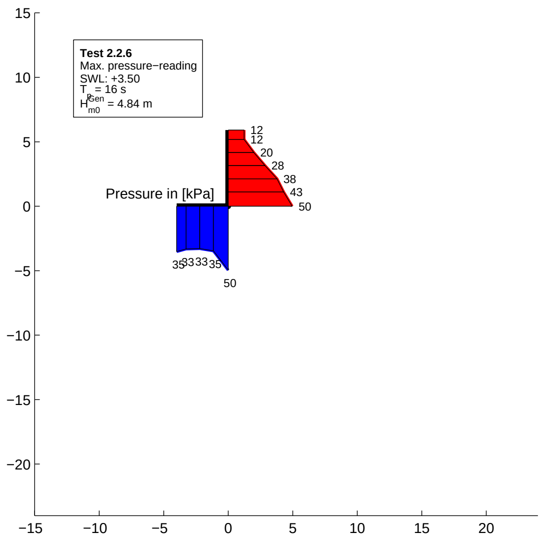

Armour Stability Photos B

Test no. 1.1.1 - SWL: +0.09, T_p: 8 s, H_{m0}^{Gen} = 2.21 m, H_{m0}^{Gen*} = 1.92 m

Position	Before	After
1		
2		

Position	Before	After
3		
4		

Test no. 1.1.2 - SWL: +0.09, $\mathbf{T_p}$: 8 s, $\mathbf{H_{m0}^{Gen}}$ = 2.72 m, $\mathbf{H_{m0}^{Gen*}}$ = 2.36 m

Position	Before	After
1		
2		

Position	Before	After
3		
4		

Test no. 1.1.3 - SWL: +0.09, T_p: 8 s, H_{m0}^{Gen} = 3.03 m, H_{m0}^{Gen*} = 2.63 m

Position	Before	After
1		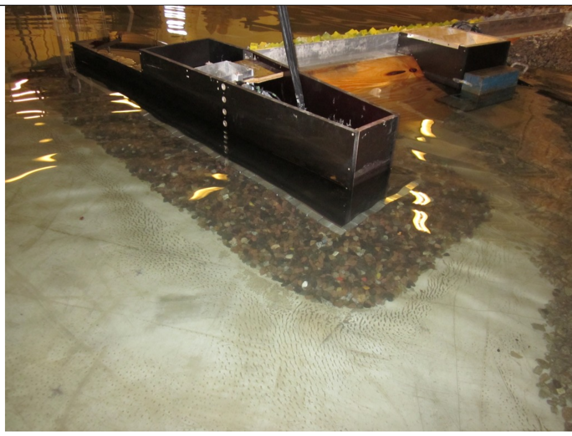
2		

Position	Before	After
3		
4		

Test no. 1.1.4 - SWL: +0.09, T_p: 8 s, H_{m0}^{Gen} = 3.57 m, H_{m0}^{Gen*} = 3.10 m

Position	Before	After
1		
2		

Position	Before	After
3	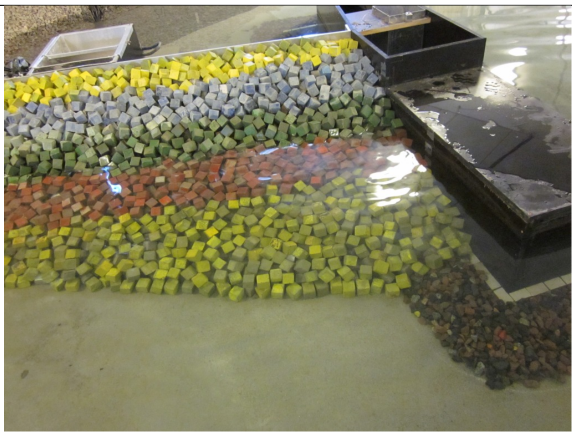	
4		

Test no. 1.1.5 - SWL: +0.09, T_p: 8 s, H_{m0}^{Gen} = 3.74 m, H_{m0}^{Gen*} = 3.25 m

Position	Before	After
1		
2	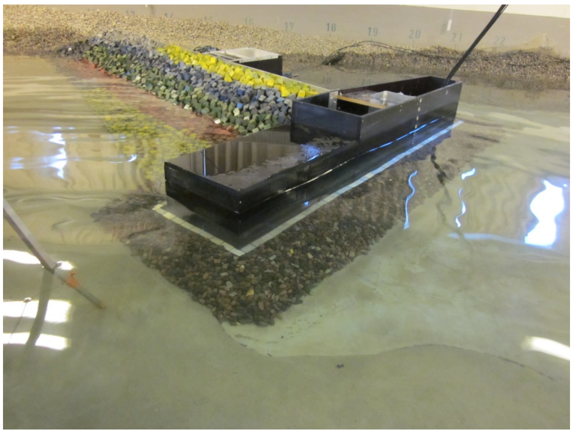	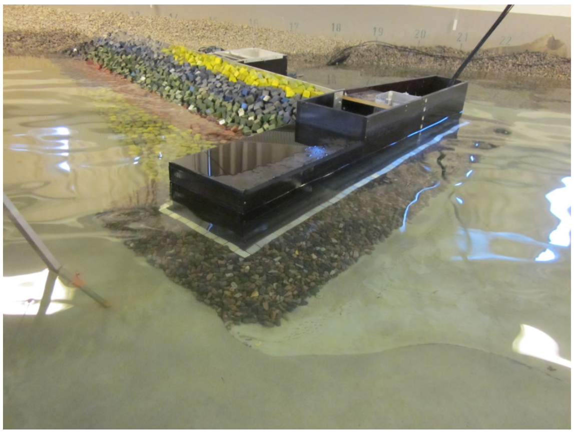

Position	Before	After
3		
4		

Test no. 1.1.6 - SWL: +0.09, T_p: 8 s, H_{m0}^{Gen} = 4.06 m, H_{m0}^{Gen*} = 3.53 m

Position	Before	After
1	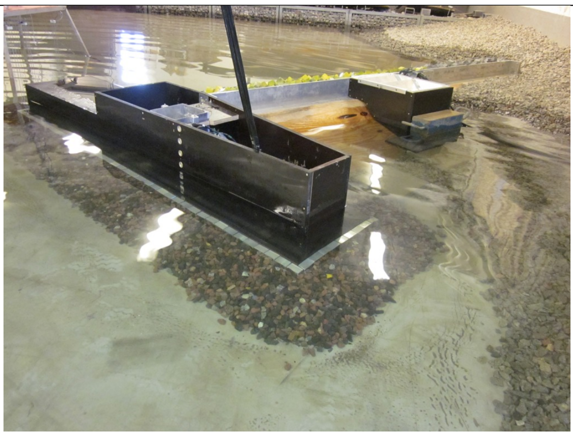	
2	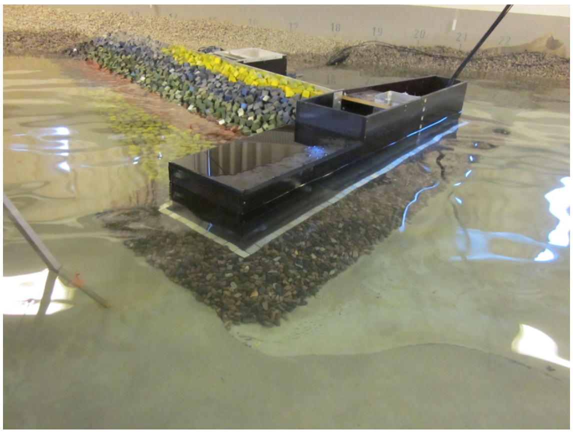	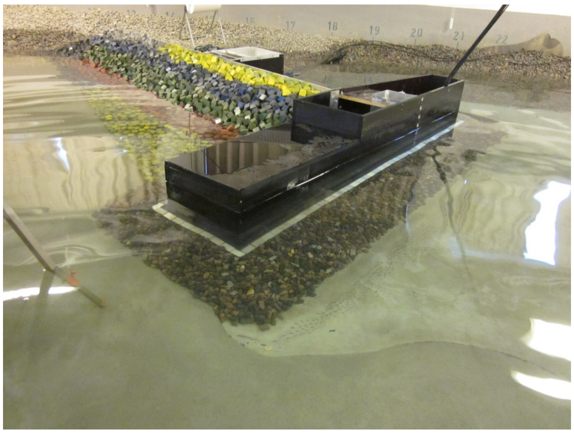

Position	Before	After
3		
4		

Test no. 1.1.7 - SWL: +0.09, T_p: 8 s, H_{m0}^{Gen} = 4.52 m, H_{m0}^{Gen*} = 3.93 m

Position	Before	After
1		
2	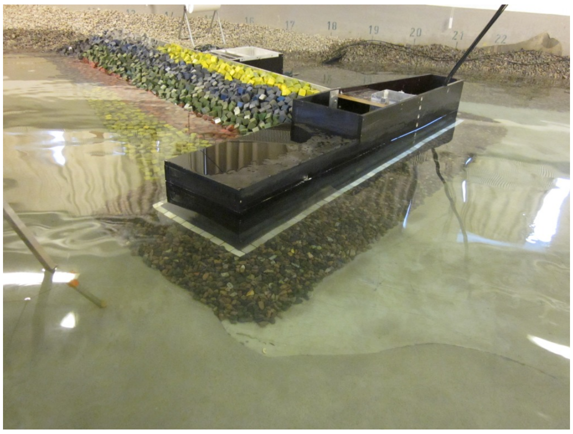	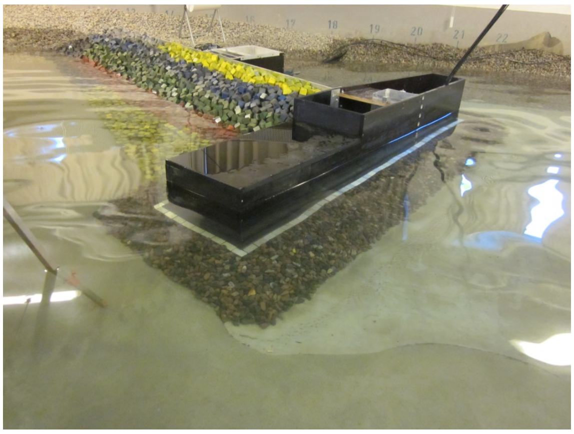

Position	Before	After
3		
4		

Test no. 1.1.7 - SWL: +0.09, T_p: 8 s, H_{m0}^{Gen} = 4.68 m, H_{m0}^{Gen*} = 4.07 m

Position	Before	After
1		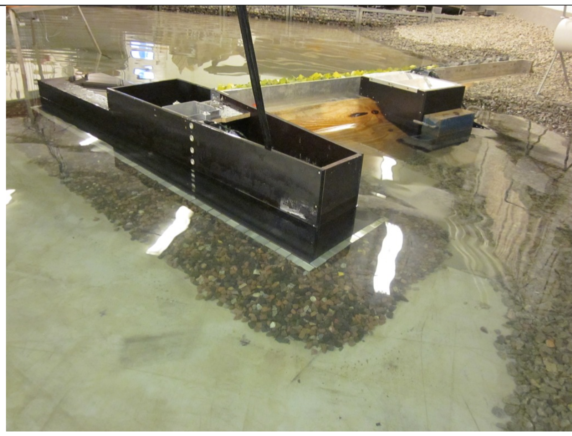
2	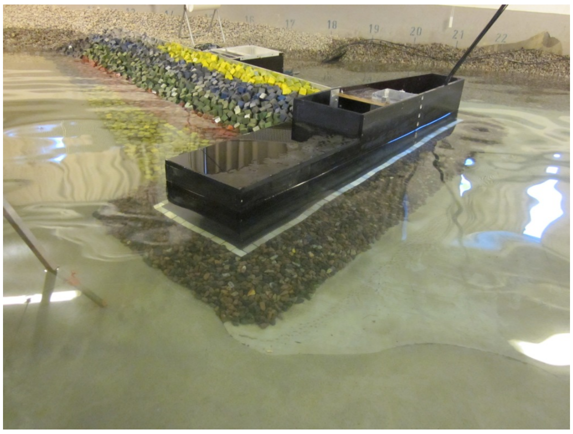	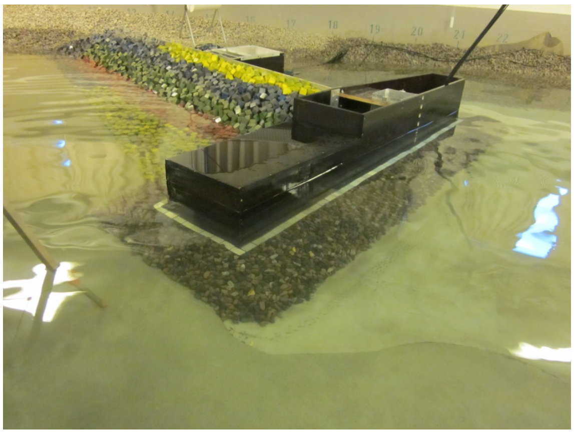

Position	Before	After
3		
4		

Test no. 1.2.1 - SWL: +0.09, T_p: 16 s, H_{m0}^{Gen} = 2.22 m, H_{m0}^{Gen*} = 1.93 m

Position	Before	After
1		
2	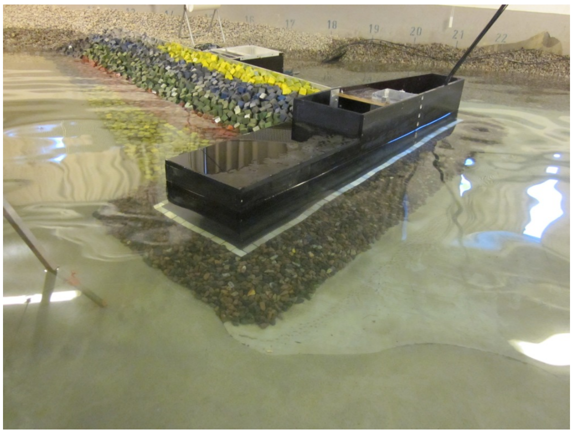	

Position	Before	After
3		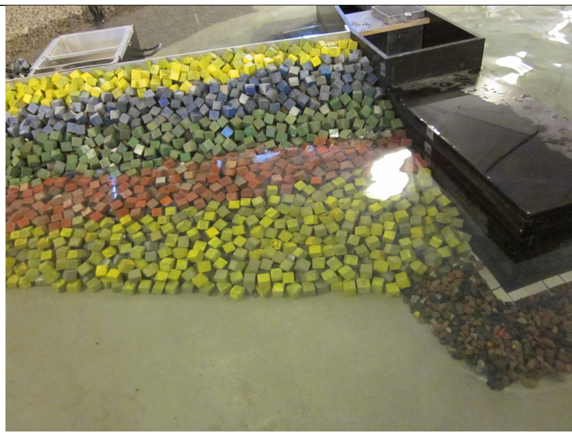
4		

Test no. 1.2.2 - SWL: +0.09, $\mathbf{T_p}$: 16 s, $\mathbf{H_{m0}^{Gen}}$ = 2.51 m, $\mathbf{H_{m0}^{Gen*}}$ = 2.18 m

Position	Before	After
1		
2		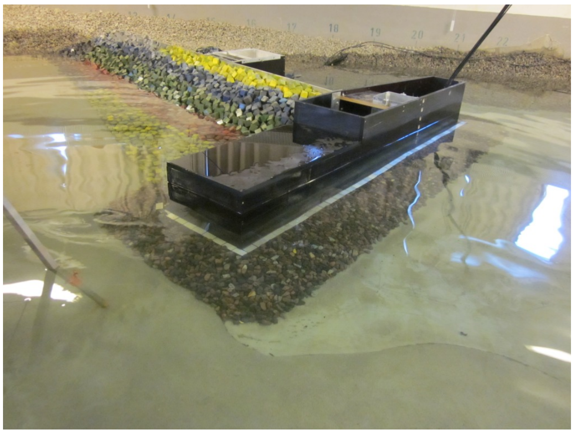

Position	Before	After
3	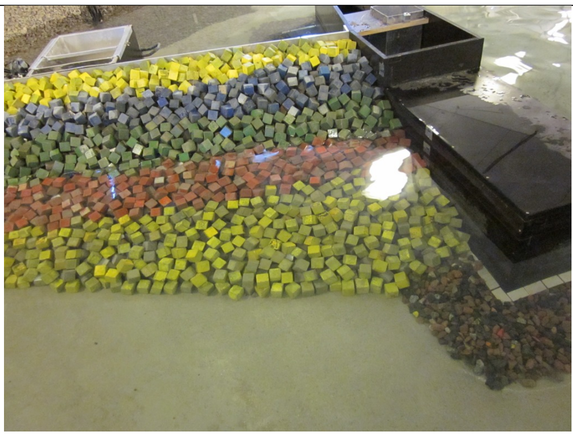	
4		

Test no. 1.2.3 - SWL: +0.09, T_p: 16 s, H_{m0}^{Gen} = 2.70 m, H_{m0}^{Gen*} = 2.35 m

Position	Before	After
1	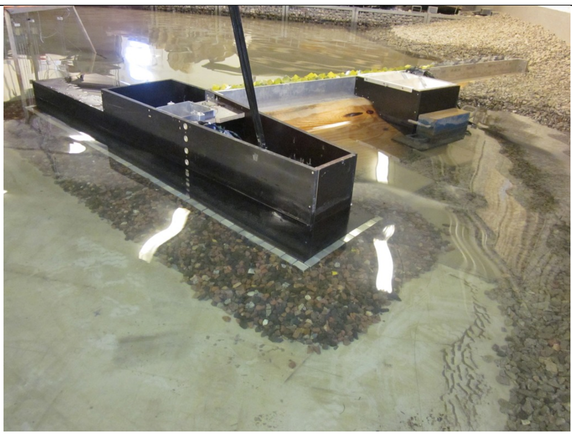	
2	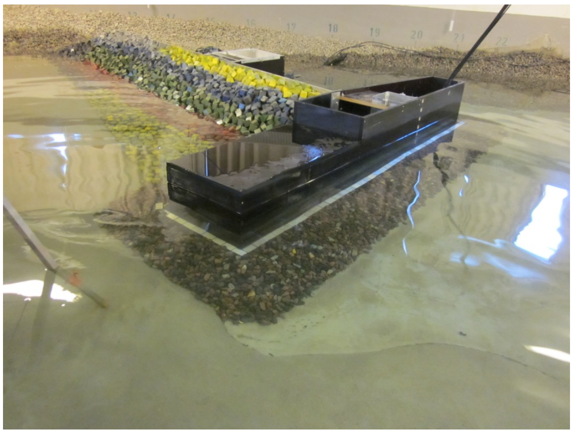	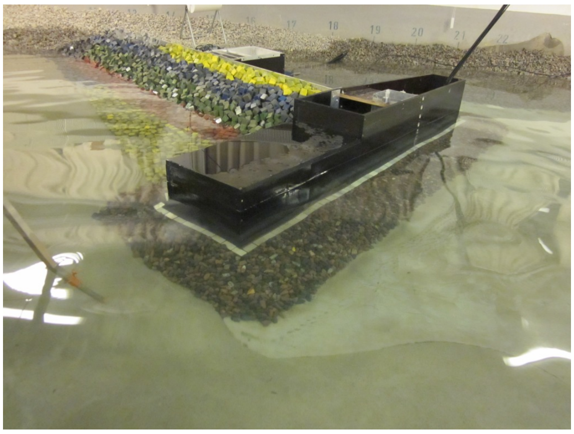

Position	Before	After
3		
4		

Test no. 1.2.4 - SWL: +0.09, T_p: 16 s, H_{m0}^{Gen} = 3.35 m, H_{m0}^{Gen*} = 2.91 m

Position	Before	After
1	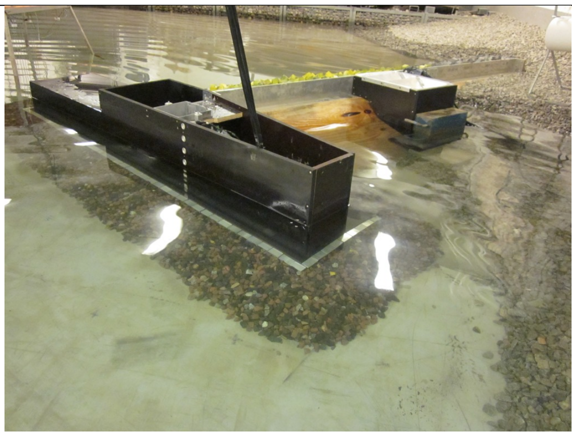	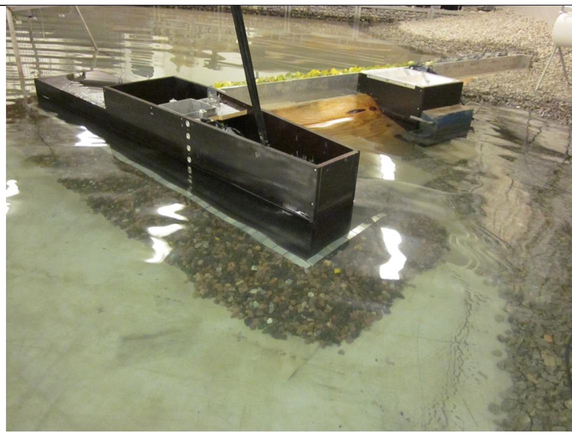
2	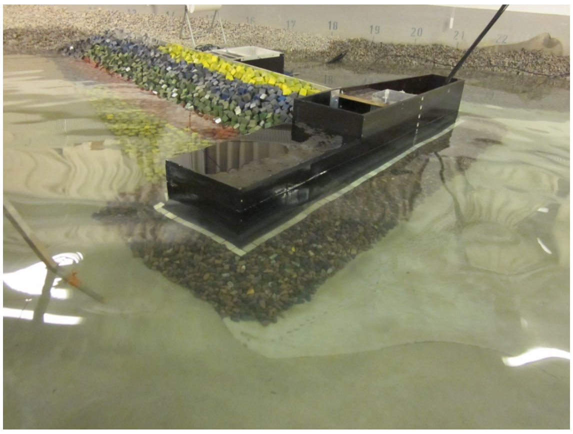	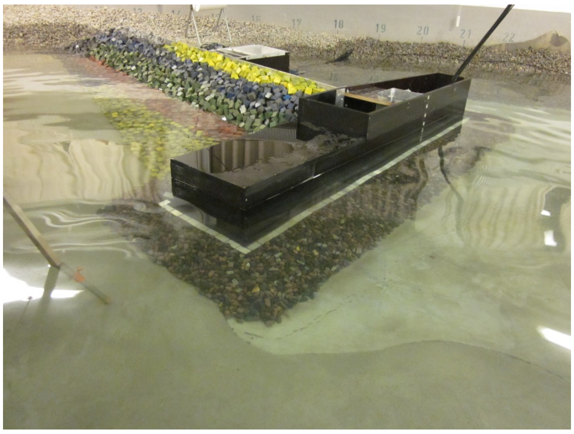

Position	Before	After
3		
4		

Test no. 1.2.5 - SWL: +0.09, T_p: 16 s, H_{m0}^{Gen} = 3.66 m, H_{m0}^{Gen*} = 3.18 m

Position	Before	After
1	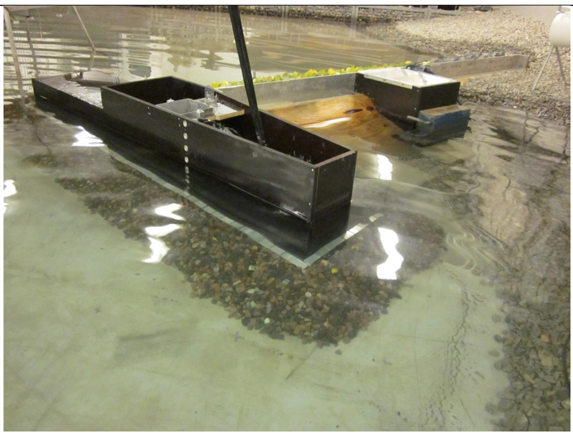	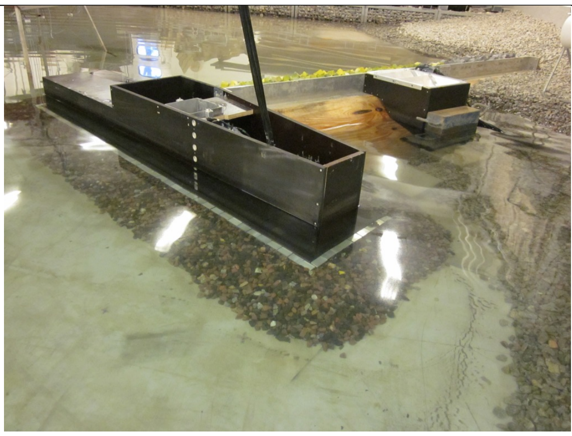
2	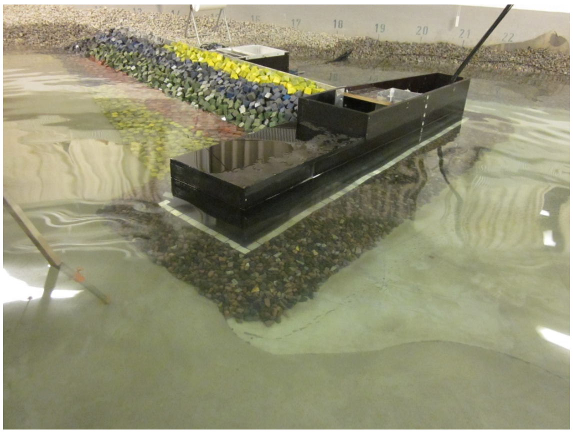	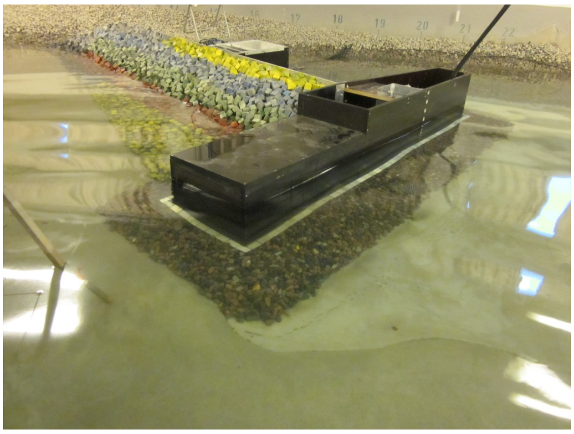

Position	Before	After
3		
4		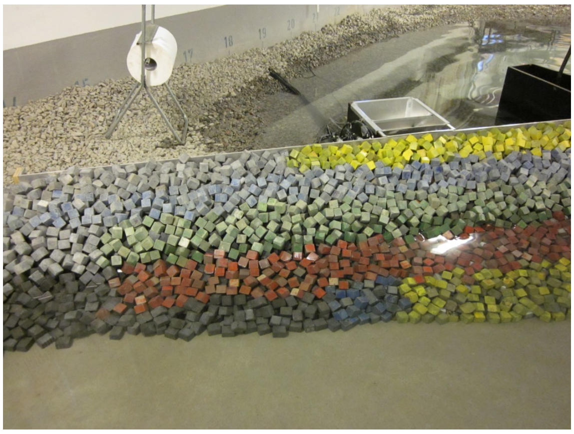

Test no. 1.2.6 - SWL: +0.09, T_p: 16 s, H_{m0}^{Gen} = 4.19 m, H_{m0}^{Gen*} = 3.64 m

Position	Before	After
1		
2	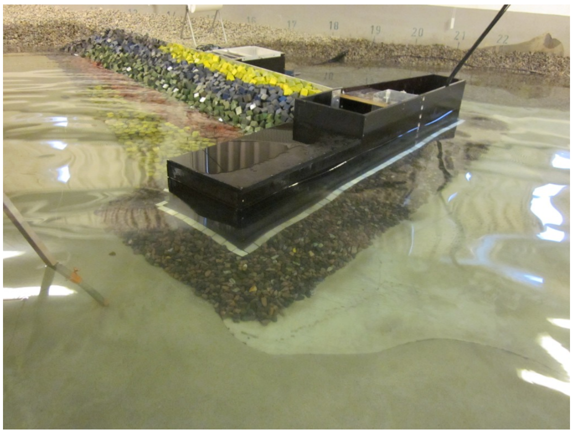	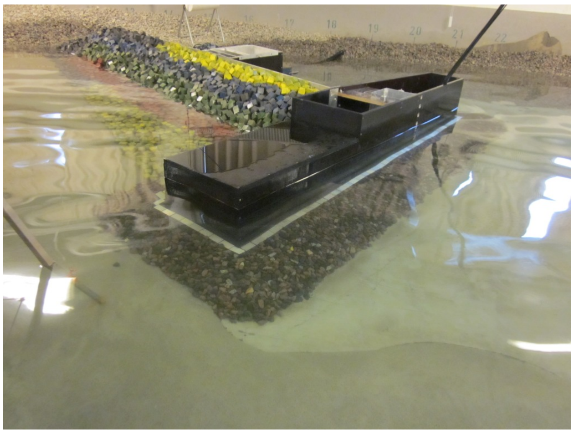

Position	Before	After
3		
4	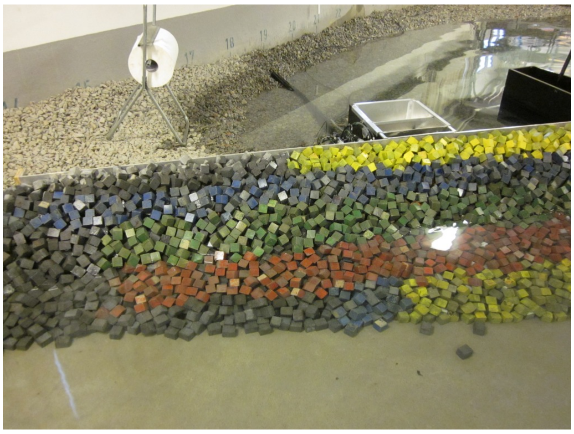	

Test no. 1.2.7 - SWL: +0.09, $\mathbf{T_p}$: 16 s, $\mathbf{H_{m0}^{Gen}}$ = 4.28 m, $\mathbf{H_{m0}^{Gen*}}$ = 3.73 m

Position	Before	After
1		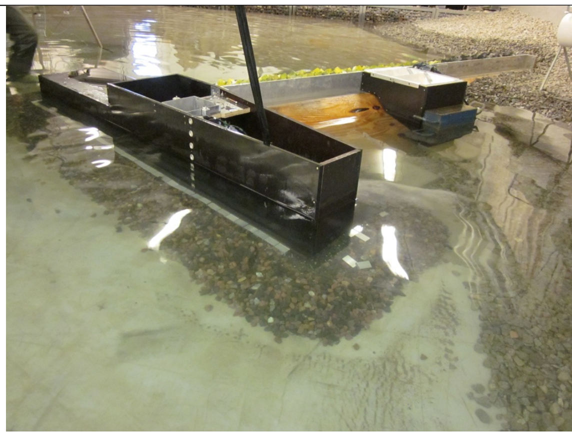
2	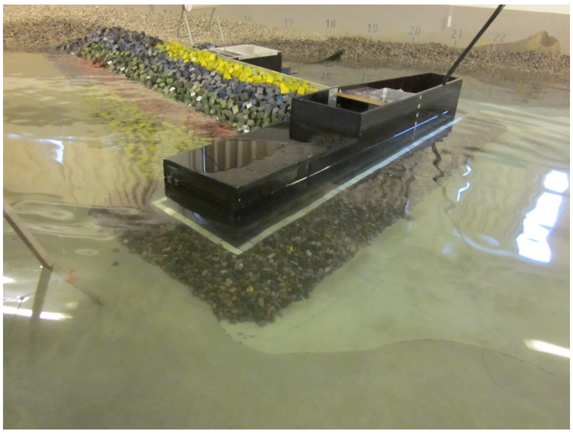	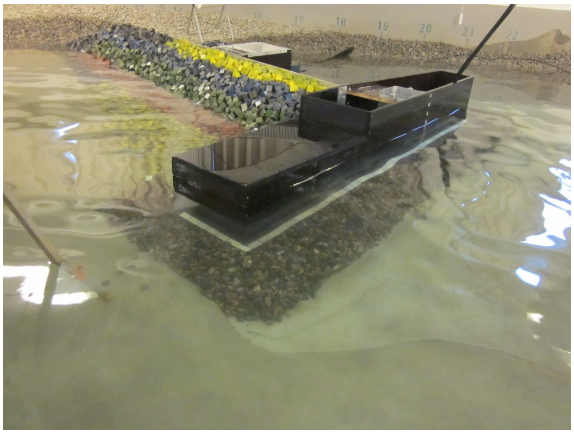

Position	Before	After
3		
4		

Test no. 2.1.1 - SWL: +3.50, T_p: 8 s, H_{m0}^{Gen} = 2.70 m, H_{m0}^{Gen*} = 2.34 m

Position	Before	After
1		
2	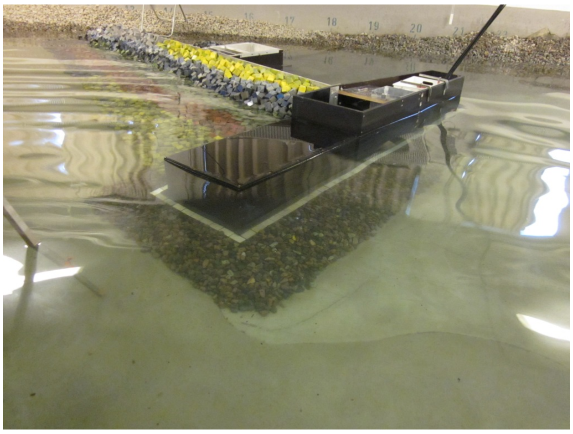	

Position	Before	After
3	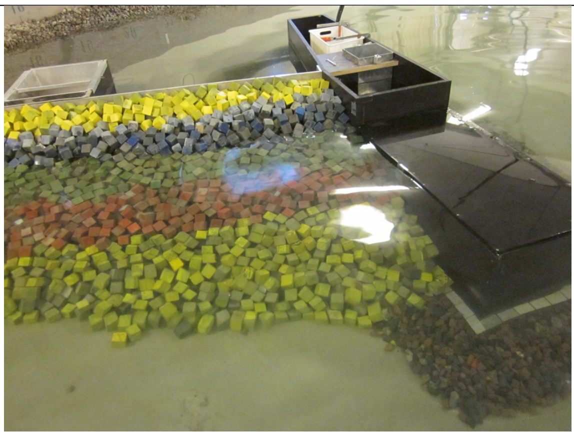	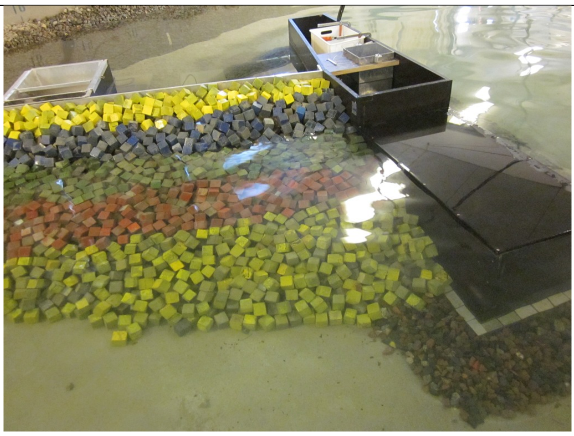
4	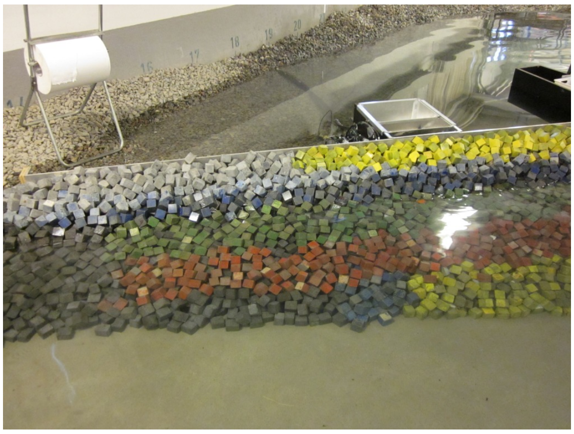	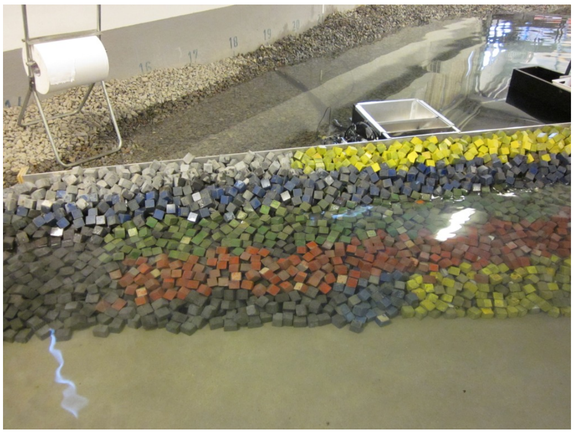

Test no. 2.1.2 - SWL: +3.50, T_p: 8 s, H_{m0}^{Gen} = 3.14 m, H_{m0}^{Gen*} = 2.73 m

Position	Before	After
1		
2		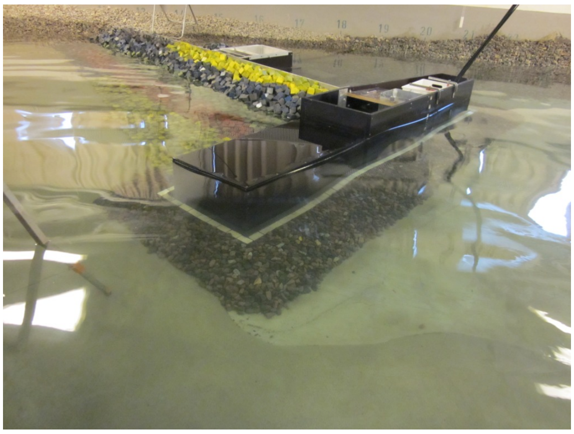

Position	Before	After
3	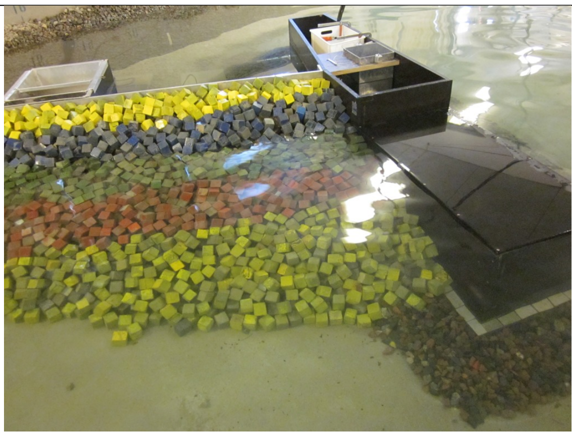	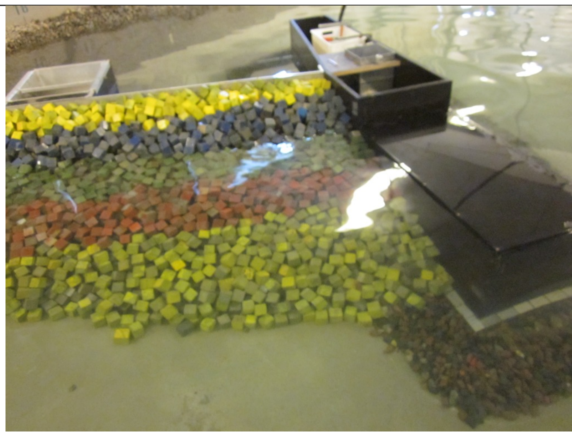
4	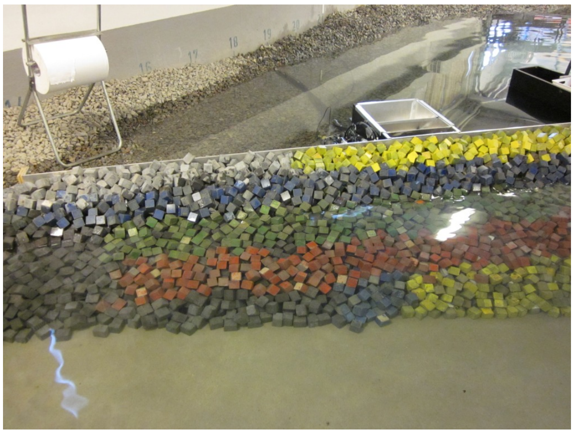	

Test no. 2.1.3 - SWL: +3.50, T_p: 8 s, H_{m0}^{Gen} = 3.31 m, H_{m0}^{Gen*} = 2.88 m

Position	Before	After
1		
2	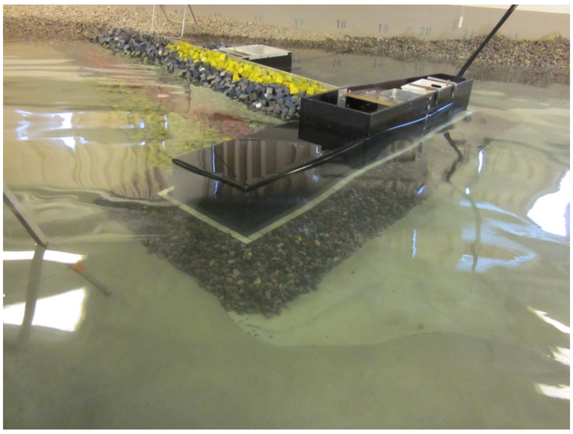	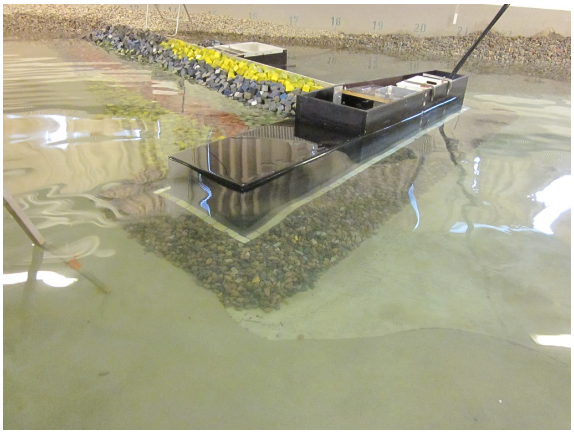

Position	Before	After
3	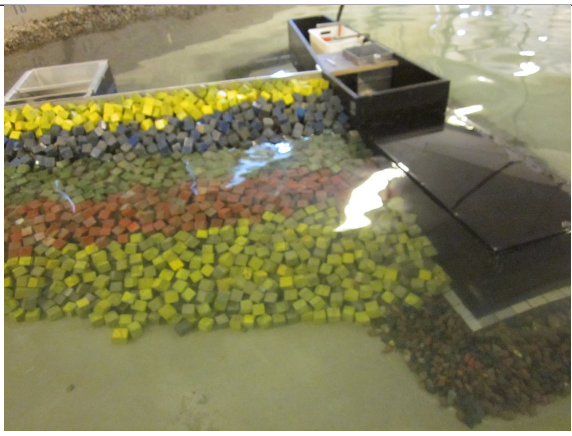	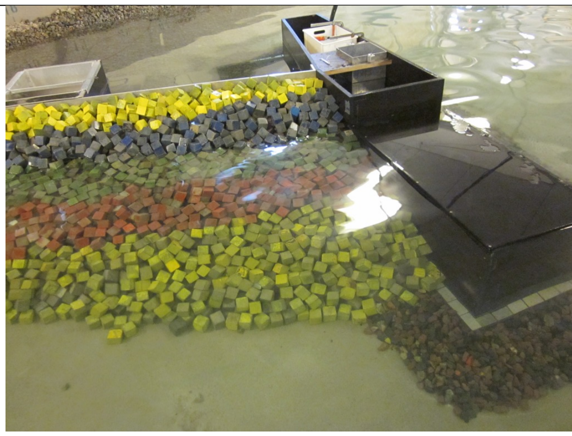
4		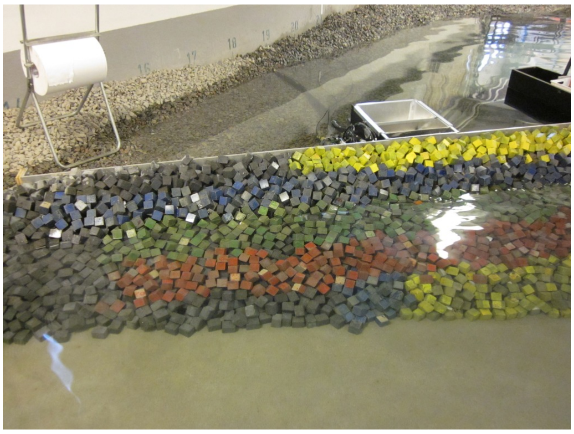

Test no. 2.1.4 - SWL: +3.50, T_p: 8 s, H_{m0}^{Gen} = 3.92 m, H_{m0}^{Gen*} = 3.41 m

Position	Before	After
1		
2	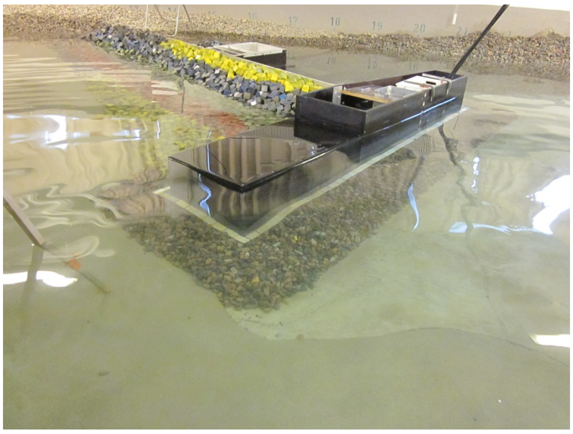	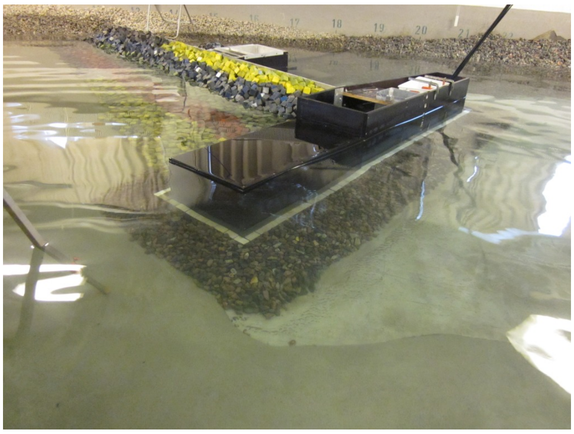

Position	Before	After
3	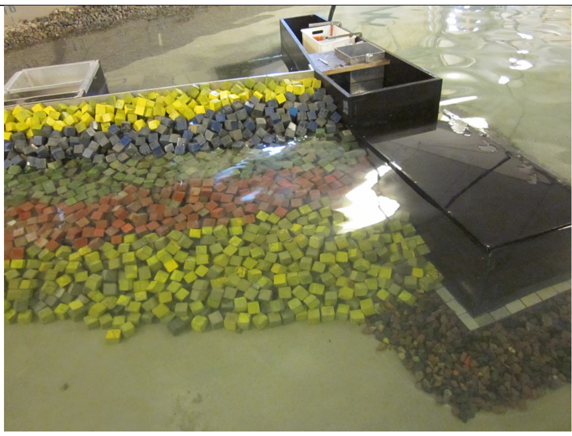	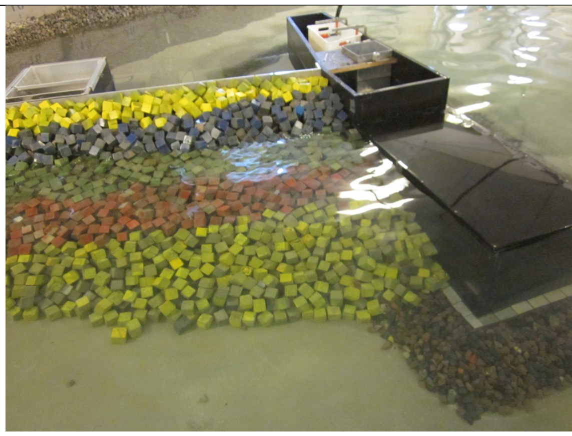
4	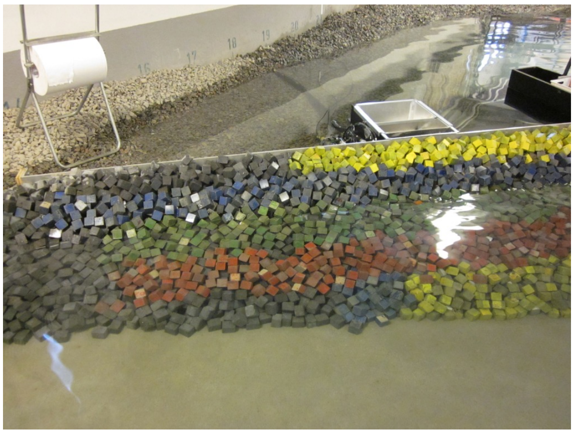	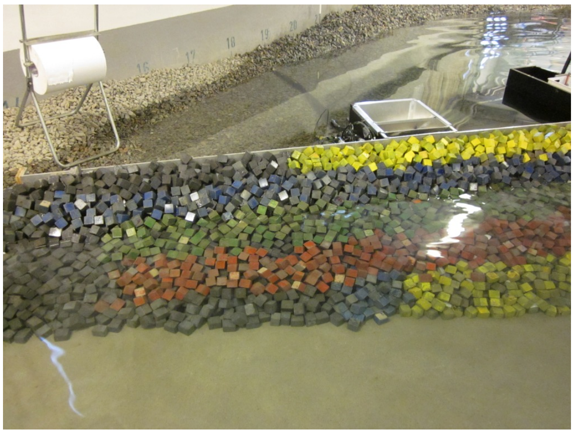

Test no. 2.1.5 - SWL: +3.50, T_p: 8 s, H_{m0}^{Gen} = 4.15 m, H_{m0}^{Gen*} = 3.61 m

Position	Before	After
1		
2	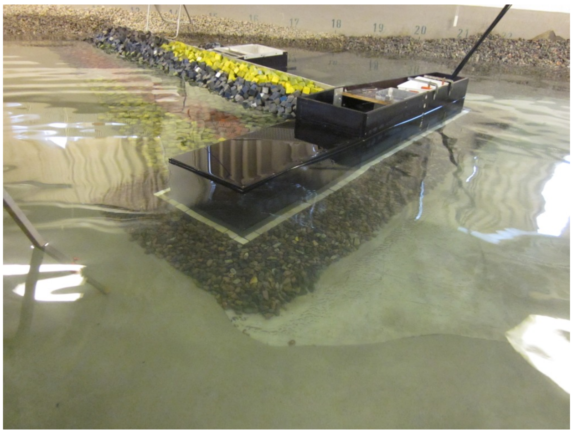	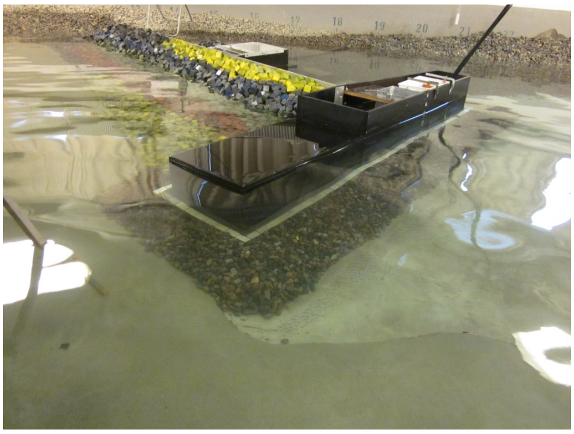

Position	Before	After
3	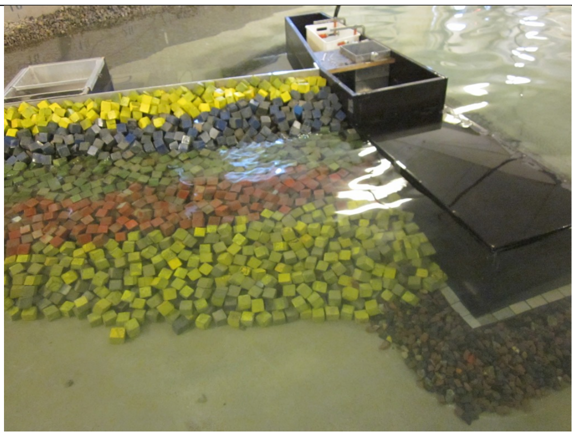	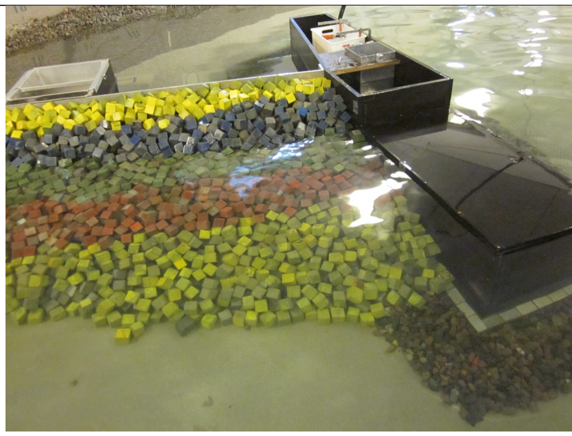
4	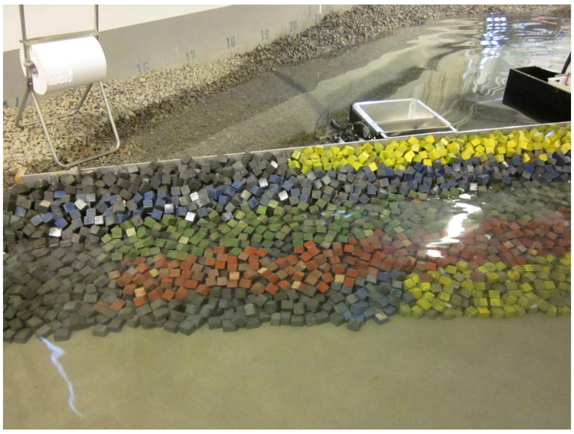	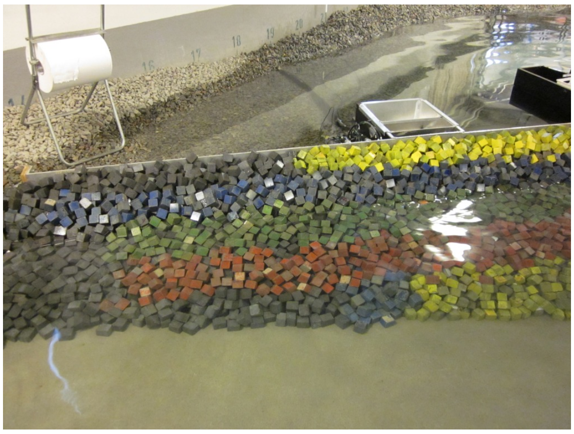

Test no. 2.1.6 - SWL: +3.50, T_p: 8 s, H_{m0}^{Gen} = 4.74 m, H_{m0}^{Gen*} = 4.12 m

Position	Before	After
1		
2	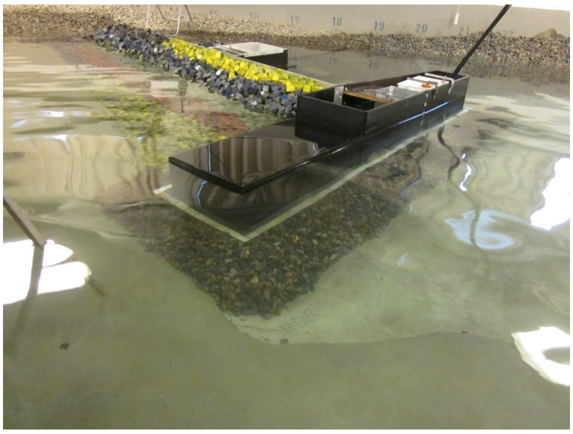	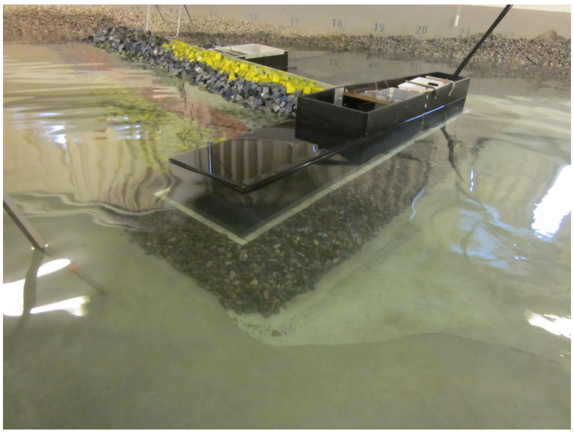

Position	Before	After
3	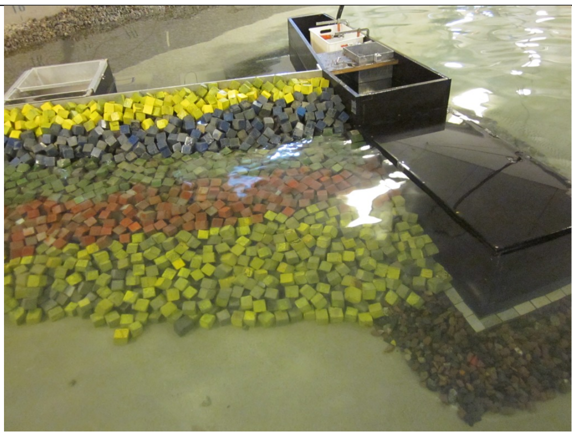	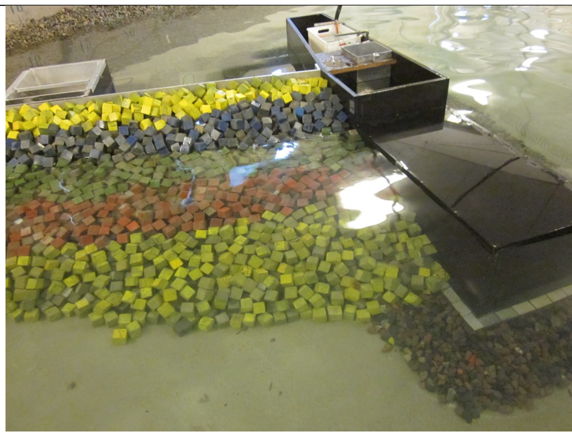
4	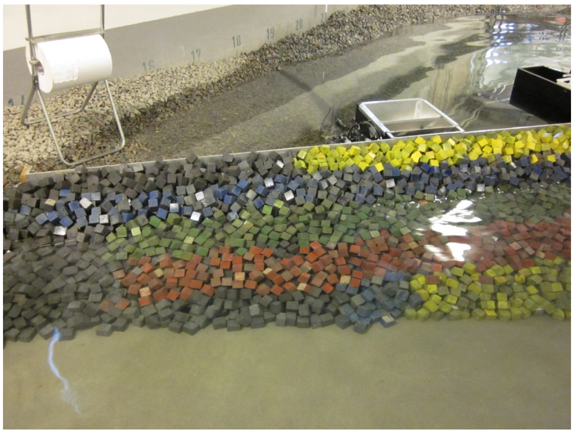	

Test no. 2.1.7 - SWL: +3.50, T_p: 8 s, H_{m0}^{Gen} = 4.87 m, H_{m0}^{Gen*} = 4.24 m

Position	Before	After
1		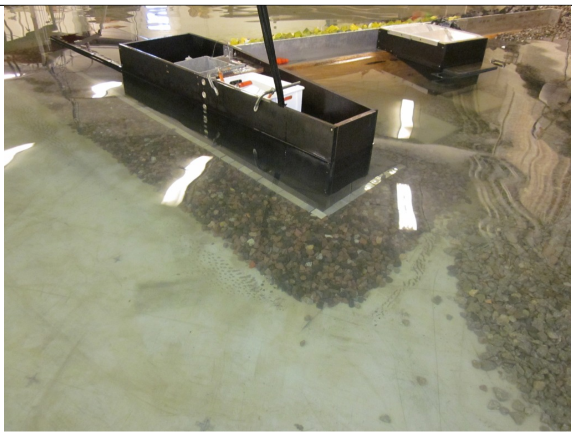
2	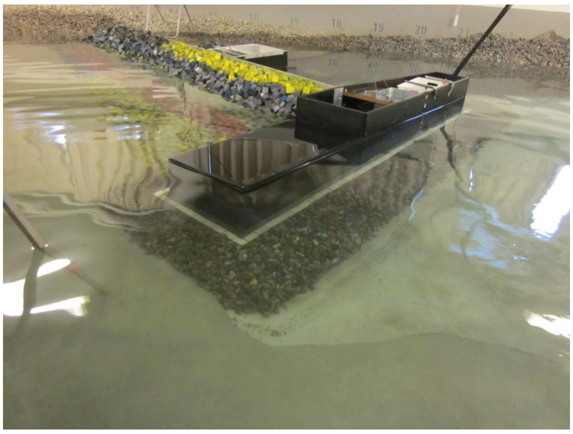	

Position	Before	After
3	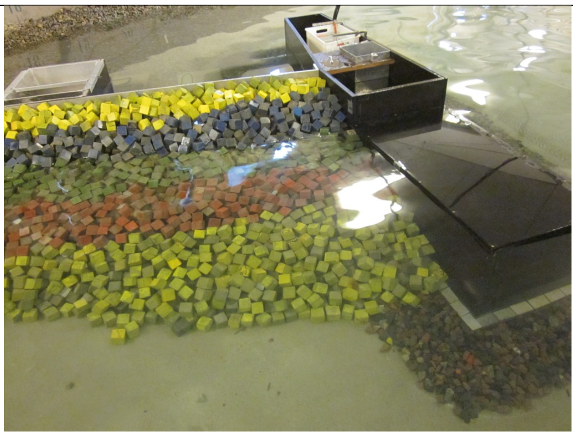	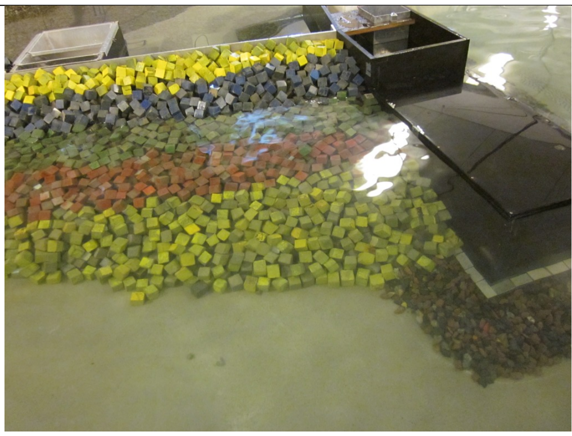
4		

Test no. 2.2.1 - SWL: +3.50, T_p: 16 s, H_{m0}^{Gen} = 2.50 m, H_{m0}^{Gen*} = 2.17 m

Position	Before	After
1	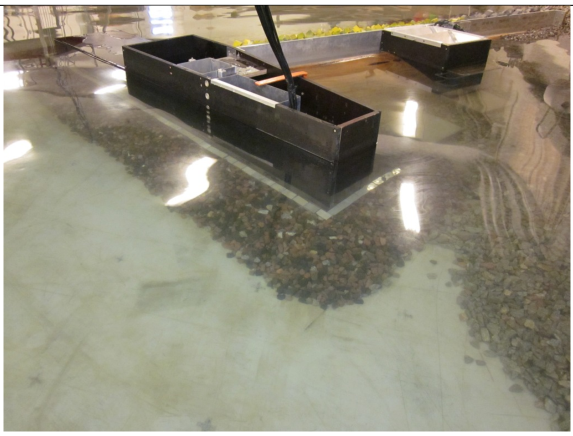	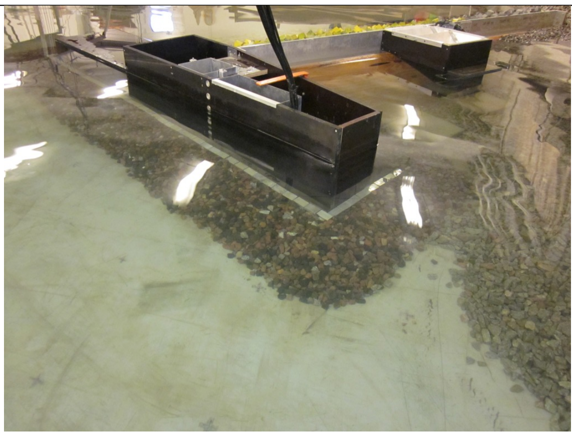
2	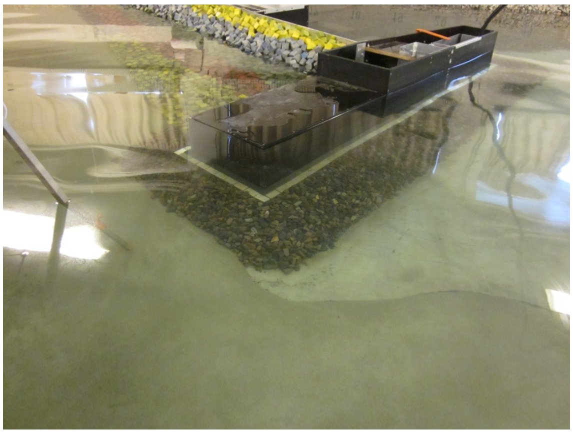	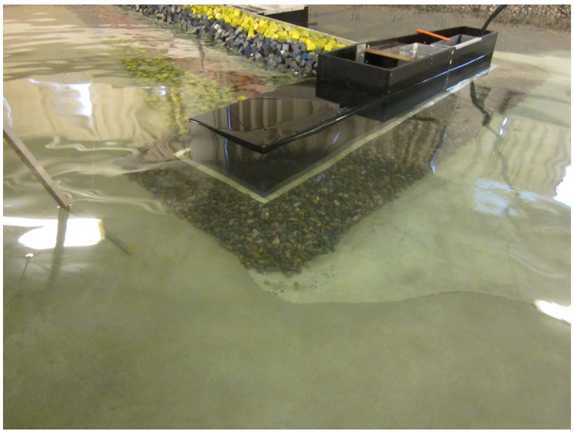

Position	Before	After
3	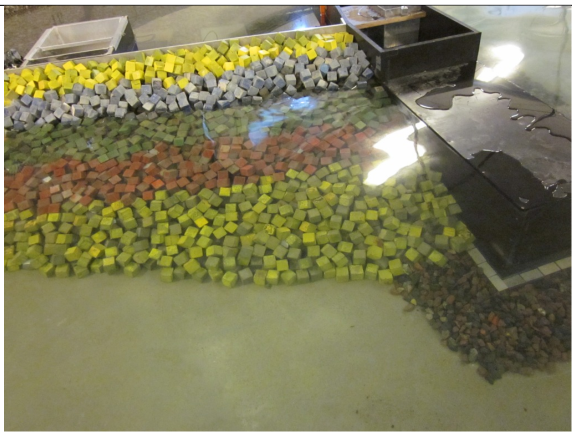	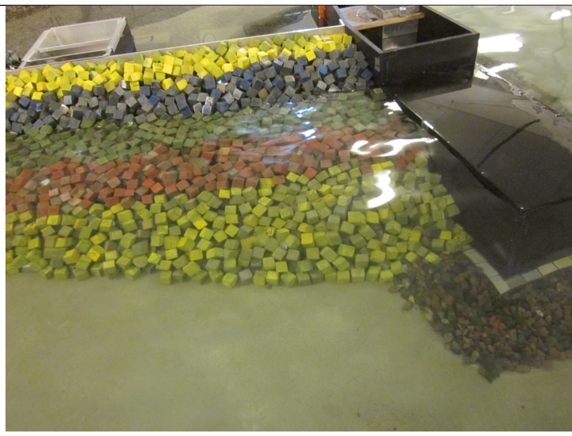
4		

Test no. 2.2.2 - SWL: +3.50, T_p: 16 s, H_{m0}^{Gen} = 3.04 m, H_{m0}^{Gen*} = 2.64 m

Position	Before	After
1	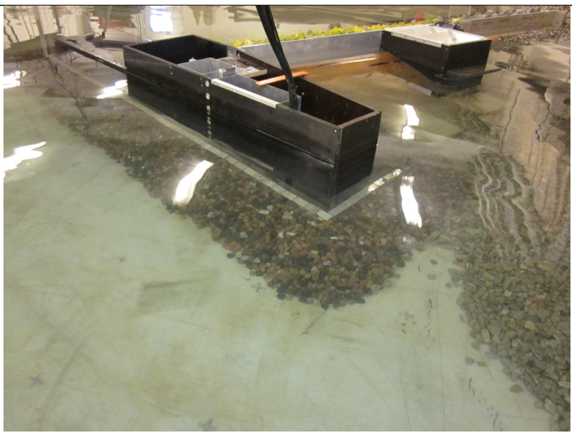	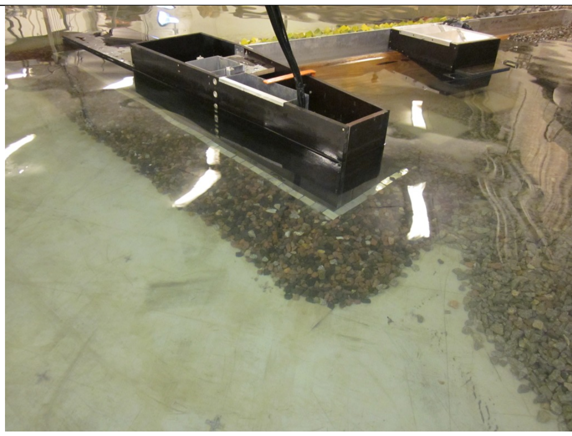
2	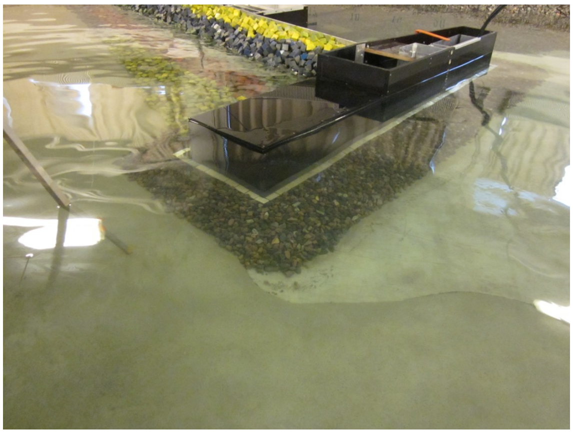	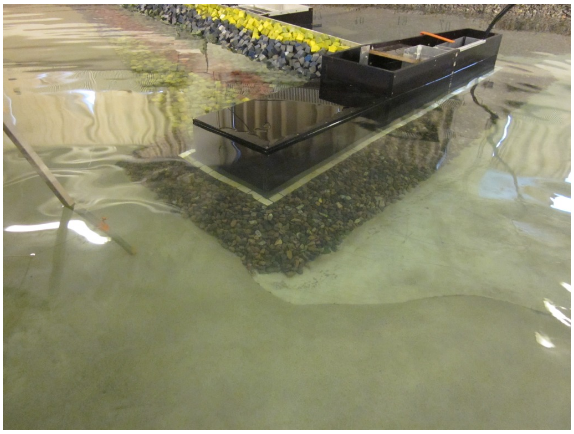

Position	Before	After
3	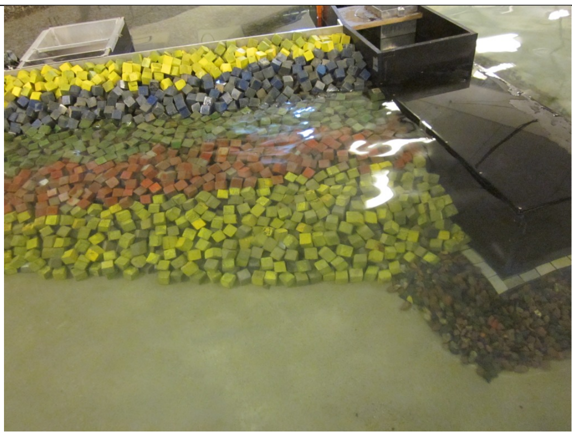	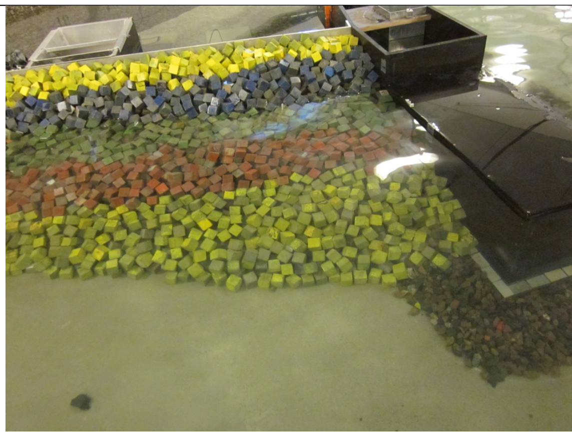
4		

Test no. 2.2.3 - SWL: +3.50, T_p: 16 s, H_{m0}^{Gen} = 3.66 m, H_{m0}^{Gen*} = 3.18 m

Position	Before	After
1	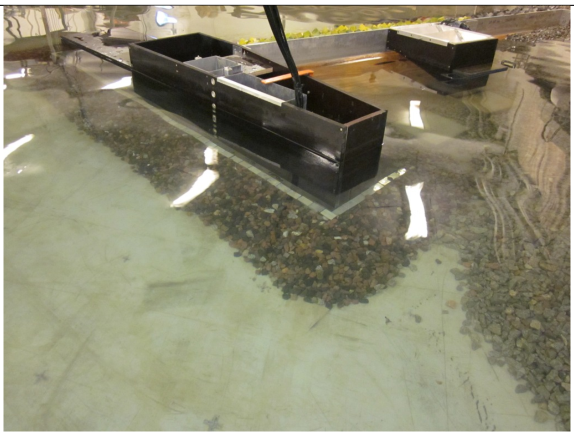	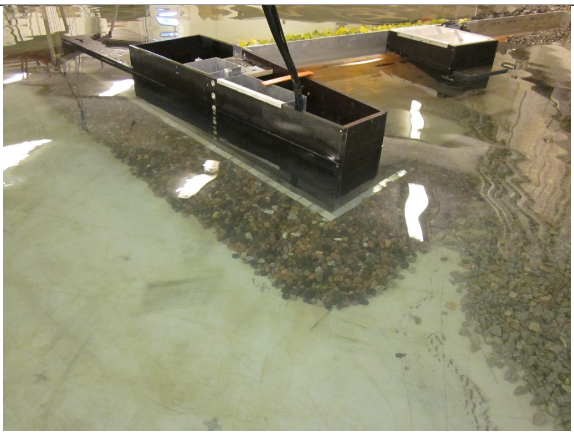
2	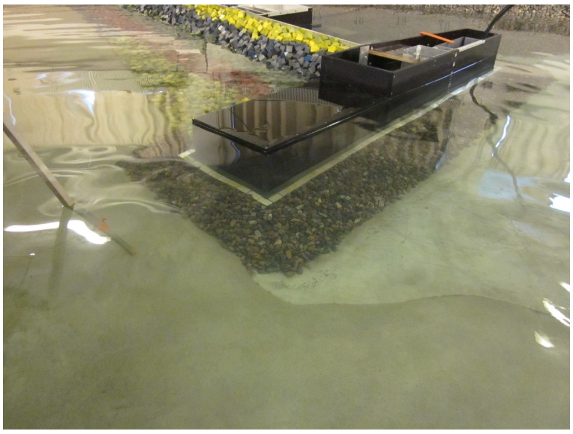	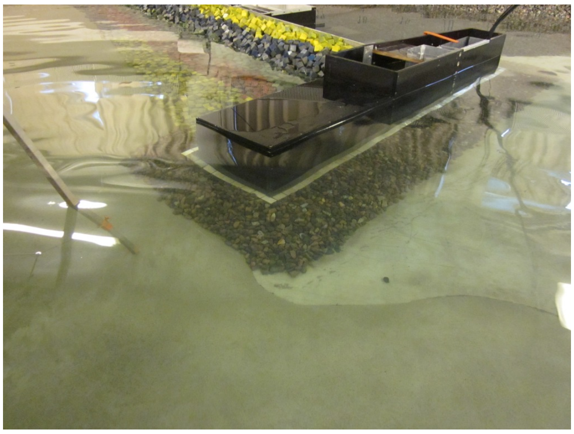

Position	Before	After
3	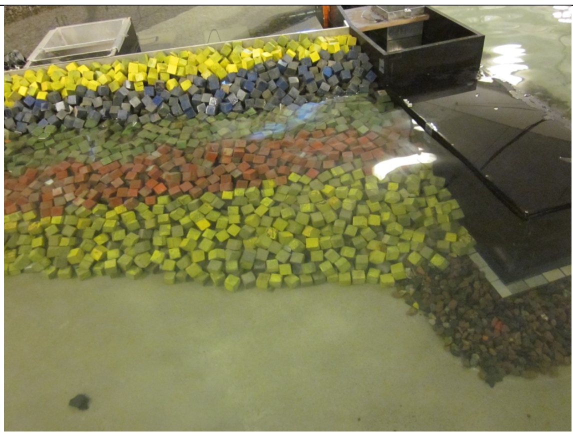	
4		

Test no. 2.2.4 - SWL: +3.50, T_p: 16 s, H_{m0}^{Gen} = 3.77 m, H_{m0}^{Gen*} = 3.27 m

Position	Before	After
1	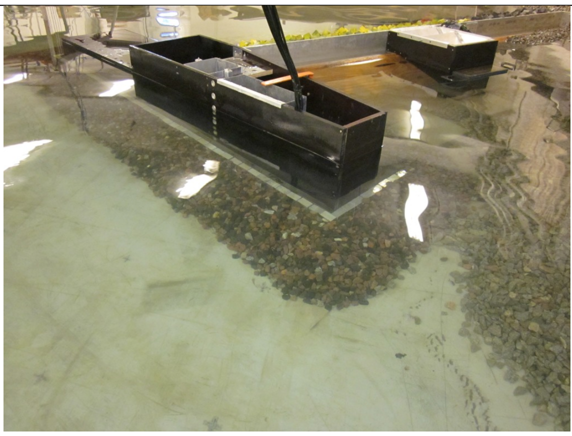	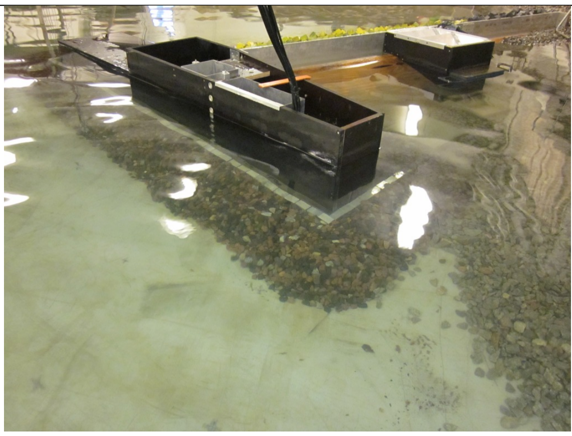
2	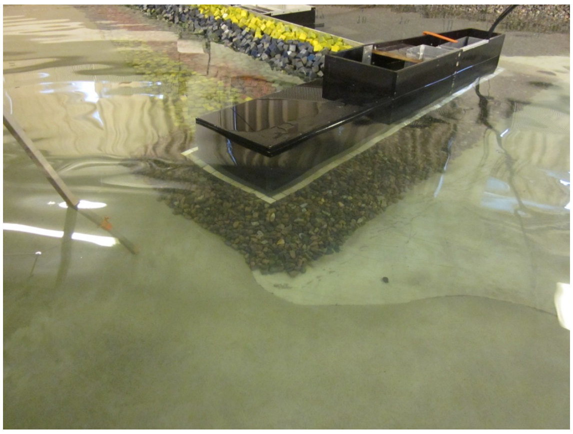	

Position	Before	After
3	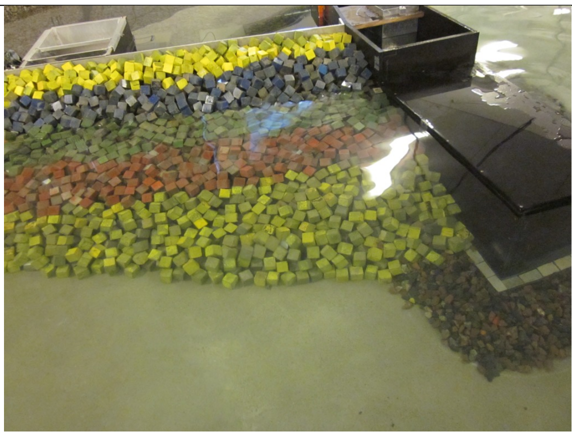	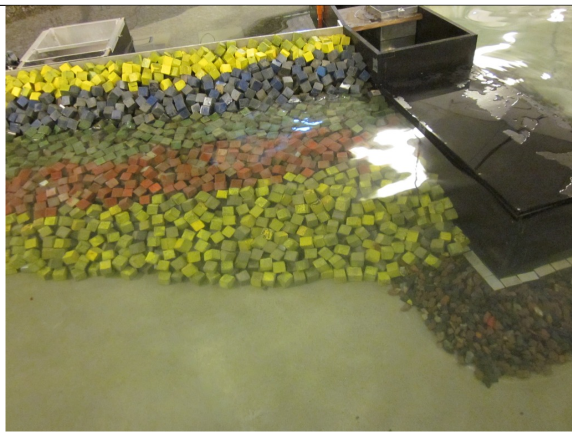
4		

Test no. 2.2.5 - SWL: +3.50, T_p: 16 s, H_{m0}^{Gen} = 4.36 m, H_{m0}^{Gen*} = 3.80 m

Position	Before	After
1	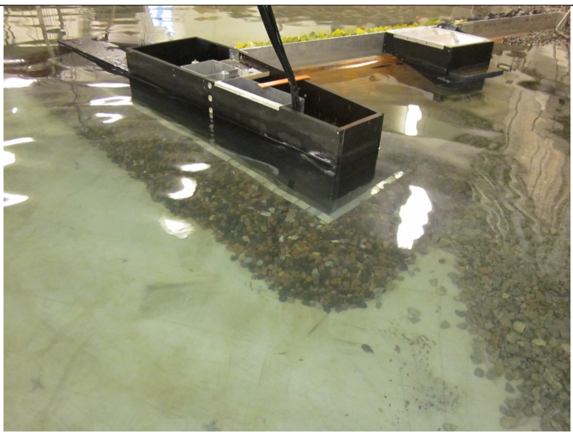	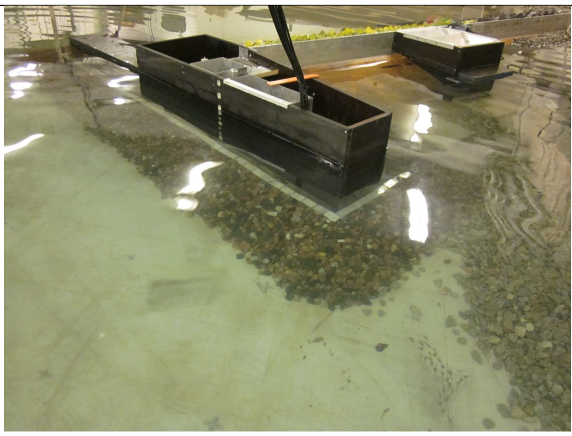
2		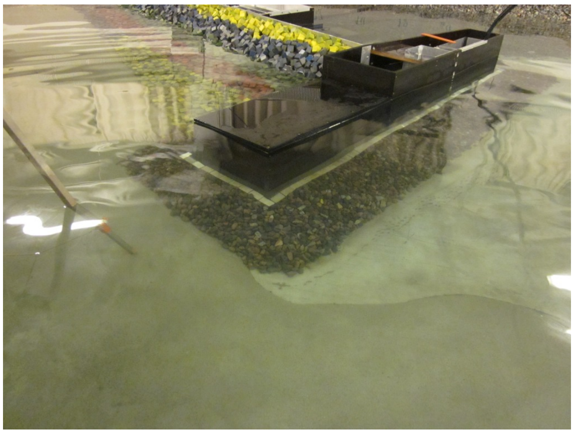

Position	Before	After
3	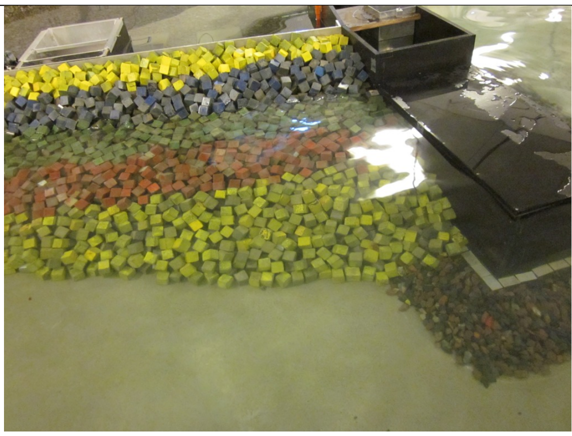	
4		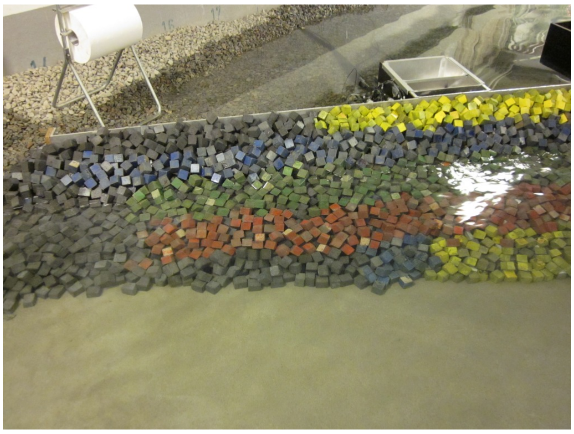

Test no. 2.2.6 - SWL: +3.50, T_p: 16 s, H_{m0}^{Gen} = 4.84 m, H_{m0}^{Gen*} = 4.21 m

Position	Before	After
1	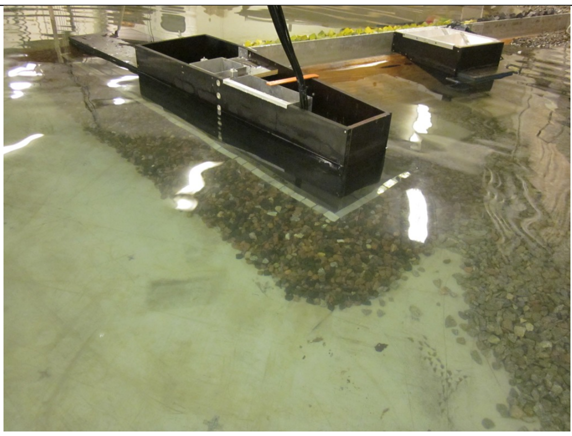	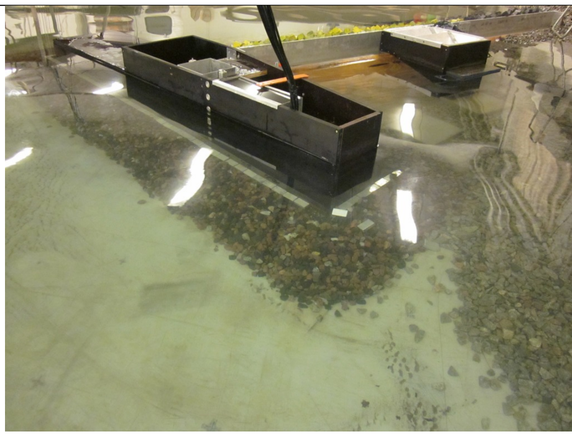
2	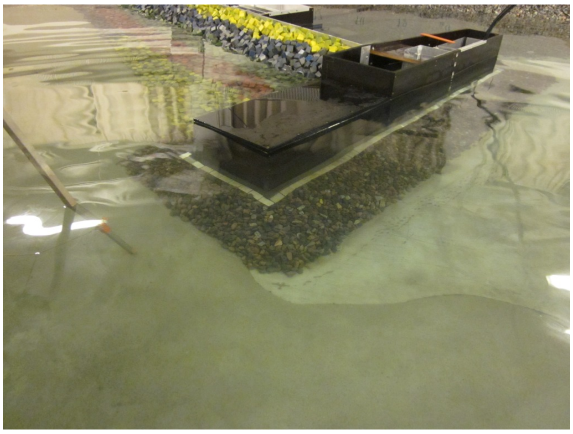	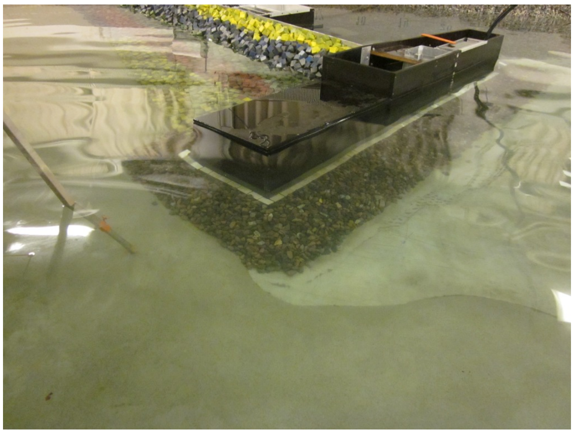

Position	Before	After
3		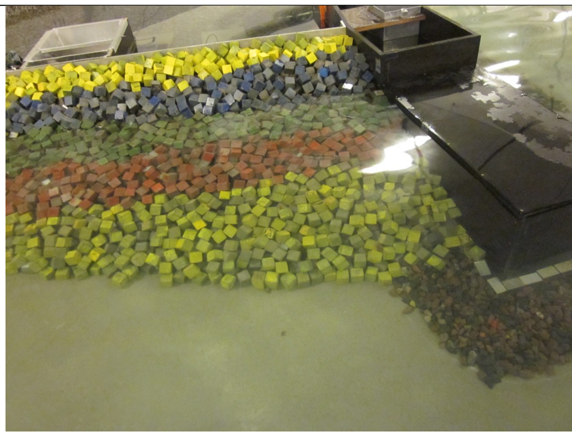
4	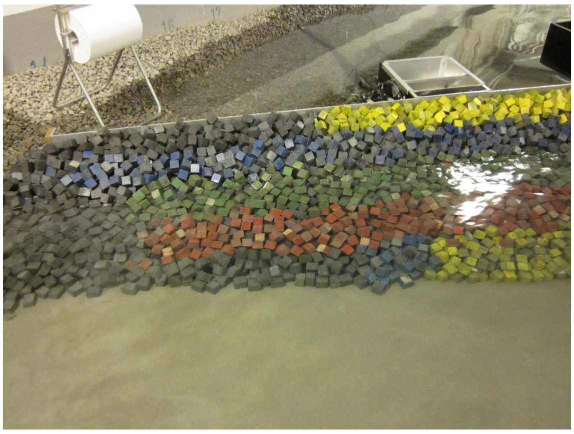	

Test no. (2.2.6) - SWL: +3.50, $\mathbf{T_p}$: 16 s, $\mathbf{H_{m0}^{Gen}}$ = 4.70 m, $\mathbf{H_{m0}^{Gen*}}$ = 4.09 m

Position	Before	After
1	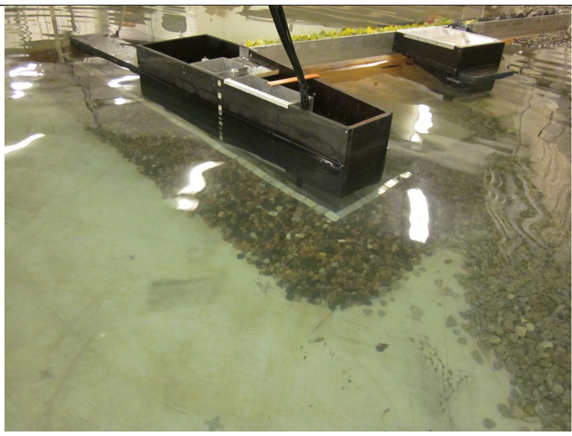	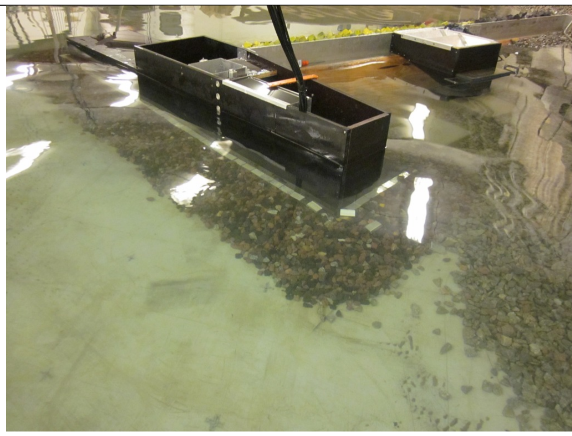
2	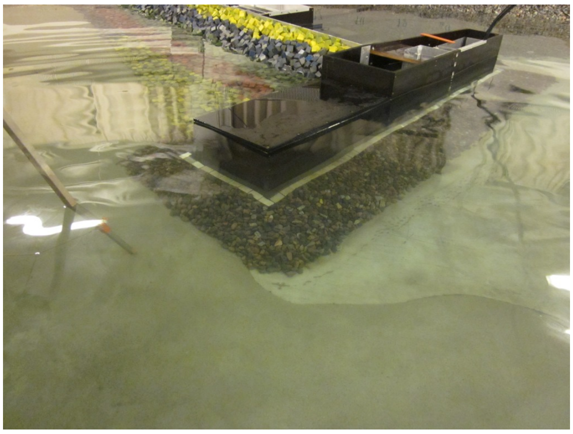	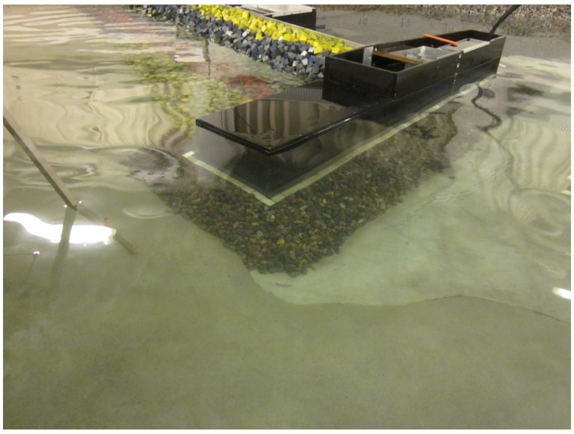

Position	Before	After
3		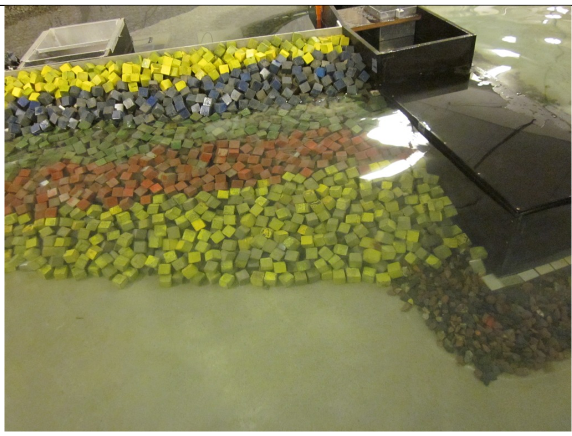
4	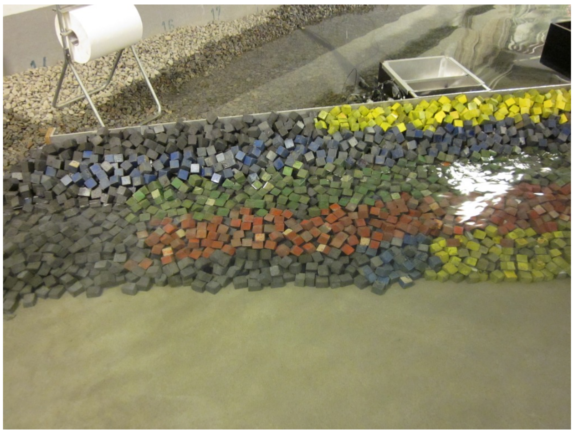	

Video Sequences of Characteristic Wave Overtopping at Rubble Mound C

Two interesting sequences have been identified for the rubble mound breakwater, with SWL = +3.5, $T_\mathrm{p} = 8$ and 16 s and $H_\mathrm{m0} \approx 4.8$ m. Regarding the overtopping for the other tests, very insignificant discharge was observed, as shown in Table 9.1.

Test no. 2.1.6, SWL: +3.50, $T_{\mathbf{p}}$: 8 s, $H_{\mathbf{m0}}^{Gen}$: 4.74 m

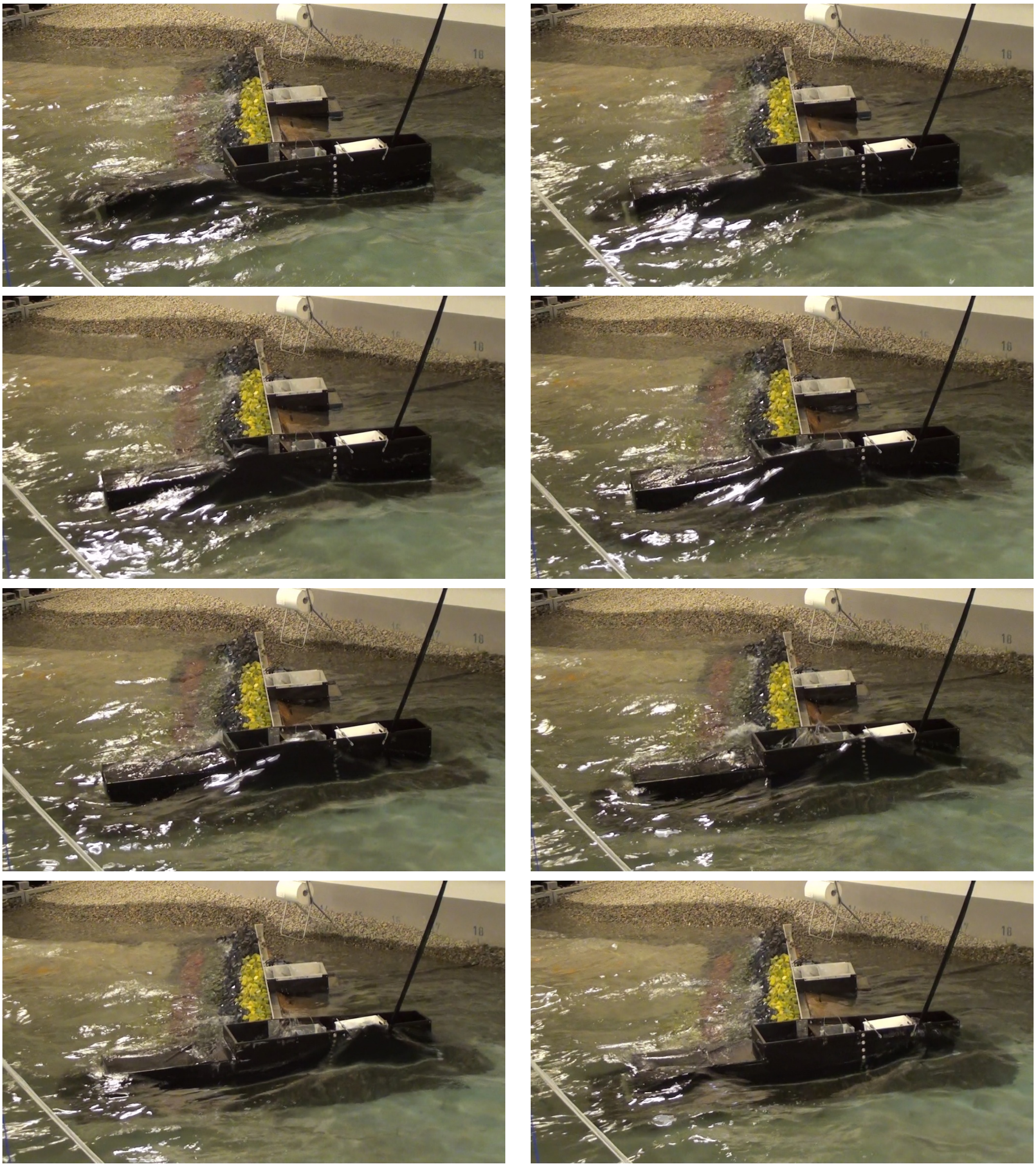

Test no. 2.2.6, SWL: +3.50, T_p: 16 s, H_{m0}^{Gen}: 4.84 m